UNIVERSITAT DE BARCELONA

The links between global climatic cycles and the diversification and migration of Arctic shorebirds

La relación entre los ciclos climáticos y la diversificación y migración de las aves limícolas árticas

Ángel Arcones Segovia

The links between global climatic cycles and the diversification and migration of Arctic shorebirds

"La relación entre los ciclos climáticos y la diversificación y migración de las aves limícolas árticas"

ÁNGEL ARCONES SEGOVIA

TESIS DOCTORAL 2019

Todas las ilustraciones de los capítulos y la contraportada han sido realizadas por María Ángeles Santamaría

All the illustrations from the chapters and the back cover have been done by María Ángeles Santamaría

Index

Agradecimientos

Llegado a este punto, tengo mucho que agradecer a mucha gente, y no se ni por dónde empezar. Esta tesis lleva mi nombre, pero es la obra de mucha gente que me ha acompañado, ayudado y apoyado durante años. Este es un camino que habría sido imposible hacer sin todos ellos.

Mi primer agradecimiento es para mi familia. Para mis padres, **Concha** y **Ángel**, que me lo han dado todo, siempre me han apoyado y me han hecho ser quien soy. A ellos les debo todo lo bueno que ha llegado y lo que llegue en el futuro. También a mis hermanas, las doctoras, **Almudena** y **Julia**, que siempre me han cuidado y han sido una referencia para mí. A **Achim**, que ya es uno más de nuestra familia, y a **Teo** y **Pablo**, los últimos en llegar y que con sus sonrisas nos llenan de alegría.

Estoy muy agradecido también a todos los que han sido mi familia científica estos años. En primer lugar, a **David**, por haberme dado la oportunidad de iniciarme y desarrollarme como científico, y por enseñarme a no conformarme nunca. También a **Xavi**, de quien siempre he disfrutado aprendiendo y que siempre ha hecho que, pese a la distancia, siempre nos sintiéramos cerca de Barcelona, que nunca es fácil y menos en los tiempos que corren.

Mi familia científica también la conforman todos mis compañeros de estos años. **Raquel**, con quien he tenido la suerte de compartir este viaje turbulento desde el inicio y cuya ayuda ha sido inestimable hasta el final. Juntos hemos salido adelante pese a las dificultades compi. **Marcos**, que desde el principio fue una especie de hermano mayor para nosotros en el Museo, y que nunca se ha dejado derrotar por los malos tiempos. **Javi**, con su siempre sorprendente mezcla de ideas, entre brillantes y locas. Y a los que sus caminos los han llevado en otras direcciones: a **Salva**, a **Guille**, a **Carlos**, a **Thijs**…

Y en esta familia también está toda la gente del Museo, que por suerte es muchísima y maravillosa. En especial quiero acordarme de todos los compañeros y compañeras con los que he compartido espacio y vida en la 1212 estos años: **Melinda**, **Chio**, **Silvia**, **Guida**, **Indra**, **Calatayud**, **Sergio**, **Jaime**, **Jorge**, **Fernanda**, **Chechu**, **Elisa**, **Manu**, **Eva** y **Mario**. Y alguno más que seguro que me olvido y luego me dará rabia. También a la gente del tupper, los compañeros de cubículo a la hora de comer. Sois tantos que a veces no cabemos todos, y tengo también tanto que agradecer que lo haré en persona cuando vayamos a por el café. Queda mucha gente por agradecer, de la 1111, de la “sala triste”, de Pinar… Todos me habéis hecho sentir que el Museo era mi casa, a pesar de todas las circunstancias que parecían querer impedirlo.

Y este viaje también se ha hecho *with a Little help from my friends.* Esos que también me han visto crecer, evolucionar, subir y bajar. Para mí son una parte importante no solo de esta tesis, sino de todo lo que soy. Son la gente a la que más admiro, y la que hace que lo malo sea menos malo y lo bueno sea mejor.

Y empiezo por **Geles**. Sin tu apoyo y tus ánimos todo este tiempo, hace mucho que no habría podido conseguir llevar a cabo esta caminata por el desierto. Tú lo has sufrido también, y ahora por fin empieza a salir el sol. Gracias por estar siempre ahí, guapita.

Tengo la suerte de tener mucha gente a la que llamar amigos, y a los que estar agradecido. Y aunque aquí no voy a poder expresar plenamente lo agradecido que os estoy (eso será tarea para cuando nos veamos), no quiero dejar de mencionar a mucha de esa gente. A mis camaradas **Andrés**, **Akbar**, **Juan**, **Raúl** y **Rober**, vecinos distantes con los que he compartido tantas aventuras, y juntos hemos pasado por los mejores y los peores momentos. A todos mis compañeros de biología, y la gente que ha llegado con ellos durante los años: **Kantala**, **Edu**, **Dani**, **Pako, María**, **Gloria**, **Sonia**, **Belén**, **Marta**, **Carlos**, **Chechu**, **Suja**, **Horcas**, **Juanillo**, **Jose**, … Esta historia es tan vuestra como mía. Y a los tetes, que recordaban cada mañana lo que cuesta levantarse, y cada día lo absurdo que es el mundo. A **Ana**, por darme apoyo y perspectiva, y evitarme crisis máximas. A **Pola** y a **Edu**, que siempre han sido una inspiración para luchar por conseguir lo que de verdad quieres. Y a todos los que me he olvidado de nombrar porque, aunque mi cabeza no dé para más, sé que estáis ahí y os lo haré saber.

Y por último a **Ángel**. Es decir, a mí mismo. Porque has sufrido mucho durante estos años, y has estado muy cerca de abandonar unas cuantas veces. Y porque has aprendido a apretar los dientes y dar más de ti mismo. Y por nunca dejar de creer. Ha sido un viaje difícil pero enriquecedor, y pronto estarás orgulloso de ello. No puedo decirte hacia donde irá el viaje ahora, pero independientemente del destino y la ruta, sé que darás lo mejor de ti. Así que, solo me queda decirte: *Naammaktsiarit!*

General introduction

Glacial cycles and diversification

Allopatry has been considered the most common mechanism of diversification at the species and population levels (Coyne & Orr, 2004; Price, 2007). This process, by definition, relies on the geographic separation of populations either though the colonization of new territories (dispersal) or the separation as a consequence of an emerging geographical barrier (vicariance). Traditionally, these vicariant events were associated with geological changes, such as continent breakups, mountain ranges or large rivers. But species sometimes display large continuous ranges with clearly differentiated populations despite a lack of apparent barriers between them, which suggests that a previous isolating factor acted between those populations and has since disappeared allowing secondary contacts. One of the first explanations proposed for such situations was the effect of historical climate and habitat changes, especially during large-scale events such as glacial cycles (Rand, 1948). Ever since, the glacial cycles of the Quaternary [from 2.6 million years ago (Mya) to the present] (Fig. 1), and especially the last glacial maximum (LGM) (ca. 21,000 years ago), have received substantial attention as promoters of allopatric diversification (e.g. Mengel, 1964; Avise & Walker, 1998; Hewitt, 1996, 2004; Weir & Schluter, 2004; Lovette, 2005).

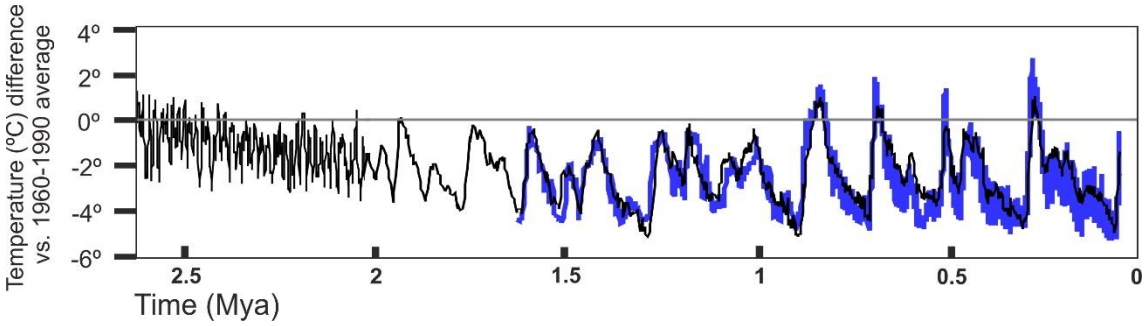

Figure 1: Changes in the global temperature during the Pleistocene, based on the estimates from EPICA community members (2004) (blue line) and Lisiecki & Raymo (2005) (black line).

Glacial cycles deeply altered the global climate (Fig. 2), modifying the distribution of habitats worldwide and in turn the distribution of many species, especially in temperate and cold regions (Webb III & Bartlein, 1992; Dynesius & Jansson, 2000). These species overcame such changes by persisting in areas of refugia during climatically unsuitable periods (Bennett & Provan, 2008; Gavin *et al*., 2014). Over multiple glacial and interglacial episodes, species would have experienced repeated contractions and expansions of their distribution ranges, leaving a genetic print on the lineages over time (Avise & Walker, 1998; Hewitt, 1999, 2000, 2004). However, molecular studies on bird species in North America challenged the idea of an increased diversification during the Pleistocene (Klicka & Zink, 1997). This sparked a debate between authors that defended a Pleistocene origin for many North American bird species and subspecies (Johnson & Cicero, 2004; Cicero & Johnson, 2006), and those advocating for an earlier origin (Zink *et al*., 2004; Zink & Klicka, 2006). When considered together, both perspectives show that the timing of the diversification in these birds is extremely dependant on the degree of relatedness between species/lineages (Lovette, 2005). While the split in some species pairs predates the Pleistocene, more closely related species diverged mostly during the Pleistocene, as well as subspecies or populations within species. But more importantly, the proximity to the glaciated areas is a key factor to explain these differences. Northern bird species, whose habitats were more affected during glacial periods, tend to show a more recent diversification than temperate and tropical species (Weir & Schluter, 2004; Lovette, 2005). This also applies to bird species in the southern hemisphere (Weir *et al*., 2016) and, to a lesser extent, to boreal mammals (Arbogast & Kenagy, 2001) and Neotropical montane species (Weir, 2006).

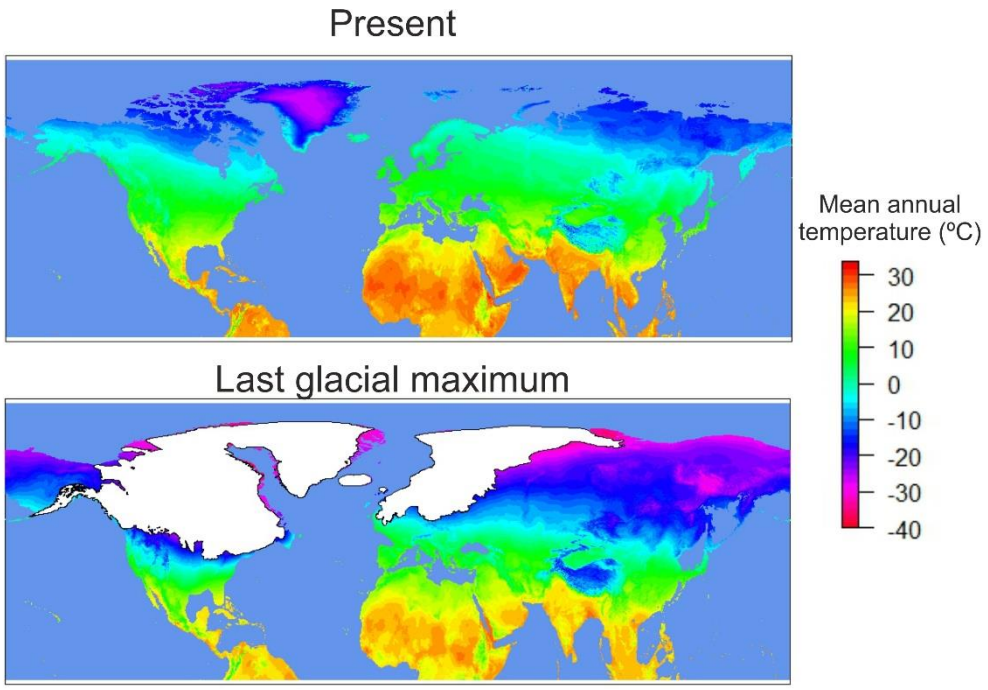

Figure 2: Mean annual temperature in the northern hemisphere in the present (representing an interglacial period) and during the last glacial maximum (ca. 21,000 years ago) with the extension of the main glaciers (in white), modified from Ehlers *et al*. (2011).

High latitude areas, in particular the Arctic and boreal regions have often been considered as "evolutionary freezers", with slow evolutionary rates and low diversity due to its harsh climatic conditions (Rohde, 1992; Wright *et al*., 2006). On top of that, some authors also attributed the low genetic diversity to the repeated action of glacial cycles (Hultén, 1937; Hewitt, 1999). But recent studies suggest the opposite, considering the Arctic as a young region (Murray, 1995) where species and their populations diversified during recent times (Weir & Schluter, 2004; Brochmann & Brysting, 2008). Recent works that built upon genetic data support a recent diversification of many Arctic species from different taxa, including plants (e.g. Abbott & Comes, 2004; Eidesen *et al*., 2013), butterflies (e.g Todisco *et al*., 2012; Kleckova, *et al*., 2015), mammals (e.g. Fedorov & Goropashnaya, 1999; Hope *et al*., 2012), reptiles (e.g. Babik *et al*., 2004; Horreo *et al*., 2018) and birds (e.g. Buehler & Baker, 2005; Jones *et al*., 2005; Maley & Winker, 2010; van Els *et al*., 2012).

These studies highlight the role of the Pleistocene glacial cycles in the diversification between and within species, and point at the refugia as a key component in allopatric speciation processes. However, most of them only suggest the existence of

the refugia based on divergence times and/or population-size changes estimated from genetic data. Although valuable, those approaches do not provide information on the spatial mechanisms involved in diversification processes. Such mechanisms are necessary to understand the relationship between the number and location of the main areas of refugia, and the emergence of the current genetic and phenotypic diversity of the species during the Pleistocene.

The definition of "refugia" is a matter of debate which has been reviewed by several authors (Bennett & Provan, 2008; Ashcroft, 2010; Stewart *et al*., 2010). In general, the term refers to geographic areas sustaining certain climatic conditions that are disappearing everywhere else (Ashcroft, 2010; Dobrowski, 2011), providing shelter for the species that are experiencing a retreat in their ranges (Keppel *et al*., 2012). As the climatic conditions become more favourable, populations emerge from the different refugia recolonizing the totality or part of their previous ranges. At this point, isolated populations can expand into a large portion of the species former distributions or make secondary contact with other populations, resulting in a new genetic landscape across the range of the species (Hewitt, 1999).

There have been some influential studies that proposed specific areas of glacial refugia as the geographic origin of subspecies across a wide number of Arctic species (Macpherson, 1965; Ploeger, 1968). These works consisted mostly in educated guesses based in the knowledge of paleoclimatic environments of their time and without any available genetic and fossil data or paleodistribution models to support them. But nonetheless, they provided a strong foundation for posterior hypotheses on the phylogeography of Arctic species, and the critical role of the areas of northern refugia on the distribution of the species during glacial periods (see Stewart & Lister, 2001; Provan & Bennett, 2008).

The knowledge about the phylogeographic histories of Arctic species has greatly advanced over the last decades, yet there still are uncertainties in the link between the genetic and geographic mechanisms involved. Genetic structure and divergence times within Arctic species suggest, but do not demonstrate, the implication of glacial cycles

in their diversification. In order to confirm such hypothesis, there is a need for an integrative approach to explore the spatial processes involved in this genetic divergence. Furthermore, this needs to be assessed for multiple species and across the whole Arctic to identify different patterns and processes, instead of generalising from the results obtained from individual species. As highlighted by Hickerson *et al*. (2010), integrating different genetic and geographic approaches across large taxonomic groups or ecologic assemblages should be a priority for future advances in phylogeography.

Birds, and especially northern species, have been the most common studied group to investigate the diversification of species during the Pleistocene (Avise & Walker, 1998; Weir & Schluter, 2004; Lovette, 2005). Even the most contentious aspects of this evolutionary process have been assessed with the study of temperate and northern bird species (Klicka & Zink, 1997; Johnson & Cicero, 2004; Zink *et al*., 2004; Cicero & Johnson, 2006; Zink & Klicka, 2006). Beyond the classic interest in birds from scientists and naturalists, their utility as a study group on this topic is also due to their widespread distributions across different habitats and regions, the large amount of Arctic and boreal species and their high intraspecific diversity.

The Arctic shorebirds

In this thesis, we used the Arctic species of shorebirds as case study group. The shorebirds (also known as waders) are one of the most representative groups of the Arctic avifauna due to the amount of species in the region and their large population densities (Järvinen & Väisänen, 1978; Meltofte *et al*., 2007). These birds constitute an ecologically homogeneous group, although not phylogenetically. They all belong to the order Charadriiformes to which also belong seagulls, terns, auks, skimmers, skuas, pratincoles and coursers. Within this order, shorebirds form a polyphyletic group with two main clades: Charadrii (plovers and allies) and Calidri (sandpipers and allies), the latter being the sister group to Lari (gulls, terns, auks and others) (Paton *et al*., 2003; Thomas *et al*., 2004; Paton & Baker, 2006; Baker *et al*., 2007).

The are 12 families and over 210 species of shorebirds distributed across all continents, reaching even Antarctica (del Hoyo *et al*., 2018). As the name shorebirds (or waders) suggests, their preferred habitats are near the water, and are usually found in wetlands, marshes or intertidal and coastal areas, where they feed mainly out of molluscs, insects and other invertebrates (Fig. 3).

Figure 3: pictures of different species of shorebirds. On the top left, a group of Eurasian Oystercatchers (*Haematopus ostralegus*) (photo: Ángel Arcones); on the top right, a Common Redshank (*Tringa totanus*) (photo: Xavier Ferrer); on the bottom left, a Dunlin (*Calidris alpina*) (photo: Xavier Ferrer); on the bottom right, a Ruddy Turnstone (*Arenaria interpres*) (photo: Marco Sannolo)

Around half of all the species have partial of full migratory behaviour (del Hoyo *et al*., 2018). Furthermore, up to 70 different species reach Arctic and subarctic areas during their breeding season (Chester, 2016), where the tundra constitutes their main habitat. The migration to those high-latitude breeding grounds often involves travelling over 5,000 kilometres, sometimes non-stop, from their non-breeding grounds in intertropical regions or temperate areas of the southern hemisphere (van de Kam *et al*., 2004). To achieve such feats, these birds display a great ability to adapt their bodies and metabolism to meet the demands of the travel. Before the spring migration, they stack up fat reserves and increase the size of their pectoral muscle and the heart, while

reducing the size of their digestive system (Piersma *et al*., 1999, 2002). The bulk of migrants arrive at the Arctic between May and early June (Meltofte 1985, Syroechkovski & Lappo, 1994, del Hoyo *et al*., 2018), and after 2-3 weeks they lay a clutch of usually four eggs (see Meltofte *et al*., 2007). Between July and August begins the autumn migration, minimizing the post-breeding stay in the Arctic to avoid a decline in food availability during their migration to the non-breeding grounds (Schneider & Harrington, 1981).

Migrating to breed in the Arctic is a very expensive strategy in terms of energy. Aside from the fat storage required for the travel, these birds also have a higher metabolic rate while staying at high latitudes due to the cooler climatic conditions (Lindström & Klaassen, 2006; Piersma *et al*., 2003). In order to make such strategy cost-efficient, other factors must be playing a key role. It has been hypothesized that peaks in the primary productivity of habitats during the spring and summer plays an important role in the migratory behaviour of birds (Ponti *et al*., 2018). In the Arctic, the period of productivity only lasts a few months during the short summer, but since suitable areas were uninhabited during the winter, the initial intra and interspecific competence during the breeding season is much lower than in tropical areas, were competing species/individuals occur year-round (Cox, 1968). Breeding in the Arctic also provides more hours of daylight for foraging (Meltofte *et al*., 2007), a lower risk of predation (McKinnon *et al*., 2012) and a lower parasite prevalence that help saving some energy expenditure in the immune system (Piersma, 1997).

As the distribution of the species changed over the glacial cycles, the long-distance migration of these and other Arctic birds would have changed too. Zink & Gardner (2017) suggested an interruption of the migration in many species during the glacial periods, although it is unclear if this was the case for Arctic species with available northern breeding areas during these periods. Upon post-glacial expansion, the migratory routes likely determined the different paths of expansion of the species, contributing in some cases to the divergence between populations during this period (Buehler *et al*., 2006; Milá *et al*., 2006, 2007; Ruegg, Hijmans, & Moritz, 2006).

Arctic shorebirds have a notable intraspecific diversity, as 21 of the 70 Arctic species have described subspecies (Engelmoer & Roselaar, 1998; del Hoyo *et al*., 2018), with a few more awaiting recognition (e.g. Barisas *et al*., 2015; Jukema *et al*., 2015; Leblanc *et al*., 2017). In his work on the geographic differentiation within Arctic geese and fowls, Ploeger (1968) extended his inference to some Arctic shorebird species, supporting similar patterns of diversification linked to the ice-free areas during the LGM. A work on the Dunlin (*Calidris alpina*) also linked the diversification of its subspecies from proposed areas of refugia (Greenwood, 1986). The first studies based on molecular analyses highlighted a very recent origin of the current diversity (Wenink *et al*., 1993, 1994, 1996; Baker *et al*., 1994; Kraaijeveld & Nieboer, 2000). However, the timing greatly varied between species. For example, *C. alpina* showed consistently older lineages than *Calidris canutus*, suggesting different evolutionary histories (Wenink *et al*., 1993, 1996; Buehler & Baker, 2005).

Additionally, multiple studies reported very shallow genetic diversity and a lack of genetic structure in Arctic shorebird species, despite having recognised phenotypic subspecies. This is the case, for example, of *C. canutus* (Baker *et al*., 1994), *Tringa totanus* (Ottvall *et al*., 2005), *Arenaria interpres* (Wenink *et al*., 1994), *Calidris maritima* (Barisas *et al*., 2015; Leblanc *et al*., 2017) and *Charadrius hiaticula* (Thies *et al*., 2018).

Some authors point out that the current phenotypic variation does not always reflect genetic differentiation (Marthinsen *et al*., 2007; Rheindt *et al*., 2011). The overall low genetic diversity has been attributed to severe changes in their ranges and population sizes in recent times (Kraaijeveld & Nieboer, 2000), which many authors consider a consequence of Pleistocene glacial cycles (Wenink *et al*., 1993, 1996; Baker *et al*., 1994; Buehler & Baker, 2005; Pruett & Winker, 2005; Thies *et al*., 2018). However, the link between glacial cycles, biogeographic changes and intraspecific diversification across this group remains mainly unknown. Previous phylogeographic studies focused around individual species (e.g. Ottvall *et al*., 2005; Marthinsen *et al*., 2007; Miller *et al*., 2013; Thies *et al*., 2018) or the comparation between only two species (Wenink *et al*., 1994; Buehler & Baker, 2005; Pruett & Winker, 2005). Moreover, these studies tend to oversee the geographic implications of the glacial and interglacial periods, and base their assumptions on the results from genetic data.

Understanding the implications of the Pleistocene glacial cycles in the diversity and distribution of Arctic species represents a key topic in phylogeography (Avise & Walker, 1998; Hewitt, 2000, 2004; Weir & Schluter, 2004; Lovette, 2005). Arctic shorebirds are representative of all the different Arctic and subarctic ecosystems, and reflect the diversity patterns that are also found in other Arctic taxa. Understanding the role of the climate in their diversification would provide a more complete picture of the recent evolution of the Arctic biodiversity. This is fundamental not only in evolutionary terms, but also to assess potential responses of Arctic species to the current climate change (Parmesan, 2006; Williams *et al*., 2013). Among birds, migratory and northern species are some of the most endangered by climate change (Crick, 2004; Huntley *et al*., 2008; Virkkala & Rajasärkkä, 2011; Barbet-Massin *et al*., 2012; Tayleur *et al*., 2016). The long-distance migrations of the Arctic shorebirds reinforce their value as indicators of the impacts of climate change in the biodiversity worldwide (Piersma & Lindström, 2004; Meltofte *et al*., 2007; Galbraith *et al*., 2014)

References

Abbott, R. J., & Comes, H. P. (2004). Evolution in the Arctic: A phylogeographic analysis of the circumarctic plant, *Saxifraga oppositifolia* (Purple saxifrage). *New Phytologist*, *161*(1), 211–224.

Arbogast, B. S., & Kenagy, G. J. (2001). Comparative phylogeography as an integrative approach to historical biogeography. *Journal of Biogeography*, *28*(7), 819–825.

Ashcroft, M. B. (2010). Identifying refugia from climate change. *Journal of Biogeography*, *37*(8), 1407–1413.

Avise, J., & Walker, D. (1998). Pleistocene phylogeographic effects on avian populations and the speciation process. *Proceedings of the Royal Society B: Biological Sciences*, *265*(October 1997), 457–463.

Babik, W., Branicki, W., Sandera, M., Litvinchuk, S., Borkin, L., Irwin, J. T., & Rafinski, J. (2004). Mitochondrial phylogeography of the moor frog, *Rana arvalis*. *Molecular Ecology*, *13*, 1469–1480.

Baker, A. J, Pereira, S. L., & Paton, T. A. (2007). Phylogenetic relationships and divergence times of Charadriiformes genera: multigene evidence for the Cretaceous origin of at least 14 clades of shorebirds. *Biology Letters*, *3*(2), 205–210.

Baker, Allan J., Piersma, T., & Rosenmeier, L. (1994). Unraveling the intraspecific phylogeography of Knots *Calidris canutus*: a progress report on the search for genetic markers. *Journal of Ornithology*, *135*(4), 599–608.

Barbet-Massin, M., Thuiller, W., & Jiguet, F. (2012). The fate of European breeding birds under climate, land-use and dispersal scenarios. *Global Change Biology*, 18(3), 881–890.

Barisas, D. A. G., Amouret, J., Hallgrímsson, G. T., Summers, R. W., & Pálsson, S. (2015). A review of the subspecies status of the Icelandic Purple Sandpiper *Calidris maritima littoralis*. *Zoological Journal of the Linnean Society*, *175*(1), 211–221.

Bennett, K. D., & Provan, J. (2008). What do we mean by "refugia"? *Quaternary Science Reviews*, *27*(27–28), 2449–2455.

Brochmann, C., & Brysting, A. K. (2008). The arctic – an evolutionary freezer? *Plant Ecology and Diversity*, *1*(2), 181–195.

Buehler, D. M., & Baker, A. J. (2005). Population Divergence Times and Historical Demography in Red Knots and Dunlins. *Condor*, *107*(3), 497–513.

Buehler, D. M., Baker, A. J., & Piersma, T. (2006). Reconstructing palaeoflyways of the late Pleistocene and early Holocene red knot (*Calidris canutus*). *Ardea*, 94(3), 485–498.

Cicero, C., & Johnson, N. K. (2006). The tempo of Avian diversification: Reply. *Evolution*, 60(2), 413.

Chester, S. (2016). *The Arctic Guide: Wildlife of the Far North*. Princeton University Press.

Cox, G. W. (1968). The Role of Competition in the Evolution of Migration. *Evolution*, *22*(1), 180–192.

Coyne, J. A., Orr A (2004) *Speciation*. Sinauer Associates Inc., Sunderland, Massachusetts.

Crick, H. Q. P. (2004). Impact of climate change on birds. *Ibis*, 146(Suppl. 1), 48–56.

del Hoyo, J., Elliott, A., Sargatal, J., Christie, D.A. & Kirwan, G. (eds.) (2018). *Handbook of the*

Birds of the World. Lynx Edicions, Barcelona.

Dobrowski, S. Z. (2011). A climatic basis for microrefugia: The influence of terrain on climate. *Global Change Biology*, *17*(2), 1022–1035.

Dynesius, M., & Jansson, R. (2000). Evolutionary Consequences of Changes in Species ' Geographical Distributions Driven by Milankovitch Climate Oscillations. *Proceedings of the National Academy of Sciences of the United States of America*, *97*(16), 9115–9120.

Ehlers, J., Gibbard, P. L., & Hughes, P. D. (Eds.). (2011). *Quaternary glaciations-extent and chronology: a closer look* (Vol. 15). Elsevier.

Eidesen, P. B., Ehrich, D., Bakkestuen, V., Alsos, I. G., Gilg, O., Taberlet, P., & Brochmann, C. (2013). Genetic roadmap of the Arctic: Plant dispersal highways, traffic barriers and capitals of diversity. *New Phytologist*, *200*(3), 898–910.

Engelmoer, M., & Roselaar, C. S. (1998). *Geographical variation in waders*. Springer Science & Business Media.

EPICA community members. (2004). Eight glacial cycles from an Antarctic ice core. Nature, 429, 623–628.

Fedorov, V. B., & Goropashnaya, A. V. (1999). The importance of ice ages in diversification of Arctic collared lemmings (*Dicrostonyx*): Evidence from the mitochondrial cytochrome b region. *Hereditas*, *130*(3), 301–307.

Galbraith, H., DesRochers, D. W., Brown, S., & Reed, J. M. (2014). Predicting vulnerabilities of North American shorebirds to climate change. *PLoS ONE*, 9(9), 21–23.

Gavin, D. G., Fitzpatrick, M. C., Gugger, P. F., Heath, K. D., Rodrıguez-Sanchez, F., Dobrowski, S. Z., … Williams, J. W. (2014). Climate refugia: joint inference from fossil records, species distribution models and phylogeography. *New Phytologist*, *204*, 37–54.

Greenwood, J. G. (1986). Geographical variation and taxonomy of the Dunlin (*Calidris alpina*). *Bulletin of the British Ornithologists' Club*, *106*, 43–42.

Hewitt, G. M. (1996). Some genetic consequences of ice ages, and their role in speciation. *Biological Journal of the Linnean Society*, *58*(July), 247–276.

Hewitt, G. M. (1999). Post-glacial re-colonization of European biota. *Biological Journal of the Linnean Society*, *68*(1–2), 87–112.

Hewitt, G. M. (2000). The genetic legacy of the quaternary ice ages. *Nature*, *405*(6789), 907–913.

Hewitt, G. M. (2004). Genetic consequences of climatic oscillations in the Quaternary. *Philosophical Transactions of the Royal Society B: Biological Sciences*, *359*, 183–195.

Hickerson, M. J., Carstens, B. C., Cavender-Bares, J., Crandall, K. A., Graham, C. H., Johnson, J. B., … Yoder, A. D. (2010). Phylogeography's past, present, and future: 10 years after Avise, 2000. *Molecular Phylogenetics and Evolution*, *54*(1), 291–301.

Hope, A. G., Speer, K. A., Demboski, J. R., Talbot, S. L., & Cook, J. A. (2012). A climate for speciation: Rapid spatial diversification within the *Sorex cinereus* complex of shrews. *Molecular Phylogenetics and Evolution*, *64*(3), 671–684.

Horreo, J. L., Pelaez, M. L., Suárez, T., Breedveld, M. C., Heulin, B., Surget-Groba, Y., … Fitze, P. S. (2018). Phylogeography, evolutionary history and effects of glaciations in a species (*Zootoca vivipara*) inhabiting multiple biogeographic regions. *Journal of Biogeography*, *45*(7), 1616–1627.

Hultén, E. (1937). *Outline of the history of arctic and boreal biota during the Quaternary period*. Stockholm: Aktiebolaget Thule.

Huntley, B., Collingham, Y. C., Willis, S. G., & Green, R. E. (2008). Potential impacts of climatic change on European breeding birds. *PLoS ONE*, 3(1).

Järvinen, O., & Väisänen, R. A. . (1978). Ecological zoogeography of north european waders, or why do so many waders breed in the north? *Oikos*, *30*(3), 496–507.

Johnson, N. K., & Cicero, C. (2004). New mitochondrial DNA data affirm the importance of Pleistocene speciation in North American birds. *Evolution*, *58*(5), 1122–1130.

Jones, K. L., Krapu, G. L., Brandt, D. A., & Ashley, M. V. (2005). Population genetic structure in migratory sandhill cranes and the role of Pleistocene glaciations. *Molecular Ecology*, *14*(9), 2645–2657.

Jukema, J., van Rhijn, J. G., & Piersma, T. (2015). Geographic variation in morphometrics, molt, and migration suggests ongoing subspeciation in Pacific Golden-Plovers (*Pluvialis fulva*). *The Auk*, *132*(3), 647–656.

Keppel, G., Van Niel, K. P., Wardell-Johnson, G. W., Yates, C. J., Byrne, M., Mucina, L., … Franklin, S. E. (2012). Refugia: Identifying and understanding safe havens for biodiversity under climate change. *Global Ecology and Biogeography*, *21*(4), 393–404.

Kleckova, I., Cesanek, M., Fric, Z., & Pellissier, L. (2015). Diversification of the cold-adapted butterfly genus *Oeneis* related to Holarctic biogeography and climatic niche shifts. *Molecular Phylogenetics and Evolution*, *92*, 255–265.

Klicka, J., & Zink, R. M. (1997). The Importance of Recent Ice Ages in Speciation: A Failed Paradigm. *Science*, *277*(5332), 1666–1669.

Kraaijeveld, K., & Nieboer, E. N. (2000). Late Quaternary paleogeography and evolution of arctic breeding waders. *Ardea*, *88*(2), 193–205.

Leblanc, N. M., Stewart, D. T., Pálsson, S., Elderkin, M. F., Mittelhauser, G., Mockford, S., … Mallory, M. L. (2017). Population structure of Purple Sandpipers (*Calidris maritima*) as revealed by mitochondrial DNA and microsatellites. *Ecology and Evolution*, (7), 3225–3242.

Lindström, Å., & Klaassen, M. (2006). High Basal Metabolic Rates of Shorebirds While in the Arctic: a Circumpolar View. *The Condor*, *105*(3), 420.

Lisiecki, L. E., & Raymo, M. E. (2005). A Pliocene-Pleistocene stack of 57 globally distributed benthic δ 18O records. Paleoceanography, 20(1), 1–17.

Lovette, I. J. (2005). Glacial cycles and the tempo of avian speciation. *Trends in Ecology and Evolution*, *20*(2), 57–59.

Macpherson, A. A. H. (1965). The origin of diversity in mammals of the Canadian arctic tundra. *Systematic Zoology*, *14*(3), 153–173.

Maley, J. M., & Winker, K. (2010). Diversification at high latitudes: Speciation of buntings in the genus *Plectrophenax* inferred from mitochondrial and nuclear markers. *Molecular Ecology*, *19*(4), 785–797.

Marthinsen, G., Wennerberg, L., & Lifjeld, J. T. (2007). Phylogeography and subspecies taxonomy of dunlins (*Calidris alpina*) in western Palearctic analyzed by DNA microsatellites and AFLP markers. *Biological Journal of the Linnean Society*, *92*, 713–726.

McKinnon, L., Picotin, M., Bolduc, E., Juillet, C., & Bêty, J. (2012). Timing of breeding, peak food availability, and effects of mismatch on chick growth in birds nesting in the High Arctic.

Canadian Journal of Zoology, *90*(8), 961–971.

Meltofte, H. (1985). Populations and breeding schedules of waders, Charadrii, in high arctic Greenland. *Bioscience, 16,* 1-43.

Meltofte, H., Piersma, T., Boyd, H., McCaffery, B., Ganter, B., Golovnyuk, V. V., … Wennerberg, L. (2007). Effects of climate variation on the breeding ecology of Arctic shorebirds. *Meddelelser Om Gronland Bioscience* (59).

Mengel, R. M. (1964) The probable history of species formation in some northern Wood warblers (Paraulidae). *Living Bird*, *3*, 9-43.

Milá, B., McCormack, J. E., Castañeda, G., Wayne, R. K., & Smith, T. B. (2007). Recent postglacial range expansion drives the rapid diversification of a songbird lineage in the genus *Junco*. *Proceedings of the Royal Society B: Biological Sciences*, 274(1626), 2653–2660.

Milá, B., Smith, T. B., & Wayne, R. K. (2006). Postglacial Population Expansion Drives the Evolution of Long-Distance Migration in a Songbird. *Evolution*, 60(11), 2403–2409.

Miller, M. P., Gratto-Trevor, C., Haig, S. M., Mizrahi, D. S., Mitchell, M. M., & Mullins, T. D. (2013). Population Genetics and Evaluation of Genetic Evidence for Subspecies in the Semipalmated Sandpiper (*Calidris pusilla*). *Waterbirds*, *36*(2), 166–178.

Murray, D. F. (1995). Causes of Arctic Plant Diversity: Origin and Evolution. In *Arctic and alpone biodiversity: patterns, causes and ecosystem consequences* (pp. 21–32), Springer, Berlin.

Ottvall, R., Höglund, J., Bensch, S., & Larsson, K. (2005). Population differentiation in the redshank (*Tringa totanus*) as revealed by mitochondrial DNA and amplified fragment length polymorphism markers. *Conservation Genetics*, *6*(3), 321–331.

Paton, T. A., & Baker, A. J. (2006). Sequences from 14 mitochondrial genes provide a well-supported phylogeny of the Charadriiform birds congruent with the nuclear RAG-1 tree. *Molecular Phylogenetics and Evolution*, *39*(3), 657–667.

Paton, T. A., Baker, A. J., Groth, J. G., & Barrowclough, G. F. (2003). RAG-1 sequences resolve phylogenetic relationships within Charadriiform birds, *29*, 268–278.

Piersma, T., & Lindström, Å. (2004). Migrating shorebirds as integrative sentinals of global environmental change. *Ibis*, 146(Suppl.1), 61–69.

Piersma, T., Lindström, Å., Drent, R. H., Tulp, I., Jukema, J., Morrison, R. I. G., … Visser, G. H. (2003). High daily energy expenditure of incubating shorebirds on High Arctic tundra: A circumpolar study. *Functional Ecology*, *17*(3), 356–362.

Piersma, T.. (1997). Do Global Patterns of Habitat Use and Migration Strategies Co-Evolve with Relative Investments in Immunocompetence due to Spatial Variation in Parasite Pressure? *Oikos*, *80*(3), 623.

Piersma, Theunis, Dietz, M. W., Dekinga, A., Nebel, S., van Gils, J. A., Battley, P. F., & Spaans, B. (1999). Reversible size-changes in stomachs of shorebirds: when, to what extent and why? *Acta Ornithologica*, *34*(2).

Piersma, Theunis, Gudmundsson, G. A., & Lilliendahl, K. (2002). Rapid Changes in the Size of Different Functional Organ and Muscle Groups during Refueling in a Long-Distance Migrating Shorebird. *Physiological and Biochemical Zoology*, *72*(4), 405–415.

Ploeger, P. L. (1968). Geographical differentation in arctic anatidae as a result of isolation during the last glacial. *Ardea*, *56*(1–2), 4–155.

Ponti, R., Arcones, A., Ferrer, X., & Vieites, D. R. (2018). Productivity as the main factor

correlating with migratory behaviour in the evolutionary history of warblers. *Journal of Zoology*, *306*(3), 197–206.

Price T (2007) *Speciation in Birds*. Roberts&Company Publishers, Greenwood Village, Colorado.

Provan, J., & Bennett, K. D. (2008). Phylogeographic insights into cryptic glacial refugia. *Trends in Ecology and Evolution*, *23*(10), 564–571.

Pruett, C. L., & Winker, K. (2005). Biological impacts of climatic change on a Beringian endemic: Cryptic refugia in the establishment and differentiation of the rock sandpiper (*Calidris ptilocnemis*). *Climatic Change*, *68*(1–2), 219–240.

Rheindt, F. E., Székely, T., Edwards, S. V., Lee, P. L. M., Burke, T., Kennerley, P. R., … Küpper, C. (2011). Conflict between genetic and phenotypic differentiation: The evolutionary history of a "lost and rediscovered" shorebird. *PLoS ONE*, *6*(11).

Rohde, K. (1992). Latitudinal gradients in species diversity: the search for the primary cause. *Oikos*, *65*(3), 514–527.

Ruegg, K. C., Hijmans, R. J., & Moritz, C. (2006). Climate change and the origin of migratory pathways in the Swainson's thush. *Journal of Biogeography*, 33, 1172–1182.

Schneider, C., & Harrington, B. A. (1981). Timing of shorebird migration in relation to prey depletion. *The Auk*, *98*(October), 801–811.

Stewart, J. R., Lister, A. M., Barnes, I., & Dalen, L. (2010). Refugia revisited: individualistic responses of species in space and time. *Proceedings of the Royal Society B: Biological Sciences*, *277*(1682), 661–671.

Stewart, John R., & Lister, A. M. (2001). Cryptic northern refugia and the origins of the modern biota. *Trends in Ecology and Evolution*, *16*(11), 608–613.

Syroechkovski, E.E., Jr. & Lappo, E.G. 1994. Migration phenology of waders (Charadrii) on the Taimyr Peninsula, northern Russia. *Ostrich*, 65: 181-190.

Tayleur, C. M., Devictor, V., Gaüzère, P., Jonzén, N., Smith, H. G., & Lindström, Å. (2016). Regional variation in climate change winners and losers highlights the rapid loss of cold-dwelling species. *Diversity and Distributions*, 22(4), 468–480.

Thies, L., Tomkovich, P., Remedios, N. dos, Lislevand, T., Pinchuk, P., Wallander, J., … Küpper, C. (2018). Population and Subspecies Differentiation in a High Latitude Breeding Wader, the Common Ringed Plover *Charadrius hiaticula*. *Ardea*, *106*(2), 163–176.

Thomas, G. H., Wills, M. A., & Székely, T. (2004). Phylogeny of shorebirds, gulls, and alcids (Aves: Charadrii) from the cytochrome-b gene: Parsimony, Bayesian inference, minimum evolution, and quartet puzzling. *Molecular Phylogenetics and Evolution*, *30*(3), 516–526.

Todisco, V., Gratton, P., Zakharov, E. V., Wheat, C. W., Sbordoni, V., & Sperling, F. A. H. (2012). Mitochondrial phylogeography of the Holarctic *Parnassius phoebus* complex supports a recent refugial model for alpine butterflies. *Journal of Biogeography*, *39*(6), 1058–1072.

van de Kam, J., Ens, B.J., Piersma, T. & Zwarts, L. (2004). *Shorebirds. An illustrated behavioural ecology*. KNNV Publishers, Utrecht

van Els, P., Cicero, C., & Klicka, J. (2012). High latitudes and high genetic diversity: Phylogeography of a widespread boreal bird, the gray jay (*Perisoreus canadensis*). *Molecular Phylogenetics and Evolution*, *63*(2), 456–465.

Virkkala, R., & Rajasärkkä, A. (2011). Climate change affects populations of northern birds in boreal protected areas. *Biology Letters*, 7, 395–398.

Webb III, T., & Bartlein, P. J. (1992). Global changes during the last 3 million years: Climatic Controls and Biotic Responses. *Annual Review of Ecology and Systematics*, *23*(1), 141–173.

Weir, J. T. (2006). Divergent Timing and Patterns of Species Accumulation in Lowland and Highland Neotropical Birds. *Evolution*, *60*(4), 842–855.

Weir, J. T., Haddrath, O., Robertson, H. A., Colbourne, R. M., & Baker, A. J. (2016). Explosive ice age diversification of kiwi. *Proceedings of the National Academy of Sciences*, *113*(38), E5580–E5587.

Weir, J. T., & Schluter, D. (2004). Ice sheets promote speciation in boreal birds. *Proceedings. Biological Sciences / The Royal Society*, *271*(1551), 1881–1887.

Wenink, P., Baker, A., Rosner, H., & Tilanus, M. (1996). Global mitochondrial DNA phylogeography of holarctic breeding dunlins (*Calidris alpina*). *Evolution*, *50*(1), 318–330.

Wenink, P. W., Baker, A. J., & Tilanus, M. G. (1993). Hypervariable-control-region sequences reveal global population structuring in a long-distance migrant shorebird, the Dunlin (*Calidris alpina*). *Proceedings of the National Academy of Sciences of the United States of America*, *90*(1), 94–98.

Wenink, P. W., Baker, A. J., & Tilanus, M. G. (1994). Mitochondrial control-region sequences in two shorebird species, the turnstone and the dunlin, and their utility in population genetic studies. *Molecular Biology and Evolution*, *11*(1), 22–31.

Wright, S., Keeling, J., & Gillman, L. (2006). The road from Santa Rosalia: A faster tempo of evolution in tropical climates. *Proceedings of the National Academy of Sciences*, *103*(20), 7718–7722.

Zink, R. M., & Gardner, A. S. (2017). Glaciation as a migratory switch. Science Advances, 3(9), e1603133.

Zink, R. M., & Klicka, J. (2006). The tempo of avian diversification: A comment on Johnson and Cicero. *Evolution*, *60*(2), 411–412.

Zink, R. M., Klicka, J., & Barber, B. R. (2004). The tempo of avian diversification during the Quaternary. *Philosophical Transactions of the Royal Society B: Biological Sciences*, *359*(1442), 215–220.

Objectives

In this thesis we aim to disentangle the role that the changes in the global climate had in the diversification and conservation of Arctic shorebirds. To achieve this goal, we take an integrative approach that combines both geographic and genetic perspectives, covering all the species possible, and exploring both past and future potential changes.

Chapter 1: In this chapter, we explored the effects of the glacial and interglacial periods on shorebird spatial diversification from a geographic perspective. The main hypothesis is that the fragmentation and isolation of the breeding populations during these periods led to the current intraspecific diversity. Combining species distribution models (SDMs) and the fossil record, we compared the distribution patterns between monotypic species and those with multiple subspecies that help explain their intraspecific diversity differences. Additionally, we examined whether this pattern changed between geographic regions, and its potential implications on the long-distance migration in these birds.

Chapter 2: The geographic mechanisms derived from the first chapter needed confirmation from a genetic point of view. Using various molecular clock and coalescent methods, we test whether the timing of the diversification supported the role of the glacial cycles in the process, and if the resulting genetic structure is related to the geographic patterns recovered.

Since the availability of specific mitochondrial molecular clock rates for shorebirds is greatly reduced, and the use of "universal" evolutionary rates is criticized, we developed a new estimation. This involved the largest analysis of this type in terms of number of species, genes, and fossil calibrations used. The goal was to provide rates for each of the mitochondrial markers, for any lineage within the avian phylogeny. The results are then applied to the genetic analyses of the Arctic shorebirds studied.

Chapter 3: In this last chapter, we explore how these Arctic species will fare against the next great challenge: the current climate change. It is expected that over the next century the Arctic shorebirds will experience changes in their breeding distribution, both in terms of range extent and latitudinal distribution. However, given the uneven geography of the Arctic region, and learning from previous chapters, we examined potential differences in responses between the main geographic regions. we also compared the effects of the current climate change in the Arctic with previous climatic scenarios. This helps to put the current situation into perspective of their most recent evolutionary history as a group, and better comprehend its implications in the distribution and conservation of this representative Arctic group.

Chapter 1:

Pleistocene glacial cycles as drivers of allopatric differentiation in Arctic shorebirds.

Authors: Arcones A., Ponti R., Ferrer X. and Vieites D.

Pleistocene glacial cycles as drivers of allopatric differentiation in Arctic shorebirds.

Abstract

During the Pleistocene, the glacial cycles severely altered the ranges of species, especially in the boreal and Arctic regions. Such changes could have favoured isolated populations that originated the current intraspecific diversity. However, the spatial mechanisms that drove this0 diversification in Arctic species are still poorly understood, and often explored for individual species only. In this work, we assess the role of the glacial and interglacial periods in the diversification and migration of the whole group of Arctic shorebirds. If the observed variation within species originated from isolated populations during the glacial cycles, we expect to find common patterns of fragmentation in the breeding ranges that explain the current subspecies. We also seek to clarify whether the long-distance migration was altered or even interrupted during glacial periods. We performed species distribution models (SDMs) to explore the changes in the breeding and non-breeding ranges of 69 species between the last glacial maximum (ca. 21,000 years ago) and the present. We also included independent evidence from the fossil record as well as estimations on the potential extension of the tundra during glacial periods to validate the results from the SDMs. Our findings show that most of the species with subspecies experienced fragmentation of their ranges, especially during the glacial periods, while the majority of the monotypic species maintained continuous ranges. Moreover, the distribution models and the fossil data support an uninterrupted long-distance migration during glacial periods, which could even play a role in maintaining populations isolated over multiple glacial cycles.

Introduction

The climate of the Planet during the Pleistocene (the last 2.5 million years) has been characterized by cycles of cold glacial and warmer interglacial periods, being more intense in the northern hemisphere (Webb & Bartlein, 1992). The duration and intensity of these glacial cycles were stable during most of the Pleistocene, but they increased during the last 900,000 years, with longer and colder periods of ca. 100,000 years each (Alley, 2000; Cohen & Gibbard, 2008). These climatic changes happened fast in a geological time-scale, abruptly altering the distribution of multiple organisms and causing alternating range contractions, expansions (Webb III & Bartlein, 1992; Hewitt, 1999) or extinctions. During glacial periods, the cold climate and large extent of ice sheets forced many temperate and especially Arctic species to shift their distribution ranges southwards, towards climatically suitable areas, usually called refugia. Most of these refugia in the Northern Hemisphere were concentrated south of 40°N (Bennett & Provan, 2008; Stewart *et al.*, 2010), although many Arctic and boreal species found refugia in more northern latitudes (Stewart & Lister, 2001; Provan & Bennett, 2008; Stewart *et al.*, 2010).

These climatic events also left their imprint on the genetic structure of many temperate boreal and Arctic species, acting as potential drivers for allopatric divergences, expansions and secondary contacts between populations (Avise *et al.*, 1998; Hewitt, 2000, 2004; Lovette, 2005). Studies on birds, mainly based on mitochondrial genetic data (mtDNA), suggested that these cycles also played a key role in the diversification of sister species or subspecies during the Pleistocene (Avise & Walker, 1998; Johnson & Cicero, 2004; Weir & Schluter, 2004), but some authors argued against a higher diversification of bird species during this period (Klicka & Zink, 1997). This sparked a debate around the true extent of the effects of the Pleistocene glacial cycles in the genetic diversification between and within bird species (Johnson & Cicero, 2004; Lovette, 2005; Cicero & Johnson, 2006; Zink & Klicka, 2006). While mtDNA has been regarded as a reliable indicator of phylogeographic structure (Zink & Barrowclough, 2008), it may not be appropriate to determine the processes involved in diversification as other nuclear genomic data may do (Edwards & Bensch, 2009). Recent works have focused mainly on the resulting spatial genetic patterns in different northern bird species (e.g. Jones *et al.*, 2005; Haring *et al.*, 2007; Zink *et al.*, 2008; Klicka *et al.*,

2011; van Els *et al.*, 2012; Miller *et al.*, 2015; Leblanc *et al.*, 2017), and a few combined them with geographic predictions (e. g. Ruegg *et al.*, 2006; Zhao *et al.*, 2012; Wang *et al.*, 2013; Li *et al.*, 2016), yet failing to propose spatially explicit hypotheses on the specific role of both the glacial and the interglacial periods in their diversification. Thus, there is a necessity of an integrative approach combining genetics, paleo and current spatial distribution modelling as well as intraspecific phenotypic variation, to disentangle the potential role of glacial cycles in the diversification of Arctic species during the Pleistocene.

The idea of the allopatric isolation during glacial periods as the main factor responsible for population diversification was proposed over 70 years ago (Rand, 1948). Despite its popularity, only a few posterior studies have dug into the detailed geographic processes involved across multiple species (Mengel, 1964; Macpherson, 1965; Ploeger, 1968; Weir & Schluter, 2004). As an example, in his study on the Arctic species of the family Anatidae, Ploeger (1968) proposed a series of areas of isolated refugia that could have harboured breeding populations during glacial periods, and directly linked them to the distribution, intraspecific variation and the origin of current subspecies. Nevertheless, the opposite mechanism is also plausible, as some recent studies suggested that the range expansions during inter-glacial periods could have been the main promoter of the diversification in some Nearctic birds (Milá *et al.*, 2006, 2007; Friis *et al.*, 2016).

Arctic shorebirds are an appropriate model system to study the impact of current and past climate change in the Artic. There are 70 species of shorebirds breeding in the Arctic and subarctic, where they are widespread. Many of them present phenotypic and genetic variation across their distribution ranges that derived in the recognition of subspecies and recent species splits. As a consequence of the strong climatic seasonality in the Arctic, with only few months of suitable temperatures but very high productivity (Pielou, 1991), shorebirds as well as other species are forced to migrate. Most Arctic shorebird species arrive at the breeding grounds in late June and stay between June and early August, they migrate back to the non-breeding grounds in temperate to tropical latitudes in August-September (Meltofte *et al.*, 2007), being some of the animal groups with the longest migrations on Earth.

During the Pleistocene glaciations, their current breeding ranges were covered by permanent ice, hence all these species were forced to shift their breeding ranges southwards. How strong was the impact of glaciations on their non-breeding ranges or whether if they lost their migratory condition during glacial periods -as it has been proposed for other bird species (Zink & Gardner, 2017)-, has not extensively been explored (Buehler *et al.*, 2006). One of the most interesting potential impacts of glacial cycles on Arctic species are not only distribution changes but their potential role as a driver of morphological and genetic diversification. Many Arctic shorebird species present some phenotypic variation across their ranges (Engelmoer & Roselaar, 1998), but most species display a shallow genetic diversity and low differentiation between lineages or subspecies (Baker *et al.*, 1994; Wenink *et al.*, 1994, 1996; Buehler & Baker, 2005; Ottvall *et al.*, 2005; Rönkä *et al.*, 2008, 2012; Trimbos *et al.*, 2014; Barisas *et al.*, 2015; Leblanc *et al.*, 2017; Thies *et al.*, 2018). This pattern has often been attributed to the effects of the Pleistocene glacial cycles in their populations (e. g. Wenink *et al.*, 1994; Kraaijeveld & Nieboer, 2000; Buehler & Baker, 2005; Pruett & Winker, 2005; Trimbos *et al.*, 2014; Thies *et al.*, 2018), but the specific role of the areas of refugia in the allopatric differentiation of the subspecies has rarely been addressed. Some areas of refugia in the western Palearctic, east Siberia and Beringia have been proposed as the potential origin of differentiation for some of the subspecies of *Limosa limosa* (Trimbos *et al.*, 2014), *Charadrius hiaticula* (Thies *et al.*, 2018) or *Calidris canutus* (Buehler *et al.*, 2006), although without spatially-explicit analyses to support them. Previous works (e.g. Ploeger, 1968) manually linked each of the proposed ice-free areas with different populations or subspecies within each of the Arctic species of Anatidae (geese, ducks and swans). Ploeger (1968) also extended his analyses to some species of Arctic shorebirds, finding great similarities in the patterns between both groups, as expected by the approach used, but it is the first proposed hypothesis yet to be tested on this link between geography, climate and intraspecific diversification.

In this work, we wanted to assess the potential effects of both the Pleistocene glacial and interglacial cycles in shaping the distribution of Arctic species and their populations, and how they could have acted as a driver of the phenotypic and genetic variation observed today by generating allopatric distribution and colonization patterns. We consider four possible competing hypotheses to explain the current phenotypic and

genetic patterns observed in Arctic shorebirds: 1) the observed variation predates the Pleistocene, hence the Pleistocene glacial cycles did not have any effect on such variation (Klicka & Zink, 1997; Zink & Klicka, 2006). 2) The observed variation originated during the Pleistocene as a consequence of allopatric isolation but during the interglacial periods, as result of the wider geographic space available after the retreat of ice sheets (Milá *et al.*, 2006, 2007; Friis *et al.*, 2016). 3) The observed variation originated during the Pleistocene by allopatric separation of breeding population species' ranges during glacial periods, into different refugia. These isolated refugia populations suffered genetic drift with no gene flow between them, driving population differentiation (Rand, 1948; Weir & Schluter, 2004). The species without observed genetic or phenotypic differentiation did not suffer such degree of isolation. 4) The Pleistocene glacial cycles caused the observed variation as a combination of allopatric isolation during both glacial and interglacial periods.

Hence, there are two main factors to address the potential role of glacial cycles in the observed spatial pattern of geographic variation in Arctic species: the time of diversification, to confirm that it happened during the Pleistocene, and the past distribution changes during glacial and interglacial periods to determine the potential existence of refugia and their connectivity. From a geographic perspective, we can expect four different distribution pattern scenarios: A) continuous distribution range both during glacial and interglacial cycles; B) continuous range during glacial cycles but fragmented during interglacials (corresponding to hypothesis 2); C) opposite to B with fragmented ranges during glaciations and continuous during interglacials (hypothesis 3); and D) fragmented in both periods (hypothesis 4). In species with current genetic and phenotypic variation, we expect to recover a fragmented allopatric distribution during the last glacial maximum (LGM) and/or interglacial periods corresponding to extant subspecies or morphotypes (scenarios B, C, D), while monotypic species will show mainly non-fragmented distributions during both glacial and interglacial cycles (scenario A). We followed an integrative approach by combining current and hindcasted species' distribution models (SDMs), fossil evidence and the known phenotypic variation within the species, to assess which geographic distribution patterns were more common and compatible with any of the former spatial hypotheses.

Methods

Present species distributions

Current distribution maps for all Arctic species were obtained from BirdLife International and NatureServe (2011) datasets. We included in the analyses 69 out of 70 species of Arctic and subarctic shorebirds (Chester, 2016). Only *Calidris subminuta* was left out, as its breeding area of occupancy consists on a series of small patches across the Palearctic and was therefore impossible to accurately model it. Model performances were poor in predicting the wintering distribution of some species, as a consequence of being too geographically restricted (*Calidris falcinellus*, *Calidris maritima*, *Calidris pygmaea*, *Calidris virgata*, *Numenius tahitiensis*, *Tringa brevipes*) or being mainly pelagic (*Phalaropus fulicarius*), hence were not included as well.

As BirdLife maps likely over represent species' distributions by including areas with unsuitable habitats where species are known to be absent, we pruned them by filtering each species' distribution map by the habitats where they are known to occur leaving out the unsuitable ones following the same procedure as in Ponti *et al.* (2018). We built habitat maps combining information from layers of land cover from GLOBCOVER (Bontemps *et al.* 2011), water bodies from Global Land Cover Facility (Carroll *et al.,* 2009) and altitude from WorldClim 1.4 (Hijmans *et al.,* 2005) at a resolution of ca. 1km^2. Within those pruned distribution maps, we sampled 10,000 random points for every species in each season (breeding vs. non-breeding), data subsequently used as presences for modelling species distributions.

After checking GBIF and eBird datasets, we did not include them as they largely lack data across most of the Arctic, especially in northern Russia where there are not many observers and records, which resulted in a biased picture of the range of most species. Most of these data also correspond to Atlases without precise coordinates, and overlapped well with our distribution datasets in the areas where eBird data are available.

Predictive variables

We used current climate as a proxy for interglacial periods, and the climate of the last glacial maximum (LGM) as a proxy for glacial periods. As predictive variables for SDMs we used monthly precipitation and temperature (maximum, minimum and mean) as climatic variables. The climate layers for the present were retrieved from WorldClim 2.0 (Fick & Hijmans, 2017) at 2.5 min resolution (ca. 5x5km). The paleoclimatic maps corresponding to the MIROC-ESM simulations for the LGM were retrieved from WorldClim 1.4 (Hijmans *et al.*, 2005) at the same resolution, and the mean between minimum and maximum temperatures was calculated to generate a mean temperature layer. Despite that there are some paleodistribution habitat maps for the last glacial maximum based on climate, those are very coarse and need to be confirmed by further works. Hence, we decided to only include climatic variables as potential predictors for the species' models, as well as for the main breeding biome for Arctic breeding shorebirds: the tundra (see below).

Species distribution models

The use of hindcasted paleodistribution models has been a useful tool to reconstruct and explore the potential changes in the distribution of multiple species during the LGM (e. g. Fløjgaard *et al.*, 2009; Nogués-Bravo, 2009; Smith *et al.*, 2013; Zink & Gardner, 2017). To model the current breeding and non-breeding distribution of Arctic shorebirds we used an ensemble approach, applying four different methods: general linear model (GLM), polynomial GLM, general additive model (GAM) and BIOCLIM, with the use of the R packages dismo (Hijmans *et al.*, 2017) and mgcv (Wood & Wood, 2015). We also tested MaxEnt and DOMAIN algorithms but both showed poor performance with our data hence they were discarded. We also tested and discarded other options, such as support vector machines (SVM) and random forests (RF) due to the bad fit to the type of absences and/or the variables used.

For each species, we trained the models using 60% of the data, and evaluated them with the remaining 40%. For the seasonal climatic conditions, we decided not to include the climatic values for the whole year. Doing this could introduce noise in the analyses since the input would represent climatic conditions not experienced by the

species, as they are not present the whole year. This is especially critical in the breeding range, where the region is mostly frozen and uninhabitable outside of the breeding season. Instead, we employed the average values of temperature and precipitation of the months corresponding to their present breeding or wintering season, according to del Hoyo *et al.* (2018), excluding the months where they mainly migrate from breeding to wintering areas or vice versa. We then created an ensemble forecast by averaging the results of all four models into a single resulting model. This helped reducing the uncertainty and potential bias of individual models (Araújo *et al.*, 2005; Araújo and New, 2006). We then evaluated each model separately, as well as the ensemble, using both the Area Under the Curve ROC (AUC) and COR (correlation) approaches. The AUC value ranges from 0.5 to 1, where 1 indicates a perfect discrimination between presences and absences and 0.5 indicates a random discrimination. If the AUC is lower than 0.5, the discrimination is less likely than random (Elith *et al.*, 2006).

To project the breeding distributions into the LGM climate, we took into account potential phenological changes, since the current length and timing of the breeding seasons could be different from those during the LGM. To do so, we hindcasted each of our trained models to the conditions of each month between April and August separately. These months covered the entire breeding season of the Arctic and subarctic shorebirds (Melofte *et al.*, 2007; del Hoyo *et al.*, 2018). After projecting every trained model separately, we merged them obtaining an ensemble forecast for the predicted presence probability for each month, and this was translated into presence-absence maps (1/0). To do so, we converted into presence (1) all values above a certain probability threshold, calculated for each species as the point where the sensibility and the specificity of the model intersect (Liu *et al.*, 2005). Having predicted presences (1) and absences (0) for each month, we summed all months to obtain the number of months where the species could potentially be present in each grid cell. Finally, we discarded the areas where species were not predicted for at least two months, which represents the minimum duration of a successful breeding season (Meltofte *et al.*, 2007; del Hoyo *et al.*, 2018). This approach was followed for the breeding season both in the present and during the LGM.

This projection month by month was ineffective for the wintering season, since it has a longer duration and the average climatic values of the season do not translate well when taking into consideration separate months. In particular the precipitation is concentrated very unevenly across the wide ranges covered, with different regions receiving most of the precipitation in different periods across the season. Thus, we projected our models into a period that spanned from October to March, both in the present and the LGM, encompassing the main months composing the wintering season for all the studied species and avoiding to overlap with the migratory period (del Hoyo *et al.*, 2018). Again, we projected each of our trained monthly models into this wintering season separately, and then combined them into an ensemble forecast which was transformed into presence-absence by applying the probability threshold approach described above.

By combining the maps from all the analysed species, we obtained potential richness maps for both seasons (breeding and non-breeding) in the present and the LGM. This allowed us to compare and visualize the changes in their distributions during the last glacial maximum as a representative of glacial periods, and the present (1970 – 2000) as a representative of interglacials.

Comparison between spatial scenarios

We reviewed the results from the SDMs species by species to assign each into one of four spatial scenarios considered (A to D in the introduction), based on the changes in their breeding ranges between the present and the LGM. We considered a range as "fragmented" when a species displayed multiple areas of their distribution in different biogeographic regions (e.g. Beringia, north of Siberia, Europe, North America) without any predicted connection between them. In the species whose main distributions were located in the continent and had a small portion of their range in an island, this gap was not considered to represent a fragmented distribution. After assigning each species to a representative scenario, we compared the results between monotypic species and species with accepted variation (e.g. subspecies), to check for differences in the frequencies of each scenario.

Analysis of latitudinal data by biogeographic region

We extracted latitudinal values for the breeding and wintering ranges of each species, separately for the Palearctic and Nearctic regions and for the main three wintering biogeographic regions (Central and South America, Africa and the Mediterranean, and Australasia). In order to explore potential overlaps between breeding and wintering seasons through time, we calculated the mean latitude of the breeding and wintering ranges of each species in the present and the LGM. We performed Mann-Whitney-Wilcoxon paired tests to test the null hypothesis of no statistical differences between the mean latitudes in the present and the past for all the species in each region. However, in the breeding range, the mean latitude might not accurately represent the distribution of species that are spread across multiple refugia at different latitudes during the LGM and the difference with their current distribution. To better explore these differences, we took four main biogeographic regions within the breeding areas: Greenland and the Western Palearctic, the Eastern Palearctic, Beringia, and the rest of the Nearctic. In each of those areas, we sampled 3,000 random points from both present and past predicted distributions of each occurring species. We took the value of the latitude of each point and built a density plot to inspect where did the predicted distribution of the species was concentrated (from south to north) in each region at both the present and the LGM.

Fossil record

We revised the available shorebird fossil data for the Pleistocene, mainly focusing on the Arctic species, from the literature and two main global databases: the Paleobiology database (Peters & McClennen, 2016) (https://paleobiodb.org) and the fosFARbase (Böhme & Ilg, 2003) (http://www.wahre-staerke.com/). We gathered all the available data for the families Scolopacidae, Charadriidae and Haematopodidae during the Pleistocene, and then filtered them to keep only the records corresponding to the Arctic shorebird species. We overlapped the distribution of fossils with the main predicted breeding and wintering areas during the LGM, to check whether the fossils and the SDMs showed spatial congruence. Since the fossil record in the high Arctic for

these birds is practically non-existent, comparisons with the interglacial breeding distribution offered no information, therefore we compared it only with the predicted distributions during the glacial period.

Predicted extension of the tundra

Arctic shorebird species reproduce mainly in the Tundra biome. The Köppen – Geiger classification system (Köppen, 1900; Köppen & Geiger, 1936) is often used by ecologists and climatologists to estimate the location and extension of the main ecosystems in the planet based on the characteristics of temperature and/or precipitation that define them. Despite recent revisions of this classification (Guetter & Kutzbach, 1990; Peel *et al.*, 2007; Belda *et al.*, 2014), the Arctic is still defined as the area where the mean temperature of the warmest month does not exceed 10°C. Furthermore, when this value is below 0°C it is considered to be polar desert. Therefore, the Tundra is defined as the region where the mean temperature of the warmest month comprises between 0°C and 10°C. By applying this criterion to the paleoclimatic layers, we predicted the extension of the Tundra during the LGM to compare it with the main areas of refugia predicted by our SDMs. We also included in this comparison the maximum extension of the ice sheets according to Ehlers *et al.* (2011).

Results

Species' distribution models

We performed models on 69 Arctic shorebird species (69 breeding and 62 wintering distributions). 77.8% of the models (102 out of 131) returned AUC values above 0.8. Only 3 models had AUC values lower than 0.7, corresponding to the breeding season of *Actitis hypoleucos* (0.63), and the wintering seasons of *Tringa flavipes* (0.66) and *Calidris himantopus* (0.68). The detailed results for each species are compiled in the Appendix 1.

Shorebird predicted richness maps for the present suggest the co-occurrence of over 30 Arctic shorebird species in large areas of both their breeding and wintering ranges (Fig. 1). Most species are distributed between 60°N and 80°N latitude during the

breeding season (Fig.1 top panels, Appendix 1), in agreement with their current distribution maps. During the LGM, the predicted breeding distributions showed a southward displacement and an overall clear wide fragmentation exemplified by the areas with the highest richness values (> 20 species) acting as putative refugia. In the Nearctic, the areas with the highest species' richness corresponded to Beringia and the northern coast of Alaska at high latitudes (over 55° N). There were also some areas with high species' richness recovered further south (between 30° N and 40° N), mainly around the Rocky Mountains and the Appalachians. Arctic species occurred as far south as central Europe (between 30° N and 55° N) in the Western Palearctic. In the Eastern Palearctic the areas with the highest richness remained at higher latitudes (over 60° N) in two main areas: one in western and central Siberia, between the Ural and Altai mountains, and the other in eastern Siberia, Kamchatka and Beringia.

During the wintering season, current species richness (Fig. 1, bottom panels) concentrates around the tropical belt in Africa and Australasia, also extending across southern Asia (India and Indochina) and surrounding the Amazonian region in South America. Although richness is higher in tropical areas, the wintering ranges of many species reach as south as the southernmost parts of South America, Africa and Oceania (ca. 35-50° S) and north to the British Islands and northwest USA (ca. 50-55° N). During the LGM, the wintering ranges contracted on the southern and northern limits, with most species not extending beyond 35° N and 35° S. During these periods, species' richness increased around the Equator, especially in Asia and Oceania, where the global seal level drop greatly increased the available land surface at those latitudes. Despite all these changes, the overall distribution of the wintering ranges during the LGM shows great overlap with their current wintering distributions.

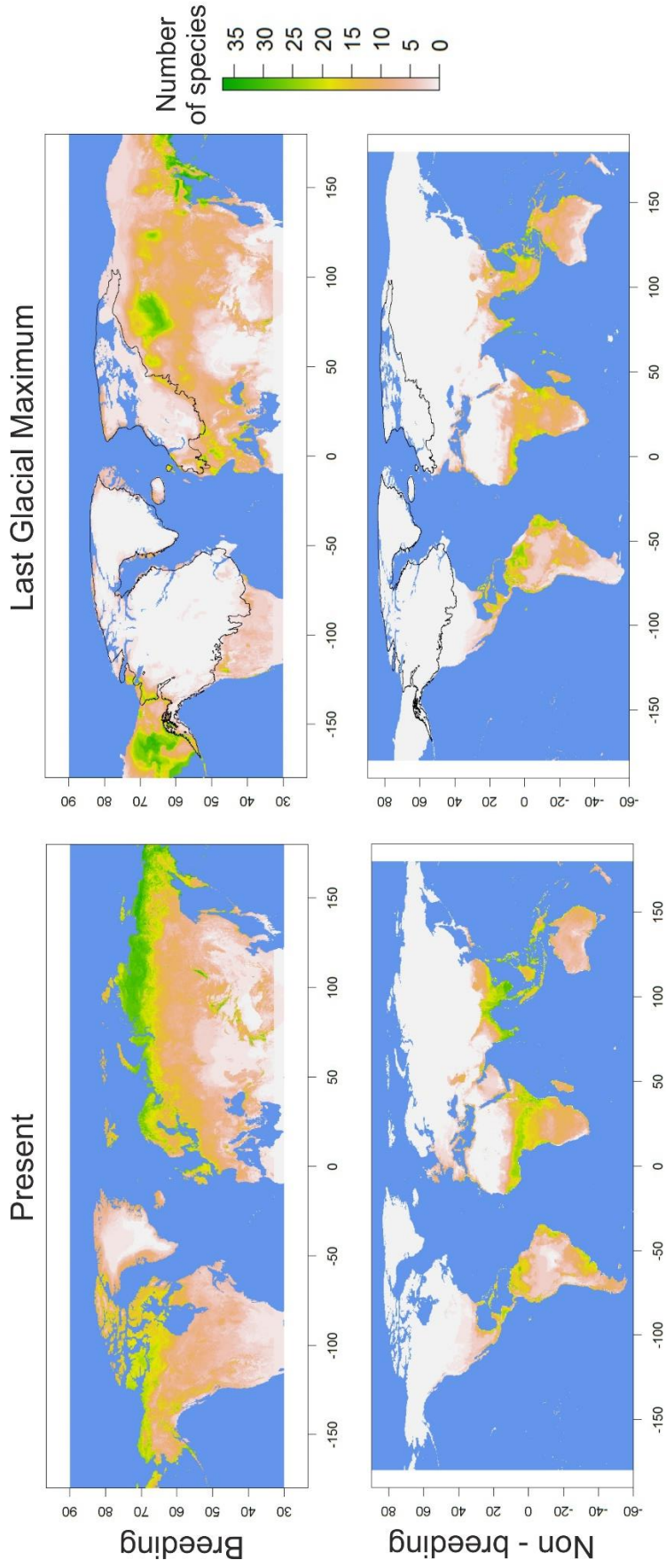

Figure 1: Potential distribution maps of Arctic shorebird species' richness in the present (left) and the LGM (right), for the breeding (top) and wintering (bottom) seasons of the studied species (69 breeding, 64 wintering). The black line represents the maximum extension of the ice during the LGM, simplified from Ehlers *et al.* (2011).

Comparison between spatial scenarios

The analysis of the distribution patterns in the present and LGM show that most of the monotypic species (>65%) did not experience large breeding range fragmentations in either period, with a continuous distribution during the LGM and the present (Fig. 2, scenario A). In contrast, the scenarios of fragmentation during the glacial period (C and D) were less frequent (30%) for these monotypic species, and in most of these cases (21% of all monotypic species) the fragmentation disappeared after the glacial period (scenario C). Only one of these species without variation, *T. brevipes*, experienced its breeding range fragmentation in the present from a single breeding area in the LGM.

On the contrary, most of the species with recognised phenotypic and/or genetic variation (>80%) showed range fragmentation during the LGM and/or the present into multiple isolated areas (scenarios C and D). In 36% of the cases (8 species), the fragmentation remained during the current interglacial (scenario D). In total, only 32% (7 species) showed no clear potential fragmentation during the glacial period (scenarios A and B), and from those the 14% (3 species) experienced range fragmentation in the current interglacial (scenario B).

The species assigned to each scenario, with or without subspecies, can be found in the Appendix 2 (Table S1)

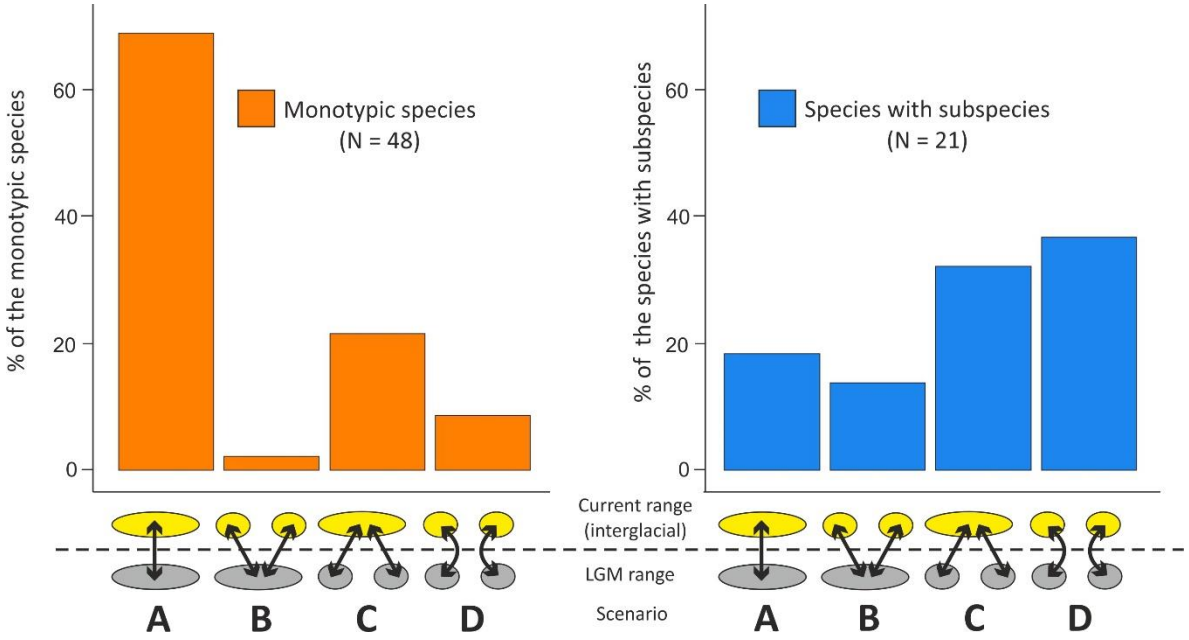

Figure 2: Percentage of the monotypic species (orange) and species with subspecies (blue) that display each general spatial scenario of continuous or fragmented breeding distribution during the LGM (grey circles) and the current interglacial (yellow circles). The scenarios represent A) single area of refugium in the LGM and continuous current range, B) single area of refugium during LGM but fragmented range in the present, C) multiple areas of refugia during the LGM but continuous range in the present, and D) multiple areas of refugia during the LGM and fragmented range in the present.

Analysis of latitudinal data by region

The comparative analysis of the mean latitude of species' ranges within and between the present and the LGM is shown in Figure 3. There is no overlap between breeding and wintering mean ranges during the LGM in any of the regions. The Mann-Whitney-Wilcoxon paired tests (V) returned statistical differences in the mean latitude between the predicted present and past species' ranges for the breeding season in the Palearctic ($V = 823$, $p < 0.0001$) and the Nearctic ($V = 609$, $p < 0.0001$). For the wintering season, the statistical test returned differences between the present and the LGM in the Afrotropic ($V = 586$, $p < 0.0001$) and Australasian regions ($V = 647$, $p < 0.0001$). However, no statistically significant differences were detected for the Neotropic mean ranges ($V = 162$, $p = 0.15$).

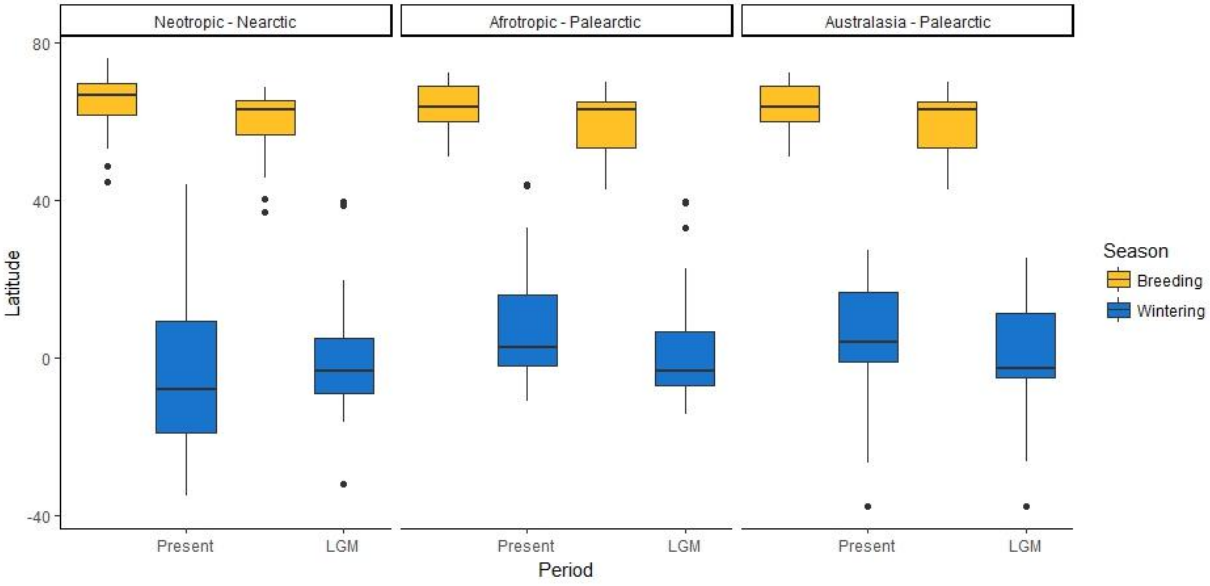

Figure 3: Boxplots representing the distribution of the predicted mean latitudes of the breeding and wintering distributions for the studied species (69) in the present and LGM in the main biogeographic regions.

The histogram representing the cumulated density of the latitudinal distribution of the predicted ranges shows different patterns in each biogeographic region (Fig. 4). In the Western Palearctic, most of the current predicted species' ranges occur between 55° N and 70° N, with also a small peak at ca. 80° N from the species in Svalbard and Greenland. During the LGM, the density of the distribution shifted southwards, with most of the ranges spanning between 40° N and 55° N, and also around 65° N. In the Nearctic the main distribution of the predicted ranges shifted from 60°-75° N in the present to 35°-50° N during the LGM. The Eastern Palearctic showed a much smaller shift of the distribution of the ranges, with the peak changing from 70° N in the present to 65°N during the LGM. In Beringia, the latitude of the ranges during the LGM and in the present overlap, both between 50° N and 75° N.

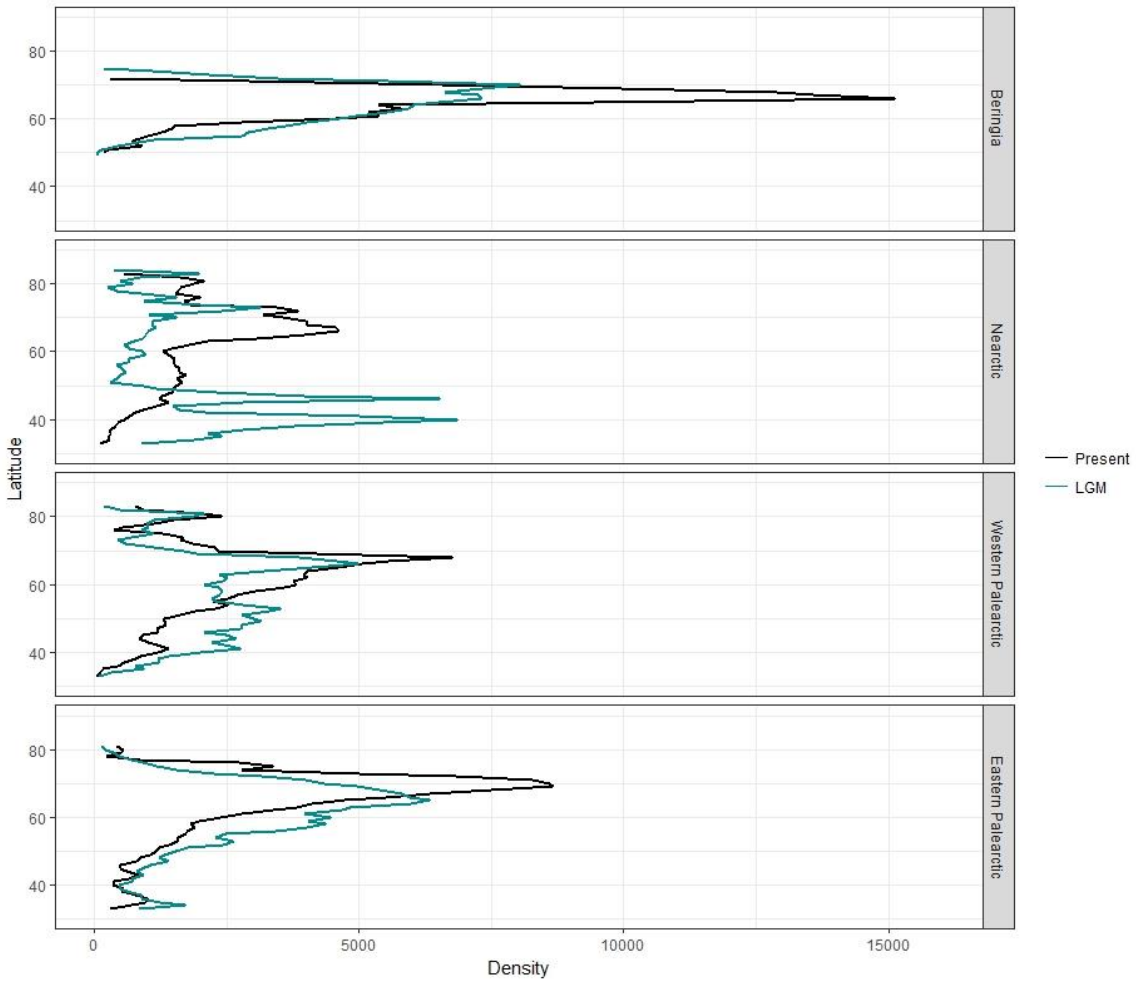

Figure 4: Histograms representing the density of the predicted breeding presence of 69 Arctic shorebird species in the latitudinal gradient (Y axis) separated in each of the regions considered. Lines represent the distribution of the shorebirds in the present (black) and the LGM (light blue).

Fossil record

Although the bird fossil record during the Pleistocene is uneven, the wetlands inhabited by shorebirds provided good conditions for the formation of fossils. After retrieving and filtering the available data from the existing databases, we gathered 191 records covering 53 of the 69 studied species, from 60 localities around the planet. These localities are all located between 52° N and 8° S, except for the Dyuktai Cave in Russia (59.3° N), and Blanche and Victoria caves in Australia (both at 37° S). Most of the localities are in Europe (n = 16, 27%) and North America (n = 30, 50%). On the other hand, there are very few localities in Oceania (n = 2), South America (n = 3) Africa (n = 3) and Asia (n = 4) for these species, and there are no records in the whole Arctic region. The table with all fossilized species present in each locality and the source can be found in the Appendix 2 (Table S2)

Predicted extension of the tundra

The model on the extension of the tundra during the LGM based on the Köppen – Geiger classification system is shown in figure 5 (below). The model suggests a continuous Tundra distribution across the Palearctic, between 50° N and 75° N in Asia and near the southern margin of the ice in Europe between 45° N and 55-60° N. In the Nearctic, the tundra also extended from coast to coast near the limit of the ice extension, as a narrow belt between 40°N and 50°N. It likely connected with Beringia through a narrow corridor along the northwest coast of North America. In some regions, the predicted tundra slightly overlapped the area of the maximum ice extension, particularly in Europe, North America, Iceland and east Beringia.

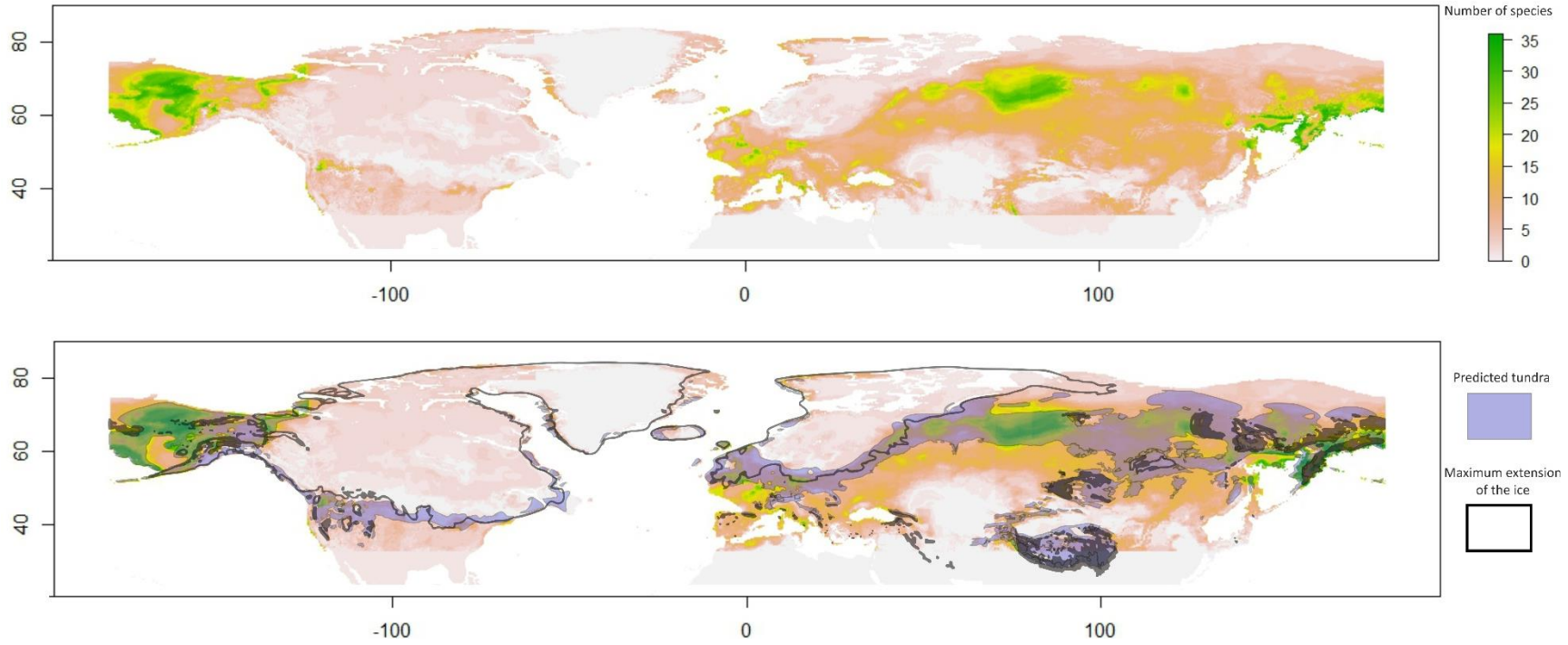

Figure 5: Above, the species richness in the breeding range during the LGM. Below, the same map overlapped to the predicted extension of the tundra according to the Köppen-Geiger classification and the maximum extension of the ice coverage during the LGM (Ehlers *et al.*, 2011).

Discussion

Several works over the past few decades have highlighted the role of Pleistocene glacial cycles in the emergence of the current diversity patterns within many bird species (see Lovette, 2005). However, the explicit mechanisms of the glacial and interglacial periods in shaping their distribution and intraspecific variation remain largely unstudied. Our results support that Pleistocene climatic cycles drove the diversification of Arctic shorebirds by creating allopatric breeding distributions during glacial, interglacial or both periods.

The majority of species with described morphological and/or genetic variation (65%) presented fragmentation of their ranges during the LGM (Fig. 2, geographic scenarios C and D and hypotheses 3 and 4), where most of their hindcasted distribution areas parallel the described subspecific variation. These scenarios include species with clear genetic differentiation between their subspecies, like *Calidris alpina* (Marthinsen *et al.*, 2007), *C. hiaticula* (Thies *et al.*, 2018) and *Limosa limosa* (Trimbos *et al.*, 2014). Some species with subspecies display a continuous distribution today (scenario C), likely the result of secondary contact after population and range expansions during the current interglacial. In these species, gene flow after secondary contact likely has been limited, while in monotypic species showing a scenario C distribution pattern, the lack of genetic and phenotypic differentiation could be the result of incomplete lineage sorting with populations not having enough time to differentiate, and/or intense gene flow after secondary contact that admixed populations. Moreover, range fragmentation during interglacials not necessarily implied isolation between near populations, as some species of Arctic shorebirds like *Calidris melanotos* are known to travel across their breeding range in order to mate with multiple partners at different locations (Kempenaers & Valcu, 2017), which reduces potential opportunites of genetic diversification between populations (D'Urban Jackson *et al.*, 2017).

The lack of range fragmentation during glacial periods seems to work strongly against intraspecific diversification, as this is by far the most common scenario found in monotypic species (>65%). On the contrary, only three species with subspecies belong

to this scenario, all of them with multiple subspecies and with a more temperate breeding distribution ranges. Those include *Charadrius vociferus* with subspecies in the Caribbean Islands and Peru, and *Tringa totanus* and *Numenius arquata* in the Tibetan Plateau. Both *T. totanus* and *N. arquata* show similar distribution patterns, where their European breeding populations reach the Arctic, while those in Asia remain further south in boreal regions. Some monotypic species with fragmented ranges like *Pluvialis fulva* and *Phalaropus lobatus* show differential phenology between populations (Jukema *et al.*, 2015; van Bemmelen *et al.*, 2019) and it is likely that subspecies will be recognized in the future (Jukema *et al.*, 2015), which will fit with the fragmentation scenarios as drivers of variation.

Our results suggest a correlation between the diversification of Arctic subspecies and LGM range fragmentation, with the result on four-five main refugia where species richness likely peaked: Beringia extending to Japan and the Korean Peninsula, central North America, Western Europe and central Russia between the Ural and Altai Mountains. This is in agreement with the ideas of Ploeger (1968) for Arctic Anatidae species, supporting the hypothesis of allopatric differentiation during glacial periods as the main driver of diversification in Arctic birds during the Pleistocene (Rand 1946, Weir & Schlutter 2004).

Range fragmentation during interglacials also likely contributed to the diversification of some species. We recovered three species with subspecies classified under the scenario B: *Charadrius melodus*, *Calidris ptilocnemis* and *C. canutus*. All three species have shown very little genetic variation between and often unclear distinction between lineages in previous studies (Buehler & Baker, 2005; Miller *et al.*, 2010; Pruett & Winker, 2005). This role of post-glacial expansion in the diversification of bird species has been proposed for other groups (Milá *et al.*, 2000, 2006, 2007; Friis *et al.*, 2016). Nearly 40% of the species with subspecies belong to the geographic scenario D, where both fragmentation during glacial and interglacial periods are recovered, and more than 80% of the species show a fragmented distribution in one or two periods, hence wide range fragmentation seems the mechanism although the potential quantitative effect of one period versus the other cannot be assessed. There is also another aspect that needs to be acknowledged which is that scenarios A to D may have changed through

time in species. Although we cannot discard this possibility, the recovered distribution patterns by our models are in agreement with the observed phenotypic and geographic variation found in most species, and this correlation should have been strong enough (likely repeated through Pleistocene climatic cycles) for this variation to be generated and persist.

Despite the changes in the climate during the LGM, large areas of steppes and tundra were available across the northern hemisphere and likely sustained populations of shorebirds and other Arctic birds, as they did with mammals (Dyke, 2005; Kienast *et al.* 2005; Willerslev *et al.*, 2014). The coastal areas at the northernmost part of the continents would have become uninhabitable for most species. Many species have their current breeding ranges restricted to those areas, but the species breeding at the highest latitudes tend to adapt their diet to tundra invertebrates during the breeding period, exploiting marine and coastal habitats only during the non-breeding season (Piersma, 2003, 2007). We can therefore expect that most or all of those "northernmost" species were also displaced to southern areas of tundra, far from the coast, during the glacial period. Our predictions on the extension and location of the tundra during the LGM, based on the Koppen – Geiger classification system (Köppen, 1900; Köppen & Geiger, 1936) are congruent with the results from previous studies using this approach (Guetter & Kutzbach, 1990; Willmes *et al.*, 2017), as well as with other predictions on the extension of the tundra and steppes (Edwards *et al.*, 2000; Harrison *et al.*, 2001; Ray & Adams, 2001; Dyke, 2005; Allen *et al.*, 2010). The distribution of the tundra during glacial periods parallels well the overall distribution of Arctic shorebirds predicted by our SDMs and covers all the areas we recovered with the highest values of species richness. Both our predictions for the tundra and the results from the SDMs also suggest that potential suitable areas could have been available beyond what it is considered the maximum extension of the glacial ice sheets in regions like central North America, western Europe and Iceland during the LGM. This could indicate potential areas of northern refugia for these birds (Stewart & Lister, 2001; Provan & Bennett, 2008), at least for a brief period of time during the summer season.

Even if suitable tundra habitats were available across the Holarctic, our results suggest that different biogeographic regions experienced different degrees of change in their climate and habitat during the LGM, which resulted in different distribution

patterns during glacial periods and posterior interglacials in each region. For instance, Beringia remained mostly ice-free and climatically stable over glacial cycles, acting as a large high-latitude refugium (Hultén 1937, Pielou 1991) and playing a key role in the diversification and post-glacial recolonization of the Arctic by plants (Abbott & Brochmann, 2003; Eidesen *et al.*, 2013), mammals (Hope *et al.*, 2013), and insects (Elias *et al.*, 2000; Kleckova *et al.*, 2015). This land connection also allowed the colonization of Palearctic fauna into the Nearctic (Davison *et al.*, 2011; Kleckova *et al.*, 2015; Koblmüller *et al.*, 2016). During interglacials, sea level rise resulted in a barrier between the Nearctic and the Palearctic for land species, and also in the isolation of populations in the Bering Sea's islands. This seems to have originated multiple local subspecies within sedentary species like *Lagopus muta* (Holder *et al.*, 2004), but also migratory species like the Arctic shorebird *C. ptilocnemis* (Pruett & Winker, 2005).

While most Arctic shorebird species in North America retreated to Beringia, some species occurred at lower latitudes, in the available territories south of the limit of the ice sheet (below 40°N) within the North American continent. This area harboured steppes and tundra (Dyke & Gulas, 2002), from which multiple Arctic and boreal species expanded to their current ranges following the retreat of the ice (e.g. Macpherson, 1965; Kurose *et al.*, 2005; Milá *et al.*, 2007; Dupuis & Sperling, 2015). The observed pattern in the Neartic is very different from the other biogeographic regions (Fig. 4), while in Beringia and the Eastern Palearctic there is a wide overlap between LGM and interglacial frequency distributions, and in the Western Palearctic there is certain overlap, in the Nearctic there is a clear gap between the peaks of the present and past, which likely had consequences on species' phenotypic and genetic variation. These different patterns suggest that the impact of Pleistocene glacial cycles on species' distributions and their potential diversification has to be studied by biogeographic region, and that it should not be extrapolated between regions as the intensity and impact of the climate effects were likely very different.

The available territories in both central North America and Beringia favoured that populations of Arctic species became isolated between those regions, which in many cases led to the distinct lineages across their current ranges in the Arctic (Macpherson, 1965; Ploeger, 1968; Sipe & Browne, 2004 Jones *et al.*, 2005). We also recovered this pattern in species like *Limnodromus griseus* and *Tringa solitaria*. A third species, *Actitis*

macularius, follows a similar pattern, but its subspecies have not been formally recognized yet.

In the Palearctic, the extension of the tundra provided multiple areas of refugia for Arctic species from East to West across the continent, with three areas of great importance: Europe, central Asia and Beringia. In Europe, where the ice sheets reached as far south as 50°N the southern peninsulas served as refugia for temperate species (e.g. Bennett & Provan, 2008; Hewitt, 2004). Arctic species, on the other hand, would have persisted in more northern refugia near the margins of the ice extension, from the British Islands to central Europe and the Baltic region, as well as in mountain ranges (Hewitt, 2004; Provan & Bennett, 2008; J. R. Stewart *et al.*, 2010). In comparison, due to the lower ice cover, the species in Asia remained at higher latitudes, between 60°N and 75°N, extending from the Urals to the Altai Mountains in central Siberia (Skrede *et al.*, 2006; Todisco *et al.*, 2012; Eidesen *et al.*, 2013; Kleckova *et al.*, 2015), as well as in east Siberia and Beringia. This array of available refugia also involved multiple routes of recolonization during interglacials, especially in Europe, where the northern latitudes were recolonized by populations from the south (Hewitt, 1999) as well as from Asia (Jaarola *et al.*, 1999; Rueness *et al.*, 2014). This pattern was also found in some genetic lineages within Arctic shorebirds' species like *C. hiaticula* (Thies *et al.*, 2018), *C. alpina (*Marthinsen *et al.*, 2007) and *T. totanus* (Ottvall *et al.*, 2005). The combination of multiple refugia with the recolonization routes likely favoured a greater diversification of the populations within species, resulting in multiple subspecies of Arctic shorebirds distributed along an East-West axis (Buehler & Baker, 2005; Marthinsen *et al.*, 2008; Trimbos *et al.*, 2014), similar to what is found for other Arctic species in the region (e.g. Jaarola & Searle, 2002; Kohli *et al.*, 2015; Horreo *et al.*, 2018).

In the western Palearctic, many subspecies are distributed in islands such as Iceland, Faeroes and Svalbard. All these islands remained isolated from the main areas of refugia in southern Europe during the LGM, either by sea or by ice sheets. Nevertheless, these territories were almost completely covered by ice during the last glacial maximum, and the availability of refugia is a subject of debate. For instance, it was generally considered that ice covered virtually all the land surface of Iceland during the LGM, rendering it uninhabitable until the end of the glacial period, when recolonization took place. This is usually called the *tabula rasa* hypothesis (see

Gabrielsen *et al.*, 2007). But some studies suggest a potential survival of some plants and animals in ice-free refugia and nunataks during the LGM (Ploeger, 1968; Rundgren & Ingolfsson, 1999), and it has been hypothesized the presence of breeding populations of migratory geese species during that period (Ploeger, 1968; Pujolar *et al.*, 2017). However, recent phylogeographic studies on Arctic shorebirds opt for the hypothesis of post-glacial colonization and rapid diversification of the subspecies of *L. l. islandica* (Trimbos *et al.*, 2014) and *C. h. psammodromus* (Thies *et al.*, 2018), as suggested for other local species of plants and animals (e.g. Gabrielsen *et al.*, 2007, Bolotov *et al.*, 2017).

Our results support the hypothesis that some species could have kept suitable breeding grounds over the summer in reduced coastal areas of Iceland, Faeroes, Svalbard and Greenland during the LGM. On the other hand, most of the subspecies in these islands are also present in the continent and/or the British Islands, and only two are completely endemic of one or more of those islands (*G. g. faeroensis* and *L. l. islandica*). Therefore, we are unable to fully resolve whether these subspecies recolonized the islands from the continent after the LGM and quickly diversified, or if on the contrary, they managed to sustain isolated breeding populations that expanded from glacial refugia, hence further studies are needed to confirm this hypothesis. In this aspect, the search for fossil data of breeding bird communities across the Arctic and especially in the North Atlantic Islands (Iceland, Faeroes, Greenland, Svalbard) should be of paramount importance to shed light on this topic.

The available fossil record of the studied species showed great congruence with the breeding and wintering ranges predicted by our SDMs during the LGM. The use of the fossil record provides an independent and alternative line of evidence to evaluate and complement the predictions on species ranges when using SDMs (Gavin *et al.*, 2014). Although classification of the fossil record as belonging to either breeding or wintering seasons is somewhat tentative, the rich fossil record of shorebirds found in Olduvai Gorge in Tanzania (Prassack, 2010, 2014; Prassack *et al.*, 2018) provides valuable information on this topic. In this locality, the fossils assigned to Scolopacidae species, mainly *Calidris sp.*, were examined for the presence or absence of medullary bone, a bone structure present only in birds during reproduction (Matthiesen, 1990a). While

fossils of birds from other clades showed presence of medullary bone, this was absent in all the samples from *Calidris*, which combined with a lack of fossils of juvenile specimens from this group indicate that they were not breeding, hence supporting that migration happened during the Pleistocene. Considering the presence of other shorebird species in Pleistocene fossil deposits across the southern hemisphere (e.g. Churcher & Smith, 1972; Campbell, 1976, 1979; Matthiesen 1990b; Meijer *et al.*, 2013; Val, 2016), the confirmation from Olduvai that they were not breeding, and the predicted southern non-breeding distributions of our models, all support as the simplest and most likely hypothesis that migration did not stop during glacial periods.

There is no clear evidence about when and how the so-called bird flyways were originated. The fragmentation and isolation of populations during glacial periods could have been reinforced by the differential use of flyways by these species (Buehler *et al.*, 2006; Piersma, 2011). During interglacial periods, populations separated in different flyways could result not only in different recolonization routes (Buehler *et al.*, 2006; Ruegg *et al.*, 2006), but also mismatches in aspects such as stopover times, arrival dates at breeding grounds and mating (Piersma, 2011), reinforcing the gap between populations or subspecies even when they overlap in their breeding or wintering territories (Wennerberg, 2001; Boulet *et al.*, 2006). This potential role of the migratory flyways in the intraspecific diversification (or lack of it) and phylogeographic histories of long-distance migratory bird species needs to be assessed in future studies.

In conclusion, our results show that the fragmentation of the breeding ranges determined and promoted the intraspecific diversification of the Arctic shorebirds during the glacial cycles of the Pleistocene. Despite severe changes in their ranges, their migratory behaviour remained largely unaltered, and likely contributed maintain the isolation between populations and their differentiation. Our study reveals the importance of the different processes involved in this diversification, and also the differences between the different regions of the Arctic. Overall, our work provides a spatial-explicit scenario for the diversification of Arctic shorebirds during the Pleistocene, which presumably reflects the evolution of other Arctic taxa, especially birds.

References

Abbott, R. J., & Brochmann, C. (2003). History and evolution of molecular the arctic flora: in the footsteps of Eric Hultén. *Molecular Ecology*, *12*, 299–313.

Allen, J. R. M., Hickler, T., Singarayer, J. S., Sykes, M. T., Valdes, P. J., & Huntley, B. (2010). Last glacial vegetation of Northern Eurasia. Quaternary Science Reviews, 29(19–20), 2604–2618.

Alley, R. B. (2000). Ice-core evidence of abrupt climate changes. *Proceedings of the National Academy of Sciences*, *97*(4), 1331–1334.

Araújo, M. B., & New, M. (2006). Ensemble forecasting of species distributions. *Trends in Ecology and Evolution, 22*(1), 42–47.

Araújo, M. B., Whittaker, R. J., Ladle, R. J., & Erhard, M. (2005). Reducing uncertainty in projections of extinction risk from climate change. Global Ecology and Biogeography, 14, 529–538.

Avise, J. C., Walker, D., & Johns, G. C. (1998). Speciation duration and Pleistocene effects on vertebrate phylogeny. *Proceeding of the Royal Society of London Series B*, *265*(June), 1707–1712.

Avise, J., & Walker, D. (1998). Pleistocene phlogeographic effects on avian populations and the speciation process. *Proceedings of the Royal Society B: Biological Sciences*, *265*(October 1997), 457–463.

Baker, A. J., Piersma, T., & Rosenmeier, L. (1994). Unraveling the intraspecific phylogeography of Knots *Calidris canutus*: a progress report on the search for genetic markers. *Journal of Ornithology*, *135*(4), 599–608.

Barisas, D. A. G., Amouret, J., Hallgrímsson, G. T., Summers, R. W., & Pálsson, S. (2015). A review of the subspecies status of the Icelandic Purple Sandpiper *Calidris maritima littoralis*. *Zoological Journal of the Linnean Society*, *175*(1), 211–221.

Belda, M., Holtanová, E., Halenka, T., & Kalvová, J. (2014). Climate classification revisited: From Köppen to Trewartha. *Climate Research*, *59*(1), 1–13.

Bennett, K. D., & Provan, J. (2008). What do we mean by “refugia”? *Quaternary Science Reviews*, *27*(27–28), 2449–2455.

BirdLife International and NatureServe. (2011). Bird species distribution maps of the world. BirdLife International, Cambridge, UK and NatureServe, Arlington, USAgton, USA.

Bolotov, I. N., Aksenova, O. V., Bespalaya, Y. V., Gofarov, M. Y., Kondakov, A. V., Paltser, I. S., … Vinarski, M. V. (2017). Origin of a divergent mtDNA lineage of a freshwater snail species, *Radix balthica*, in Iceland: cryptic glacial refugia or a postglacial founder event? *Hydrobiologia*, *787*(1), 73–98.

Böhme, M.& Ilg, A. (2003). fosFARbase, www.wahre-staerke.com/

Boulet, M., Norris, D. R., & Boulet, M. (2006). Introduction: the Past and Present of Migratory Connectivity. *Ornithological Monographs*, (61), 1–13.

Bontemps, S., Defourny, P., Van Bogaert, E., Kalogirou, V., & Arino, O. (2011). GLOBCOVER 2009: Products Description and Validation Report.

Buehler, D. M., & Baker, A. J. (2005). Population divergence times and historical demography in Red Knots and Dunlins. *Condor*, *107*, 497–513.

Buehler, D. M., Baker, A. J., & Piersma, T. (2006). Reconstructing palaeoflyways of the late Pleistocene and early Holocene red knot (*Calidris canutus*). *Ardea*, *94*(3), 485–498.

Carroll, M. L., Townshend, J. R., DiMiceli, C. M., Noojipady, P., & Sohlberg, R. A. (2009). A new global raster water mask at 250 m resolution. *International Journal of Digital Earth, 2*(4), 291–308.

Chester, S. (2016). *The Arctic Guide: Wildlife of the Far North*. Princeton University Press.

Churcher, C. S., & Smith, P. E. L. (1972). Kom Ombo: Preliminary Report on the Fauna of Late Paleolithic Sites in Upper Egypt. *Science, 177*, 259–261.

Cicero, C., & Johnson, N. K. (2006). The tempo of Avian diversification: Reply. *Evolution*, *60*(2), 413.

Cohen, K. M., & Gibbard, P. L. (2008). Global chronostratigraphical correlation table for the last 2.7 million years. *Episodes*, *31*(2), 243–247.

D'Urban Jackson, J., dos Remedios, N., Maher, K. H., Zefania, S., Haig, S., Oyler-McCance, S., … Küpper, C. (2017). Polygamy slows down population divergence in shorebirds. *Evolution*, *71*(5), 1313–1326.

del Hoyo, J., Elliott, A., Sargatal, J., Christie, D.A. & Kirwan, G. (eds.) (2018). *Handbook of the Birds of the World*. Lynx Edicions, Barcelona.

Davison, J., Ho, S. Y. W., Bray, S. C., Korsten, M., Tammeleht, E., Hindrikson, M., … Saarma, U. (2011). Late-Quaternary biogeographic scenarios for the brown bear (*Ursus arctos*), a wild mammal model species. *Quaternary Science Reviews*, *30*(3–4), 418–430.

Dupuis, J. R., & Sperling, F. A. H. (2015). Repeated reticulate evolution in North American *Papilio machaon* group swallowtail butterflies. *PLoS ONE*, *10*(10), 1–26.

Dyke, A. S. (2005). Late Quaternary Vegetation History of Northern North America Based on Pollen, Macrofossil, and Faunal Remains. *Géographie Physique et Quaternaire*, *59*(2–3), 211.

Dyke, G. J., & Gulas, B. (2002). The Fossil Galliform Bird *Paraortygoides* from the Lower Eocene of the United Kingdom. *American Museum Novitates*, *3360*(1), 1–14.

Edwards, M. E., Anderson, P. M., Brubaker, L. B., Ager, T. A., Andreev, A. A., Cwynar, L. C., … Yu, G. (2000). Pollen-based biomes for Beringia. *Journal of Biogeography*, *27*(3), 521–554.

Edwards, S., & Bensch, S. (2009). Looking forwards or looking backwards in avian phylogeography? A comment on Zink and Barrowclough 2008. *Molecular Ecology*, *18*(14), 2930–2933.

Eidesen, P. B., Ehrich, D., Bakkestuen, V., Alsos, I. G., Gilg, O., Taberlet, P., & Brochmann, C. (2013). Genetic roadmap of the Arctic: Plant dispersal highways, traffic barriers and

capitals of diversity. *New Phytologist*, *200*(3), 898–910.

Elias, S. A., Berman, D., & Alfimov, A. (2000). Late pleistocene beetle faunas of beringia: Where east met west. *Journal of Biogeography*, *27*(6), 1349–1363.

Elith, J., H. Graham, C., P. Anderson, R., Dudík, M., Ferrier, S., Guisan, A., … E. Zimmermann, N. (2006). Novel methods improve prediction of species' distributions from occurrence data. *Ecography, 29*(2), 129–151.

Ehlers, J., Gibbard, P. L., & Hughes, P. D. (Eds.). (2011). *Quaternary glaciations-extent and chronology: a closer look* (Vol. 15). Elsevier.

Engelmoer, M., & Roselaar, C. S. (1998). *Geographical variation in waders*. Springer Science & Business Media.

Fick, S. E., & Hijmans, R. J. (2017). WorldClim 2: new 1-km spatial resolution climate surfaces for global land areas. *International Journal of Climatology, 37*(12), 4302–4315.

Fløjgaard, C., Normand, S., Skov, F., & Svenning, J. C. (2009). Ice age distributions of European small mammals: Insights from species distribution modelling. *Journal of Biogeography, 36*(6), 1152–1163.

Friis, G., Aleixandre, P., Rodríguez-Estrella, R., Navarro-Sigüenza, A. G., & Milá, B. (2016). Rapid postglacial diversification and long-term stasis within the songbird genus *Junco*: phylogeographic and phylogenomic evidence. *Molecular Ecology*, *25*(24), 6175–6195.

Gabrielsen, T. M., Landvik, J. Y., Nordal, I., Elven, R., & Brochmann, C. (2007). Glacial Survival or tabula rasa? The History of North Atlantic Biota Revisited. *Taxon*, 52(3), 417.

Gavin, D. G., Fitzpatrick, M. C., Gugger, P. F., Heath, K. D., Rodrıguez-Sanchez, F., Dobrowski, S. Z., … Williams, J. W. (2014). Climate refugia: joint inference from fossil records, species distribution models and phylogeography. *New Phytologist*, *204*, 37–54.

Guetter, P. J., & Kutzbach, J. E. (1990). A modified Köppen classification applied to model simulations of glacial and interglacial climates. *Climatic Change*, *16*, 193–215.

Haring, E., Gamauf, A., & Kryukov, A. (2007). Phylogeographic patterns in widespread corvid birds. *Molecular Phylogenetics and Evolution*, *45*(3), 840–862.

Harrison, S. P., Yu, G., Takahara, H., & Prentice, I. C. (2001). Palaeovegetation: Diversity of temperate plants in east Asia. *Nature*, *413*(September), 129–130.

Hewitt, G. M. (1999). Post-glacial re-colonization of European biota. *Biological Journal of the Linnean Society*, *68*(1–2), 87–112.

Hewitt, G. M. (2000). The genetic legacy of the quaternary ice ages. *Nature*, *405*(6789), 907–913.

Hewitt, G. M. (2004). Genetic consequences of climatic oscillations in the Quaternary. *Philosophical Transactions of the Royal Society B: Biological Sciences*, *359*, 183–195.

Hijmans, A. R. J., Phillips, S., Leathwick, J., Elith, J., & Hijmans, M. R. J. (2017). Package 'dismo'

Hijmans, R. J., Cameron, S. E., Parra, J. L., Jones, P. G., & Jarvis, A. (2005). Very high resolution interpolated climate surfaces for global land areas. *International Journal of Climatology,*

25(15), 1965–1978.

Holder, K., Montgomerie, R., & Friesen, V. L. (2004). Genetic diversity and management of Nearctic rock ptarmigan (*Lagopus mutus*). *Canadian Journal of Zoology*, *82*(4), 564–575.

Hope, A. G., Takebayashi, N., Galbreath, K. E., Talbot, S. L., & Cook, J. A. (2013). Temporal , spatial and ecological dynamics of speciation among amphi-Beringian small mammals. *Journal of Biogeography*, *40*, 415–429.

Horreo, J. L., Pelaez, M. L., Suárez, T., Breedveld, M. C., Heulin, B., Surget-Groba, Y., … Fitze, P. S. (2018). Phylogeography, evolutionary history and effects of glaciations in a species (*Zootoca vivipara*) inhabiting multiple biogeographic regions. *Journal of Biogeography*, *45*(7), 1616–1627.

Hulten, E. (1937). *Outline of the history of arctic and boreal biota during the quaternary period*. Bokforlags Aktiebolaget Thule. Stockholm

Jaarola, M., & Searle, J. B. (2002). Phylogeography of field voles (*Microtus agrestis*) in Eurasia inferred from mitochondrial DNA sequences. *Molecular Ecology*, *11*, 2613–2621.

Jaarola, M., Tegelström, H., & Fredga, K. (1999). Colonization history in Fennoscandian rodents. *Biological Journal of the Linnean Society*, *68*(1–2), 113–127.

Johnson, N. K., & Cicero, C. (2004). New mitochondrial DNA data affirm the importance of Pleistocene speciation in North American birds. *Evolution*, *58*(5), 1122–1130.

Jones, K. L., Krapu, G. L., Brandt, D. A., & Ashley, M. V. (2005). Population genetic structure in migratory sandhill cranes and the role of Pleistocene glaciations. *Molecular Ecology*, *14*(9), 2645–2657.

Kempenaers, B., & Valcu, M. (2017). Breeding site sampling across the Arctic by individual males of a polygynous shorebird. *Nature*, *541*(7638), 528–531.

Kleckova, I., Cesanek, M., Fric, Z., & Pellissier, L. (2015). Diversification of the cold-adapted butterfly genus *Oeneis* related to Holarctic biogeography and climatic niche shifts. *Molecular Phylogenetics and Evolution*, *92*, 255–265.

Klicka, J., Spellman, G. M., Winker, K., Chua, V., & Smith, B. T. (2011). A Phylogeographic and population genetic analysis of a widespread, sedentary North American bird: the Hairy Woodpecker (*Picoides villosus*). *The Auk*, *128*(2), 346–362.

Klicka, J., & Zink, R. M. (1997). The Importance of Recent Ice Ages in Speciation: A Failed Paradigm. *Science*, *277*(5332), 1666–1669.

Koblmüller, S., Vilà, C., Lorente-Galdos, B., Dabad, M., Ramirez, O., Marques-Bonet, T., … Leonard, J. A. (2016). Whole mitochondrial genomes illuminate ancient intercontinental dispersals of grey wolves (*Canis lupus*). *Journal of Biogeography*, *43*(9), 1728–1738.

Kohli, B. A., Fedorov, V. B., Waltari, E., & Cook, J. A. (2015). Phylogeography of a Holarctic rodent (*Myodes rutilus*): Testing high-latitude biogeographical hypotheses and the dynamics of range shifts. *Journal of Biogeography*, *42*(2), 377–389.

Köppen, W. (1900). Versuche einer Klassifikation der Klimate, vorzugsweise nach ihren Beziehungen zur Pflanzenwelt. *Geographische Zeitschrift*, *6*(12), 657–679.

Köppen, W., & Geiger, R. (1936). Das Geographische System der Klimate. *Handbuch Der Klimatologie*, (c), 7–30.

Kraaijeveld, K., & Nieboer, E. N. (2000). Late Quaternary paleogeography and evolution of arctic breeding waders. *Ardea*, *88*(2), 193–205.

Kurose, N., Abramov, A. V., & Masuda, R. (2005). Comparative Phylogeography between the Ermine Mustela erminea and the Least Weasel *M. nivalis* of Palaearctic and Nearctic Regions, Based on Analysis of Mitochondrial DNA Control Region Sequences. *Zoological Science*, *22*(10), 1069–1078.

Leblanc, N. M., Stewart, D. T., Pálsson, S., Elderkin, M. F., Mittelhauser, G., Mockford, S., … Mallory, M. L. (2017). Population structure of Purple Sandpipers (*Calidris maritima*) as revealed by mitochondrial DNA and microsatellites. *Ecology and Evolution*, (7), 3225–3242.

Li, X., Dong, F., Lei, F., Alström, P., Zhang, R., Ödeen, A., … Yang, X. (2016). Shaped by uneven Pleistocene climate: Mitochondrial phylogeographic pattern and population history of white wagtail *Motacilla alba* (Aves: Passeriformes). *Journal of Avian Biology*, *47*(2), 263–274.

Lovette, I. J. (2005). Glacial cycles and the tempo of avian speciation. *Trends in Ecology and Evolution*, *20*(2), 57–59.

Macpherson, A. A. H. (1965). The origin of diversity in mammals of the Canadian arctic tundra. *Systematic Zoology*, *14*(3), 153–173.

Marthinsen, G., Wennerberg, L., & Lifjeld, J. T. (2007). Phylogeography and subspecies taxonomy of dunlins (*Calidris alpina*) in western Palearctic analyzed by DNA microsatellites and AFLP markers. *Biological Journal of the Linnean Society*, *92*, 713–726.

Marthinsen, G., Wennerberg, L., Pierce, E. P., & Lifjeld, J. T. (2008). Phylogeographic origin and genetic diversity of dunlin *Calidris alpina* in Svalbard. *Polar Biology*, *31*(11), 1409–1420.

Matthiesen, D. G. (1990a). Avian medullary bone in the fossil record, an example from the Early Pleistocene of Olduvai Gorge, Tanzania. *Journal of Vertebrate Paleontology, 9*, 34A.

Matthiesen, D. G. (1990b). Prodromus of the paleoecology of the Plio-Pleistocene fossil birds from the early man sites of Omo and Hadar, Ethiopia, and Olduvai Gorge, Tanzania. In Paper presented at the International Conference for Archaeozoology, Washington D.C., June, 1990.

Meijer, H. J., Sutikna, T., Saptomo, E. W., Awe, R. D., Jatmiko, Wasisto, S., ... & Tocheri, M. W. (2013). Late Pleistocene-Holocene non-Passerine Avifauna of Liang Bua (Flores, Indonesia). *Journal of Vertebrate Paleontology, 33*(4), 877-894.

Meltofte, H., Piersma, T., Boyd, H., McCaffery, B., Ganter, B., Golovnyuk, V. V., … Wennerberg, L. (2007). Effects of climate variation on the breeding ecology of Arctic shorebirds. *Meddelelser Om Gronland Bioscience* (Vol. 59).

Mengel, R. M. (1964) The probable history of species formation in some northern Wood warblers (Paraulidae). *Living Bird, 3*, 9-43.

Milá, B., Girman, D. J., Kimura, M., & Smith, T. B. (2000). Genetic evidence for the effect of a postglacial population expansion on the phylogeography of a North American songbird. *Proceedings of the Royal Society B: Biological Sciences*, *267*(1447), 1033–1040.

Milá, B., McCormack, J. E., Castañeda, G., Wayne, R. K., & Smith, T. B. (2007). Recent postglacial range expansion drives the rapid diversification of a songbird lineage in the genus *Junco*. *Proceedings of the Royal Society B: Biological Sciences*, *274*(1626), 2653–2660.

Milá, B., Smith, T. B., & Wayne, R. K. (2006). Postglacial Population Expansion Drives the Evolution of Long-Distance Migration in a Songbird. *Evolution*, *60*(11), 2403–2409.

Miller, M. P., Haig, S. M., Gratto-Trevor, C. L., Mullins, T. D., Iller, M. A. R. K. P. M., Aig, S. U. M. H., … Ullins, T. H. D. M. (2010). Subspecies Status and Population Genetic Structure in Piping Plover (*Charadrius melodus*). *The Auk*, *127*(1), 57–71.

Miller, M. P., Haig, S. M., Mullins, T. D., Ruan, L., Casler, B., Dondua, A., … Lanctot, R. B. (2015). Intercontinental genetic structure and gene flow in Dunlin (*Calidris alpina*), a potential vector of avian influenza. *Evolutionary Applications*, *8*(2), 149–171.

Nogués-Bravo, D. (2009). Predicting the past distribution of species climatic niches. *Global Ecology and Biogeography, 18*(5), 521–531.

Ottvall, R., Höglund, J., Bensch, S., & Larsson, K. (2005). Population differentiation in the redshank (*Tringa totanus*) as revealed by mitochondrial DNA and amplified fragment length polymorphism markers. *Conservation Genetics*, *6*(3), 321–331.

Peel, M. C., Finlayson, B. L., & McMahon, T. A. (2007). Updated World Map of the Köppen-Geiger Climate Classification. *Hydrol. Earth Systm. Sci. Discuss.*, *4*, 439–473.

Peters, S. E. & McClennen, M. (2016). The Paleobiology Database application programing interface. *Paleobiology*, *42*, 1–7.

Pielou, E. C. (1991). *After the ice age: the return of life to glaciated North America*. University of Chicago Press.

Piersma, T. (2003). " Coastal" versus" inland" shorebird species: interlinked fundamental dichotomies between their life-and demographic histories?. *Bulletin-Wader Study Group*, *100*, 5-9.

Piersma, T. (2007). Using the power of comparison to explain habitat use and migration strategies of shorebirds worldwide. *Journal of Ornithology, 148*(1), 45.

Piersma, T. (2011). Flyway evolution is too fast to be explained by the modern synthesis: Proposals for an “extended” evolutionary research agenda. *Journal of Ornithology*, *152*(1 SUPPL), 151–159.

Ploeger, P. L. (1968). Geographical differentiation in arctic Anatidae as a result of isolation during the last glacial. *Ardea*, *56*(1–2), 4–155.

Ponti, R., Arcones, A., Ferrer, X., & Vieites, D. R. (2018). Productivity as the main factor correlating with migratory behaviour in the evolutionary history of warblers. *Journal of*

Zoology, *306*(3), 197–206.

Prassack, K. A. (2010). Late Pliocene avifauna from the hominid-bearing *Zinjanthropus* land surface at Olduvai Gorge, Tanzania. In Proceedings of the VII International Meeting of the Society of Avian Paleontology and Evolution, ed. W.E. Boles and T.H. Worthy. *Records of the Australian Museum, 62*(1), 185–192.

Prassack, K. A. (2014). Landscape distribution and ecology of Plio-Pleistocene avifaunal communities from Lowermost Bed II, Olduvai Gorge, Tanzania. *Journal of Human Evolution, 70*(1), 1–15.

Prassack, K. A., Pante, M. C., Njau, J. K., & de la Torre, I. (2018). The paleoecology of Pleistocene birds from Middle Bed II, at Olduvai Gorge, Tanzania, and the environmental context of the Oldowan-Acheulean transition. *Journal of Human Evolution*, 120, 32–47.

Provan, J., & Bennett, K. D. (2008). Phylogeographic insights into cryptic glacial refugia. *Trends in Ecology and Evolution*, *23*(10), 564–571.

Pruett, C. L., & Winker, K. (2005). Biological impacts of climatic change on a Beringian endemic: Cryptic refugia in the establishment and differentiation of the rock sandpiper (*Calidris ptilocnemis*). *Climatic Change*, *68*(1–2), 219–240.

Pujolar, J. M., Dalén, L., Hansen, M. M., & Madsen, J. (2017). Demographic inference from whole-genome and RAD sequencing data suggests alternating human impacts on goose populations since the last ice age. *Molecular Ecology*, *26*(22), 6270–6283.

Rand, A. L. (1948). Glaciation, An Isolating Factor in Speciation. *Evolution*, *2*(4), 314–321.

Ray, N., & Adams, J. M. (2001). A GIS-based vegetation map of the world at the Last Glacial A GIS-based Vegetation Map of the World at the Last Glacial Maximum (25,000-15,000 BP). *Internet Archaeology*, *11*.

Rönkä, A., Kvist, L., Karvonen, J., Koivula, K., Pakanen, V. M., Schamel, D., & Tracy, D. M. (2008). Population genetic structure in the Temminck's stint *Calidris temminckii*, with an emphasis on Fennoscandian populations. *Conservation Genetics*, *9*(1), 29–37.

Rönkä, N., Kvist, L., Pakanen, V. M., Rönkä, A., Degtyaryev, V., Tomkovich, P., … Koivula, K. (2012). Phylogeography of the Temminck's Stint (*Calidris temminckii*): Historical vicariance but little present genetic structure in a regionally endangered Palearctic wader. *Diversity and Distributions*, *18*(7), 704–716.

Ruegg, K. C., Hijmans, R. J., & Moritz, C. (2006). Climate change and the origin of migratory pathways in the Swainson's Thrush. *Journal of Biogeography*, *33*, 1172–1182.

Rueness, E. K., Naidenko, S., Trosvik, P., & Stenseth, N. C. (2014). Large-scale genetic structuring of a widely distributed carnivore - The eurasian lynx (*Lynx lynx*). *PLoS ONE*, *9*(4), 1–11.

Rundgren, M., & Ingolfsson, O. (1999). in Iceland during Plant survival periods of glaciation? *Journal of Biogeography*, *26*(2), 387–396.

Sipe, T. W., & Browne, R. A. (2004). Phylogeography of Masked (*Sorex cinereus*) and Smoky Shrews (Sorex Fumeus) in the Southern Appalachians. *Journal of Mammalogy*, *85*(5),

875–885.

Skrede, I., Eidesen, P. B., Portela, R. P., & Brochmann, C. (2006). Refugia , differentiation and postglacial migration in arctic- alpine Eurasia , exemplified by the mountain avens (*Dryas octopetala* L.). *Molecular Ecology*, *15*, 1827–1840.

Smith, S. E., Gregory, R. D., Anderson, B. J., & Thomas, C. D. (2013). The past, present and potential future distributions of cold-adapted bird species. *Diversity and Distributions, 19*(3), 352–362.

Stewart, J. R., & Lister, A. M. (2001). Cryptic northern refugia and the origins of the modern biota. *Trends in Ecology and Evolution*, *16*(11), 608–613.

Stewart, J. R., Lister, A. M., Barnes, I., & Dalen, L. (2010). Refugia revisited: individualistic responses of species in space and time. *Proceedings of the Royal Society B: Biological Sciences*, *277*(1682), 661–671.

Thies, L., Tomkovich, P., Remedios, N. dos, Lislevand, T., Pinchuk, P., Wallander, J., … Küpper, C. (2018). Population and Subspecies Differentiation in a High Latitude Breeding Wader, the Common Ringed Plover *Charadrius hiaticula*. *Ardea*, *106*(2), 163–176.

Todisco, V., Gratton, P., Zakharov, E. V., Wheat, C. W., Sbordoni, V., & Sperling, F. A. H. (2012). Mitochondrial phylogeography of the Holarctic *Parnassius phoebus* complex supports a recent refugial model for alpine butterflies. *Journal of Biogeography*, *39*(6), 1058–1072.

Trimbos, K. B., Doorenweerd, C., Kraaijeveld, K., Musters, C. J. M., Groen, N. M., Knijff, P., … De Snoo, G. R. (2014). Patterns in nuclear and mitochondrial DNA reveal historical and recent isolation in the black-tailed godwit (*Limosa limosa*). *PLoS ONE*, *9*(1).

Val, A. (2016). New data on the avifauna from the Middle Stone Age layers of Sibudu Cave, South Africa: Taphonomic and palaeoenvironmental implications*. Quaternary International, 421*, 173–189.

van Els, P., Cicero, C., & Klicka, J. (2012). High latitudes and high genetic diversity: Phylogeography of a widespread boreal bird, the gray jay (*Perisoreus canadensis*). *Molecular Phylogenetics and Evolution*, *63*(2), 456–465.

Wang, W., Mckay, B. D., Dai, C., Zhao, N., Zhang, R., Qu, Y., … Lei, F. (2013). Glacial expansion and diversification of an East Asian montane bird, the green-backed tit (*Parus monticolus*). *Journal of Biogeography*, *40*(6), 1156–1169.

Webb III, T., & Bartlein, P. J. (1992). Global changes during the last 3 million years: Climatic Controls and Biotic Responses. *Annual Review of Ecology and Systematics*, *23*(1), 141–173.

Weir, J. T., & Schluter, D. (2004). Ice sheets promote speciation in boreal birds. *Proceedings. Biological Sciences / The Royal Society*, *271*(1551), 1881–1887.

Wenink, P., Baker, A., Rosner, H., & Tilanus, M. (1996). Global mitochondrial DNA phylogeography of holarctic breeding dunlins (*Calidris alpina*). *Evolution*, *50*(1), 318–330.

Wenink, P. W., Baker, A. J., & Tilanus, M. G. (1994). Mitochondrial control-region sequences in

two shorebird species, the turnstone and the dunlin, and their utility in population genetic studies. *Molecular Biology and Evolution*, *11*(1), 22–31.

Wennerberg, L. (2001). Breeding origin and migation pattern of dunlin (*Calidris alpina*) revealed by mitochondrial DNA analysis. *Molecular Ecology*, *10*, 1111–1120.

Willmes, C., Becker, D., Brocks, S., Hütt, C., & Bareth, G. (2017). High Resolution Köppen-Geiger Classifications of Paleoclimate Simulations. *Transactions in GIS*, *21*(1), 57–73.

Wood, S., & Wood, M. S. (2015). Package 'mgcv'. R package version, 1, 29.

Zhao, N., Dai, C., Wang, W., Zhang, R., Qu, Y., Song, G., … Lei, F. (2012). Pleistocene climate changes shaped the divergence and demography of Asian populations of the great tit *Parus major*: Evidence from phylogeographic analysis and ecological niche models. *Journal of Avian Biology*, *43*(4), 297–310.

Zink, R. M., & Barrowclough, G. F. (2008). Mitochondrial DNA under siege in avian phylogeography. *Molecular Ecology*, *17*(9), 2107–2121.

Zink, R. M., & Gardner, A. S. (2017). Glaciation as a migratory switch. *Science Advances*, *3*(9), e1603133.

Zink, R. M., & Klicka, J. (2006). The tempo of avian diversification: A comment on Johnson and Cicero. *Evolution*, *60*(2), 411–412.

Zink, R. M., Pavlova, A., Drovetski, S., & Rohwer, S. (2008). Mitochondrial phylogeographies of five widespread Eurasian bird species. *Journal of Ornithology*, *149*(3), 399–413.

Chapter 2:

New mitochondrial DNA substitution rates reveal patterns of recent diversification in Arctic shorebirds linked to longer glacial cycles.

Authors: Arcones A., Ponti R., Ferrer X. and Vieites D.

New mitochondrial DNA substitution rates reveal patterns of recent diversification in Arctic shorebirds linked to longer glacial cycles.

Abstract

The Pleistocene glacial cycles are usually considered as the origin of many of the current intraspecific diversity in Arctic shorebirds. The geographic changes in the breeding ranges between glacial and interglacial periods support this process of diversification across this clade. However, this needs to be confirmed with genetic data, to evaluate if the patterns and timing of diversification support the Pleistocene origin. Dating divergence times from DNA data requires the use of reliable and specific substitution rates. In the case of mitochondrial DNA (mtDNA), such rates are often unavailable and analyses are based on "universal" rates from other taxa or DNA sources. To avoid the error induced from those rates, we performed a novel calibration of the molecular clock rates for each of the mtDNA genes across the bird phylogenetic tree. The obtained rates, specific for each gene and lineage in the tree, allowed us to explore the diversification within 10 species of Arctic shorebirds. Using phylogenetic and coalescent methods, we confirmed that most of the intraspecific diversification in Arctic shorebirds developed during the Pleistocene, and especially during the Middle and Late Pleistocene, coinciding with longer and more intense glacial periods. The patterns of diversification show parallelisms between shorebird species that experienced similar changes of their breeding ranges during glacial and interglacial periods. Species with a higher degree of isolation of their populations, especially during glacial periods, display older and better-defined lineages than those from areas more affected by the glaciation or that became isolated during the interglacial. The diversification patterns found in Arctic shorebirds also show great parallelism with previous results in some Arctic species, highlighting the importance of integrating different evolutionary histories to understand the origin of Arctic biodiversity.

Introduction

Pleistocene glacial cycles have been suggested as potential drivers of diversification in Arctic species (see Chapter 1). To confirm this hypothesis, there are two main factors to explore the potential role of glacial cycles in the observed patterns of geographic variation in Arctic species: the time of diversification, to confirm that it happened during the Pleistocene, and the past distribution changes during glacial and interglacial periods to determine the potential existence of refugia and their connectivity, or lack of, in parallel to the observed genetic and phenotypic variation in species.

From a geographic perspective, seminal papers (Rand, 1948; Macpherson, 1965; Ploeger, 1968; Greenwood, 1986) proposed the retreat into isolated refugia during cold glacial periods as the potential cause of geographic isolation and diversification, which correlated to the actual observed variation in Arctic species, like geese and shorebirds (Ploeger, 1968). However, interglacial periods could have also affected the genetic and phenotypic variation of Arctic species as they expanded their ranges back to northern latitudes, an alternative hypothesis that has been neglected so far. In the Chapter 1 of this thesis, we performed explicit analyses that show that range fragmentation into large biogeographic regions driven by glacial climatic cycles parallel the observed intraspecific variation in shorebirds. The majority of species with recognized subspecific variation presented fragmentation of their ranges during glacial, interglacial or both periods, and the fragmentation of their ranges overlaps with their subspecies distributions. Hence, both glacial and interglacial periods seem to have played an important role in the diversification of Arctic species. Genetic data constitute an independent dataset to confirm this hypothesis as, in order to be true, the origin and divergence of extant subspecies had to happen during the last 2.5 million years (My). The expansions and contractions of ranges, often involving fragmentation, left genetic signatures in species (Avise & Walker, 1998; Hewitt, 1996, 2000, 2004), including population demographic changes (Jaarola *et al.*, 1999; Hewitt, 2000; Flagstad & Røed, 2003; Buehler & Baker,

2005; Jones *et al.*, 2005; Milá *et al.*, 2007), although those does not necessarily have to be related to the origin of the subspecies.

Another interesting aspect to explore is the potential scenario of simultaneous temporal diversification of Arctic species or whether each species diversified independently. The Pleistocene was characterized by an alternation of cold glacial and warm interglacial periods, some of which were longer and more intense than others (EPICA community members, 2004; Lisiecki & Raymo, 2005; Cohen & Gibbard, 2008; Jouzel *et al.*, 2007). It may be possible that some of these periods had a more profound impact on the genetic and phenotypic variation of Arctic species, hence they diverged at the same time. Many works have provided coalescent and Bayesian time estimates of the origin of subspecies of Arctic species (Abbott & Comes, 2004; Weir & Schluter, 2004; Buehler & Baker, 2005; Todisco *et al.*, 2012; Eidesen *et al.*, 2013; Hope *et al.*, 2012; Kleckova *et al.*, 2015), but the confidence intervals of such estimates are very large. Also, so far there has not been a comparative study that analysed multiple species at the same time with the same approach and methods to test this hypothesis on Arctic species. Using shorebirds as a model, here we want to test if the observed intraspecific genetic variation observed in Arctic shorebird species originated during the Pleistocene, if there is an overlap in time in such diversification, and if the diversification correlates with a particular period.

As confidence intervals in divergence time estimates are expected to be larger than the duration of any particular glacial or interglacial period, we consider two main periods in the Pleistocene based on the length of Milankovitch cycles. Since the beginning of the Pleistocene, glacials and interglacials gained in duration and intensity, but since around 900,000 years ago, the Milankovitch cycles showed much larger amplitudes and durations until the last glacial maximum about 22,000 years ago (EPICA community members, 2004; Lisiecki & Raymo, 2005; Jouzel *et al.*, 2007). We hypothesize that most Arctic species where more affected during this last period and consequently their diversification peaked during the last 900,000 years.

A proper testing of those hypotheses relies on robust coalescent or phylogenetic estimates of divergence times. Fossils can be used to calibrate divergence times of particular nodes on a phylogeny, but the fossil record is scarce in the Arctic (Peters & McClennen, 2016), and fossils are unlikely assigned to particular subspecies. Hence, when performing analyses on intraspecific divergences, they have to rely on mutation rates for the loci of interest (Lovette, 2004; Pereira & Baker, 2006). Mitochondrial DNA (mtDNA) is generally regarded as a useful resource to assess recent evolutionary histories and especially in phylogeographic studies on bird species (Zink & Barrowclough, 2008). For years, many of these studies estimated divergence times based on the "universal" molecular clock rate of 2% divergence per million years, which translates to approximately 0.01 substitutions per site per lineage per million years (s/s/l/My). This rate was originally estimated based on data from humans and chimpanzees (Brown *et al.*, 1979) and was supported by similar rates obtained for other vertebrates (Wilson *et al.*, 1985) and a couple genera of geese (Shields & Wilson, 1987), and more recently in a reanalysis extended to birds in general (Weir & Schluter, 2008). But the validity of this universal molecular clock for any mtDNA loci in any bird species has been heavily criticized (Garcia-moreno, 2004; Lovette, 2004) and all the large mitogenomic analyses performed over the past 15 years reflect a lack of "standard" rates across the avian tree of life and between the different mtDNA markers (Pereira & Baker, 2006; Pacheco *et al.*, 2011; Nabholz *et al.*, 2016). However, the results of these studies have high variation between them, and more importantly, they often fail to provide rates that are specific for the mtDNA gene in the actual taxonomic group of interest. To overcome this problem, we here performed our own mitogenomic calibration of the avian molecular clock for each mtDNA gene in each lineage within the tree, including several shorebirds, and then applied those resulting rates to the dating of the diversification in our studied species.

Although phylogenetic molecular clock analyses are the most common approach to estimate divergence times, the use of other complementary statistical methods can enhance the validation of results. Coalescent-based methods have become a powerful tool to infer evolutionary histories under more complex scenarios, incorporating demographic changes into the model (Hickerson *et al.*, 2007, 2010; Beaumont *et al.*, 2010). One of these methods is approximate Bayesian computation (ABC), which allows

testing between alternative hypotheses in order evaluate which evolutionary scenario fits the data better (Csilléry *et al.*, 2010). This has often been used to infer the phylogeography and timing of diversification events between lineages during the Pleistocene in relation to changes in the climate (e.g. Shafer *et al.*, 2010; Zigouris *et al.*, 2013; Fasanella *et al.*, 2014; Castellanos-Morales *et al.*, 2016).

Here we used Arctic shorebirds as a model group, because it harbours species with suitable characteristics to test the proposed hypotheses. Arctic and subarctic shorebirds are one of the most migratory groups of organisms on Earth. They comprise 70 species belonging to 18 genera (Chester, 2016), spanning throughout the Arctic and subarctic regions during reproduction, performing long migrations to Eurasia, Africa, Australasia or South America (del Hoyo, 2018). Some species occur throughout the Arctic, while others are restricted to smaller areas. Widespread species can show no intraspecific phenotypic variation and genetic uniformity or have several well-defined morphological subspecies (Engelmoer & Roselaar, 1998) with or without genetic differentiation. Previous works hypothesized that their diversification may be related to Pleistocene glaciations (Buehler & Baker, 2005; Buehler *et al.*, 2006; Piersma & Drent, 2003; Wenink *et al.*, 1993, 1996), and in the first chapter we provided explicit spatial scenarios suggesting that range fragmentation caused by glacial cycles correlate to the observed spatial differentiation.

There are not many species of Arctic shorebirds for which genetic data are available across their distribution ranges. For some with such data, Pleistocene vicariant events, when populations were fragmented in different refugia not connected between them, together with a strong philopatry have been advocated to explain the genetic structure within species or the genetic differentiation between subspecies [e.g. *Calidris alpina*, (Buehler & Baker, 2005; Wenink *et al.*, 1993, 1994, 1996); *Calidris canutus* (Baker *et al.*, 1994; Buehler & Baker, 2005); *Calidris maritima* (Barisas *et al.*, 2015; Leblanc *et al.*, 2017), *Calidris ptilocnemis* (Pruett & Winker, 2005); *Limosa limosa*, (Höglund *et al.*, 2009; Trimbos *et al.*, 2014)]. In other species, like *Arenaria interpres* (Wenink *et al.*, 1994), *Calidris fuscicollis* (Wennerberg *et al.*, 2002) or *Tringa totanus* (Ottvall *et al.*, 2005) there is no signature of population genetic structure across their ranges, suggesting that different species may have experienced different historical processes

within the Arctic. A comparative analysis with multiple species to assess their potential parallel diversification through time is lacking.

We here provide novel estimates of mutation rates across birds, including Arctic shorebirds, that were used to estimate their intraspecific diversification and origin of subspecies, test their potential overlap in time, and perform explicit coalescent hypothesis testing of different time scenarios. Those analyses constitute an independent line of evidence to the geographic and climatic scenarios, to support the hypothesis of glacial cycles as the main drivers of the diversification in Arctic species.

Methods

Complete mitochondrial genomes

We assembled the most comprehensive dataset available so far of complete bird mitochondrial genomes from Genbank. To retrieve the genomes, we modified the Mitobank script (Abascal *et al.*, 2007) in BioPerl, providing complete or nearly complete bird genomes for 622 species representing 33 modern bird orders, including some extinct species. Of these 622 species sampled, including some that are now extinct, 17 belonged to palaeognaths (Ostrich, tinamous and allies), 94 to the Galloanserae clade (chickens, quails, geese, fowls and allies) and 511 to the Neoaves (all other avian groups) clade, of which 259 were Passeriformes (Accession Numbers: see Appendix 3). Only 5 orders were left unrepresented due to the lack of species' mtgenome data available: Mesitornithiformes (Mesites), Pterocliformes (Sandgrouses and allies), Opisthocomiformes (Hoatzin), Leptosomiformes (Cuckoo rollers) and Cariamiformes (Seriemas and allies).

In two cases, there were some missing data for some species that were completed from different individuals: *Psittacus erithacus* for ND6 (accession number KM611474) and *Accipiter gularis* for ND1 (EU583261).

After excluding the D-loop and the tRNAs, the result was a combined dataset of 12950 base pairs. Alignments were done gene by gene as global alignments are not possible because of gene rearrangements and complexity of the genomes (Mueller & Boore, 2005). Alignment was performed using the software Genious v.9 (https://www.geneious.com). Due to the high variability of some regions of the mitochondrial DNA, and especially in 3rd codon positions, we applied a translation alignment. This implies translating the sequences into aminoacids for the alignment, and then returning to the original nucleotide sequence. The genes were then concatenated into a single sequence per species.

We computed a phylogenetic tree using RaxML (Stamatakis, 2014) as a test to detect troublesome sequences that could be introducing error in the process. This resulted in the exclusion of *Larus vegae* (GenBank accession number: NC_029383) from the following analyses, after a clearly wrong placement in the obtained tree.

Fossil time constraints

In order to accurately determine divergence times and evolutionary rates, analyses must include a number of independent fossil constraints to time-calibrate the phylogenetic tree (Near & Sanderson, 2004; Benton & Donoghue, 2007; Magallón *et al.*, 2013). In our case, these calibrations are based on the fossil record. In accordance with recent recommendations (Ho & Duchêne, 2014; Zheng & Wiens, 2015), we aimed to include the higher number of calibrations as possible across the tree to maximize the accuracy of our results.

After a thorough review of the bibliography, we studied 77 reliable fossil reliable calibrations. Out of these 77, 25 were included into the analyses based on their informative value and compatibility with our dataset (Fig. 1). Following the recommendations from Parham *et al.* (2012) and Fourment & Holmes (2014), we used a conservative minimum age based on the chronostratigraphic evidence of each fossil, and we did not impose any hard maximum ages.

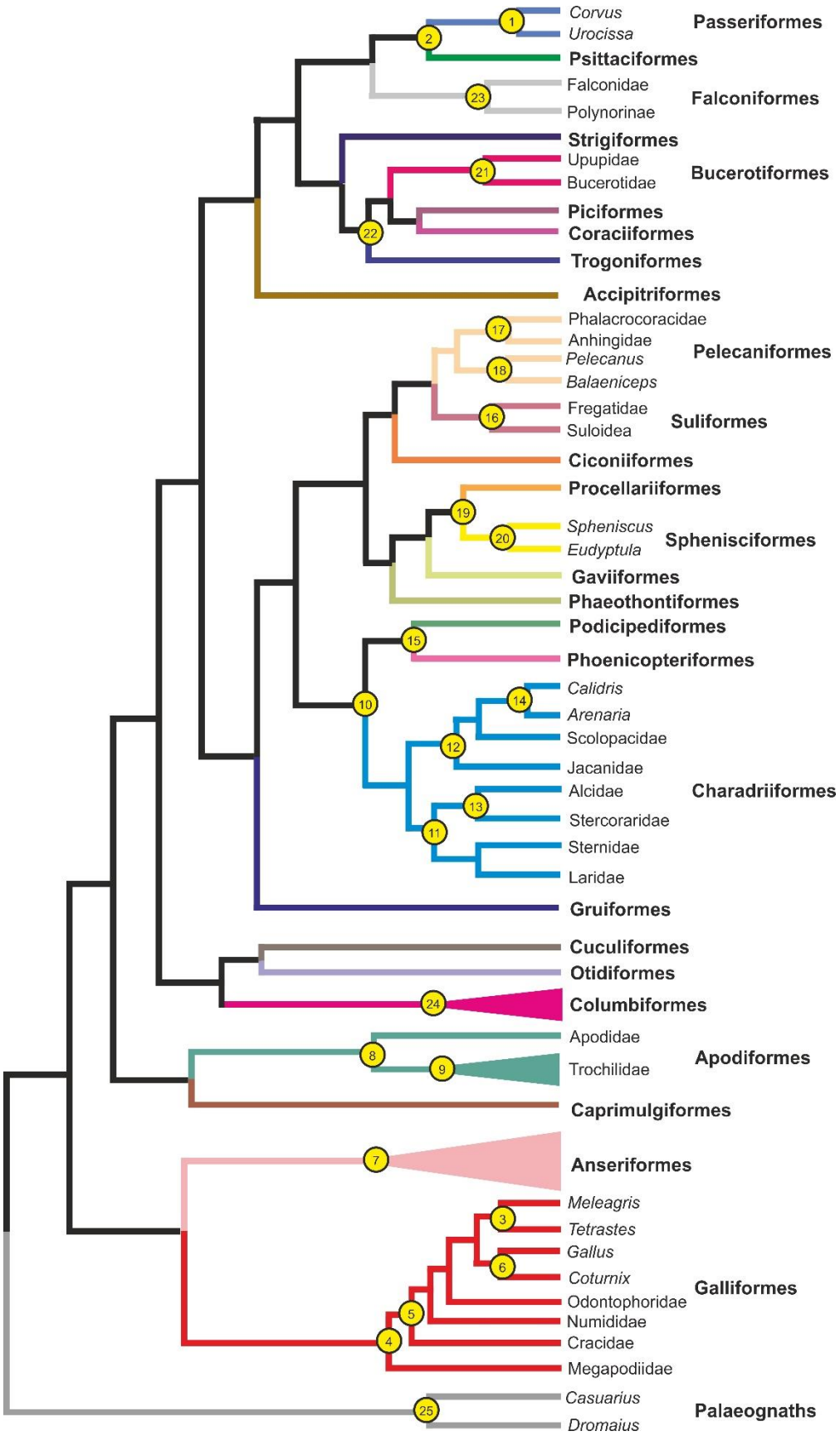

Figure 1: Cladogram summarizing the relationships between orders used for the analyse, with the 25 fossil calibrations in the corresponding nodes indicated by yellow circles (numbers are detailed in the text).

1) Split *Corvus / Urocissa* - *Miocitta galbreathi*

The minimum time constraint for the split between *Corvus* and *Urocissa* (Scofield *et al.*, 2017) can be inferred by *Miocitta galbreathi*, which is identified as a corvid from the late Miocene (15.97–13.6Mya) of North America. This fossil has been reported from the Pawnee Creek formation associated with Kennesaw local fauna [Upper Miocene (Galbreath, 1953)], in Colorado USA (Brodkorb, 1972; Becker, 1987a). Jønsson *et al.* (2016) suggested that *M. galbreathi* is more closely related to the genus *Corvus* than *Urocissa/Cissa* magpies; hence, we used the minimum constraint of 13.6 Mya on the divergence of *Corvus* and *Urocissa* genus.

2) Split Psittaciformes / Passeriformes -*Pulchrapollia gracilis*

The fossil *Pulchrapollia gracilis* was recovered from the London Clay Formation at Walton on the Naze, England. The Walton Member is related to the 14 upper part of Chron C24r and to calcareous plankton zone NP10-11 (Rhodes *et al.*, 1999). Given the difficulty to precise dating Chron C24r, Ksepka and Clarke (2015) suggest selecting the youngest estimate for the top of C24r (53.5 Mya). *P. gracilis* presented unique morphological similarities with extant parrots, sitting this fossil as a stem position of Psittaciformes. Here we use *P. gracilis* to calibrate the node in the split of Psittaciformes and Passeriformes with a minimum time constraint of 53.5 Mya.

3) Crown Meleagridinae + Tetraoninae - *Rhegminornis calobates*

When *Rhegminornis* was described, it was assigned to the order Charadriiformes (Wetmore, 1943). Olson and Farrand (1974) restudied this fossil placing it to Galliformes. They described it as a Meleagridae species and it has been used as calibration constraint between Meleagris and the grouse and ptarmigan (Pearson *et al.*, 2016; Stein *et al.*, 2015). It was found in the Lower Miocene deposits at Thomas Farm, 8 miles north of Bell, Gilchrist County, Florida. If we consider the minimum age of the lower Miocene, we would use 16 Mya as minimum time constraint for this node.

4) Crown Galliformes - *Gallinuloides wyomingensis*

Both *Gallinuloides* (Mayr, 2004) and *Paraortygoides* (Dyke and Gulas, 2002) fossils are valid for the calibration constraint of the stem Galliformes, as they are sister taxa (Ksepka, 2009). Several authors (van Tuinen *et al.*, 2004; Chen *et al.*, 2015; Kan *et al.*, 2010; Pereira *et al.*, 2006) used *Gallinuloides* as calibration for the stem Numididae - Phasianidae based in Dyke (2003), but Mayr and Weidig (2004) placed this fossil at the base of Galliformes.

The holotype of *Gallinuloides* was found in the Fossil Butte Member of the Green River Formation, Kemmerer, Wyoming, USA (Mayr and Weidig, 2004). Smith *et al.* (2008) dated with 40Ar/39Ar method the Fossil Butte Member assigning an age of (51.66 ± 0.09 Mya). We used the minimum age of the strata for our calibrations (51.57 Mya).

5) Crown Cracide + Numididae + Phasianidae - *Procrax*

Procrax fossil was described by Tordov 1957, from fresh-water limestone at the top of the Chadron formation from the lower Oligocene, NE 1/4 Sec. 4, T1S, R17E, in Pennington County, South Dakota. Van Tionen and Dyke (2004) used this fossil as calibration constraint; although, Ksepka (2009) remarked that there is not a phylogenetic analysis with this fossil that confirmed its correct placement. We used the minimum age of the lower Oligocene for our calibrations (33.9 Mya).

6) Crown *Gallus* + *Coturnix* - *Schaubortyx*

The fossil *Schaubortyx* has been considered as the most recent common ancestor of *Gallus* and *Coturnix* (Eastman, 1905). This fossil has been described from the freshwater limestone of Armissan, near Narbonne (Aude) (Eastman, 1905) assigned to the Chattian geological period (28 - 23.03 Mya) (Aguilar and Michaux, 1977). Several papers attributed a time constraint for divergence time analyses to this split around 32 to 38 Mya (Kan *et al.*, 2010; Chen *et al.*, 2015; Pereira *et al.*, 2006; van Tuinen & Dyke, 2004; Li *et al.*, 2015; Pereira & Baker, 2006). Although these papers refer to the Chattian period, they use ages corresponding to the Bartonian to Ruppelian. Here, we use a conservative age corresponding to the late Chattian as a minimum time constraint of

23.03 Mya. There is not a phylogenetic analysis confirming the position of *Schaubortyx* taxon as the ancestor of crown *Gallus* and *Coturnix* (Ksepka, 2009), but its placement this position seems not to be controversial.

7) Crown Anatidae - *Vegavis iaai*

This fossil was described by Clarke *et al.* (2005), from the Sandwich Bluff Member of the Lopez de Bertodano Formation at Sandwich Bluff, Vega Island, Antarctica. According to Ksepka & Clarke (2015), the fossil was found near a deposit that lies 50 below the K-Pg boundary, and was dated to be 67 Mya on the base and about 66 on the top, when taking 65.5 Mya as a reference for de K-Pg boundary. Since the new reference is 66My, then the top part of the biozone of *Vegavis* is 66.5 Mya, making this the youngest possible age, and thus the minimum age for this node.

8. Split Apodidae / Trochilidae - *Eocypselus vincenti*

Eocypselus vincenti is considered as the most recent common ancestor of the Apodiformes. This fossil was described by Harrison in 1984 from the lower Eocene (Ypresian) (Division A, London Clay. Walton on the Naze, Essex (England). We did not find the age of the strata. According to Ericson *et al.* (2016), we used the age from the Ypresian in the lower Eocene, around 53 Mya.

9) Crown Trochilidae - *Eurotrochilus inexpectatus*

Eurotrochilus inexpectatus is considered the oldest modern-type hummingbird, described by Mayr (2004). It was found in Frauenweiler south of Wiesloch (Baden-Württemberg, Germany). The fossil was recovered from clay pit of the Bott-Eder GmbH ("Grube Unterfeld"), corresponding to the early Oligocene, Rupelian period (30 to 34 Mya). We used 30 Mya as a minimum time constraint to calibrate the crown of hummingbirds, considering the minimum age from the Rupelian to be conservative (Ornelas *et al.*, 2014).

10) Split Charadriiformes / sister taxa - *Charadriiformes incertae*

The minimum time constraint from the Order Charadriiformes and its sister taxa is defined by a fossil with genus and species unknown, described by Mayr (2000a). Mayr (2000a) referred the fossil to Charadriiformes based on some apomorphies of the coracoid, humerus and carpometacarpos. However, the relationships of this fossil within the Order Charadriiformes are unclear. The fossil was recovered in "Grube Messel", located near Darmstadt in Hessen, Germany. The deposits from Messel originated in the Lower Middle Eocene. According with 40Ar/39Ar methods, the igneous rocks were dated to 47.8 ± 0.2 Mya, corresponding to the biostratigraphic reference level MP11 (the Geiseltalian European Land Mammal Age, estimated at 47.5-46.5 Mya) (Mertz and Renne, 2005; Smith, 2015). We used the inferior limit of the Geiseltalian (46.5 Mya) as minimum time constraint to calibrate the split of Charadriiformes from its sister taxa.

11) Crown Laromorphae (Laridae, Sternidae and allies) - *Laricola elegans*

Laricola fossil remains were recovered from Saint-Gérand-le-Puy (Early Miocene) and Billy-Créchy (Late Oligocene) in France. Although different *Laricola* species were found, only *Laricola elegans* was complete enough to be considered as potential calibration taxon, and included in phylogenetic analyses. The unresolved phylogenetic analyses from De Pietri (2011), suggest positioning this taxon as calibration point of the base of Laromorphae (Smith, 2015). The strata where *Laricola* remains were found in Créchy corresponds to the Miocene-Oligocene boundary, Paleogene mammalian zones MP25-M30, with an estimated age of 24.1-23.6 Mya (Hugueney *et al.*, 2003). Considering a conservative approach, we used the 23.6 Mya as minimum time constraint to calibrate the base of Laromorphae.

12) Split Jacanidae / other Scolopacidae – *Nupharanassa bulotorum*

Nupharanassa bolutorum, as well as other jacanas were recovered from the Quarry M, Fayum Province, in Egypt. The strata corresponded to the upper sequence of the Jebel Qatrani Formation from the Lower Oligocene, dated as 33-30 Mya. Those fossil remains were assigned to the family Jacanidae given their tarsometatarsi, distinctive in

having the huge distal doramen, broad tendinal groove and flattened shaft (Rasmussen *et al.*, 1987). Although the species *Nupharanassa tolutaria* has been considered older than *Nupharanassa bolutorum*, no phylogenetic studies have been conducted with this species (Smith, 2015). Thus, *N. bolutorum* is considered as a good calibration point to calibrate de divergence of the family Jacanidae from other scolopacids. We used 30 Mya as minimum time constraint for this node.

13) Split Pan-Alcidae / Stercorariidae - Pan-Alcidae incertae sedis

A Pan-Alcidae incertae sedis fossil was recovered from the locality of Hardie Mine in Georgia, USA (Chandler and Parmley, 2002). This fossil was placed in the group of pan-alcids given the apomorphic dorsoventrally flattened shaft and proximally extended dorsal supracondylar process of the humeri, that differs from other charadriiforms (Smith, 2011). The sediments exposed in Hardie Mine corresponded to the Clinchfield Formation. The sediments together with the fauna recovered in these strata as rays, sharks, mammals, snakes and dinocysts support the age of Late Eocene of this species. Other dinocyst assemblage from Georgia and South Carolina were placed in calcareus nannofosil zone NP19/20, that was dated 36-34.2 Mya (Smith, 2015). Therefore, the conservative age used for the divergence of Pan-Alcidae and Stercorariidae was 34.2 Mya.

14) Crown Calidrinae (*Calidris* and allies) - *Mirolia brevirostrata*

The specimens of *Mirolia brevirostrata* were placed in the subfamilie Calidridinae based on the apomorphies of the cranium and postcranium (Ballmann, 2004). These remains have been recoved from Nördlinger Ries basin, in Bavaria, Germany. This basin is an impact crater and has been dated as 14.8 ± 0.7 Mya. However, using the fossil fauna of the crater, the age has been dated in the Middle Miocene (Astaracian, MN 6) 16-11Ma (Smith, 2015). As the age of the fauna is not exact, the Serravallian-Tortonian boundary age is recommended to date the remains (11.62 Mya) (Smith, 2015); then we used 11.62 Mya as minimum time constraint for the basal node of Calidrinae.

15) Split Phoenicopteriformes / Podicipediformes - *Adelalopus hoogbutseliensis*

Adelalopus hoosbutseliensis presents singular morphological features in the coracoid, furcula and trochlea metatarsi that place it to the family Palaelodidae. This family is known from the Oligocene to the Pliocene of Europe, America and Australia (Olson and Feduccia, 1980) within the Order Phoenicopteriformes. *Adelalopus hoosbutseliensis* is the oldest known Phoenicopteriform species found in Hoogbutsel near Boutersem, in Brabant, Belgium. The remains were found in the strata MP 21 that corresponds to the Lower Oligocene (Mayr and Smith, 2002). We used this fossil to calibrate the node corresponding to the divergence of Phoenicopteriformes from its sister taxa (Podicipediformes) with a minimum time constraint of 27.8 Mya.

16) Split Fregatidae / Suloidea - *Limnofregata hasegawai*

The especies *Limnofregata azygosternon* was described by Olson (1977) and assigned to the genus *Limnofregata*, within the family Fregatidae. Further phylogenetic analyses recovered this genus as the base of the family Fregatidae based on synapomorphies that include the cranial, axial and pectoral characters (Smith 2010). These remains were collected near Kemmerer in Lincoln County, Wyoming; however, the exact place is unknown. Several specimens from another species from the genus *Limnofregata*, *L. haseqawais* were collected from a more precise locality. Those remains were found in F-2 Facies in the middle unit of the Fossil Butte Member of the Green River Formation. Multicrystal analyses from a K-feldspar tuff (FQ-1) at the top of the middle unit of the Fossil Butte Member, from Fossil-Fowkes Basin have determined that the deposits are late early Eocene, with and age of 51.97 ± 0.16 (Smith and Ksepka, 2015). We used the minimum age (51.8 Mya) as constraint for the divergence of Fregatidae and Suloidea.

17) Split Phalacrocoracidae / Anhingidae - ?*Borvocarbo stoeffelensis*

?*Borvocarbo stoeffelensis* fossil remains were found in Lagerstätte Enspel, near Bad Marienberg in Westerwald, Rheinland-Pfalz, Germany. This species was placed together with Phalacrocoracidae clade given three synamoporphies represented in the

mandible and the pes of the skeleton (Smith, 2010). The deposits from Enspel correspond to the upper Oligocene mammal Paleogene, in the level 28 (Mertz *et al.*, 2007; Smith and Ksepka, 2015). The Enspel lacustrine deposits were dated using laser fusion 40Ar/39Ar radiometric dating of volcanic feldspars from the lower and upper basaltic flows, yielding ages of 24.56 ± 0.04 to 24.79 ± 0.05 Mya (Mertz *et al.*, 2007). Therefore, the conservative age used for the divergence of Phalacrocoracidae and Anhingidae was 24.5 Mya. Similarly, the species *?Oligocorax* described in Mayr (2001) and placed within the family Phalacrocoracidae and also found in the deposits from Lagerstätte Enspel, in the level 28, could also serve as a calibration for this split.

18) Crown Balaenicipitidae - *Goliathia andrewsi*

Goliathia andrewsi was found in Faym Province, lower sequence, in the Jebel Qatrani Formation (Rasmussen *et al.*, 1987). This species was assigned to the family Balaenicipitidae given its distinctive flattened shafand. *G. andewsi* is the oldest fossil found of this family (Smith, 2013). The remains were found in the horizon Quarry M, upper sequence, dated by Seiffert (2006) as Early Oligocene. Hence, we used 30 Mya as the minimum time constraint to calibrate the crown group of Balaenicipitidae.

19) Split Sphenisciformes / Procellariiformes - *Waimanu manneringi*

The holotype of *Waimanu manneringi* (Slack *et al.*, 2006) was placed within Spheniciformes given distinct characters: as some thoracic vertebrae that are not heterocoelous, synsacrum has 11–12 ankylosed vertebrae, not well developed hypotarsal crests and grooves of the tarsometatarsus. Multiple analyses using morphology and molecular data place *Waimanu* as the most basal penguin taxon (Slack *et al*., 2006; Ksepka and Clarke, 2010). This specimen was collected from the basal Waipara Greensand, Waipara River in New Zealand (Slack *et al.*, 2006). The top of the Waipara Greensand corresponds to the Paleocene-Eocene boundary given the calcareous nannofossils 61.6 – 60.5 Mya (Cooper, 2004, Kepska and Clarke, 2015). The youngest possible age (60.5 Mya) is used as a hard-minimum age for the divergence between Sphenisciformes and Procellariiformes.

20) Split *Spheniscus* / *Eudyptula* - *Spheniscus muizoni*

According to Göhlich (2007), *Spheniscus muizoni* is the oldest fossil record of the extant penguin genus *Spheniscus*. This specimen was found in Cerro La Bruja, in the Department of Ica (Peru). The remains were from Pisco Formation, latest middle/earliest late Miocene, ca. 13 –11 Mya (Muizon, 1988). Postcranial bones of this species recovered from Pisco Formation presented osteological features that allow assigning them to the genus *Spheniscus*. Hence, we considered 11 Mya as the minimum age for the calibration between *Spheniscus* and *Eudyptula*.

21) Crown Uppupidae + Phoeniculidae - *Messelirrisor grandis*/*Messelirrisor halcyrostris*

The taxa *Messelirrisor grandis* was described by Mayr (2000b). The fossil remains were recovered from Messel near Darmstadt, Germany. The deposits of Messel originated in a deep crater lake about 49 Mya in the Lower Middle Eocene. Phylogenetic analyses based in morphological characters were performed by Mayr (2006), placing this taxon as the sister species of all Bucerotiformes (stem of Upupidae and Phoeniculidae). Ksepka and Clarke (2015) choose the other species of the genus (*Messelirrisor halcyrostris*) from the same strata as fossil for calibrations. The age of the strata was calculated by incorporating the dating of the deposits below (40Ar/39Ar age of the basalt chimney below Lake Messel) where the fossil was found (ca. 47.8) and the estimated time of the deposition of the lacustrine sediments above the basalt chimney (1My after) (Mertz *et al.*, 2004). We used as a minimum age constraint 46.6 Mya.

22) Trogoniformes - *Primotrogon ? pumilio*

Mayr (2005) described *Primotrogon ? pumilio* as the oldest species of Trogoniformes. This fossil was discovered in Messel, near Darmstadt, Hessen, Germany originated in a lake of tectonic or volcanic origin, from the Lower Middle Eocene dated as 49 Mya. This species shares with modern trogons the heterodactyl feet, which is a distinctive character only known for trogons. As previously said in the explanation of

Messelirrisor halcyrostris, the estimated time of deposits of the lacustrine sediments above the basalt chimney is 46.6 Mya (Mertz *et al.*, 2004). We used 49 Mya as minimum time constraint to calibrate the node corresponding to the split of the lineage of Trogoniformes from the sister taxa.

23) Split Falconidae/Polynorinae - *Pediohierax ramenta*

Pediohierax ramenta was described by Wetmore (1936) as *Falco ramenta*, while Becker (1987b) revised its taxonomic position moving it to the genus *Pediohierax*. This fossil represents the first known species of Falconidae and the most recent common ancestor of the subfamily Falconinae.

The holotype of *P. ramenta* was found at the "Merychippus Quarry, Dawes Co., Nebraska. However, other specimens were found at Boulder Quarry, Echo Quarry, Thomson Quarry and Observation Quarry. Excluding the Observation Quarry, all specimens are from Sheep Creek or Olcott Formations, Sioux Co., Nebraska. Based on the dating of a vitric tuff on top of one of the localities, Thomson quarry (late Hemingfordian, ca. 16.3Mya), the minimum age of *P. ramenta* is approximately 16.5 ± 0.6 Mya (Becker, 1987b). We used 15.9Ma as the minimum time constraint to calibrate the split between Falconidae and Polynorinae.

24) Crown Columbiformes - *Gerandia calcaria*

Gerandia calcaria is the earliest dove known, from the early Miocene (Aquitanian) of France between 23 – 20.4 Mya (Gradstein & Ogg, 2004). It was described as *Columba calcaria* from a single humérus; and renamed later as *Gerandia* (Olson 1985). We use the minimum age of the Aquitanian, 20.3 Mya, as a minimum time constraint for the basal node of Columbiformes.

25) Split *Casuarius* / *Dromaius* - *Emuarius gidju*

Emuarius gidju was firstly described as *Dromaius gidju* by Patterson and Rich (1987), from the Miocene Kutjamarpu local fauna of central Australia. The type of the

fossil was recovered from the Wipajiri Formation, Lake Ngapakaldi, Etadunna Station, eastern Lake Eyre basin, South Australia. However, given the similarity of hindlimb characters to both cassowaries and emus, Boles (1992) assigned this fossil to the genus *Emuarius*. Other specimens assigned to this species were found from the Oligocene and Miocene in Riversleigh deposits, northwestern Queensland. Those deposits are considered closer to the Lower Miocene or even Upper Oligocene (25 Mya) (Boles, 1992; Archer *et al.*, 1989). We consider as a minimum age of this taxon around 23 Mya to calibrate the divergence between *Casuarius* and *Dromaius*.

Rate estimates

We performed Bayesian analyses as implemented in BEAST2 v.2.4.7 (Bouckaert *et al.*, 2014) to estimate the substitution rate per locus. The choice of this software was based on its capability to accommodate different parameters into the analysis (such as substitution models for each codon position and multiple options of relaxed molecular clock), as well as the capability of recovering a rate for each gene in all the nodes of the tree.

We set independent partitions for every gene to estimate each molecular clock rate, and for every codon position to fit the nucleotide substitution models selected. We used PartitionFinder (Lanfear *et al.*, 2012) to find the best substitution model for each codon position in each gene (Table 1).

We selected the lognormal relaxed clock implemented in BEAST2. In order to avoid misleading results due to the clock selection, we also ran an analysis under a random local clock model to compare between results. Due to the fast rate of change in mtDNA, saturation becomes an issue affecting the topology at deeper nodes. To minimize this problem, we constrained the topology of the tree by grouping species' sequences into their corresponding orders, as well as the phylogenetic relationships between orders based on the results from Prum *et al.* (2015). Relationships between Galliformes families were also constrained to fit that topology. The phylogenetic tree was computed using all genes combined, following a birth-death Yule model.

Given the complexity of the analysis, the MCMC chain needed a large number of generations in order to reach stability. We ran the chain for 1 billion (1.000 million) generations, discarding the first 500 million as pre-burn-in and sampling every 5000 states. To avoid results based on a local maximum, a second 600 million chain was run independently to compare. The random local clock analysis also ran for 500 million generations.

Additionally, we ran an analysis using only the information from the priors, to determine whether the posterior probability of the results is driven solely by the priors, or if the data are also introducing information into the final results.

GENE	POSITION 1	POSITION 2	POSITION 3
12S	TN93+I+G	TN93+I+G	TN93+I+G
16S	TN93+I+G	TN93+I+G	TN93+I+G
ATP6	TN93+I+G	TN93+I+G	TN93+I+G
ATP8	TN93+I+G	TN93+I+G	TN93+I+G
CO1	TN93+I+G	TN93+I+G	TN93+I+G
CO2	TN93+I+G	TN93+I+G	TN93+I+G
CO3	TN93+I+G	TN93+I+G	TN93+I+G
CYTB	TN93+I+G	TN93+I+G	TN93+G
ND1	TN93+I+G	TN93+I+G	TN93+G
ND2	TN93+I+G	TN93+I+G	TN93+G
ND3	HKY+G	HKY+G	HKY+G
ND4L	TN93+I+G	TN93+I+G	TN93+I+G
ND4	TN93+I+G	TN93+I+G	TN93+I+G
ND5	TN93+I+G	TN93+I+G	TN93+G
ND6	TN93+I+G	TN93+I+G	TN93+I+G

Table 1: nucleotide substitution models employed for each partition by locus of the complete mitochondrial genomes in the BEAST2 analyses

We also ran an aminoacid analysis, using the same specifications as in the main analysis, except for the substitution models, where we used MTREV for each of the partitioned markers as implemented in BEAST2. Aminoacid sequences are much more conserved than nucleotide sequences. Therefore, this allowed us to compare both analyses in order to determine the effect of the saturation of mtDNA in the topology and divergence time estimates.

Shorebird mtDNA genetic data

There are no nuclear DNA datasets available for shorebirds covering their full range, and fresh tissues were not available to us to generate such datasets. We assembled mitochondrial DNA datasets for Arctic shorebird species for which genetic data are available. We increased the number of sequences from published datasets available in Genbank by incorporating many unpublished data from the BarCodingofLife initiative (http://www.boldsystems.org) (accession numbers: Appendix 4). For most species there were less than two sequences available for each population to compare, often with large parts of their ranges unsampled and/or with different genetic markers for different populations. Hence, we considered all Arctic-breeding or boreal-breeding species and discarded the ones for which data were incomplete or absent. After this filtering, only 10 species had suitable data for analyses: five of them from the family Charadriidae (*Charadrius hiaticula, Pluvialis squatarola, Pluvialis fulva, Pluvialis apricaria and Pluvialis dominica*) and five from Scolopacidae (*A. interpres, C. alpina, C. canutus, C. ptilocnemis* and *L. limosa*). All these species have described morphological subspecies with various degrees of differentiation at the genetic level, except for *P. fulva* and *P. dominica* which are monotypic. All four *Pluvialis* species were analysed as a single group to compare the patterns of intraspecific diversity with the speciation of closely related Arctic species. The mitochondrial markers used were the subunit 1 of the cytochrome C oxidase (COI) in *A.interpres*, *C. canutus*, *C. hiaticula*, *L. limosa*, *P. apricaria*, *P. dominic*a, *P. fulva* and *P. squatarola*; the Cytochrome B (CytB) in *C. alpina*; and the subunit 2 of the NADH dehydrogenase (ND2) in *C. ptilocnemis*.

Every dataset was aligned using Clustal-Wallis as implemented in Bioedit and corrected by eye. We then used PartitionFinder to determine the best substitution model for each of them for further analyses.

Molecular clock analyses

To determine the diversification between and within species, we performed divergence time analyses by assembling time-calibrated Bayesian phylogenies for each species using the software BEAST2 (v 2.4.4). We applied a strict molecular clock model given the low rate variation and genetic diversity expected when working at the intraspecific level, as recommended by Ho *et al.* (2017), as well as by the authors of the software (Drummond & Rambaut, 2015). As substitution rate, we used the values obtained from the calibration of the mitochondrial molecular clock analyses. We considered the rate that specifically belongs to the crown group of each species in each corresponding mtDNA marker: for the COI, 0.0013 s/s/l/My in Scolopacidae and 0.0014 s/s/l/My in Charadriidae; for Cyt b, 0.0015 s/s/l/My (Scolopacidae); and for ND2, 0.0025 s/s/l/My (Scolopacidae). Following recommendations made by Drummond & Rambaut (2014) we set a constant population size tree prior, given the nature of the available data and the fact that we are not aiming to explore complex population dynamics. The Bayesian analyses were run for 100 million steps, sampling every 2000 steps. We then used Tracer v 1.4 to check the stabilization of the MCMC chains and the posterior distribution of all estimated parameters.

Genetic diversity and population size changes:

We used DNAsp v6 (Rozas *et al.*, 2017) to calculate indices of genetic diversity (haplotype diversity, nucleotide diversity), as well as the values of Fu´s F (Fu, 1997), Fu and Li´s F* and D* (Fu & Li, 1993) and Tajima's D (Tajima, 1989) to measure departures from a neutral model of evolution in the form of recent population expansions or bottlenecks. We included, for these analyses only, other monotypic species of Arctic shorebirds not included in the molecular clock analysis due to uneven sampling and lack of representation from all populations across their ranges. We estimated these values

from all the available GenBank sequences for *C. maritima* (Cyt b), *Calidris melanotos* (COI), *Phalaropus fulicarius* (COI), *Tringa erythropus* (COI) and *Tringa nebularia* (COI). The inclusion of these monotypic species, whose ranges were potentially fragmented during the LGM (see Chapter 1), allowed us to compare potential mismatches in the demographic histories between monotypic species and those with subspecies.

ABC coalescent hypothesis testing:

We used coalescent approximate Bayesian computation (ABC) implemented in DIYABC 2.1.0 (Cornuet *et al.*, 2008). This method allows testing different hypothesis by defining scenarios of lineage diversification for which different likelihoods are calculated. Hence, we defined six non-overlapping scenarios to test hypotheses on lineage diversification. From the most recent to the oldest period, we defined scenario 1 from the end of the Last Glacial maximum to the Present [Holocene, from 11,700 years ago (ya) to the present]. Scenario 2 spans from 430,000 to 11,700 ya, a period of multiple long (ca. 100 ky) glacial cycles with short (< 30 ky) but warm interglacial periods in between (EPICA community members, 2004; Jouzel *et al.*, 2007). Scenario 3 spans from 940,000 ya to 430,000 ya, a period in the Middle Pleistocene when the duration and ice accumulation during glacial periods increased from the previous cycles, reaching the 100-ky duration (Jouzel *et al.*, 2007). Scenario 4 spans from 1,200,000 to 940,000 ya, a transition period between the Early Pleistocene and the Middle Pleistocene where glacial and interglacial periods showed lower amplitude than in scenarios 2 and 3 but started to gain amplitude and intensity (Lisiecki & Raymo, 2005; Cohen & Gibbard, 2008). Scenario 5 spans from 2,595,000 ya to 1,200,000 ya in the Early Pleistocene, where the climatic cycles were shorter and with a lower amplitude. Scenario 6 corresponds to the Pliocene, spanning from 5,300,000 ya to 2,595,000 ya and it was included to cover the case that some species' diversification predated the Pleistocene.

We applied this approach to compare intraspecific divergence in species showing clear genetic structure in the BEAST analyses, with lineages congruent with their described populations or subspecies emerging within or shortly before the Pleistocene: in *C. alpina* between Alaskan and Siberian lineages and between Canadian and European lineages; in *C. ptilocnemis* between *C. p. ptilocnemis* and the other subspecies from the

continental coast and Aleutian Islands; and in *L. limosa* between *L. l. limosa* (western Palearctic) and *L. l. islandica* (Iceland).

We used large uniform priors (10 – 2,000,000) for the present and ancestral effective population sizes. For the substitutions per generation, we transformed the same rates used in the molecular clock analyses, as well as the HKY substitution model. We assumed a generation time of 2 years (Kees *et al.*, 2001). For each comparison, we simulated datasets of 10 million points. We calculated the posterior probability of each scenario using the logistic regression method implemented in DIYABC.

Results

Molecular rate estimates

Log-normal analyses provided a tree topology with most nodes recovered as highly supported (>98% of nodes above 0.9 posterior probability) and fully resolved. The Maximum Clade Credibility method implemented in TreeAnnotator forcefully prevents polytomies, but no signs of conflict were found in the resolution of any of the nodes of the tree. Results from the sample from prior differed from those from the main analyses, indicating that the recovered posterior probabilities are not just a product of the priors, as the data are also responsible for the obtained results. The random clock analysis returned a phylogeny where most of the nodes of the tree were younger than 1 Mya. Thus, we considered this method unreliable and discarded it as an alternative. The topology of the amino acid tree (not shown) matched the topology obtained from nucleotides except minor differences at the position of certain tips, affecting under 5% of the species.

The resulting phylogenetic tree had an overall high support, with over 98% of the nodes with a posterior probability above 0.9. We recovered a root age (Palaeognatha / Neognatha split) at 88.3Mya (95% CI = 90.9 – 85.4 Mya). The split between Neoaves and Galloanserae is recovered at 87.9 Mya (90.7 – 85.3). The divergence between all extant avian orders occurred before or around the transition between the Cretaceous and the

Paleogene, 66My before present, and most of their diversification took place during the Paleogene and Neogene (phylogenetic tree in Appendix 6 Fig. S1).

In general, the fossil-calibrated nodes returned ages several million years older than the minimum age established. The only two exceptions were the calibrations for the Sphenisciformes / Procellariiformes split (minimum age = 60.5Mya) and the *Dromaius* / *Casuarius* split (min. age = 23.03Mya). In both cases, the posterior distribution was potentially clipped by the hard minimum bound of the prior, but still displayed normal distribution and the mean ages were slightly older than the minimum constraint (not shown).

Our approach allowed us to obtain substitution rates for each gene across each node of the tree. We found variation in the rates between genes, and to a lesser extent between lineages in the tree in each gene. The highly conserved ribosomal genes 12S and 16S showed the lowest mean substitution rate over the whole tree (0.00107 and 0.00043 s/s/l/My, respectively), while ND2, ATP6 and ATP8 returned the highest overall rate values (0.00227, 0.00215 and 0.00260 s/s/l/My, respectively) (Fig.1). Overall, the rate values in each gene showed very little variation across the branches of the tree (Fig. 2), and there were no major differences in the overall mitochondrial rates between orders (Fig. 3). Only the order Otidiformes showed values distributed mostly below the overall average, although this is the only order represented by just a single species, and could be affected by a punctual underestimation of the rates. The values of the rates per gene for each order can be found in the Appendix 5 (Table S1).

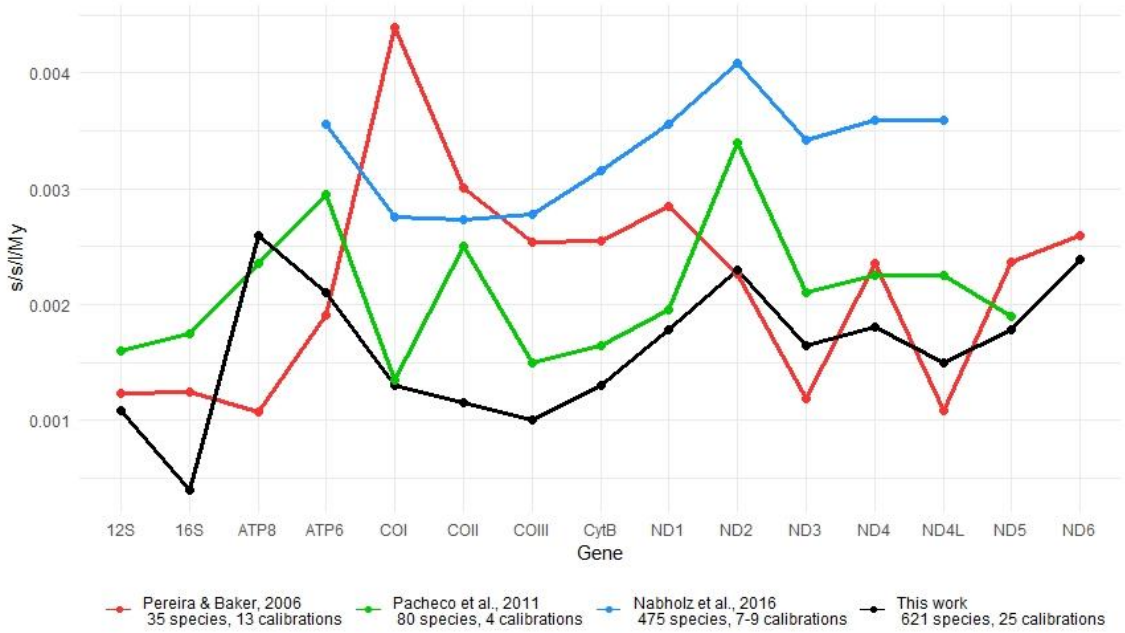

Figure 1: Comparison of the mean substitution rate estimates for each mitochondrial gene, between previous mitogenomic studies and our results (black line), with the number of species and fossil calibrations included in each analysis.

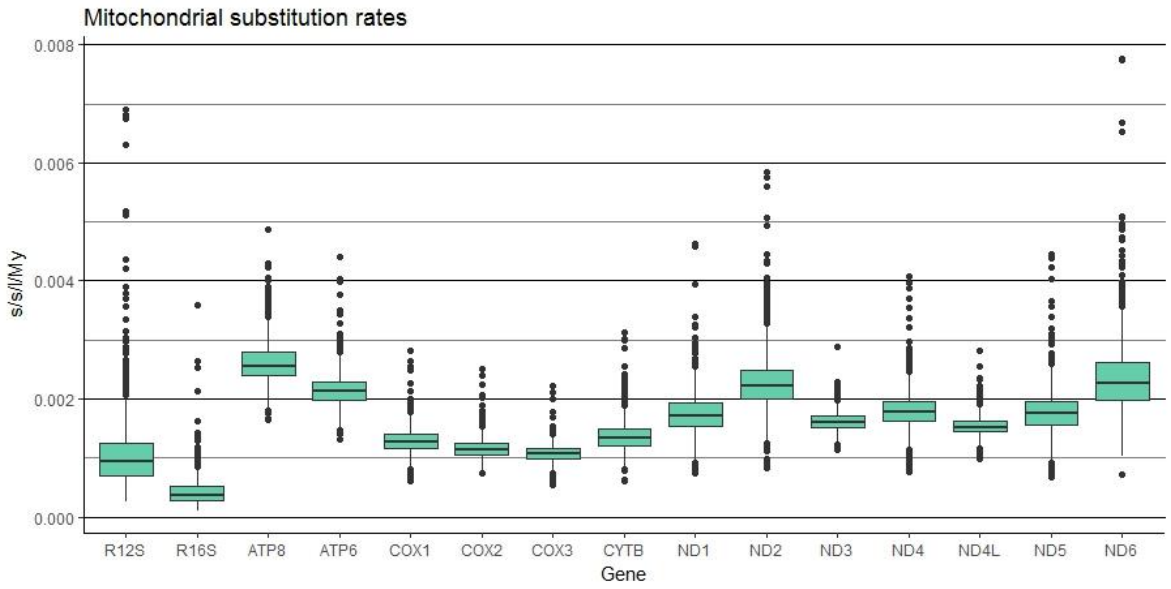

Figure 2: boxplot of the substitution rate values (in substitutions / site / lineage / million years) from every node of the mitogenomic tree, for each of the 15 mitochondrial genes analysed.

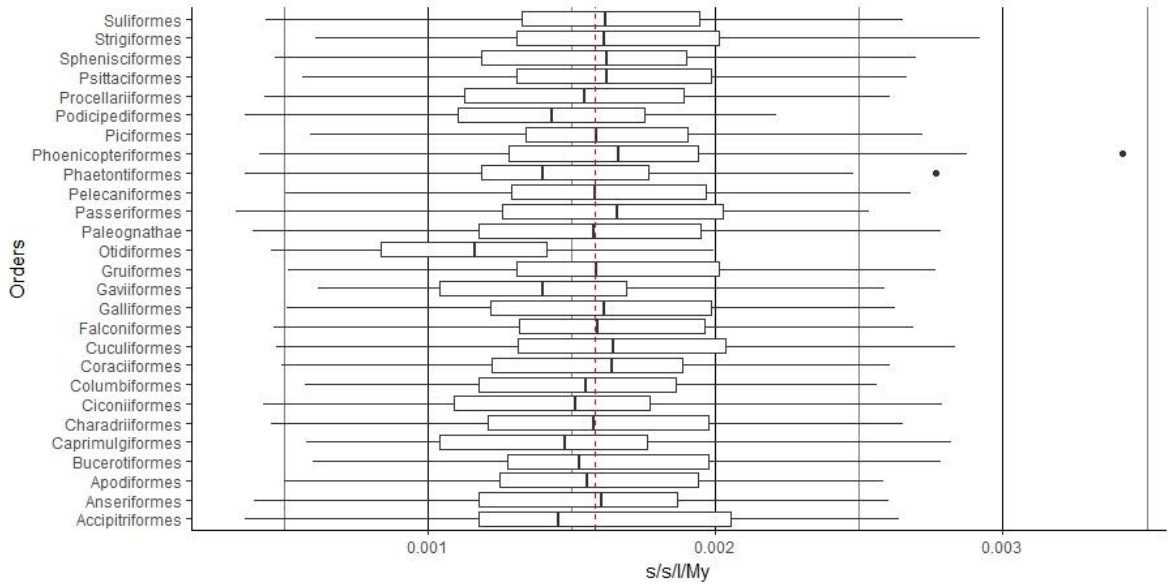

Figure 3: boxplot of the average substitution rate values (in substitutions / site / lineage / million years) of all 15 mitochondrial genes analysed for each of the orders of birds.

Divergence time analyses of shorebirds

The molecular clock analyses performed in BEAST2 allowed us to recover the main lineages within species, the relationships between them and the timing of the splits. Given the wide variety of diversity patterns, some species showed a clear genetic diversification, while others do not present genetic structure.

In *C. alpina*, we recovered 4 main lineages: north and eastern Russia, Alaska, Canada and Europe (Fig. 5). There is also a clear split in the phylogenetic tree, with the Russian and Alaskan lineages forming a clade, and those from Europe and Canada as another clade. Within the Russian lineage, the samples from the subspecies *C. a. actites* (from the north of the Shakalin Island) constitute a separate clade from all the other samples, which comprise *C. a. shakalina*, *C. a. kistchinski* and samples from the Taymyr region. The Alaskan lineage contains 4 samples identified as *C. a. shakalina*. No distinctive groups or geographical structure were found within this lineage. We recovered the separation of both lineages at 5.3 Mya (95% confidence interval = 7.5 – 3 Mya) (Fig. 5). The most recent common ancestor (MRCA) of all the samples within the Russian lineage dates back to 2.5 Mya (CI = 4.1 – 1 Mya), and 3 Mya (CI = 4.9 – 1.5 Mya) in the Alaskan lineage (Fig. 6). In the populations from Canada and Europe, there was no evidence of further geographic structure. The split between these two lineages in our

analysis was recovered at 3 Mya (CI = 5.6 – 1 Mya) (Fig. 5). The MRCAs of the samples within each of these lineages are dated at 1.8 Mya in the Canadian population (CI = 3.4 – 0.5 Mya) and 1.3 in Europe (CI = 2.9 – 0.2 Mya) (Fig. 6).

In *C. ptilocnemis* we recovered a lineage formed by *C. p. quarta*, from the Kamchatka peninsula, separated from all the other samples at 1 Mya (CI = 1.7 – 0.6 Mya) (Fig. 5), and with a diversification from its MRCA within the population at 0.06 Mya (CI = 0.2 – 0 Mya) (Fig. 6), although this result represents just 2 samples. Among the remaining samples, we recovered two separated lineages: one containing *C. p. ptilocnemis* (Bering Sea islands) and a single *C. p. tschuktschorum* sample, and the other containing both *C. p. tschuktschorum* (continental Alaska and Siberia) and *C. p. couesi* (Aleutian Islands). The separation between these two populations is dated at 0.6 Mya (CI = 0.96 – 0.28 Mya) (Fig. 5). The MRCA within the lineage containing *C. p. tschuktschorum* and *C. p. couersi* is recovered at 0.5 Mya (CI = 0.7 – 0.2 Mya) (Fig. 6). Within *C. p. ptilocnemis* the age of the MRCA is estimated at 0.2 Mya (CI = 0.4 – 0 Mya).

Within *L. limosa* we recovered a split between the subspecies from the eastern Palearctic (*L. l. melanuroides*) and all those from the western Palearctic at 6.4 Mya (CI = 9.9 – 3.2 Mya) (Fig. 5). *L. l. limosa* forms a paraphyletic group, since it also contains *L. l. islandica*. The separation between *L. l. islandica* and *L. l. limosa* is dated at 0.75 Mya (CI = 1.44 – 0.25 Mya) (Fig. 5). The ages of the MRCA of each of the subspecies are 1 Mya in *L. l. limosa* (CI = 2 – 0.3 Mya), 0.3 Mya in *L. l. melanuroides* (CI = 1 – 0 Mya) and 0.1 Mya in *L. l. islandica* (CI = 0.3 – 0 Mya) (Fig. 6).

In the genus *Pluvialis*, the estimated divergence times between species trace back to the Miocene period (23 – 5.3 Mya) (Fig. 5). The species from the eastern and western Palearctic (*P. fulva* and *P. apricaria*, respectively) were recovered as sister species, with the Nearctic species (*P. dominica*) as their closest relative. The nearly circumpolar *P. squatarola* diverged from the other 3 species at the basal split of the resulting tree (Fig. 6).

Despite the old ages of the species, no geographical structure was recovered within them. Only two of the species, *P. apricaria* and *P. squatarola* have described morphological subspecies, but we found no differentiation between them in the genetic analyses. The ages for the MRCA of the samples within each of the species are 0.9 Mya

in *P. apricaria* (CI = 1.8 – 0.3 Mya), 1.2 Mya in *P. fulva* (CI = 2.2 – 0.3 Mya) and *P. dominica* (CI = 2.6 – 0.3), and 1.8 in *P. squatarola* (CI = 3 – 0.7 Mya) (Fig. 6).

A. interpres, *C. canutus* and *C. hiaticula* showed no geographic structure (Fig. 5) for the mtDNA marker used, despite the fact that all three have described subspecies (Engelmoer & Roselaar, 1998; del Hoyo, 2018; Thies *et al.*, 2018).

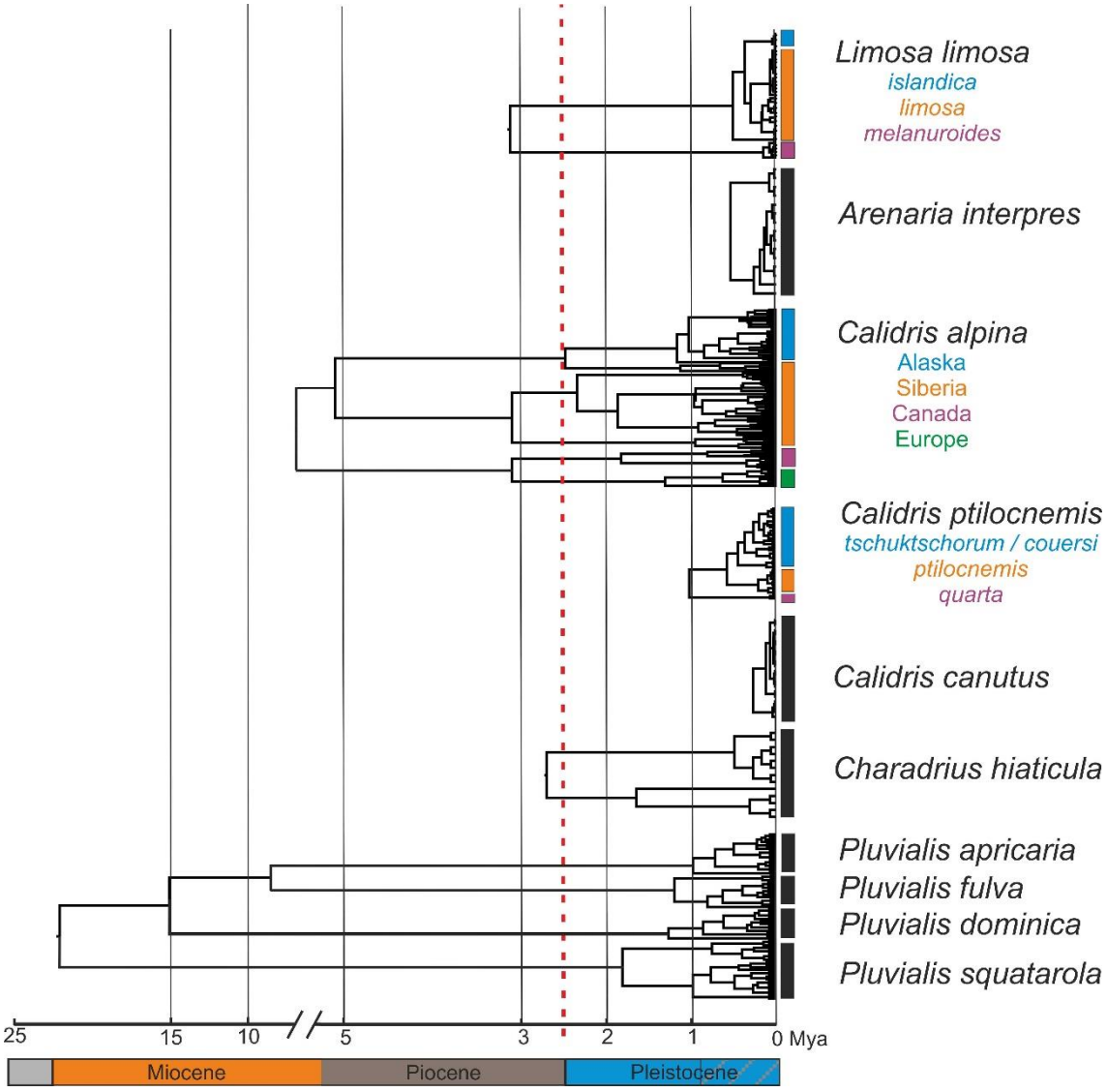

Figure 5: Bayesian phylogenetic chronograms for the studied species. Colours represent the different geographically structured lineages recovered. Black bars represent lack of geographic structure in the results despite the existence of subspecies in some cases. The red dotted line represents the beginning of the Pleistocene period.

Genetic diversity and population size changes

Haplotype diversity in the studied species ranged from 0.8 in *C. ptilocnemis* (Hd = 0.878) and *C. alpina* (Hd = 0.849) to below 0.3 in *P. dominica* (Hd = 0.295) and *P. apricaria* (0.118) (Table 2). Only three species showed more than five haplotypes: *L. limosa* (h = 7), *C. ptilocnemis* (h = 13) and *C. alpina* (h = 29). *C. canutus* and *P. apricaria* had the lowest values of nucleotide diversity (π = 0.00058 and π =0.00019), respectively. None of the studied species with subspecies showed a statistically significant deviation from neutrality in the Tajima's D and Fu and Li's F* and D* tests ($p > 0.10$ in all cases). Obtained values of Fu's F were close to 0 in all the species except *C. alpina* (-18.548) and *C. ptilocnemis* (-4.735) (Table 2).

Comparatively, the monotypic species analysed showed a similar range of haplotype diversity (Hd = 0.02 – 0.7) and overall low nucleotide diversity (π = 0.0004 – 0.0033) (Table 2). Neutrality tests showed statistically significant deviations with $p < 0.05$ in *P. fulicarius* for both tests and in *C. maritima* for the Fu and Li's tests. Results were non-significant, but with $p < 0.10$, in the Tajima's D test for *C. maritima* and for both tests in *T. erythropus*. In all these cases, values for Fu's F, Fu and Li's F* and D*, and Tajima's D were negative, indicating an excess of rare alleles (Table 2).

		Haplotypes			Nucleotide divers.	Fu's F	Fu and Li's test				Tajima's D	
Species	**N**	**h**	**Hd**	**var**	**π**	**F**	**F***		**D***		**D**	
A. interpres	15	4	0.600	0.012	0.00111	-1.161	-1.138	-	-1.081	-	-0.764	-
C. alpina	139	29	0.849	0.000	0.00852	-18.548	-1.619	-	-1.596	-	-0.961	-
C. canutus	20	2	0.337	0.012	0.00058	0.721	0.652	-	0.649	-	0.352	-
C. ptilocnemis	40	13	0.860	0.002	0.00218	-4.735	-0.572	-	-0.165	-	-1.130	-
C. hiaticula	13	4	0.603	0.017	0.00506	2.132	1.019	-	0.791	-	0.186	-
L. limosa	77	7	0.541	0.004	0.00519	2.986	0.432	-	0.706	-	-0.247	-
P. apricaria	17	2	0.118	0.010	0.00019	-0.748	-1.591	-	-1.477	-	-1.163	-
P. dominica	13	3	0.295	0.024	0.00153	-1.401	-1.922	-	-1.776	-	-1.468	-
P. fulva	14	3	0.626	0.011	0.00124	0.206	0.911	-	0.935	-	0.415	-
P. squatarola	25	5	0.603	0.006	0.00143	-1.699	-1.820	-	-1.850	-	-0.865	-
C. maritima	285	17	0.548	0.001	0.00181	-9.203	-2.464	**	-2.356	**	-1.565	*
C. melanotos	23	4	0.605	0.006	0.00134	-0.694	-0.263	-	-0.174	-	-0.367	-
P. fulicarius	33	5	0.023	0.009	0.0004	-4.611	-3.166	**	-3.074	**	-1.888	**
T. erythropus	9	4	0.583	0.033	0.00151	-1.238	-1.940	*	-1.799	*	-1.609	*
T. nebularia	12	5	0.727	0.013	0.00339	-0.113	-0.366	-	-0.503	-	0.199	-

significance: ** $p < 0.05$; *$p < 0.10$; - not significative

Table 2: DNAsp results for all the analysed species, including number of samples (N), number of haplotypes (h), haplotype diversity (Hd) and its variance (var), nucleotide diversity (π) and the neutrality tests and their significance. The dashed line separates the species included in the molecular clock analyses (above) and those included only in this analysis (below).

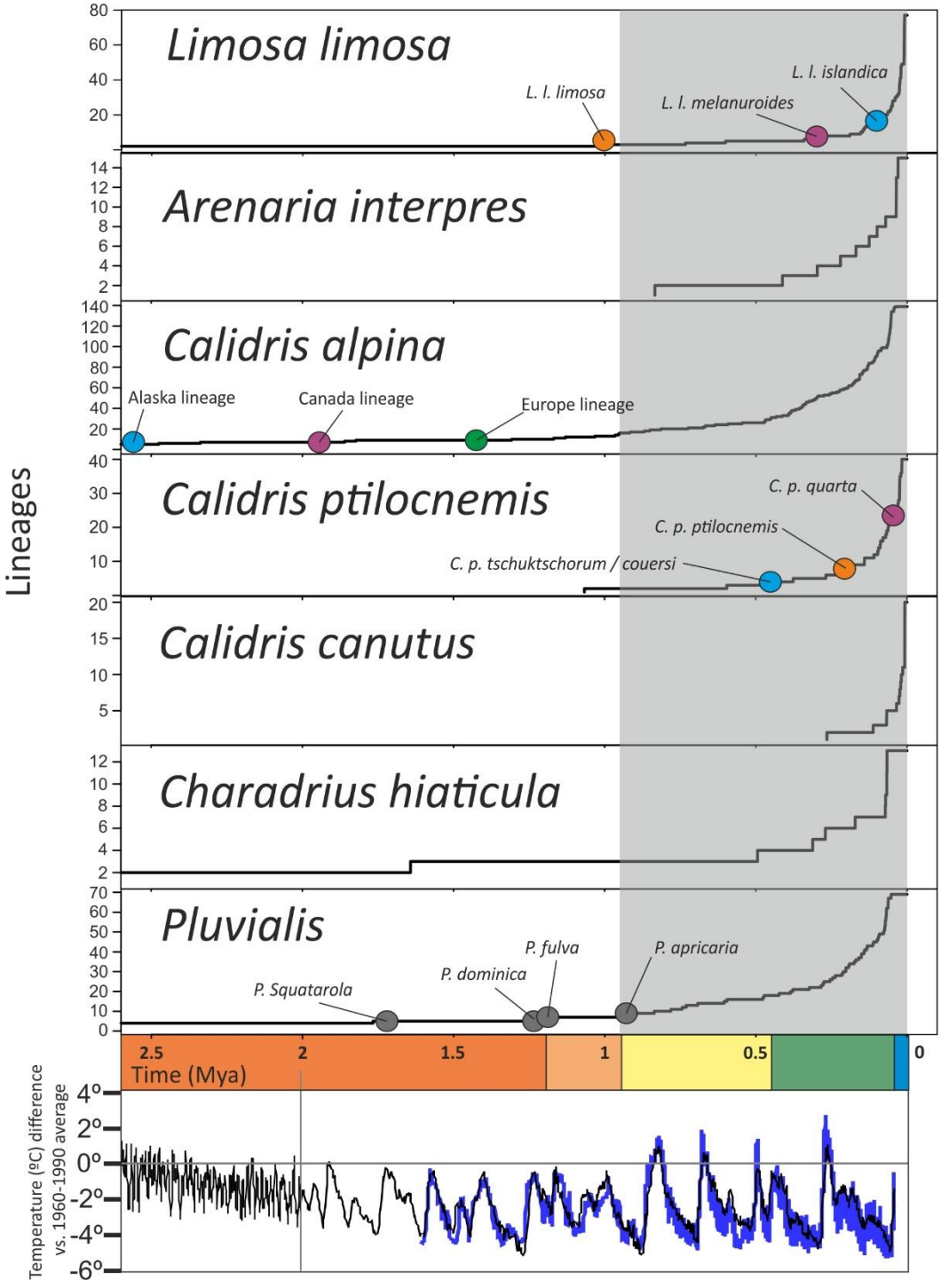

Figure 6: Above, accumulation of lineages through time (LTT) in each of the Bayesian phylogenetic trees. The dots represent the estimated MRCA of all the samples within the defined population in each species, with colours following the same code as in figure 1. Below, the variation of the temperature during the Pleistocene as estimated by Lisiecki & Raymo (2005) and EPICA community members (2004) (black line); and Jouzel *et al.* (2007) (blue line). Colours in the X axis mark the temporal scenarios used in the ABC analyses: The Early Pleistocene (dark orange), the transition from Early to Middle Pleistocene (light orange), the Middle Pleistocene (yellow), the Late Pleistocene (green) and the Holocene (blue). The grey area represents the period of increase in duration and amplitude of the glacial periods.

ABC hypothesis testing

In *C. alpina*, the ABC analysis assigned the divergence between the Asian and Alaskan lineages to the scenario 6 (pre-Pleistocene) as the most likely (probability = 0.40) (Fig. 7), while the split between European and North American lineages returns two scenarios as the most likely ones for this split: scenario 6 (pre-Pleistocene) (prob. = 0.32) or scenario 5 (early Pleistocene, 2.6 – 1.2 Mya) (prob. = 0.31) (Fig. 7).

In *C. ptilocnemis*, no ABC analysis was performed on the split of *C. p. quarta*, as only 2 samples represent this subespecies. For the split between the continental populations and those from the Bering Sea, ABC analyses returned the scenario 2 (late Pleistocene, 460 – 11.7 kya) as the most likely (p = 0.33) (Fig. 7).

For the split between *L. l. limosa* and *L. l. melanuroides*, three temporal scenarios had similar high probabilities: scenario 2 (460 – 11.7 kya) (p= 0.23), scenario 3 (940 – 460 kya) (p = 0.27) and scenario 4 (1.2 Mya – 940 kya) (p = 0.24) (Fig. 7).

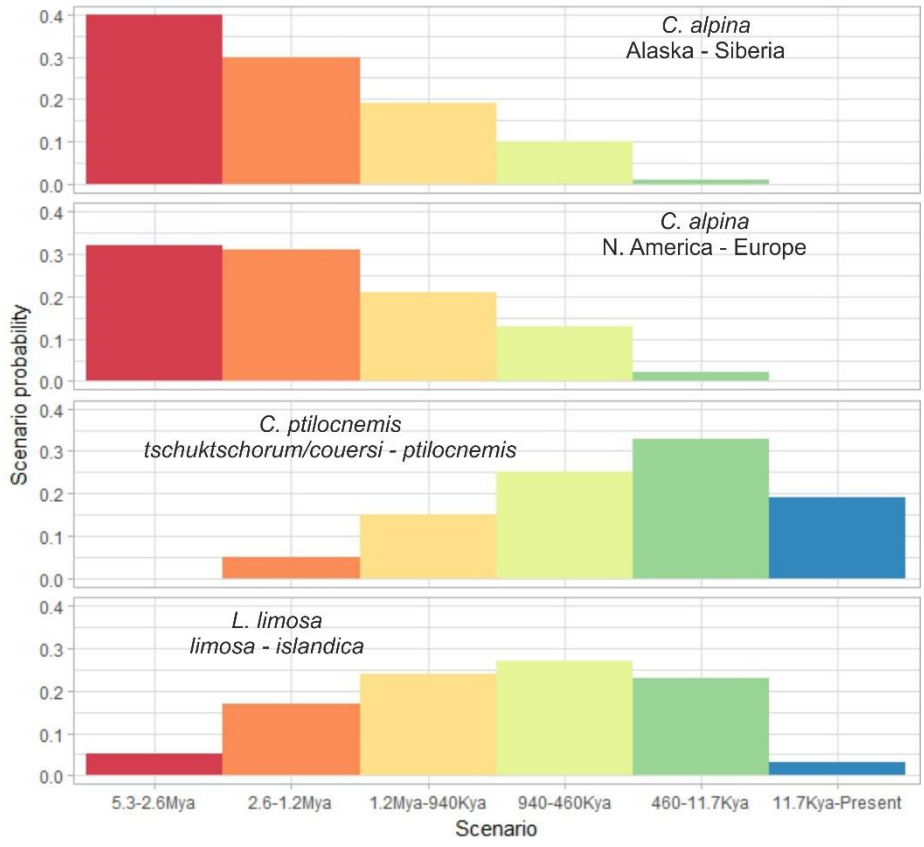

Figure 7: Posterior probability of each of the temporal scenarios in the ABC analyses for lineage divergence: The Pliocene (red), the Early Pleistocene (dark orange), the transition from Early to Middle Pleistocene (light orange), the Middle Pleistocene (yellow), the Late Pleistocene (green) and the Holocene (blue).

Discussion

Several works explored the phylogeographic variation of Arctic shorebirds and their diversification during the Pleistocene, yet there still was a need for an integrative comparative analysis including multiple species to address the potential role of Pleistocene glacial cycles in their diversification. In the Chapter 1 we tested several spatial hypotheses that could explain the observed intraspecific variation as well as global biodiversity patterns of Arctic shorebirds, suggesting that the fragmentation of their ranges during glacial and / or interglacial periods drove their diversification. To confirm that this diversification happened during the Pleistocene in parallel to the proposed spatial-climatic mechanisms, we needed a time calibration of these events, which is here confirmed with genetic data. The molecular methods used in this chapter, analysing species with different distributions and diversity patterns under a common framework, allow us to support that the diversification time in most species happened during the Pleistocene and mainly overlapping with longer and more intense glacial periods.

Shorebird fossils cannot be reliably assigned to subspecies to determine intraspecific variation and often they cannot even be assigned to species, as fossil remains usually consist in bone fragments instead of full skeletons, and the lack of fossils from Arctic regions prevents also ancient DNA molecular studies. Hence, any estimation of the times of divergence within or between species relies on mutation rates applied to current genetic data. So far, mitochondrial DNA has been widely used to infer relationships within and between shorebird species (Baker *et al.*, 1994, 2007; Wenink *et al.*, 1996; Pereira *et al.*, 2007; Marthinsen *et al.*, 2008; Pruett & Winker, 2008; Miller *et al.*, 2013 Trimbos *et al.*, 2014; Barisas *et al.*, 2015), and mutation rates from other bird groups were applied to infer diversification times (Baker *et al.*, 1994; Wenink *et al.*, 1996; Buehler & Baker, 2005; Barisas *et al.*, 2015). We here addressed this issue by compiling a large dataset of mitogenomic data, including several shorebird species, and the most comprehensive set of fossils to serve as calibration constraints to infer divergences times and mutation rates per locus for each bird species included, which

can then be used in intraspecific analyses.

Our analyses represent the most comprehensive ones of this type ever performed, both in terms of species coverage and fossil calibrations used, and for the first time provide lineage-specific rates for each of the mtDNA genes for the main extant bird groups. Also, by including several shorebird species, specific mutation rates for shorebirds were applied to our intraspecific datasets with confidence. The relationships obtained in the avian phylogeny at species, genus and family levels are overall congruent with previous large-scale analyses performed with mitochondrial and nuclear DNA data (e.g. Brown *et al*., 2008; Hackett *et al.*, 2008; Pacheco *et al*., 2011; Claramunt & Cracraft, 2015). The root age in our tree falls within the interval of the most recent estimations for the origin of modern birds (Jarvis *et al*., 2014; Prum *et al*., 2015), and support an origin of most of the current lineages around the transition from the Cretaceous to the Paleogene (Brown *et al*., 2008; Claramunt & Cracraft, 2015). Although the focus of this work is not on the detailed phylogenetic relationships between bird species, our results showed slight discrepancies in the placement of Achanthisittidae, which we recovered together with the sub-oscines instead of as the sister taxa of all other Passeriformes (Barker *et al.*, 2004; Olson *et al*., 2013; Ericson *et al.*, 2014), and also in the position of the Ostrich (*Struthio camelus*) that recent genomic analyses place at the base of all Paleognaths (Mitchell *et al.* 2014; Yonezawa *et al*. 2017). Both cases represent isolated lineages at the base of old taxonomic groups, where the resolution power of the mtDNA is often insufficient to fully clarify these relationships, and have a reduced effect the overall topology and dating of the phylogenetic tree.

Results from previous mitogenomic studies (Pereira & Baker, 2006; Pacheco *et al.*, 2011; Nabholz *et al.*, 2016) showed significant variances, lacking full agreement in the values obtained. But, in all cases, they found lower rates than the so-called “standard” molecular clock of 0.01 s/s/l/My (Fig. 1). Our results also do not fully match those from previous rate estimations by gene, but nevertheless the obtained values fall within the range of the variation between previous works (Fig. 1). Furthermore, the differences in mean rate values between genes in our study parallel the values obtained in the most recent study on bird mutation rates, which previously was the most taxonomic-rich and phylogenetically updated analysis (Nabholz *et al.*, 2016) (Fig. 1, blue line), being our mutation rate estimates lower than in Nabholz *et al.* (2016).

Differences in mutation rates can be the consequence of several causes, from the inclusion or elimination of third codon positions that are generally saturated at deeper phylogenetic levels but not within species, to the impact of hard maximum bounds in fossil time constraints that force younger ages in the phylogeny (Ho *et al.*, 2005, 2007, 2008), and even the choice of software or other specific parameters could be introducing variation (Drummond & Rambaut, 2015). Given the variety of methodologies that have been used in previous mitogenomic rate estimations for birds (Pereira & Baker, 2006; Pacheco *et al.*, 2011; Nabholz *et al.*, 2016), we are unable to assess whether the differences between our work and previous studies are caused by one or several of the mentioned causes, or by any other cause. In any case, we are confident that given our large taxonomic coverage, the amount of reliable fossil calibrations and the methodology applied (e.g. no maximum-age constraints, very long Bayesian MCMC runs reaching stabilization), our results provide a reliable estimation of the molecular clock substitution rates in birds, and as such we applied them in our phylogenetic analyses. Furthermore, these results contradict the hypothesis of a universal molecular clock for all bird lineages and mitochondrial genes, something in which previous mitogenomic analyses also agreed on (Pereira & Baker, 2006; Pacheco *et al.*, 2011; Nabholz *et al.*, 2016), but was already criticized (Garcia-moreno, 2004; Lovette, 2004).

According to our results, the variation in rate values between mitochondrial genes was much more marked than the variation within each gene between linages of the tree (Figs. 2 and 3; Appendix 5). However, the use of general rate values should be avoided, in favour of taxon-specific rates from the closest lineage available. Previous divergence time estimations within Arctic shorebird lineages using mtDNA were based on the standard molecular clock rate (Pruett & Winker, 2005; Rönkä *et al.*, 2012), or in general rates for the Control Region across all bird lineages (Wenink *et al.*, 1996; Buehler & Baker, 2005; Ottvall *et al.*, 2005). In contrast, we based our analyses on our new rate estimations, specific for each marker and the lineage of each species, to obtain more accurate estimations that are comparable between them.

The time calibrated genealogies for the 10 species included in this study support a Pleistocene diversification within species, except for *Calidris alpina* that predates the

Pleistocene for the main genetic lineages, with subsequent Pleistocene diversification of several populations and subspecies. These results were also confirmed with ABC hypothesis testing analyses. Most of the observed intraspecific diversification took place in the second half of the Pleistocene, especially during the last 900,000 years, coinciding with an increased intensity and duration of the glacial periods. Hence, this genetic evidence supports the spatial geographic hypotheses presented in Chapter 1, and in combination they strongly highlight the Pleistocene climatic cycles as the main driver of the current patterns of diversity within these Arctic species.

We found that despite having morphologically differentiated subspecies, most Arctic shorebirds show very little genetic diversity, shallow differentiation between populations and no genetic structure in the analysed genetic datasets, something that it has also been reported in previous studies (Baker *et al.*, 1994; Wenink *et al.*, 1994; Ottvall *et al.*, 2005; Miller *et al.*, 2010; Miller *et al.*, 2013; Barisas *et al.*, 2015). Regarding the lack of genetic structure, it is important to acknowledge that the samples used in this study were not always collected for this purpose, so not all populations and subspecies are properly sampled and this could hinder our ability to identify population genetic structure in some species. The Arctic is a vast region with difficult access where not many researchers work across it, hence gathering tissues from breeding localities of most species and subspecies is very complicated. We are aware that the use of nuclear genomic markers would have benefitted this work, but the impossibility to get access to tissue samples impeded the generation of such datasets. So far, mitochondrial genetic data are the only source of information the community has, and further studies should try to incorporate nuclear genomic data to have a more precise picture of the diversification of these species.

The older divergence times and best-defined lineages found in *C. alpina* and *L. limosa* likely developed from populations isolated by tens of thousands of kilometres during glacial periods (see Chapter 1) that, despite secondary contacts, remained acting as independent breeding populations over glacial cycles across longer periods of time. The opposite would be the cases of *C. canutus* and *A. interpres*, whose divergence times are very recent. The available mtDNA data did not allow us to recover the described subspecies or any degree of genetic structure within these species. In both cases, their breeding ranges are constrained to the northernmost parts of the Arctic during the

breeding season, in areas that were unavailable during the LGM, and must have been colonized very recently via expansion from areas of glacial refugia. This, together with our results, point towards a very quick and recent phenotypic diversification of their current subspecies without a genetic signal in their mitochondrial DNA. This is in line with the findings from previous studies on these species, which agree in the recent origin of the populations (Baker *et al.*, 1994; Wenink *et al.*, 1994; Buehler & Baker, 2005) and the key role of post glacial expansion in their differentiation (Buehler *et al.*, 2006).

In the case of *C. ptilocnemis*, both the divergence time and ABC analyses confirm that all the lineages diverged from each other and diversified over the last half of the Pleistocene. Despite its very recent origin, its genetic structure seems the result of the geographic changes in its breeding range in Beringia during this period. Aside from the climatic and habitat changes in the region, oscillations in the sea level between glacial and interglacial periods significantly altered the available extension of emerged land and the connectivity between the islands and the continents. This has been considered a main factor in shaping the current diversity of this species (Pruett & Winker, 2005), and seems to have some degree of parallelism in other bird species in the region (Holder *et al.*, 2004; Pruett & Winker, 2008).

C. ptilocnemis is another species with a predicted continuous breeding range during the LGM. However, as a Beringian endemic species, its populations became isolated during the interglacials due to the sea level rise, which over multiple cycles shaped the main lineages within the species, as recovered in our results.

In the *Pluvialis* genus both monotypic species and species with subspecies lack genetic structure. Despite old divergence times between sister species (> 5 Mya) most of the diversification within each species took place during the Pleistocene, also peaking during the period of longer glacials.

P. apricaria and *C. hiaticula* have similar distribution patterns of their subspecies along the western Palearctic. Although both lack genetic structure, our results suggest that their intraspecific diversification happened during the Late Pleistocene. Recent

studies employing different DNA markers have successfully recovered some geographic structure in *C. hiaticula*, highlighting the combination of lineages from central Europe and west Siberia in the distribution of the subspecies, and the low diversification in the Icelandic population (Thies *et al.,* 2018). This mixture of Siberian and European lineages, especially in northern Scandinavia, is also found in other Arctic species, and is the result of the recolonization process from multiple important areas of Arctic glacial refugia during the LGM (Jaarola *et al.*, 1999; Hewitt, 2004). But more remarkably, European lineages of Arctic shorebirds are usually younger compared to lineages in Asia or North America, as seen in our results from *L. limosa*, *C. alpina* and *Pluvialis*. It could be possible that the notable intensity of the LGM and likely other glacial periods in the western Palearctic disrupted any possible stabilization of long-lasting lineages in the region (especially in Iceland and other Atlantic islands), resulting in younger and less genetically structured local subspecies within the Arctic shorebirds. This is also the case of our results for the Icelandic populations of *C. hiaticula* and *L. limosa*, in line with previous findings in those species (Trimbos *et al.*, 2014, Thies *et al.*, 2018), as well as in other migratory birds (Holder *et al*., 2004; Tiedermann *et al*., 2004; Ruokonen *et al.* 2005; Johnson *et al*., 2007; Pujolar *et al*., 2017). This idea however requires a more extensive sampling and including other sources of DNA data (nuclear, SNPs) for it to be successfully tested in the future across multiple species of Arctic shorebirds and other Arctic birds.

Whether phenotypic variation, including subspecific status, is reflected in mitochondrial DNA or not is critical to disentangle the evolutionary and biogeographic history of these Arctic species. Humphries & Winker (2011) argued that studying isolated parts of the mitochondrial or nuclear genomes could result insufficient to portray the recent evolutionary processes in arctic birds. Recent studies combining different types of genetic markers with better resolution have proven successful (e.g. Rönkä *et al.*, 2012, Trimbos *et al.*, 2014, Thies *et al.*, 2018). Nevertheless, identifying the genetic lineages corresponding to phenotypic subspecies or populations in most species remain elusive (e.g. Ottvall *et al.*, 2005; Marthinsen *et al.*, 2007; Miller *et al.*, 2013; Leblanc *et al.*, 2017). Furthermore, it seems likely that the loci that are involved in phenotypic differentiation are not in the mitochondria. The subspecific plumage differences may have arose recently by strong disruptive selection of nuclear regions involved in feather coloration,

or they have resulted from different responses to environmental conditions across the Arctic. Differences in bill length can be achieved in very short evolutionary times as this character is controlled by few loci (Abzhanov *et al.*, 2006), and with higher or lower expression levels bill lengths can change in few generations and become fixed by selective processes.

In summary, our results provide substantial support for an increased diversification in Arctic shorebirds during the Pleistocene glacial cycles. Most of their intraspecific diversity originated in the second half of the period, as the glacial cycles gained in amplitude and duration. By comparing the genetic patterns across multiple Arctic shorebird species, we found similarities in the timing and pattern of diversification between species with similar distributions, which also parallel previous findings in other Arctic taxa, especially birds and mammals. Finally, we provide the most complete estimation of the molecular clock rates for the mtDNA in birds. This will allow for more precise divergence time estimations in future studies, with specific rates for any study group and mitochondrial gene used.

References

Abascal, F., Posada, D., & Zardoya, R. (2007). MtArt: A new model of amino acid replacement for Arthropoda. *Molecular Biology and Evolution*, *24*(1), 1–5.

Abbott, R. J., & Comes, H. P. (2004). Evolution in the Arctic: A phylogeographic analysis of the circumarctic plant, *Saxifraga oppositifolia* (Purple saxifrage). *New Phytologist*, *161*(1), 211–224.

Abzhanov, A., Kuo, W. P., Hartmann, C., Grant, B. R., Grant, P. R., & Tabin, C. J. (2006). The calmodulin pathway and evolution of elongated beak morphology in Darwin's finches. *Nature*, *442*(7102), 563–567.

Archer, M., S. Hand, H. Godthelp, & D. Megirian. (1989). Fossil mammals of Riversleigh, northwestern Queensland: Preliminary overview of biostratigraphy, correlation and environmental change. *Australian Zoologist, 25*(2), 29-65.

Avise, J., & Walker, D. (1998). Pleistocene phylogeographic effects on avian populations and the speciation process. *Proceedings of the Royal Society B: Biological Sciences*, *265*, 457–463.

Baker, A. J, Pereira, S. L., & Paton, T. A. (2007). Phylogenetic relationships and divergence times of Charadriiformes genera: multigene evidence for the Cretaceous origin of at least 14 clades of shorebirds. *Biology Letters*, *3*(2), 205–210.

Baker, Allan J., Piersma, T., & Rosenmeier, L. (1994). Unraveling the intraspecific phylogeography of Knots *Calidris canutus*: a progress report on the search for genetic markers. *Journal of Ornithology*, *135*(4), 599–608.

Ballmann, P. (2004). Fossil Calidridinae (Aves: Charadriiformes) from the Middle Miocene of the Nördlinger Ries. *Bonner Zoologische Beiträge, 52,* 101-114.

Barisas, D. A. G., Amouret, J., Hallgrímsson, G. T., Summers, R. W., & Pálsson, S. (2015). A review of the subspecies status of the Icelandic Purple Sandpiper *Calidris maritima* littoralis. *Zoological Journal of the Linnean Society*, *175*(1), 211–221.

Barker, F. K., Cibois, A., Schikler, P., Feinstein, J., & Cracraft, J. (2004). Phylogeny and diversification of the largest avian radiation. *Proceedings of the National Academy of Sciences, 101*(30), 11040–11045.

Beaumont, M. A., Nielsen, R., Robert, C., Hey, J., Gaggiotti, O., Knowles, L., … Excoffier, L. (2010). In defence of model-based inference in phylogeography. *Molecular Ecology*, *19*(3), 436–446.

Becker, J.J. (1987a). *Neogene Avian Localities of North America*. Smithsonian Institution Press, Washington, DC.

Becker, J. J. (1987b). Revision of *"Falco" ramenta* Wetmore and the Neogene evolution of the Falconidae. *The Auk*, *104*(2), 270-276.

Benton, M. J., & Donoghue, P. C. J. (2007). Paleontological evidence to date the tree of life. *Molecular Biology and Evolution*, *24*(1), 26–53.

Boles, W. E. (1992). Revision of *Dromaius gidju* (Patterson & Rich, 1987) from Riversleigh, northwestern Queensland, Australia, with a reassessment of its generic position. *Natural History Museum of LA County Science Series, 36*, 195-208.

Bouckaert, R., Heled, J., Kühnert, D., Vaughan, T., Wu, C. H., Xie, D., ... & Drummond, A. J. (2014). BEAST 2: a software platform for Bayesian evolutionary analysis. *PLoS computational biology*, *10*(4), e1003537.

Brodkorb, P. (1972). Neogene Fossil Jays from the Great Plains. *The Condor*, *74*(3), 347–349.

Brown, W. M., George, M., & Wilson, A. C. (1979). Rapid evolution of animal mitochondrial DNA. *Proceedings of the National Academy of Sciences of the United States of America*, *76*(4), 1967–1971.

Brown, J. W., Rest, J. S., García-moreno, J., Sorenson, M. D., & Mindell, D. P. (2008). Strong mitochondrial DNA support for a Cretaceous origin of modern avian lineages. *BMC Biology, 6*(6), 1–18.

Buehler, D.M., & Baker, A. J. (2005). Population Divergence Times and Historical Demography in Red Knots and Dunlins. *Condor*, *107*(3), 497–513.

Buehler, D. M, Baker, A. J., & Piersma, T. (2006). Reconstructing palaeoflyways of the late Pleistocene and early Holocene red knot (*Calidris canutus*). *Ardea*, *94*(3), 485–498.

Castellanos-Morales, G., Gámez, N., Castillo-Gámez, R. A., & Eguiarte, L. E. (2016). Peripatric speciation of an endemic species driven by Pleistocene climate change: The case of the Mexican prairie dog (*Cynomys mexicanus*). *Molecular Phylogenetics and Evolution*, *94*, 171–181.

Chandler, R.M. & Parmley, D. (2002). The earliest North American record of an auk (Aves: Alcidae) from the Late Eocene of central Georgia. *Oriole, 68*, 7-9.

Chen, D., Chang, J., Li, S. H., Liu, Y., Liang, W., Zhou, F., Yao, C. Te & Zhang, Z. (2015). Was the exposed continental shelf a long-distance colonization route in the ice age? The Southeast Asia origin of Hainan and Taiwan partridges. *Molecular Phylogenetics and Evolution, 83*, 167–173.

Chester, S. (2016). *The Arctic Guide: Wildlife of the Far North*. Princeton University Press.

Claramunt, S., & Cracraft, J. (2015). A new time tree reveals Earth history's imprint on the evolution of modern birds. *Science Advances, 1*(11), 1–14.

Clarke, J. A., Tambussi, C. P., Noriega, J. I., Erickson, G. M., & Ketcham, R. A. (2005). Definitive fossil evidence for the extant avian radiation in the Cretaceous. *Nature, 433*(7023), 305-308.

Cohen, K. M., & Gibbard, P. L. (2008). Global chronostratigraphical correlation table for the last 2.7 million years. *Episodes*, *31*(2), 243–247.

Cooper, R. A. (2004). *The New Zealand Geological Timescale 2004/2*. Institute of geological & nuclear sciences.

Cornuet, J. M., Santos, F., Beaumont, M. A., Robert, C. P., Marin, J. M., Balding, D. J., … Estoup, A. (2008). Inferring population history with DIY ABC: A user-friendly approach to approximate Bayesian computation. *Bioinformatics*, *24*(23), 2713–2719.

Csilléry, K., Blum, M. G. B., Gaggiotti, O. E., & François, O. (2010). Approximate Bayesian Computation (ABC) in practice. *Trends in Ecology and Evolution*, *25*(7), 410–418.

del Hoyo, J., Elliott, A., Sargatal, J., Christie, D.A. & Kirwan, G. (eds.) (2018). *Handbook of the Birds of the World*. Lynx Edicions, Barcelona.

De Pietri, V.L., Costeur, L., Guntert, M., & Mayr, G. (2011). A revision of the Lari (Aves, Charadriiformes) from the early Miocene of Saint-Gérand-le-Puy (Allier, France). *Journal of Vertebrate Paleontology, 31*, 812-828.

Drummond, A. J., & Rambaut, A. (2015). *Bayesian evolutionay analysis with BEAST 2*. Cambridge University Press.

Dyke, G. J. (2003). The fossil record and molecular clocks: Basal radiations within the Neornithes. In: Smith, P., Donoghue, P. (eds) *Telling the evolutionary time: molecular clocks and the fossil record*, 263-277.

Dyke, G. J., & Gulas, B. E. (2002). The fossil galliform bird *Paraortygoides* from the Lower Eocene of the United Kingdom. *American Museum Novitates*, 1-14.

Dyke, G. J., Gulas, B. E., & Crowe, T. M. (2003). Suprageneric relationships of galliform birds (Aves, Galliformes): A cladistic analysis of morphological characters. *Zoological Journal of the Linnean Society*, *137*(2), 227–244.

Eidesen, P. B., Ehrich, D., Bakkestuen, V., Alsos, I. G., Gilg, O., Taberlet, P., & Brochmann, C. (2013). Genetic roadmap of the Arctic: Plant dispersal highways, traffic barriers and capitals of diversity. *New Phytologist*, *200*(3), 898–910.

Engelmoer, M., & Roselaar, C. S. (1998). *Geographical variation in waders*. Springer Science & Business Media.

EPICA community members. (2004). Eight glacial cycles from an Antarctic ice core. *Nature*, *429*, 623–628.

Ericson, P. G. P., Klopfstein, S., Irestedt, M., Nguyen, J. M. T., & Nylander, J. A. A. (2014). Dating the diversification of the major lineages of Passeriformes (Aves*). BMC Evolutionary Biology, 14*, 8.

Fasanella, M., Premoli, A. C., Urdampilleta, J. D., González, M. L., & Chiapella, J. O. (2017). How did a grass reach Antarctica? The Patagonian connection of *Deschampsia antarctica* (Poaceae). *Botanical Journal of the Linnean Society*, *185*(4), 511–524.

Flagstad, Ø., & Røed, K. H. (2003). Refugial origins of Reindeer (*Rangifer tarandus*) inferred from Mitochondrial DNA Sequences. *Evolution*, *57*(3), 658–670.

Fourment, M., & Holmes, E. (2014). Novel non-parametric models to estimate evolutionary rates and divergence times from heterochronous sequence data. *BMC Evolutionary Biology*, *14*(1), 163.

Fu, Y. X. (1997). Statistical tests of neutrality of mutations against population growth, hitchhiking and background selection. *Genetics 147*, 915–925.

Fu, Y. X., & Li, W. H. (1993). Statistical tests of neutrality of mutations. *Genetics*, *133*(3), 693-709.

Galbreath, Edwin C. (1953). A contribution to the Tertiary geology and paleontology of northeastern Colorado. *University of Kansas Paleontological Contributions* (Vertebrata), No. 4

Garcia-Moreno, J. (2004). Is there a universal mtDNA clock for birds? *Journal of Avian Biology*, *35*(6), 465–468.

Göhlich, U.B. (2007). The oldest fossil record of the extant penguin genus *Spheniscus*—a new species from the Miocene of Peru. *Acta Palaeontologica Polonica 52* (2): 285–298.

Gradstein, F., & Ogg, J. (2004). Geologic time scale 2004–why, how, and where next!. *Lethaia*, *37*(2), 175-181.

Greenwood, J. G. (1986). Geographical variation and taxonomy of the Dunlin (*Calidris alpina*). *Bulletin of the British Ornithologists' Club*, *106*, 43–42.

Hackett, S. J., Kimball, R. T., Reddy, S., Bowie, R. C. K., Braun, E. L., Braun, M. J., … Yuri, T. (2008). A phylogenomic study of birds reveals their evolutionary history. *Science, 320(*5884), 1763–1768.

Hewitt, G. M. (1996). Some genetic consequences of ice ages, and their role in speciation. *Biological Journal of the Linnaean Society*, *58*(July), 247–276.

Hewitt, G. M. (2000). The genetic legacy of the quaternary ice ages. *Nature*, *405*(6789), 907–913.

Hewitt, G. M. (2004). Genetic consequences of climatic oscillations in the Quaternary. *Philosophical Transactions of the Royal Society B: Biological Sciences*, *359*, 183–195.

Hickerson, M. J., Carstens, B. C., Cavender-Bares, J., Crandall, K. A., Graham, C. H., Johnson, J. B., … Yoder, A. D. (2010). Phylogeography's past, present, and future: 10 years after Avise, 2000. *Molecular Phylogenetics and Evolution*, *54*(1), 291–301.

Hickerson, Michael J., Stahl, E. A., & Lessios, H. A. (2007). Test for Simultaneous Divergence Using Approximate Bayesian Computation. *Evolution*, *60*(12), 2435–2453.

Ho, S. Y. W, & Duchêne, S. (2014). Molecular-clock methods for estimating evolutionary rates and timescales. *Molecular Ecology*, *23*(24), 5947–5965.

Ho, S.Y.W., Duchene, S., Hua, X., Ritchie, A. M., Duchene, D. A., & Bromham, L. D. (2017). Bayesian molecular dating: opening up the black box. *Biological Reviews*, *93*(2), 1165-1191.

Ho, S. Y. W, Phillips, M. J., Cooper, A., & Drummond, A. J. (2005). Time dependency of molecular rate estimates and systematic overestimation of recent divergence times. *Molecular Biology and Evolution*, *22*(7), 1561–1568.

Ho, S. Y.W., Saarma, U., Barnett, R., Haile, J., & Shapiro, B. (2008). The effect of inappropriate calibration: Three case studies in molecular ecology. *PLoS ONE*, *3*(2).

Ho, S. Y. W, Shapiro, B., Phillips, M. J., Cooper, A., & Drummond, A. J. (2007). Evidence for Time Dependency of Molecular Rate Estimates. *Systematic Bi*, *56*(3), 515–522.

Höglund, J., Johansson, T., Beintema, A., & Schekkerman, H. (2009). Phylogeography of the Black-tailed Godwit *Limosa limosa*: Substructuring revealed by mtDNA control region sequences. *Journal of Ornithology*, *150*(1), 45–53.

Holder, K., Montgomerie, R., & Friesen, V. L. (2004). Genetic diversity and management of Nearctic rock ptarmigan (*Lagopus mutus*). *Canadian Journal of Zoology*, *82*(4), 564–575.

Hope, A. G., Speer, K. A., Demboski, J. R., Talbot, S. L., & Cook, J. A. (2012). A climate for speciation: Rapid spatial diversification within the *Sorex cinereus* complex of shrews. *Molecular Phylogenetics and Evolution*, *64*(3), 671–684.

Hosner, P. A., Braun, E. L. & Kimball, R. T. (2016). Rapid and recent diversification of curassows, guans, and chachalacas (Galliformes: Cracidae) out of Mesoamerica: Phylogeny inferred from mitochondrial, intron, and ultraconserved element sequences. *Molecular Phylogenetics and Evolution, 102*, 320–330.

Humphries, E. M., & Winker, K. (2011). Discord reigns among nuclear, mitochondrial and phenotypic estimates of divergence in nine lineages of trans-Beringian birds. *Molecular Ecology*, *20*(3), 573–583.

Inoue, K., Monroe, E. M., Elderkin, C. L., & Berg, D. J. (2014). Phylogeographic and population genetic analyses reveal Pleistocene isolation followed by high gene flow in a wide ranging, but endangered, freshwater mussel. *Heredity*, *112*(3), 282–290.

Jaarola, M., Tegelström, H., & Fredga, K. (1999). Colonization history in Fennoscandian rodents. *Biological Journal of the Linnean Society*, *68*(1–2), 113–127.

Jarvis, E. D., Mirarab, S., Aberer, A. J., Li, B., Houde, P., Li, C., ... & Suh, A. (2014). Whole-genome analyses resolve early branches in the tree of life of modern birds. Science, 346(6215), 1320-1331.

Jones, K. L., Krapu, G. L., Brandt, D. A., & Ashley, M. V. (2005). Population genetic structure in migratory sandhill cranes and the role of Pleistocene glaciations. *Molecular Ecology*, *14*(9), 2645–2657.

Johnson, J. A., Burnham, K. K., Burnham, W. A., & Mindell, D. P. (2007). Genetic structure among continental and island populations of gyrfalcons. *Molecular Ecology*, *16*(15), 3145-3160.

Jønsson, K.A., Fabre, P.-H., Kennedy, J.D., Holt, B.G., Borregaard, M.K., Rahbek, C., Fjeldså, J., (2016). A supermatrix phylogeny of corvoid passerine birds (Aves: Corvides). *Molecular phylogenetics and evolution, 94* (Part A), 87–94.

Jouzel, J., Cattani, O., Dreyfus, G., Falourd, S., Hoffmann, G., Nouet, J., … Schilt, A. (2007). Orbital and millennial Antarctic climate variability over the past 800,000 years. *Science*, *317*(5839), 793–796.

Kan, X. Z., Li, X. F., Lei, Z. P., Chen, L., Gao, H., Yang, Z. Y., ... & Qian, C. J. (2010). Estimation of divergence times for major lineages of galliform birds: evidence from complete mitochondrial genome sequences. *African Journal of Biotechnology, 9*(21), 3073-3078.

Kees, C. J., Boyd, H., & Piersma, T. (2001). Changing balance between survival and recruitment explains population trends in Red Knots *Calidris canutus islandica* wintering in Britain, 1969-1995. *Ardea*, *89*(2), 301–317.

Kleckova, I., Cesanek, M., Fric, Z., & Pellissier, L. (2015). Diversification of the cold-adapted butterfly genus *Oeneis* related to Holarctic biogeography and climatic niche shifts. *Molecular Phylogenetics and Evolution*, *92*, 255–265.

Ksepka, D. T. (2009). Broken gears in the avian molecular clock: new phylogenetic analyses support stem galliform status for *Gallinuloides wyomingensis* and rallid affinities for *Amitabha urbsinterdictensis*. *Cladistics, 25*(2), 173-197.

Ksepka, D. T., & Clarke, J. A. (2010). The basal penguin (Aves: Sphenisciformes) *Perudyptes devriesi* and a phylogenetic evaluation of the penguin fossil record. *Bulletin of the American Museum of Natural History, 2010*(337), 1-78.

Ksepka, D., & Clarke, J. (2015). Phylogenetically vetted and stratigraphically constrained fossil calibrations within Aves. *Palaeontologia Electronica*, *18*(1), 1–25.

Lanfear, R., Calcott, B., Ho, S. Y., & Guindon, S. (2012). PartitionFinder: combined selection of partitioning schemes and substitution models for phylogenetic analyses. *Molecular biology and evolution*, *29*(6), 1695-1701.

Leblanc, N. M., Stewart, D. T., Pálsson, S., Elderkin, M. F., Mittelhauser, G., Mockford, S., … Mallory, M. L. (2017). Population structure of Purple Sandpipers (*Calidris maritima*) as revealed by mitochondrial DNA and microsatellites. *Ecology and Evolution*, (7), 3225–3242.

Lisiecki, L. E., & Raymo, M. E. (2005). A Pliocene-Pleistocene stack of 57 globally distributed benthic δ 18O records. *Paleoceanography*, *20*(1), 1–17.

Lovette, I. J. (2004). Mitochondrial dating and mixed support for the “2% rule” in birds. *The Auk*, *121*(1), 1–6.

Macpherson, A. A. H. (1965). The origin of diversity in mammals of the Canadian arctic tundra. *Systematic Zoology*, *14*(3), 153–173.

Magallón, S., Hilu, K. W., & Quandt, D. (2013). Land plant evolutionary timeline: Gene effects are secondary to fossil constraints in relaxed clock estimation of age and substitution rates. *American Journal of Botany*, *100*(3), 556–573.

Marthinsen, G., Wennerberg, L., & Lifjeld, J. T. (2007). Phylogeography and subspecies taxonomy of dunlins (*Calidris alpina*) in western Palearctic analyzed by DNA microsatellites and AFLP markers. *Biological Journal of the Linnean Society*, *92*, 713–726.

Marthinsen, G., Wennerberg, L., Pierce, E. P., & Lifjeld, J. T. (2008). Phylogeographic origin and genetic diversity of dunlin *Calidris alpina* in Svalbard. *Polar Biology*, *31*(11), 1409–1420.

Mayr, G. (2000a). Charadriiform birds from the Early Oligocene of Céreste (France) and the Middle Eocene of Messel (Hessen, Germany). *Geobios, 33*, 625-636

Mayr, G. (2000b). Tiny hoopoe-like birds from the Middle Eocene of Messel (Germany). *The Auk*, *117*(4), 964-970.

Mayr, G. (2001). A cormorant from the late Oligocene of Enspel, Germany (Aves, Pelecaniformes, Phalacrocoracidae). *Senckenbergiana lethaea*, *81*(2), 329-333.

Mayr, G. (2004). Old World fossil record of modern-type hummingbirds. *Science, 304*(5672), 861-864.

Mayr, G. (2005). New trogons from the early Tertiary of Germany. *Ibis, 147*, 512-518.

Mayr, G. (2006). New specimens of the Eocene Messelirrisoridae (Aves: *Bucerotes*), with comments on the preservation of uropygial gland waxes in fossil birds from Messel and the phylogenetic affinities of Bucerotes. *Paläontologische Zeitschrift*, *80*(4), 390-405.

Mayr G, Smith R. (2002) Avian remains from the lowermost Oligocene of Hoogbutsel (Belgium). *Bulletin de l'Institut Royal des Sciences Naturelles de Belgique Sciences de la Terre, 72*, 139–150.

Mayr, G., & Weidig, I. (2004). The Early Eocene bird *Gallinuloides wyomingensis*—a stem group representative of Galliformes. *Acta Palaeontologica Polonica*, *49*(2), 211–217.

Mertz, D.F., Harms, F.-J., Gabriel, G., & Felder, M. (2004). Arbeitstreffen in der Forschungsstation Grube Messel mit neuen Ergebnissen aus der Messel-Forschun. *Natur und Museum, 134*, 289-290.

Mertz, D.F. & Renne, P.R. (2005). A numerical age for the Messel fossil deposit (UNESCO World Heritage Site) derived from 40Ar/39Ar dating on a basaltic rock fragment. *Courier Forschungsinstitut Senckenberg, 255*, 67-75.

Mertz, D.F., Renne, P.R., Wuttke, M., & Mödden, C. (2007). A numerically calibrated reference level (MP28) for the terrestrial mammal-based biozonation of the European Upper Oligocene. *International Journal of Earth Sciences, 96* (2),353–361.

Milá, B., McCormack, J. E., Castañeda, G., Wayne, R. K., & Smith, T. B. (2007). Recent postglacial range expansion drives the rapid diversification of a songbird lineage in the genus *Junco*. *Proceedings of the Royal Society B: Biological Sciences*, *274*(1626), 2653–2660.

Miller, M. P., Gratto-Trevor, C., Haig, S. M., Mizrahi, D. S., Mitchell, M. M., & Mullins, T. D. (2013). Population Genetics and Evaluation of Genetic Evidence for Subspecies in the Semipalmated Sandpiper (*Calidris pusilla*). *Waterbirds*, *36*(2), 166–178.

Miller, M. P., Haig, S. M., Gratto-Trevor, C. L., & Mullins, T. D. (2010). Subspecies Status and Population Genetic Structure in Piping Plover (*Charadrius melodus*). *The Auk*, *127*(1), 57–71.

Mitchell, K. J., Llamas, B., Soubrier, J., Rawlence, N. J., Worthy, T. H., Wood, J., … Cooper, A. (2014). Ancient DNA reveals elephant birds and kiwi are sister taxa and clarifies ratite bird evolution. *Science, 344*(6186), 898–900.

Mueller, R. L., & Boore, J. L. (2005). Molecular mechanisms of extensive mitochondrial gene rearrangement in Plethodontid salamanders. *Molecular Biology and Evolution*, *22*(10), 2104–2112.

Muizon, C. (1988). Les vertébrés fossiles de la formation Pisco (Pérou). III – Les odontocètes (Cetacea, Mammalia) du Miocène. *Travaux de l' Institut Français d'Études Andines, 42,* 1–244.

Nabholz, B., Lanfear, R., & Fuchs, J. (2016). Body mass-corrected molecular rate for bird mitochondrial DNA. *Molecular Ecology*, 4438–4449.

Near, T. J., & Sanderson, M. J. (2004). Assessing the quality of molecular divergence time estimates by fossil calibrations and fossil-based model selection. *Philosophical Transactions of the Royal Society B: Biological Sciences*, *359*(1450), 1477–1483.

Ohlson, J., Irestedt, M., Ericson, P. G. P., & Fjeldså, J. (2013). Phylogeny and classification of the New World suboscines (Aves, Passeriformes). *Zootaxa, 3613*(1), 1–35.

Olson, S. L. (1977). A Lower Eocene frigatebird from the Green River Formation of Wyoming (Pelecaniformes: Fregatidae). *Smithsonian Contributions to Paleobiology*.

Olson, S.L. (1985). The fossil record of birds. In: Farner, D.S., King, J.R., Parkes, K.C. (Eds.), *Avian Biology*. Academic Press, New York, Vol. VIII, pp. 79–238.

Olson, S. L., & Farrand, J. (1974). Rhegminornis restudied : A Tiny Miocene. *The Wilson*, *86*(2), 114–120.

Olson,S.L. & Feduccia,A. (1980). Relationships and Evolution of Flamingos (Aves: Phoenicopteridae). *Smithsonian Contributions to Zoology,316*, 1-73

Ornelas, J. F., González, C., los Monteros, A. E., Rodríguez-Gómez, F., & García-Feria, L. M. (2014). In and out of Mesoamerica: temporal divergence of *Amazilia* hummingbirds predates the orthodox account of the completion of the Isthmus of Panama. *Journal of Biogeography, 41*(1), 168-181.

Ottvall, R., Höglund, J., Bensch, S., & Larsson, K. (2005). Population differentiation in the redshank (*Tringa totanus*) as revealed by mitochondrial DNA and amplified fragment length polymorphism markers. *Conservation Genetics*, *6*(3), 321–331.

Pacheco, M. A., Battistuzzi, F. U., Lentino, M., Aguilar, R. F., Kumar, S., & Escalante, A. A. (2011). Evolution of modern birds revealed by mitogenomics: Timing the radiation and origin of major orders. *Molecular Biology and Evolution*, *28*(6), 1927–1942.

Parham, J. F., Donoghue, P. C. J., Bell, C. J., Calway, T. D., Head, J. J., Holroyd, P. A., … Benton, M. J. (2012). Best practices for justifying fossil calibrations. *Systematic Biology*, *61*(2), 346–359.

Pereira, S. L., & Baker, A. J. (2006). A mitogenomic timescale for birds detects variable phylogenetic rates of molecular evolution and refutes the standard molecular clock. *Molecular Biology and Evolution*, *23*(9), 1731–1740.

Pereira, S. L., Johnson, K. P., Clayton, D. H., & Baker, A. J. (2007). Mitochondrial and nuclear DNA sequences support a Cretaceous origin of Columbiformes and a dispersal-driven radiation in the Paleogene, *56*(4), 656–672.

Persons, N. W., Hosner, P. A., Meiklejohn, K. A., Braun, E. L. & Kimball, R. T. 2016 Sorting out relationships among the grouse and ptarmigan using intron, mitochondrial, and ultra-conserved element sequences. *Molecular phylogenetics and evolution 98*, 123–132.

Peters, S. E. & McClennen, M. (2016). The Paleobiology Database application programing interface. *Paleobiology*, *42*, 1–7.

Piersma, T., & Drent, J. (2003). Phenotypic flexibility and the evolution of organismal design. *Trends in Ecology and Evolution*, *18*(5), 228–233.

Ploeger, P. L. (1968). Geographical differentation in Arctic Anatidae as a result of isolation during the last glacial. *Ardea*, *56*(1–2), 4–155.

Pruett, C. L., & Winker, K. (2005). Biological impacts of climatic change on a Beringian endemic: Cryptic refugia in the establishment and differentiation of the rock sandpiper (*Calidris ptilocnemis*). *Climatic Change*, *68*(1–2), 219–240.

Pruett, C. L., & Winker, K. (2008). Evidence for cryptic northern refugia among high- and temperate-latitude species in Beringia. *Climatic Change*, *86*(1–2), 23–27.

Prum, R. O., Berv, J. S., Dornburg, A., Field, D. J., Townsend, J. P., Lemmon, E. M., & Lemmon, A. R. (2015). A comprehensive phylogeny of birds (Aves) using targeted next-generation DNA sequencing. *Nature*, *526*, 569–573.

Pujolar, J. M., Dalén, L., Hansen, M. M., & Madsen, J. (2017). Demographic inference from whole-genome and RAD sequencing data suggests alternating human impacts on goose populations since the last ice age. *Molecular ecology*, *26*(22), 6270-6283.

Rand, A. L. (1948). Glaciation, An Isolating Factor in Speciation. *Evolution*, *2*(4), 314–321.

Rasmussen, D.T., Olson, S.L., & Simons, E.L. (1987). Fossil birds from the Oligocene Jebel Qatrani Formation, Fayum Province, Egypt. *Smithsonian Contributions to Paleobiology, 62*.

Rhodes, G.M., Ali, J.R., Hailwood, E.A., King, C., and Gibson, T.G. (1999). Magnetostratigraphic correlation of Paleogene sequences from northwest Europe and North America. *Geology, 27*, 451-454.

Rönkä, N., Kvist, L., Pakanen, V. M., Rönkä, A., Degtyaryev, V., Tomkovich, P., … Koivula, K. (2012). Phylogeography of the Temminck's Stint (*Calidris temminckii*): Historical vicariance but little present genetic structure in a regionally endangered Palearctic wader. *Diversity and Distributions*, *18*(7), 704–716.

Rozas, J., Ferrer-Mata, A., Sánchez-DelBarrio, J. C., Guirao-Rico, S., Librado, P., Ramos-Onsins, S. E., & Sánchez-Gracia, A. (2017). DnaSP 6: DNA sequence polymorphism analysis of large data sets. *Molecular biology and evolution*, *34*(12), 3299-3302.

Ruokonen, M., Aarvak, T., & Madsen, J. (2005). Colonization history of the high-arctic pink-footed goose *Anser brachyrhynchus*. *Molecular Ecology*, *14*(1), 171-178.

Scofield, R. P., Mitchell, K. J., Wood, J. R., De Pietri, V. L., Jarvie, S., Llamas, B., & Cooper, A. (2017). The origin and phylogenetic relationships of the New Zealand ravens. *Molecular phylogenetics and evolution, 106*, 136-143

Seiffert, E.R. (2006). Revised age estimates for the later Paleogene mammal faunas of Egypt and Oman. *Proceedings of the National Academy of Sciences, 103* (13), 5000-5005.

Shafer, A. B. A., Cullingham, C. I., Côté, S. D., & Coltman, D. W. (2010). Of glaciers and refugia: A decade of study sheds new light on the phylogeography of northwestern North America. *Molecular Ecology*, *19*(21), 4589–4621.

Shields, G. F., & Wilson, A. C. (1987). Calibration of Mitochondrial DNA Evolution in Geese. *Journal of Molecular Evolution*, *24*, 212–217.

Slack, K.E., Jones, C.M., Ando, T., Harrison, G.L., Fordyce, R.E., Arnason, U., & Penny, D. (2006) Early penguin fossils, plus mitochondrial genomes, calibrate avian evolution. *Molecular Biology and Evolution, 23*, 1144–1155.

Smith, N.D. (2010) Phylogenetic Analysis of Pelecaniformes (Aves) Based on Osteological Data: Implications for Waterbird Phylogeny and Fossil Calibration Studies. *PLoS ONE, 5* (10), e13354.

Smith, N.A. (2011). *Systematics and evolution of extinct and extant Pan-Alcidae (Aves, Charadriiformes): combined phylogenetic analyses, divergence estimation, and paleoclimatic interactions*. PhD Dissertation. The University of Texas at Austin.

Smith, N.D. & Ksepka, D.T. (2015) Five well-supported fossil calibrations within the "Waterbird" assemblage (Tetrapoda, Aves). *Palaeontologia Electronica, 18*, 1–21.

Stamatakis, A. (2014). RAxML Version 8: A tool for Phylogenetic Analysis and Post-Analysis of Large Phylogenies. *Bioinformatics, 30* (9), 1312-1313

Stein, R. W., Brown, J. W., & Mooers, A. Ø. (2015). A molecular genetic time scale demonstrates Cretaceous origins and multiple diversification rate shifts within the order Galliformes (Aves). *Molecular phylogenetics and evolution, 92*, 155-164.

Tajima, F. (1989). Statistical method for testing the neutral mutation hypothesis by DNA polymorphism. *Genetics 123*, 585–595.

Tiedemann, R., Paulus, K. B., Scheer, M., Von Kistowski, K. G., Skírnisson, K., Bloch, D., & Dam, M. (2004). Mitochondrial DNA and microsatellite variation in the eider duck (Somateria mollissima) indicate stepwise postglacial colonization of Europe and limited current long-distance dispersal. *Molecular Ecology*, *13*(6), 1481-1494.

Thies, L., Tomkovich, P., dos Remedios, N., Lislevand, T., Pinchuk, P., Wallander, J., ... & Küpper, C. (2018). Population and subspecies differentiation in a high latitude breeding wader, the Common Ringed Plover *Charadrius hiaticula*. *Ardea*, *106*(2), 163-177.

Todisco, V., Gratton, P., Zakharov, E. V., Wheat, C. W., Sbordoni, V., & Sperling, F. A. H. (2012). Mitochondrial phylogeography of the Holarctic *Parnassius phoebus* complex supports a recent refugial model for alpine butterflies. *Journal of Biogeography*, *39*(6), 1058–1072.

Tordov, H.B., Macdonald, J.R., 1957. A new bird (family Cracidae) from the early Oligocene of South Dakota. *Auk 74*, 174–184.

Trimbos, K. B., Doorenweerd, C., Kraaijeveld, K., Musters, C. J. M., Groen, N. M., Knijff, P., … De Snoo, G. R. (2014). Patterns in nuclear and mitochondrial DNA reveal historical and recent isolation in the black-tailed godwit (*Limosa limosa*). *PLoS ONE*, *9*(1).

van Tuinen, M. and G. J. Dyke (2004). Calibration of galliform molecular clocks using multiple fossils and genetic partitions. *Molecular Phylogenetics and Evolution 30*(1): 74-86.

Weir, J. T., & Schluter, D. (2008). Calibrating the avian molecular clock. *Molecular Ecology*, *17*(10), 2321–2328.

Weir, Jason T., & Schluter, D. (2004). Ice sheets promote speciation in boreal birds. *Proceedings. Biological Sciences / The Royal Society*, *271*(1551), 1881–1887.

Wenink, P., Baker, A., Rosner, H., & Tilanus, M. (1996). Global mitochondrial DNA phylogeography of holarctic breeding dunlins (*Calidris alpina*). *Evolution*, *50*(1), 318–330.

Wenink, P. W., Baker, A. J., & Tilanus, M. G. (1993). Hypervariable-control-region sequences reveal global population structuring in a long-distance migrant shorebird, the Dunlin (*Calidris alpina*). *Proceedings of the National Academy of Sciences of the United States of America*, *90*(1), 94–98.

Wenink, P. W., Baker, A. J., & Tilanus, M. G. (1994). Mitochondrial control-region sequences in two shorebird species, the turnstone and the dunlin, and their utility in population genetic studies. *Molecular Biology and Evolution*, *11*(1), 22–31.

Wennerberg, L., Klaassen, M., & Lindström, Å. (2002). Geographical variation and population structure in the White-rumped Sandpiper *Calidris fuscicollis* as shown by morphology,

mitochondrial DNA and carbon isotope ratios. *Oecologia*, *131*(3), 380–390.

Wetmore, A. (1936). Two new species of hawks from the Miocene of Nebraska. *Proceedings of the United States National Museum*.

Wetmore, A. (1943). Fossil birds from the Tertiary deposits of Florida. In *Proceedings of the New England Zoological Club* (22), 59-68.

Wilson, A. C., Cann, R. L., Carrii, S. M., George, M., Gyllenstenis, U. L. F. B., Kathleen, M., … Sage, R. D. (1985). Mitochondrial DNA and two perspectives on evolutionary genetics. *Biological Journal of the Linnean Society*, *26*, 375–400.

Yonezawa, T., Segawa, T., Mori, H., Campos, P. F., Hongoh, Y., Endo, H., … Hasegawa, M. (2017). Phylogenomics and morphology of extinct Paleognaths reveal the origin and evolution of the Ratites. *Current Biology, 27(1)*, 68–77.

Zheng, Y., & Wiens, J. J. (2015). Do missing data influence the accuracy of divergence-time estimation with BEAST? *Molecular Phylogenetics and Evolution*, *85*, 41–49.

Zigouris, J., Schaefer, J. A., Fortin, C., & Kyle, C. J. (2013). Phylogeography and post-glacial recolonization in wolverines (*Gulo gulo*) from across their circumpolar distribution. *PLoS ONE*, *8*(12), 1–13.

Zink, R. M., & Barrowclough, G. F. (2008). Mitochondrial DNA under siege in avian phylogeography. *Molecular Ecology*, *17*(9), 2107–2121.

Chapter 3:

Stairway to northern haven? Uneven climate change effects in the ranges of Arctic shorebirds between the Nearctic and the Palearctic.

Authors: Arcones A., Ponti R., Ferrer X. and Vieites D.

Stairway to northern haven? Uneven climate change effects in the ranges of Arctic shorebirds between the Nearctic and the Palearctic.

Abstract

The Arctic is among the most threatened regions of the planet under the pressure of the current climate change. Arctic species have persisted over multiple warm and cold periods during the Pleistocene and Holocene, but the fast rate of the current changes represent an unprecedented scenario. In this work we explore the potential changes in the breeding ranges of the Arctic shorebirds under different scenarios of climate change for the current century. Arctic shorebirds are one of the best representatives of the Arctic avifauna, and their distribution and diversity have been shaped by the extreme changes in the climate of the region in the last 2.5 million years. Species' distribution models for 69 species show an overall northward shift of their breeding ranges, combined with a severe reduction at the southern margins. However, these effects greatly vary between biogeographic regions. In the Palearctic, species display greater signs of future range reduction and fragmentation given the lack of available land at more northern latitudes to extend their ranges. Meanwhile in the Nearctic, the Arctic Archipelago potentially provides an opportunity for the species to avoid loss of their breeding range extent. But even if these species have available northern territories to overcome increasing temperatures, as it likely happened in the Arctic in recent periods, the speed of the current changes greatly exceeds previous climatic oscillations. Even under the most optimistic climate change scenarios, the capacity of these species and their habitats to adapt or move in time to the new situation will be critical for their survival and the conservation of the diversity generated during the glacial cycles.

Introduction

Current climate change has proven to be a major threat for global biodiversity (Butchart *et al.*, 2010; Bellard *et al.*, 2012; Urban, 2015), and its effects are predicted to keep developing throughout this century and beyond (Sala *et al.*, 2000; Pereira *et al.*, 2010;). These effects include habitat loss, population declines, fragmentation of the distribution ranges, and alteration of the behavioural and physiological ecology of species (Crick, 2004; Hickling *et al.*, 2006; Parmesan, 2006; Chen *et al.*, 2011; Bellard *et al.*, 2012; Urban, 2015). Among vertebrates, birds can be prone to suffer global change effects depending on their distribution, migratory condition, population sizes and human-made habitat changes in their breeding and wintering ranges (Crick, 2004; La Sorte & Jetz, 2010; Saino *et al.*, 2011). Many species are displaying some of the clearest responses to climate change, especially in the form of changes in their distribution ranges and phenology (Crick, 2004; Jetz *et al.*, 2007; Huntley *et al.*, 2008; Gregory *et al.*, 2009; Barbet-Massin *et al.*, 2012; Brommer *et al.*, 2012). At higher latitudes, in the boreal and Arctic regions, climate change may be disproportionately threatening species distributed across these northern latitudes (Loarie *et al.*, 2009; Laaksonen & Lehikoinen, 2013; Virkkala & Lehikoinen, 2017) while the populations of those with primarily temperate and tropical distributions seem to be increasing (Virkkala & Rajasärkkä, 2011a, 2011b)

The Arctic region is one of the most pristine areas in the planet, mainly because its climatic conditions hinder the establishment of humans and the development that accompanies them. This region extends around the north pole and spans beyond the Arctic Circle (ca. 66.5°N) with a classic limit around the 10°C isotherm (Köppen, 1900; Köppen & Geiger, 1936), and its environment includes the polar desert, the tundra and the northern limit of the taiga/boreal forests. Climatic conditions are extreme, with a very strong seasonality changing from brief cool summers (3-12°C), to long and very cold winters with temperatures below -30°C (Pielou, 1991). Many species have evolved adaptations to cope with this extreme physical and climatic environment year-round, while others follow different life-history strategies like short or long-distance migration to southern latitudes, mainly birds and mammals in land. Furthermore, these species have overcome multiple cycles of glacial periods and warm interglacials during the

Pleistocene, especially over the last 900,000 years (EPICA community members, 2004; Jouzel *et al.*, 2007). During these cycles, the species experienced successive expansions and contractions of their range and their populations, which determined their distribution and actual diversity (Hulten, 1937; Rand, 1948; Macpherson, 1965; Ploeger, 1968; Hewitt, 2000, 2004). The current global warming is driving very fast changes in the Arctic region (Pearson *et al.*, 2013; Hobbie *et al.*, 2017), heading towards a climate similar to what the Earth experienced more than 30 million years ago (Mya), during periods where the Arctic polar cap was reduced (Burke *et al.*, 2018).

In this chapter we explored the potential consequences of the current climate change in the future distribution and conservation of the Arctic land avifauna. To do so, we focused our study in one of the most representative groups of Arctic birds, the shorebirds, which are among the most important in the region in terms of both number of species and population sizes. As seen in the Chapters 1 and 2, the diversity within these species is linked to changes in the climate, especially those that affect their breeding territories. Under the current climate change, Arctic species that diversified over multiple glacial cycles could face an unprecedented fragmentation of their ranges and decrease of their populations, threatening their diversity and conservation of many subspecies and populations (Lagerholm *et al.*, 2017).

In their Arctic breeding grounds, Arctic shorebirds are already facing changes in their ecology, phenology and habitat availability (Rehfisch & Crick, 2003; Meltofte *et al.*, 2007; Galbraith *et al.*, 2014). Over the next century, these effects could even be more pronounced, leading to an increasing extinction risk (Galbraith *et al.*, 2014). In addition, as long-distance migrants, their distribution and conservation status provide key insights on world-wide effects of climate change (Piersma & Lindström, 2004; Galbraith *et al.*, 2014). Both migratory birds and other northern latitude species have been identified as two of the most vulnerable targets to the impacts of climate change (Both *et al.*, 2006; Huntley *et al.*, 2006; Virkkala *et al.*, 2008; Laaksonen & Lehikoinen, 2013).

In this work, we aim to assess the potential impacts of climate change in the future distribution of the Arctic shorebirds over the 21st century, and the implications in their

diversity and conservation, using Species Distribution Models (SDMs). The SDMs have proven to be an useful tool when examining the potential effects of potential changes in the distribution ranges of species due to climate change (Thuiller, 2004; Araújo & Peterson, 2012; Barbet-Massin *et al.*, 2012). Traditional views of climatic changes during the Pleistocene and for the near future usually consider the entire northern hemisphere as a common region. Studies on the distribution of birds are usually focus on a single continent (e.g Huntley *et al.*, 2008; Barbet-Massin *et al.*, 2012) or regions within them (Saalfeld, *et al.*, 2013; Gillings *et al.*, 2015; Stralberg *et al.*, 2016). However, the Arctic have experienced different effects in different regions over recent climatic cycles (see Chapter 1). Therefore, we explore here the changes in the ranges of the shorebirds across the Arctic, but with a focus on whether potential differences exist between the two main biogeographic regions involved, the Palearctic and the Nearctic, and what effects can this have in their worldwide conservation.

Furthermore, we seek to put the current changes in the Arctic into a historical context, comparing the expected future scenarios with past warm and cold periods during the Late Quaternary. The goal for this is to measure how the extension and composition of the Arctic responded during recent climatic cycles, and how the current change compares to them. We expect that, over the 21st century, the Arctic could decrease drastically reaching extensions similar to those experienced during the warmest periods of the Late Quaternary, or even beyond. And although Arctic species survived those periods, we also try to take into an account how current climate change is driving those changes in much shorter periods of time, and what implications can this have for the Arctic shorebirds and the Arctic avifauna in general.

Methods

Spatio-temporal evolution of Arctic environments

We used the Koppen – Geiger classification system (Köppen, 1900; Köppen & Geiger, 1936) to estimate the potential extension of the Arctic and its different ecosystems over different time periods. This classification system is very popular among climatologists and ecologists to define the boundaries of the different macroclimates and their associated biomes around the globe, based solely on certain climatic variables

that define them. This allows to study past and future biome changes at a global scale (Guetter & Kutzbach, 1990; Rubel & Kottek, 2010; Feng *et al.*, 2012; Chen & Chen, 2013; Willmes *et al.*, 2017). Despite recent revisions of the classification (Guetter & Kutzbach, 1990; Peel *et al.*, 2007; Belda *et al.*, 2014), the Arctic remains defined as the region where the mean temperature of the warmest month is below 10°C. Within this definition of the Arctic, the temperature values between 0°C and 10°C correspond to the tundra and below 0°C represent the polar desert and ice-covered areas.

We applied this classification to evaluate the extent of the Arctic in seven different time periods: the last interglacial period (LIG), around 130,000 years ago (ya); the Last Glacial Maximum (LGM), around 21,000 ya; the Mid-Holocene warm period, around 6,000 ya, the pre-industrial period, between 1750 – 1800; the present, between 1970 – 2000; and the periods around 2050 (2040 – 2060) and 2070 (2060 – 2080). We used the available climatic raster layers at a resolution of 5x5 km for each period (Hijmans *et al.*, 2005; Otto-Bliesner *et al.*, 2006; Lima-Ribeiro *et al.*, 2015; Fick & Hijmans, 2017). We estimated the extension of the tundra and polar desert based on the mean temperature values of July or August, selecting whichever was higher on each pixel. We then compared the extension, measured as number of pixels, of the tundra and polar desert separately, as well as the Arctic as a whole on each period; and compared them using the pre-industrial period as the reference. We also estimated the rate of change of the Arctic surface over time using as a measure the percentage of gain/loss per century, again using the values of Arctic extent during the preindustrial period as the baseline to compare with.

Species presence data

We analysed migratory shorebird species with breeding distribution ranges comprising all or most Arctic and subarctic regions. After testing 70 species matching that criterion, we included 69 in the final analyses (see Chapter 1). According to the IUCN Red List (IUCN, 2018), 12 species are considered as Near Threatened (NT) (*Calidris canutus, Calidris ferruginea, Calidris pusilla, Calidris ruficollis, Calidris subruficollis, Charadrius melodus, Gallinago media, Haematopus ostralegus, Limosa lapponica, Limosa limosa, Numenius arquata* and *Tringa brevipes)*, 1 as Vulnerable (VU) (*Numenius*

tahitiensis), 2 as Endangered (EN) (*Calidris tenuirostris* and *Numenius madagascariensis*) and 1 as Critically Endangered (CR) (*Calidris pygmaea*).

The distribution ranges obtained from BirdLife International and NatureServe (2011) andfiltered by habitat following the process described in Chapter 1. We sampled 10,000 random points across the distribution of each species to use as presence points.

Climatic variables

We used macroclimate variables to predict the distribution of species, due to its proven effectiveness in large spatial scale studies (Barbet-Massin *et al.*, 2012; Jiménez-Valverde *et al.*, 2011; Pigot *et al.*, 2010). We retrieved monthly precipitation and temperature (minimum, maximum and mean) maps from WorldClim 2.0 (Fick & Hijmans, 2017) for the present period (1970 – 2000). For the future, we considered three different scenarios based on the Representative Concentration Pathways (RCPs) of greenhouse gases proposed by the fifth Intergovernmental Panel on Climate Change (IPCC, 2014): RCP 2.6, assuming the emissions reaching its peak by around 2020 and decline thereafter; RCP 4.5, which represents emissions peaking by 2040 and a stabilization afterwards; and RCP 8.5, which assumes that emissions keep increasing at the current rate throughout the 21st century. For this, we averaged all the models available in WorldClim 1.4 (Hijmans *et al.* 2005) for two future periods: the years 2050 (average for 2041 – 2060) and 2070 (2061 – 2080). Since only minimum and maximum temperature values are available, we calculated mean temperature as the average between them. Both sets of climatic layers, present and future, were retrieved at a resolution of 2.5 minutes (ca. 5 x 5 km).

Niche modelling and forecasting

We applied four different SDM methods: general linear model (GLM), polynomial GLM, general additive model (GAM) and BIOCLIM algorithm, as implemented in the R packages dismo (Hijmans *et al.*, 2017) and mgcv (Wood & Wood, 2015). We also tested MaxEnt, DOMAIN, support vector machine (SVM) and random forest (RF) algorithms, but they all showed poor performance with our data and were discarded.

Each species was modelled independently, using 60% of the presence data for the training and 40% to evaluate the models. Since the species only stay in their breeding range for a short available period over the year, we only included the climatic variables corresponding to the breeding season. We trained each model with the average monthly values of each species' breeding season, according to the phenological information in del Hoyo *et al.* (2018). We combined the results of the four models by averaging them into an ensemble forecast, to reduce the potential uncertainty introduced by individual models in certain cases (Araújo *et al.*, 2005; Araújo and New, 2006). We evaluated the discrimination of each of the models and the ensemble forecast based on the values of the Area Under the Curve ROC (AUC) and COR (correlation). We expected models to return values of AUC higher than 0.5 (random discrimination of the model) (Elith *et al.*, 2006), and ideally over 0.7 (good discrimination).

Changes in the climate could potentially cause changes in the timing and length of available breeding grounds of these Arctic species. To take this into account, we applied the same methodology of month-by-month hindcasting as in the Chapter 1. We combined all the species' potential distributions to obtain richness maps for the present and each of the future scenarios.

Changes in species' distributions

For each species' predicted distribution, we calculated values of mean latitude and extent size (in number of pixels) to estimate the changes between the present and each of the future scenarios. We estimated the number of species in each region that experiences changes greater than 10% (increase or decrease) in their extent size by 2070 in each climate change scenario. Additionally, we sampled the latitude of 2,000 random points from each species in each of the forecasts (present and future). We combined the data from all the species into a density plot, which represents how the set of species is distributed along a latitudinal gradient. All these analyses were done separately for the Palearctic (including eastern Greenland) and the Nearctic. The goal for this was to discern potential differences between continents in the potential changes experienced by the Arctic shorebirds, since each region has different geographical constraints at high latitudes.

Results

Changes in the extent of the Arctic

The predicted extension of the Arctic and its environments is predicted to change substantially between the examined periods (Figs. 1 & 2). The LIG, around 120,000 ya, represents the warmest of all the past periods (Fig. 1), where the estimated size of the Arctic is only 60% of the extension calculated for the preindustrial period, and with only 38% of the polar desert extent in comparison. The LGM represents the coldest period of the series (Fig. 1). The Arctic extent in this period is four times greater than during the preindustrial period (Fig. 2, top), with more than twice the extension of tundra and over six times the extension of polar desert (not shown in Fig. 2). After the LGM, in the Holocene, the Arctic experienced another warm period in the Mid-Holocene (Fig. 1), where the total extent was 71% of the size compared to the preindustrial period. The following scenarios show a decrease over the past two centuries, from the preindustrial period to the present with a 9% reduction. The forecasts for the 21st century suggest that this trend further accentuates in all climate change scenarios, with reductions between 18% (RCP 2.6) and 38% (RCP 8.5) by 2070 (Fig. 2). Despite the reduction in the extension of the Arctic, our results show that the areas of polar desert (ice and barren areas) switch to tundra as the climate becomes warmer (Fig. 1). This translates in a greater reduction of the polar desert (between 47% and 64% by 2070) than the tundra (between 2% and 24%). The climate change predictions for the extension of the Arctic by the late 21st century are comparable to the scenarios recovered for previous periods like the LIG and the Mid-Holocene warm periods. However, the changes in the temperature leading to those warm periods happened over thousands of years (Fig. 1). We recovered that the decrease in size of the Arctic from the preindustrial period to the present and over the next century greatly exceeds previous events like the post-glacial warming (Table 2). Furthermore, this rate of reduction in the extent of the Arctic (measured in percentage points per 100 years compared to the preindustrial) increases significantly over time. It reaches its highest values in the period from the present to the end of the next century (between 10-34% /100y).

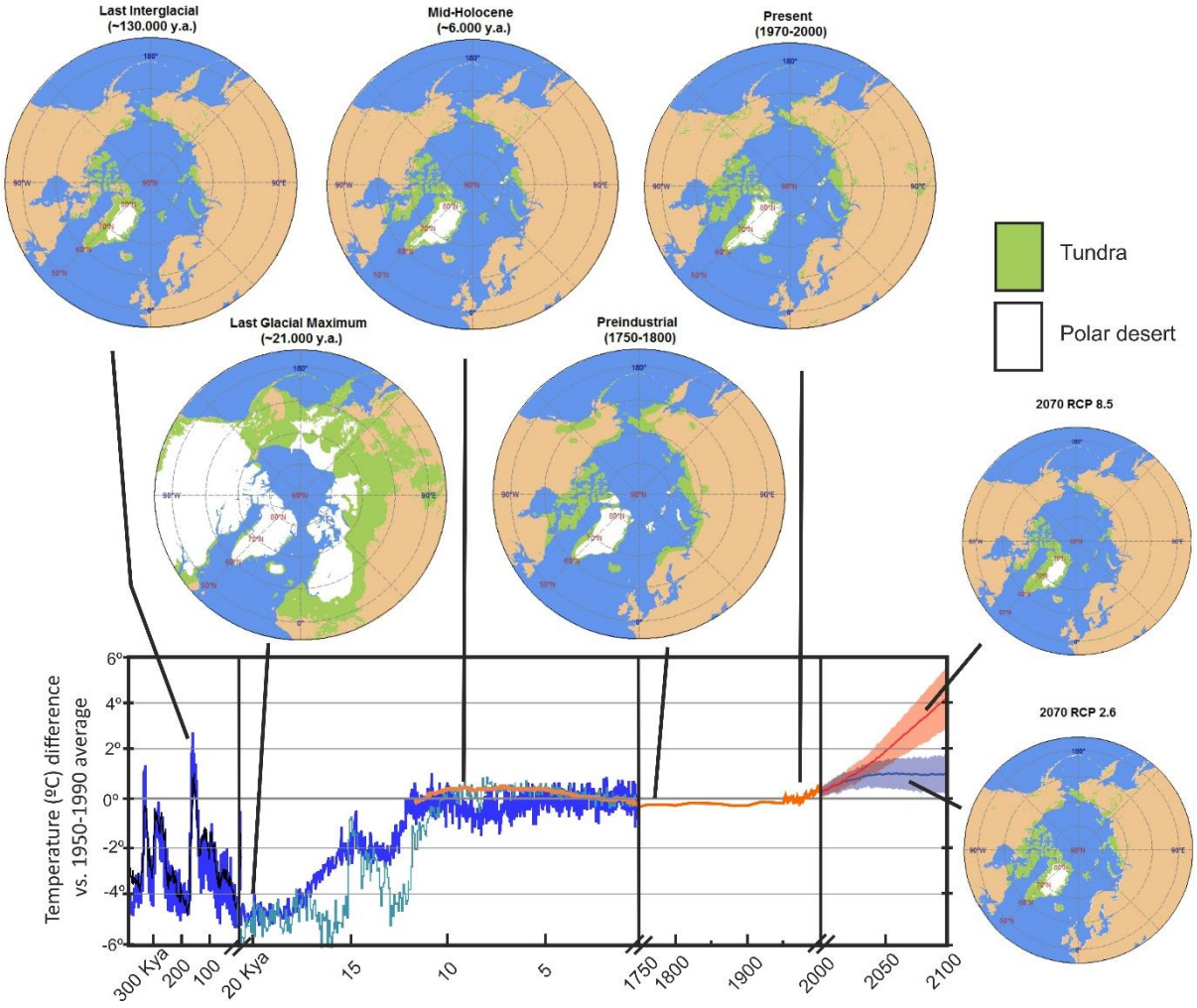

Figure 1: Estimated extension of the Arctic in different periods over the last 300,000 years and for the next century (circles), along with historical and future predicted changes in global temperature (bottom graph). Past temperatures from EPICA community members (2004) (blue); North Greenland Ice Core Project members (2004) (clear blue); Lisiecki & Raymo (2005) (black) and Marcott *et al.*, (2013) (orange). Future temperature forecasts from IPCC (2014).

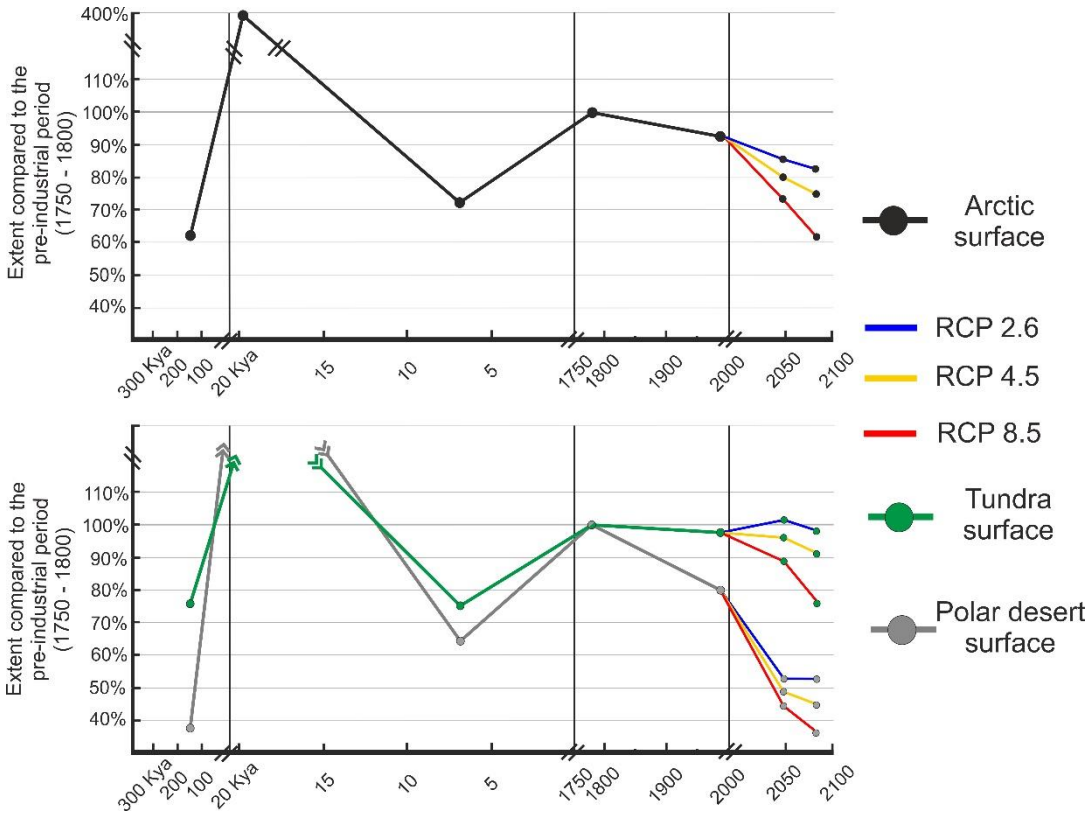

Figure 2: Changes in the predicted extension of the whole Arctic region (top) and its environments (bottom) in the studied periods, following the same X axis (time) as in Fig. 1., with future trends according to each RCP model.

Transition	Scenario	Arctic	Tundra	Polar desert
LGM to Mid-Holocene	H	-2.2 % / 100y	-1.1 % / 100y	-4 % / 100y
Mid-Holocene to preindustrial	H	0.52 % / 100y	0.5 % / 100y	0.4 % / 100y
Preindustrial to present	H	-4.3 % / 100y	-1.4 % / 100y	-9.5 % / 100y
Preindustrial to 2070	RCP 2.6	-6.13 % / 100y	-0.7 % / 100y	-15.9 % / 100y
	RCP 8.5	-12.9 % / 100y	-8.1 % / 100y	-21.7 % / 100y
Present to 2070	RCP 2.6	-10.6 % / 100y	1.2 % / 100y	-31.8 % / 100y
	RCP 8.5	-34.11 % / 100y	-24.7 % / 100y	-51.8 % / 100y

Table 1: Rates of change in the extension of the Arctic, the tundra and the polar desert between historical (H) and future (RCPs) scenarios, measured as percentage points increased (positive) or decreased (negative) per 100 years, considering the preindustrial period as the reference.

Species' distribution models

Over 84% (58 out of 69) of the ensemble forecasts for the breeding distributions returned and AUC higher than 0.8. Only *Actitis hypoleucos* (0.62) showed AUC values lower than 0.7.

The resulting shorebird species' richness maps show values of up to 36 co-occurring species in the Arctic in the present (Fig. 3). This region of high-predicted species richness (over 20 species) covers the whole northern part of the Palearctic as a continuous band mainly between 65°N and 75°N. In the Nearctic it covers the coast of Alaska and the Canadian Arctic, except for the northernmost islands where the species richness is lower (below 15 species). The climatic change predictions show that the high-richness areas will become a narrower band that is restricted to the coast in both the Palearctic and the Nearctic, and some discontinuities will appear.

By 2050 the high-richness areas of the east and central Siberia will no longer be connected under any scenario, as the species richness in the coasts of the East Siberian Sea decreases below 15 species, except around the mouth of the Kolyma River. Similarly, the models predict high-richness areas in the future along the north and west coasts of Alaska, at the same time that species richness in southern areas of the region will decrease. In addition, under higher-emission scenarios the species richness will decrease below 15 species in continental Canada, remaining above those values only in the Arctic Archipelago, and the north of the Northwest Territories and Labrador Peninsula. In the western Palearctic, only the north of Scandinavia will maintain richness values of over 20 species in all future scenarios, declining below 15 species everywhere else in the region.

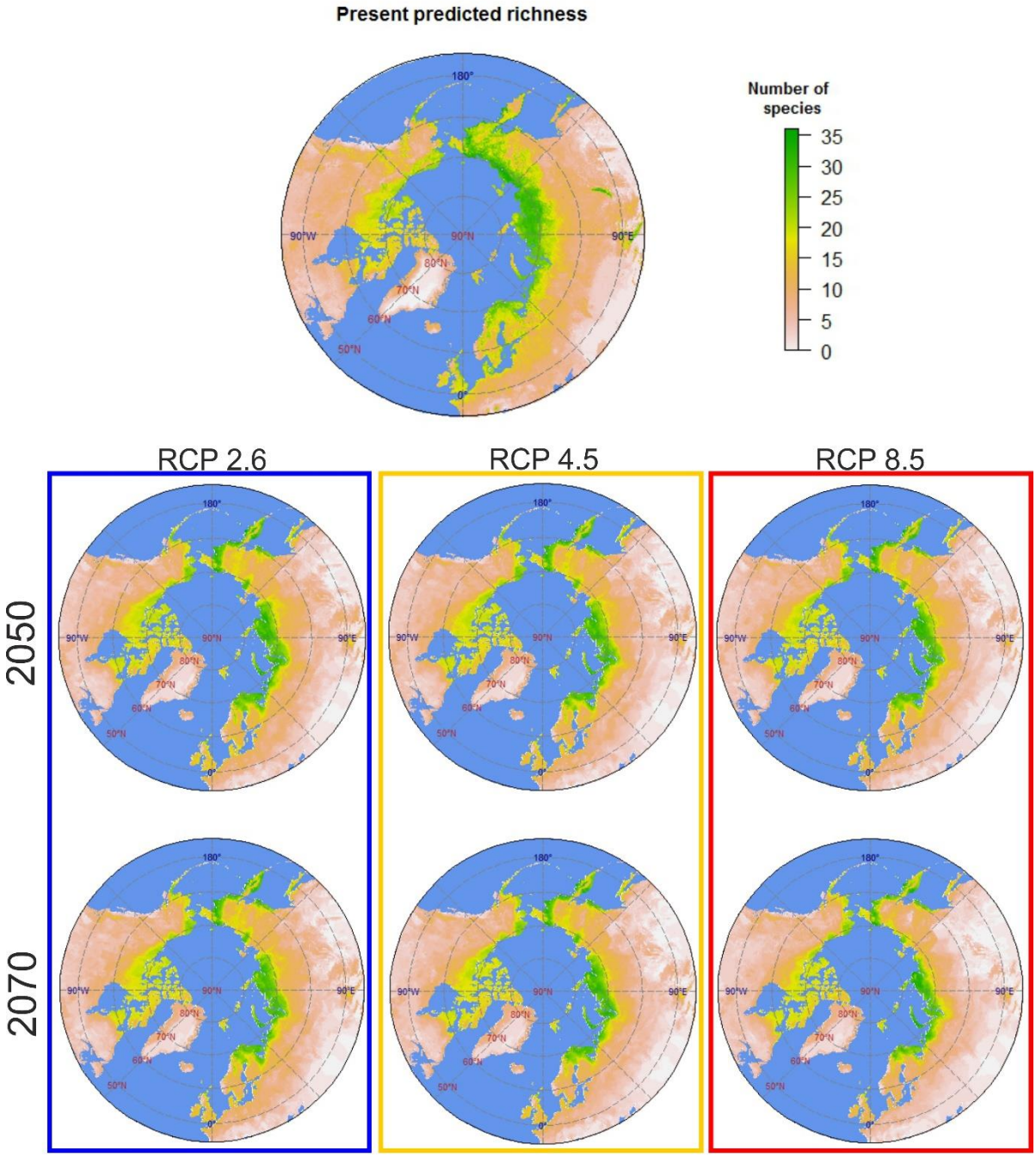

Figure 3: Predicted species' richness maps for the present and each of the climate change scenarios (RCPs) by 2050 and 2070.

Changes in species' ranges

On average, the mean latitude of the species' predicted range by 2070 will increase between 2 and 2.5 degrees in the Nearctic, and between 1.5 and 2 degrees in the Palearctic. However, these results do not properly reflect the changes at the northern and southern margins of their distributions. The distribution of the random samples from the species' ranges provides a better indicator of the latitudes at which they concentrate. In the histogram (Fig. 4), the density peaks between 68°N and 70°N in the Nearctic and the Palearctic both for the present and all future scenarios. Comparing the predicted changes above and below the Arctic Polar Circle returns a general trend increase of density of distributions in the north and decrease in the south. This change is more pronounced in the Nearctic, with up to 24% decrease in density of species' distributions below the Arctic Polar Circle and 10.5% increase above, by 2070. In contrast, in the Palearctic the density decreases 12% below the Arctic Polar Circle by 2070, increasing only 3% above it.

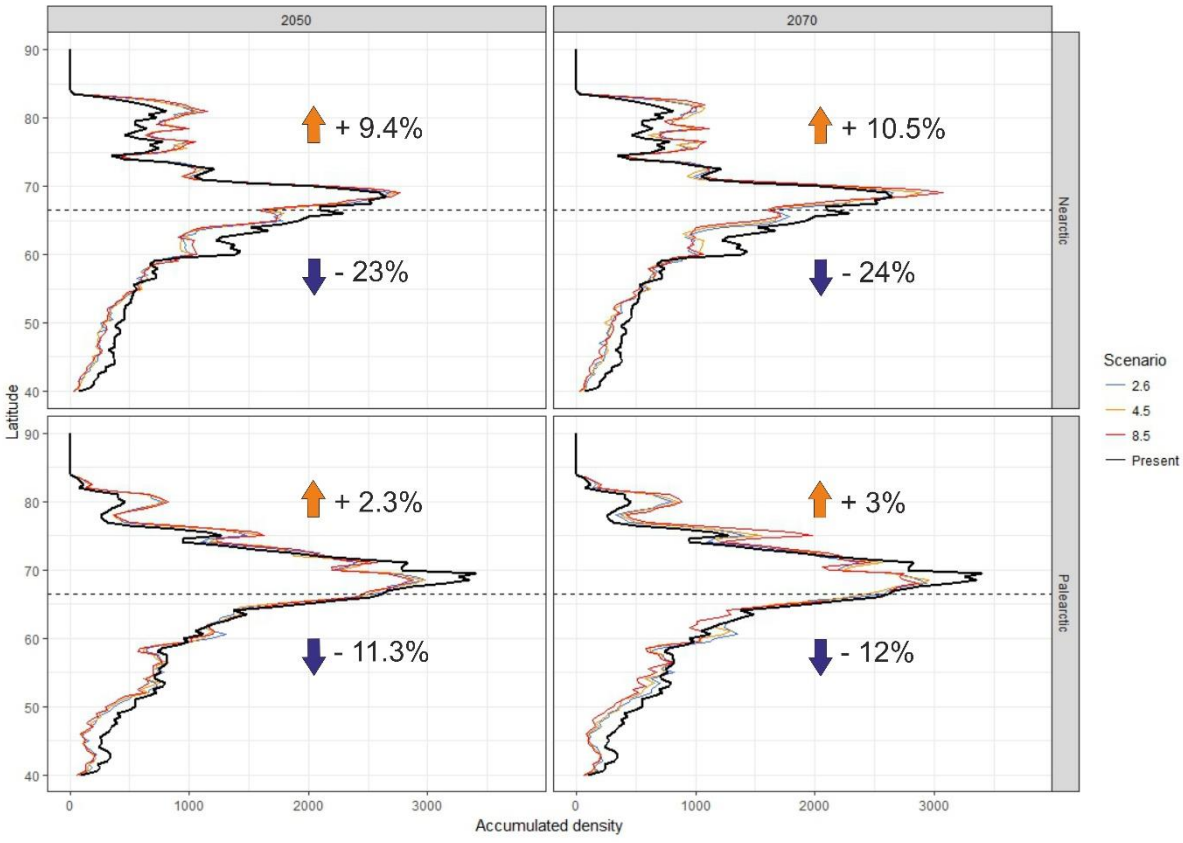

Figure 4: Density of the predicted distribution of the Arctic shorebird species across a latitudinal gradient (Y axis) in the periods round year 2050 (left) and 2070 (right) compared to the present gradient (black line), in the Nearctic (top) and Palearctic (bottom). Colours represent different IPCC climate change scenarios (RCPs). Arrows indicate an increase (orange) or decrease (blue) in the density above or below the Arctic Polar Circle (dashed line), with the percentage of change.

We recovered that, by 2070, 50% of the species in the Palearctic reduced (over 20% change) their predicted area under the scenario RCP 2.6, compared to the present extent. This percentage increases to 77% under scenario RCP 8.5 (Fig. 5). Comparatively, very few species (<10%) showed signs of potential future expansions greater than 20% in extent in all three scenarios. The percentage of species in this region with less than 20% of gain or loss in range extent between now and 2070 will drop from 43% of the species when considering RCP 2.6, to only 13% of the species with the scenario RCP 8.5. In this region, the species with the greatest reduction in range extent by 2070 are *Charadrius mongolus*, *Calidris alpina* and *Calidris ptilocnemis*, all with an estimated decrease between 50-70% in all climate change scenarios. On the other hand, *Limosa limosa* is predicted to increase its range between 30% and 50%, and *Numenius phaeopus* only increases under scenarios RCP 4.5 (69% increase) and RCP 8.5 (54%).

In the Nearctic, a lower proportion of species will show a reduction of their extent compared to the Palearctic, between 27% and 36% of the species depending on the climate change scenario (Fig. 5). In this region, there is a higher percentage of species potentially remaining stable than in the Palearctic, ranging between 44% and 50% of the species. The percentage of species potentially increasing their range extent is 22% under the scenarios RCP 2.6 and RCP 4.5, but drops to 16% under scenario RCP 8.5. The Nearctic species with the greater expected range reduction by 2070 are *Numenius tahitiensis, Calidris himantopus, Calidris alba* and *Calidris mauri*, with reductions of over 50% of their ranges in all scenarios and over 80% in some cases. In contrast, *Gallinago delicata, Charadrius vociferus, Limnodromus scolopaceus* and *Numenius americanus* will increase their predicted ranges by over 50%, and over 80% in some scenarios.

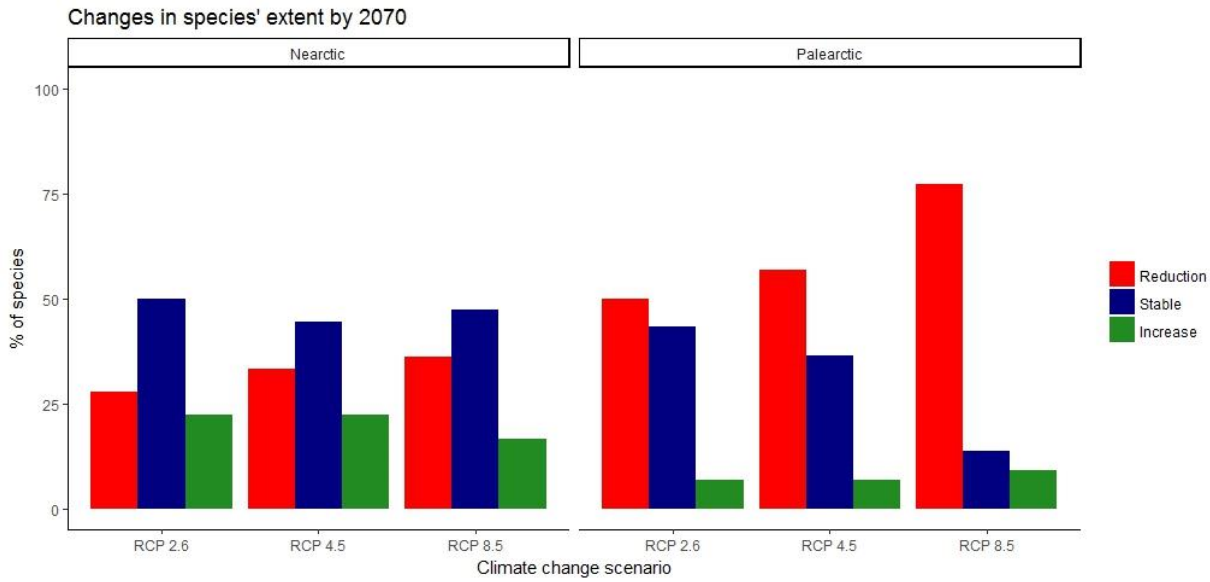

Figure 5: Percentage of species that will experience changes in their predicted extent size by 2070 in the Nearctic (left) and Palearctic (right) under the three different IPCC climate change scenarios (RCPs). Colours represent type of change: over 20% decrease (red), over 20% increase (green); or no change greater than 20% (blue).

Discussion

Our results show that climate change is altering the distribution of Arctic shorebirds, and even in the most optimistic scenarios it represents a major threat to their conservation. The main predicted consequences are the loss of the current distribution ranges in many species, changes in the richness at high latitudes and potential loss of local diversity of subspecies. This situation is recovered across the whole Arctic region, although there are notable differences in the responses of the two main biogeographic regions, as the Nearctic could offer better future conditions for the conservation of Arctic shorebird species than the Palearctic.

Overall, Arctic shorebirds seem to be gradually shifting their breeding ranges towards higher latitudes in parallel to climatic changes. Such poleward shift in the ranges of bird species has been regarded as one of the most notable effects derived from climate change (Huntley *et al.*, 2008; Barbet-Massin *et al.*, 2012; Brommer *et al.*, 2012;

Virkkala & Lehikoinen, 2014, 2017). However, our results also suggest that this displacement involves not only an expansion to the north, but must importantly disappearances at the southern margin of their distribution. This trend has been previously suggested for other northern bird species in northern Europe (Virkkala & Rajasärkkä, 2011a, 2011b; Brommer *et al.*, 2012; Kujala *et al.*, 2013; Virkkala & Lehikoinen, 2014, 2017), but our results show that it is extensible to the whole Arctic region. The loss of the southern margin in northern species is also related to the poleward expansion of temperate species in those areas, in detriment of the more vulnerable northern migratory species (Virkkala *et al.*, 2008; Laaksonen & Lehikoinen, 2013).

However, our results suggest that the derived effects from these poleward shifts in the distribution vary greatly between the Palearctic and Nearctic regions. In the Palearctic, where the northernmost limit of the continent with the Arctic ocean acts as a hard boundary, the species will be unable to expand further north as the climatic conditions change, as there is no more available land. We recovered very low increases in the density of species' ranges above the Arctic Polar Circle in this region, which is congruent with the fact that most Arctic species are already distributed at the northernmost part of the continent, leaving them more vulnerable to range reductions without chances to expand any further (Virkkala *et al.*, 2008). Moreover, the percentage of species that experience severe (>20%) range reduction in the Palearctic (between 50% and 77%) greatly exceeds the percentage predicted for the Nearctic (between 27% and 36%).

Despite a greater expected reduction at the southern margins of species' ranges in this region (up to 12%), the availability of large extensions of land at high latitudes (70 - 80°N) seems to be a benefit for Nearctic species. Currently, some species of shorebirds like the Turnstone (*Arenaria interpres*), the Red Knot (*Calidris canutus*) and the Sanderling (*C. alba*) inhabit those northern areas of the Nearctic in the Arctic Archipelago, but their presence is mostly restricted to the rocky areas in the coastline, since most of the inland areas are mainly barren land (Walker *et al.*, 2005). However, climate change is quicky altering the vegetation of this region, by often causing an increase in shrubslands (Sturm *et al.*, 2001; Forbes *et al.*, 2010), but also by quickly

expanding the tundra into areas where vegetation was previously sparse or even absent (Jia *et al.*, 2003; Pearson *et al.*, 2013; Keenan & Riley, 2018). As a result, if the northward expansion of the habitat matched the rapid changes in the Arctic climate, the Nearctic could provide better opportunities for the Arctic shorebirds to cope with the effects of global warming at a continental scale. Otherwise, the mismatch between climate and habitat could result in a dramatic reduction of available breeding sites, and consequently of population sizes, well beyond current predictions. Furthermore, all the species that are predicted to suffer the greatest range reductions now have very restricted ranges, either occurring only in small areas (like *N. tahitiensis* and *C. mauri* in the Nearctic, *C. ptilocnemis* and *C. mongolus* in the Palearctic) or at the northernmost latitudes (*C. alba* in the Nearctic, *C. alpina* in the Palearctic). On the contrary, species that are predicted to expand their ranges tend to have large distributions across temperate and sub-Arctic regions, like *N. americanus*, *C. vociferus* and *G. delicata* in the Nearctic and *L. limosa* in the Palearctic. This supports the idea of a future scenario where the temperate widespread species will be the "winners" over the more restricted northern species (Virkkala *et al.*, 2008; Tayleur *et al.*, 2016).

But even if expected scenarios for the next century show a severe reduction of the Arctic habitat, these species experienced similar conditions over their recent evolutionary history. During the previous interglacial, and even during the Mid-Holocene, warm periods led to a subsequent reduction of the environments in the Arctic (McFarlin *et al.*, 2018). These glacial – interglacial cycles during the Pleistocene, as seen in the previous chapters, had a key role in the diversification of their populations. The fragmentation of ranges in areas of refugia due to changes in the climate led to the current diversity of subspecies and populations. While the fragmentation (or lack of it) during glacial periods was the most important factor to explain the diversity within most species, the interglacials also contributed to the isolation of the Arctic populations. Regarding refugia, most of the literature is focused more on the Late Quaternary than in the current climate change (Keppel *et al.*, 2012). These potential future refugia are of great importance in terms of identifying key areas in the conservation of the species (Araújo *et al.*, 2004; Pyke & Fischer, 2005; Hannah *et al.*, 2007), and some of the areas

highlighted in this work, like the north coast of Alaska, are already gathering attention (Fuller *et al*., 2008; Saalfeld *et al*., 2013).

However, while in previous occasions the warmer and colder periods took thousands of years of gradual change to develop, the current climatic change is concentrating the same amount of change in just a few centuries. By the end of the 21st century, the Arctic would reach previously experienced conditions but at a rate never experienced before in the Late Quaternary (IPCC, 2014). Our results suggest that the current rate of reduction in Arctic size is well over the experienced during the post-glacial warming since the LGM. Furthermore, this rate has increased in the last years and will double over the next decades, even in the most optimistic scenarios. Should the trend continue, and over the following century the climate of the planet would resemble that of the Pliocene or the Eocene in the worst scenario (Burke *et al.*, 2018). This high velocity of climate change is a major concern in the conservation of species, especially for those whose low dispersal ability limits their capacity to occupy suitable areas (Williams & Blois, 2018). With few exceptions, Arctic-breeding shorebirds are long distance migrants, and it is assumed that dispersal ability would not be an obstacle in reaching suitable areas. But beyond habitat availability, climate change poses many other challenges for this group of birds (Rehfisch & Crick, 2003; Meltofte *et al.*, 2007; Galbraith *et al.*, 2014). Changes in synchronicity with the peak of food resources in the migratory stopovers and the breeding sites demand that the migratory shorebirds adapt their phenology to a quickly changing global scenario (Tulp & Schekkerman, 2007; McGowan *et al.*, 2011; McKinnon *et al.*, 2012; Galbraith *et al.*, 2014; Saalfeld *et al.*, 2019). Although some populations seem to be succesfully profiting from these changes (Alves *et al.*, 2019), most of the evidence suggest an overall declining trend of populations in Europe (Lindström *et al.*, 2015) and North America (Bart *et al.*, 2007). Furthermore, expected sea-level rise of up to 80cm by 2100 (Church *et al.*, 2013) will cause the disappearance of intertidal areas that are key for fuelling during migrations as well as in breeding and wintering areas (Galbraith *et al.*, 2002). All these factors could have a deep impact on the Arctic shorebird populations, reducing their presence in the Arctic beyond the predictions from the models.

Our results highlight that climate change represents a major threat for the conservation of Arctic shorebirds and other northern and migratory bird species across the planet, especially in the Palearctic region. The changes in the ranges of these species are an already ongoing process, and their consequences will likely be greatly aggravated in the scenarios resulting from higher emissions. Despite the ability of these birds to overcome severe climatic changes, the current trend greatly surpasses the rate of previous events. The result of this extreme and sudden warming challenges the capability of these Arctic species to quickly adapt their distribution and phenology beyond anything they have experienced in their recent evolutionary history. This remarks the need for immediate measures to reduce these emissions in order to minimize the negative impacts on the already vulnerable Arctic ecosystem.

References

Alves, J. A., Gunnarsson, T. G., Sutherland, W. J., Potts, P. M., & Gill, J. A. (2019). Linking warming effects on phenology, demography and range expansion in a migratory bird population. *Ecology and Evolution*.

Araújo, M. B., Cabeza, M., Thuiller, W., Hannah, L., & Williams, P. H. (2004). Would climate change drive species out of reserves? An assessment of existing reserve-selection methods. *Global Change Biology, 10*(9), 1618–1626.

Araújo, M. B., & New, M. (2006). Ensemble forecasting of species distributions. *Trends in Ecology and Evolution, 22*(1), 42–47.

Araújo, M. B., & Peterson, A. T. (2012). Uses and misuses of bioclimatic envelope modeling. *Ecology*, *93*(7), 1527–1539.

Araújo, M.B., Whittaker, R.J., Ladle, R.J., & Erhard, M. (2005) Reducing uncertainty in projections of extinction risk from climate change. *Global Ecology and Biogeography*, *14*, 529–538.

Barbet-Massin, M., Thuiller, W., & Jiguet, F. (2012). The fate of European breeding birds under climate, land-use and dispersal scenarios. *Global Change Biology*, *18*(3), 881–890.

Bart, J., Brown, S., Harrington, B., & Guy Morrison, R. I. (2007). Survey trends of North American shorebirds: Population declines or shifting distributions? *Journal of Avian Biology, 38*(1), 73–82.

Belda, M., Holtanová, E., Halenka, T., & Kalvová, J. (2014). Climate classification revisited: From Köppen to Trewartha. *Climate Research, 59*(1), 1–13.

Bellard, C., Bertelsmeier, C., Leadley, P., Thuiller, W., & Courchamp, F. (2012). Impacts of climate change on the future of biodiversity. *Ecology Letters*, *15*(4), 365–377.

BirdLife International and NatureServe (2011) Bird species distribution maps of the world. BirdLife International, Cambridge, UK and NatureServe, Arlington, USA,

Both, C., Bouwhuis, S., Lessells, C. M., & Visser, M. E. (2006). Climate change and population declines in a long-distance migratory bird. *Nature*, *441*(1), 81–83.

Brommer, J. E., Lehikoinen, A., & Valkama, J. (2012). The Breeding Ranges of Central European and Arctic Bird Species Move Poleward. *PLoS ONE*, *7*(9), 1–7.

Bontemps, S., Defourny, P., Van Bogaert, E., Kalogirou, V. and Arino, O. 2011. GLOBCOVER 2009: Products Description and Validation Report.: 1–17.

Burke, K. D., Williams, J. W., Otto-Bliesner, B. L., Haywood, A. M., Burke, K. D., Chandler, M. A., & Lunt, D. J. (2018). Pliocene and Eocene provide best analogs for near-future climates. *Proceedings of the National Academy of Sciences, 115*(52), 13288–13293.

Butchart, S. H. M., Walpole, M., Collen, B., van Strien, A., Scharlemann, J. P. W., Almond, R. E. A., … Watson, R. (2010). Global Biodiversity: Indicators of Recent Declines. *Science*, *328*(5982), 1164–1168.

Chen, D., & Chen, H. W. (2013). Using the Köppen classification to quantify climate variation and change: An example for 1901-2010. *Environmental Development, 6*(1), 69–79.

Chen, I., Hill, J. K., Ohlemüller, R., Roy, D. B., & Thomas, C. D. (2011). Rapid range shifts of species of climate warming. *Science*, *333*, 1024–1026.

Church, J. A., Clark, P. U., Cazenave, A., Gregory, J. M., Jevrejeva, S., Levermann, A., … Unnikrishnan, A. S. (2013). Sea level change. In *Climate Change 2013: The Physical Science Basis. Contribution of Working Group I to the Fifth Assessment Report of the Intergovernmental Panel on Climate Change*. (pp. 1137–1216). Cambridge University Press, Cambridge, United Kingdom and New York, NY, USA.

Crick, H.Q.F. (2004). The impact of climate change on birds. *Ibis, 146* Volume146 (1): 48-56.

del Hoyo, J., Elliott, A., Sargatal, J., Christie, D.A. & de Juana, E. (eds.). 2018. *Handbook of the Birds of the World Alive*. Lynx Edicions, Barcelona. (retrieved from http://www.hbw.com/).

Elith, J., H. Graham, C., P. Anderson, R., *et al.* (2006) Novel methods improve prediction of species' distributions from occurrence data. *Ecography*, *29*, 129–151.

EPICA community members. (2004). Eight glacial cycles from an Antarctic ice core. *Nature, 429*, 623–628.

Feng, S., Ho, C. H., Hu, Q., Oglesby, R. J., Jeong, S. J., & Kim, B. M. (2012). Evaluating observed and projected future climate changes for the Arctic using the Köppen-Trewartha climate classification. *Climate Dynamics, 38*(7–8), 1359–1373.

Fick, S.E. & Hijmans, R.J. (2017) WorldClim 2: new 1-km spatial resolution climate surfaces for global land areas. *International Journal of Climatology*, 37, 4302–4315

Forbes, B. C., Fauria, M. M., & Zetterberg, P. (2010). Russian Arctic warming and “greening” are closely tracked by tundra shrub willows. *Global Change Biology, 16*(5), 1542–1554.

Fuller, T., Morton, D. P., & Sarkar, S. (2008). Incorporating uncertainty about species' potential distributions under climate change into the selection of conservation areas with a case study from the Arctic Coastal Plain of Alaska. *Biological Conservation, 141*(6), 1547–1559.

Galbraith, H., DesRochers, D. W., Brown, S., & Reed, J. M. (2014). Predicting vulnerabilities of North American shorebirds to climate change. *PLoS ONE, 9*(9), 21–23.

Galbraith, H., Jones, R., Park, R., Clough, J., Herrod-Julius, S., Harrington, B., & Page, G. W. (2002). Global climate change and sea level rise: potential losses of intertidal habitat for shorebirds. *Waterbirds, 25*(2), 173–183.

Gillings, S., Balmer, D. E., & Fuller, R. J. (2015). Directionality of recent bird distribution shifts and climate change in Great Britain. *Global Change Biology*, *21*(6), 2155–2168.

Gregory, R. D., Willis, S. G., Jiguet, F., Voříšek, P., Klvaňová, A., van Strien, A., … Green, R. E. (2009). An indicator of the impact of climatic change on European bird populations. *PLoS ONE*, *4*(3).

Guetter, P. J., & Kutzbach, J. E. (1990). A modified Köppen classification applied to model simlutaions of glacial and interglacial climates. *Climatic Change, 16*, 193–215.

Hannah, L., Midgley, G., Andelman, S., Araújo, M., Hughes, G., Martinez-meyer, E., … Williams, P. (2007). Protected area needs in a changing climate. *Frontiers in Ecology and the Environment, 5*(3), 131–138.

Hewitt, G. (2000) The genetic legacy of the quaternary ice ages. *Nature*, 405, 907–913.

Hewitt, G. (2004) Genetic consequences of climatic oscillations in the Quaternary. *Philosophical Transactions of the Royal Society B: Biological Sciences*, 359, 183–195.

Hickling, R., Roy, D. B., Hill, J. K., Fox, R., & Thomas, C. D. (2006). The distributions of a wide range of taxonomic groups are expanding polewards. *Global Change Biology, 12*(3), 450–455.

Hijmans, A. R. J., Phillips, S., Leathwick, J., Elith, J., & Hijmans, M.R.J. (2017) Package "dismo".

Hijmans, A. R. J., Cameron, S.E., Parra, J.L., Jones, P.G., & Jarvis, A. (2005) Very high resolution interpolated climate surfaces for global land areas. *International Journal of Climatology,* 25, 1965–1978.

Hobbie, J. E., Shaver, G. R., Rastetter, E. B., Cherry, J. E., Goetz, S. J., Guay, K. C., … Kling, G. W. (2017). Ecosystem responses to climate change at a Low Arctic and a High Arctic long-term research site. *Ambio, 46*(s1), 160–173.

Hultén, E. (1937). *Outline of the history of arctic and boreal biota during the quaternary period*. Bokforlags Aktiebolaget Thule. Stockholm

Huntley, B., Collingham, Y. C., Green, R. E., Hilton, G. M., Rahbek, C., & Willis, S. G. (2006). Potential impacts of climatic change upon geographical distribution of birds. *Ibis*, *148*, 8–28.

Huntley, B., Collingham, Y. C., Willis, S. G., & Green, R. E. (2008). Potential impacts of climatic change on European breeding birds. *PLoS ONE*, *3*(1).

IPCC. (2014) Climate change 2014: *Synthesis report. Contribution of Working Groups I, II, and III to the Fifth Assessment Report of the Intergovernmental Panel on Climate Change* [Core Writing Team, Pachauri, R.K. & Meyer, L.A. (eds.)]. Geneva, Switzerland: IPCC, 151 pp

IUCN 2018. *The IUCN Red List of Threatened Species. Version 2018-1*. http://www.iucnredlist.org

Jia, G. J., Epstein, H. E., & Walker, D. A. (2003). Greening of arctic Alaska, 1981-2001. *Geophysical Research Letters, 30*(20), 3–6.

Jetz, W., Wilcove, D. S., & Dobson, A. P. (2007). Projected impacts of climate and land-use change on the global diversity of birds. *PLoS Biology*, *5*(6), 1211–1219.

Jiménez-Valverde, A., Barve, N., Lira-Noriega, A., Maher, S. P., Nakazawa, Y., Papeş, M., … Peterson, A. T. (2011). Dominant climate influences on North American bird distributions. *Global Ecology and Biogeography*, *20*(1), 114–118.

Jouzel, J., Cattani, O., Dreyfus, G., Falourd, S., Hoffmann, G., Nouet, J., … Schilt, A. (2007). Orbital and Millennial Antarctic Climate Variability over the past 800,000 years. *Science, 317*(5839), 793–796.

Keenan, T. F., & Riley, W. J. (2018). Greening of the land surface in the world's cold regions consistent with recent warming. *Nature Climate Change, 8*(9), 825.

Keppel, G., Van Niel, K. P., Wardell-Johnson, G. W., Yates, C. J., Byrne, M., Mucina, L., … Franklin, S. E. (2012). Refugia: Identifying and understanding safe havens for biodiversity under climate change. *Global Ecology and Biogeography, 21*(4), 393–404.

Köppen, W. (1900). Versuche einer Klassifikation der Klimate, vorzugsweise nach ihren Beziehungen zur Pflanzenwelt. *Geographische Zeitschrift, 6*(12), 657–679.

Köppen, W., & Geiger, R. (1936). Das Geographische System der Klimate. *Handbuch Der Klimatologie, 46*.

Kraaijeveld, K., & Nieboer, E. N. (2000). Late Quaternary paleogeography and evolution of arctic breeding waders. *Ardea, 88*(2), 193–205.

Kujala, H., Vepsäläinen, V., Zuckerberg, B., & Brommer, J. E. (2013). Range margin shifts of birds revisited - the role of spatiotemporally varying survey effort. *Global Change Biology*, *19*(2), 420–430.

La Sorte, F. a, & Jetz, W. (2010). Avian distributions under climate change: towards improved projections. *The Journal of Experimental Biology, 213*(6), 862–869.

Laaksonen, T., & Lehikoinen, A. (2013). Population trends in boreal birds: Continuing declines in agricultural, northern, and long-distance migrant species. *Biological Conservation*, *168*, 99–107.

Lagerholm, V. K., Sandoval-Castellanos, E., Vaniscotte, A., Potapova, O. R., Tomek, T., Bochenski, Z. M., … Stewart, J. R. (2017). Range shifts or extinction? Ancient DNA and distribution modelling reveal past and future responses to climate warming in cold-adapted birds. *Global Change Biology, 23(*4), 1425–1435.

Lima-Ribeiro M. S.; Varela S.; González-Hernández J.; Oliveira G.; Diniz-Filho J. A. F.; Terribile L. C. (2015) ecoClimate: a database of climate data from multiple models for past, present, and future for macroecologists and biogeographers. *Biodiversity Informatics 10*, 1-21.

Lindström, Å., Green, M., Husby, M., Kålås, J. A., & Lehikoinen, A. (2015). Large-scale monitoring of waders on their boreal and arctic breeding grounds in northern Europe. *Ardea, 103*(1), 3–15.

Lisiecki, L. E., & Raymo, M. E. (2005). A Pliocene-Pleistocene stack of 57 globally distributed benthic δ 18O records. *Paleoceanography, 20*(1), 1–17.

Loarie, S. R., Duffy, P. B., Hamilton, H., Asner, G. P., Field, C. B., & Ackerly, D. D. (2009). The velocity of climate change. *Nature, 462*(7276), 1052–1055.

Macpherson, A. A. H. (1965). The origin of diversity in mammals of the Canadian arctic tundra. *Systematic Zoology, 14*(3), 153–173.

Marcott, S. A., Shakun, J. D., Clark, P. U., & Mix, A. C. (2013). A reconstruction of regional and global temperature for the past 11,300 years. *Science, 339*(6124), 1198–1201.

McFarlin, J. M., Axford, Y., Osburn, M. R., Kelly, M. A., Osterberg, E. C., & Farnsworth, L. B. (2018). Pronounced summer warming in northwest Greenland during the Holocene and Last Interglacial. *Proceedings of the National Academy of Sciences, 115*(25), 6357–6362.

McGowan, C. P., Hines, J. E., Nichols, J. D., Lyons, J. E., Smith, D. R., Kalasz, K. S., … Kendall, W. (2011). Demographic consequences of migratory stopover: linking red knot survival to horseshoe crab spawning abundance. *Ecosphere, 2*(6)

McKinnon, L., Picotin, M., Bolduc, E., Juillet, C., & Bêty, J. (2012). Timing of breeding, peak food availability, and effects of mismatch on chick growth in birds nesting in the High Arctic. *Canadian Journal of Zoology, 90*(8), 961–971.

Meltofte, H., Piersma, T., Boyd, H., McCaffery, B., Ganter, B., Golovnyuk, V. V., … Wennerberg, L. (2007). *Effects of Climate Variation on The Breeding Ecology of Arctic Shorebirds*. Meddelelser Om Gronland Bioscience (Vol. 59).

North Greenland Ice Core Project members. (2004). High-resolution record of Northern Hemispher climate extending in the last interglacial period. *Nature, 431*(September), 147–151.

Otto-Bliesner, B. L., Marshall, S. J., Overpeck, J. T., Miller, G. H., & Hu, A. (2006). Simulating Arctic Climate Warmth and Icefield Retreat in the Last Interglaciation. *Science, 311*(2006), 1751–1755.

Parmesan, C. (2006). Ecological and Evolutionary Responses to Recent Climate Change. *Annual Review of Ecology, Evolution, and Systematics*, *37*(1), 637–669.

Pearson, R. G., Phillips, S. J., Loranty, M. M., Beck, P. S. A., Damoulas, T., Knight, S. J., & Goetz, S. J. (2013). Shifts in Arctic vegetation and associated feedbacks under climate change. *Nature Climate Change, 3*(7), 673–677.

Peel, M. C., Finlayson, B. L., & McMahon, T. A. (2007). Updated World Map of the Köppen-Geiger Climate Classification. *Hydrology and earth system sciences discussion*, *4*(2), 439–473.

Pereira, H. M., Leadley, P. W., Proenca, V., Alkemade, R., Scharlemann, J. P. W., Fernandez-Manjarres, J. F., … Walpole, M. (2010). Scenarios for Global Biodiversity in the 21st Century. *Science*, *330*, 1496–1502.

Pielou, E. C. (1991). *After the ice age: the return of life to glaciated North America*. University of Chicago Press.

Piersma, T., & Lindström, Å. (2004). Migrating shorebirds as integrative sentinals of global environmental change. *Ibis, 146*(Suppl.1), 61–69.

Pigot, A. L., Owens, I. P. F., & Orme, C. D. L. (2010). The environmental limits to geographic range expansion in birds. *Ecology Letters*, *13*(6), 705–715.

Ploeger, P. L. (1968). Geographical differentiation in arctic Anatidae as a result of isolation during the last glacial. *Ardea, 56*(1–2), 4–155.

Pyke, C. R., & Fischer, D. T. (2005). Selection of bioclimatically representative biological reserve systems under climate change. *Biological Conservation, 121*(3), 429–441.

Rand, A. L. (1948). Glaciation, An Isolating Factor in Speciation. *Evolution, 2*(4), 314–321.

Rebelo, H., Tarroso, P., & Jones, G. (2010). Predicted impact of climate change on european bats in relation to their biogeographic patterns. *Global Change Biology*, *16*(2), 561–576.

Rehfisch, M. M., & Crick, H. Q. P. (2003). Predicting climate change on Arctic-breeding waders. *Wader Study Group Bulletin, 100*, 86–95.

Rubel, F., & Kottek, M. (2010). Observed and projected climate shifts 1901-2100 depicted by world maps of the Köppen-Geiger climate classification. *Meteorologische Zeitschrift, 19*(2), 135–141.

Saalfeld, S.T., McEwen, D. C., Kesler, D., M.G., B., Cunningham, J., Doll, A., … Lanctot., R. B. (2019). Phenological mismatch in Arctic-breeding birds: impact of earlier summers and unpredictable weather conditions on food availability and chick growth. *Ecology and Evolution*.

Saalfeld, S. T., Lanctot, R. B., Brown, S. C., Saalfeld, D. T., & Johnson, J. a. (2013). Predicting breeding shorebird distributions on the Arctic Coastal Plain of Alaska. *Ecosphere*, *4*(1), 277–293.

Saino, N., Ambrosini, R., Rubolini, D., Von Hardenberg, J., Provenzale, A., Hüppop, K., … Sokolov, L. (2011). Climate warming, ecological mismatch at arrival and population decline in migratory birds. *Proceedings of the Royal Society B: Biological Sciences, 278*, 835–842.

Sala, O. E., Iii, F. S. C., Armesto, J. J., Berlow, E., Dirzo, R., Huber-sanwald, E., … Wall, D. H. (2000). Global Biodiversity Scenarios for the Year 2100 Global Biodiversity Scenarios for the Year 2100. *Science*, *287*, 1770–1774.

Schröter, D., Cramer, W., Leemans, R., Prentice, I. C., Araújo, M. B., Arnell, N. W., … Zierl, B. (2005). Ecology: Ecosystem service supply and vulnerability to global change in Europe. *Science*, *310*(5752), 1333–1337.

Stralberg, D., Matsuoka, S. M., Handel, C. M., Bayne, E. M., Schmiegelow, F. K. A., & Hamann, A. (2016). Biogeography of boreal passerine range dynamics in western North America: past, present, and future. *Ecography*, *39*, 1–17.

Sturm, M., Racine, C., Tape, K., Cronin, T. W., Caldwell, R. L., & Marshall, J. (2001). Increasing shrub abundances in the Arctic. *Nature, 411*, 2001–2002.

Tayleur, C. M., Devictor, V., Gaüzère, P., Jonzén, N., Smith, H. G., & Lindström, Å. (2016). Regional variation in climate change winners and losers highlights the rapid loss of cold-dwelling species. *Diversity and Distributions*, *22*(4), 468–480.

Thuiller, W. (2004). Patterns and uncertainties of species' range shifts under climate change. *Global Change Biology*, *10*(12), 2020–2027.

Tulp, I., & Schekkerman, H. (2007). Has Prey Availability for Arctic Birds Advanced with Climate Change? Hindcasting the abundance of tundra arthropods using weather and seasonal variation. *Arctic, 61*(1), 48–60.

Urban, M. C. (2015). Accelerting extinction risk from climate change. *Science*, *348*(6234), 571–573.

Virkkala, R., Heikkinen, R. K., Leikola, N., & Luoto, M. (2008). Projected large-scale range reductions of northern-boreal land bird species due to climate change. *Biological Conservation*, *141*(5), 1343–1353.

Virkkala, R., & Lehikoinen, A. (2014). Patterns of climate-induced density shifts of species: Poleward shifts faster in northern boreal birds than in southern birds. *Global Change Biology*, *20*(10), 2995–3003.

Virkkala, R., & Lehikoinen, A. (2017). Birds on the move in the face of climate change: High species turnover in northern Europe. *Ecology and Evolution*, *7*(20), 8201–8209.

Virkkala, R., & Rajasärkkä, A. (2011a). Climate change affects populations of northern birds in boreal protected areas. *Biology Letters, 7*, 395–398.

Virkkala, R., & Rajasärkkä, A. (2011b). Northward density shift of bird species in boreal protected areas due to climate change. *Boreal Environment Research, 16*(supp. B), 2–13.

Walker, D. a, Raynolds, M. K., Daniëls, F. J., Einarsson, E., Elvebakk, A., Gould, W. a, … CAVM Team. (2005). The Circumpolar Arctic vegetation map. *Journal of Vegetation Science, 16*(16), 267–282.

Williams, J. E., & Blois, J. L. (2018). Range shifts in response to past and future climate change: Can climate velocities and species' dispersal capabilities explain variation in mammalian range shifts? *Journal of Biogeography, 45*(9), 2175–2189.

Willmes, C., Becker, D., Brocks, S., Hütt, C., & Bareth, G. (2017). High Resolution Köppen-Geiger Classifications of Paleoclimate Simulations. *Transactions in GIS, 21*(1), 57–73.

Wood, S., & Wood, M. S. (2015). Package ‘mgcv’. R package version, 1, 29.

Integrative discussion

In this thesis we have explored the effects of the Pleistocene glacial cycles in the diversity, distribution and migration of Arctic shorebirds. By using an integrative approach, combining spatial-explicit scenarios and genetic analyses for multiple species, we show that the fragmentation of the breeding distribution during these cycles promoted species' intraspecific diversification, especially during the Pleistocene period when glacial periods increased in intensity and duration. Our results show that past climatic changes have played a key role in shaping the diversity and distribution of these birds, driving quick changes over short periods of time. This allows us to better understand the potential impacts of the climate change in these representative Arctic species.

The role of the Pleistocene glacial cycles in the diversification of plant and animal species is a topic that has gathered substantial interest (Hewitt, 1996, 1999, 2000; Avise & Walker, 1998). It has even been argued against an increased diversification during this period, using Nearctic birds as study group (Klicka & Zink, 1997; Zink & Klicka, 2006). However, further reanalyses supported a recent timing for many events of inter- and intraspecific diversification (Johnson & Cicero, 2004; Lovette, 2005; Cicero & Johnson, 2006). Moreover, this process seems to be especially important in the diversification of species at higher latitudes, whose ranges were more in contact with the areas affected by the expansion of ice sheets (Weir & Schluter, 2004; Pruett & Winker, 2008; van Els *et al.*, 2012; Weir *et al.*, 2016).

Arctic shorebirds have received considerable attention when studying species' diversification at high latitudes. Previous works on different species reported an overall very shallow genetic diversity and recent diversification (Wenink *et al.*, 1994, 1996; Wennerberg, *et al.*, 2002; Buehler & Baker, 2005; Ottvall *et al.*, 2005; Trimbos *et al.*, 2014; Barisas *et al.*, 2015 Thies *et al.*, 2018).

This pattern has often been attributed to the effects of the fragmented breeding populations and population bottlenecks in the areas of refugia during glacial cycles, and a posterior recovery during interglacials (Buehler & Baker, 2005; Pruett & Winker, 2005, 2008; Trimbos *et al.*, 2014; Leblanc *et al.*, 2017; Thies *et al.*, 2018). But these processes are not necessarily exclusive of glacial periods, as some species can also have fragmented distributions during interglacials (Kraaijeveld & Nieboer, 2000; Stewart & Dalén, 2008). Frequently, the geographic details of the species' putative Arctic refugia are omitted in the literature. Studies assume their existence but oversee key aspects such as their location, the number of available independent breeding areas and the changes between periods (e. g. Buehler & Baker, 2005; Pruett & Winker, 2005; Trimbos *et al.*, 2014). These result in inferences based solely from the patterns provided by genetic data, ignoring the spatial mechanisms involved, and usually focused on individual species. Early studies on the potential distribution of species during the Last Glacial Maximum (LGM), highlighted a correlation between areas of refugia and the origin of subspecies in certain Arctic shorebirds (Greenwood, 1986; Ploeger, 1968), which had some parallelism with Arctic geese and ducks (Ploeger, 1968).

In the Chapter 1, we highlighted the importance of the different distribution patterns during both glacial and interglacial periods in the intraspecific diversification of Arctic shorebirds. The results show that the majority of species with subspecies experienced potential fragmentation of their breeding ranges during glacial and/or interglacial periods. On the other hand, monotypic species predominantly displayed a continuous range during both periods, with retreat to a single refugium during the LGM. This is in agreement with the original hypothesis of the Pleistocene glacial cycles as the main driver of diversification though isolation of breeding populations (Rand, 1948; Ploeger, 1968). But our work also extended it further. First, we showed that in many species the glacial cycles prevented their diversification by keeping all their populations together. Furthermore, while the glacial refugia seemed to be the main source of allopatric differentiation, the post-glacial expansions would have still played a role in the diversification of certain species. This fits the previous findings in northern bird species where fragmentation during glacial periods is the most common suggested process (Rand, 1948; Mengel, 1964; Ploeger, 1968; Weir & Schluter, 2004), but post-glacial expansions and interglacial climate also contributed to the isolation and recent

diversification in some species (Kraaijeveld & Nieboer, 2000; Milá, *et al.*, 2006, 2007; Friis *et al.*, 2016)

Our results also show that, despite changes in the breeding distribution, almost all species of Arctic shorebirds maintained their long-distance migration during the LGM. This contradicts the generality of the glaciations as a "migratory switch", proposed for some migratory birds in North America (Zink & Gardner, 2017). The predicted non-breeding ranges remained stable during that period, especially around tropical areas, and in general the overlap between breeding and non-breeding ranges was predicted to be minimal or non-existent. Additionally, the studies on the fossils specimens of *Calidris* in Olduvai Gorge (Tanzania) across the Pleistocene showed a lack of medullary bone, which is a structure only present during the breeding period, and absence of juveniles. This indicates that the same non-breeding areas where occupied during the Pleistocene to the present, and therefore supports that Arctic shorebirds remained migrating even during glacial periods.

It is possible that the different flyways used by species and subspecies are linked to their areas of refugia. However, we cannot conclude whether the different flyways promoted the geographic fragmentation or if it was the other way around. In any case, it is likely that the parallel migratory routes for different populations reinforced the divergence between them. This is especially important upon post-glacial expansions, where different populations expanded north maintaining their main migratory routes (Ruegg & Smith, 2002; Buehler *et al.*, 2006; Ruegg *et al.*, 2006). Even with secondary contacts, breeding populations from different flyways can remain acting as independent units, as different migration routes often involve different phenological timings and morphological traits (Buehler *et al.*, 2006; Meltofte *et al.*, 2007; Maley & Winker, 2010; Jukema *et al.*, 2015).

Validation of the spatial mechanisms of diversification proposed in Chapter 1 required the use of genetic data. Previous analyses of divergence times in Arctic shorebirds were performed for individual species, and based on mitochondrial mutation rates generalised from other sources (e. g. Buehler & Baker, 2005; Ottvall *et al.*, 2005;

Pruett & Winker, 2005; Rönkä *et al.*, 2012). The use of these "universal" rates for any studied taxa or any mitochondrial gene, has been very criticized (Garcia-moreno, 2004; Lovette, 2004; Pereira & Baker, 2006). Furthermore, estimations of the rates based on the analysis of complete mitochondrial genomes argued against the universality of such rates between different genes or lineages (Pereira & Baker, 2006; Pacheco *et al.*, 2011; Nabholz *et al.*, 2016). The estimation of the rates performed in this thesis represents the largest analysis of this type ever done so far, both in number of species included (621) and reliable fossil calibrations used (25). The results, as in previous studies, contradict the generality of the mutation rate values (Pereira & Baker, 2006; Pacheco *et al.*, 2011; Nabholz *et al.*, 2016). We therefore advise against the use of the "standard molecular clock" rate, or any form of "universal" rates. Instead, we here provide specific rate estimations for every mitochondrial gene, for many lineages of the avian phylogenetic tree. This allowed us to apply rates that were more specific for the lineages of shorebirds studied and the mitochondrial genes used in our analyses of divergence times.

The molecular clock and coalescent analyses, performed simultaneously for multiple species with different patterns of diversity, support an overall recent diversification of Arctic shorebirds during the Pleistocene. The divergence time recovered between some species (*Pluvialis sp.*) or subspecies (in *Calidris alpina* and *Limosa limosa*) predate the Pleistocene period, which is still in agreement with previous works (Johnson & Cicero, 2004; Weir & Schluter, 2004; Lovette, 2005; Cicero & Johnson, 2006). However, most of the intraspecific diversification in all the studied species took place within the Pleistocene, and especially during the last 900,000 years. This period is known for an increase in the intensity and duration of the glacial cycles, where longer glacial periods (~100,000 years) with greater ice accumulation were only interrupted by shorter warm interglacials (~30,000 years) (EPICA community members, 2004; Lisiecki & Raymo, 2005; Jouzel *et al.*, 2007).

The species with greater isolation between their main populations during both glacial and interglacial periods, like *L. limosa* and *C. alpina* shower older and better-defined genetic lineages, which is consistent with previous findings (Buehler & Baker, 2005; Trimbos *et al.*, 2014). On the other hand, some species showed little or no genetic structure, and a very recent overall diversification. These species tend to show similar distribution patterns during both glacial and interglacial periods, like *Charadrius*

hiaticula and *Pluvialis apricaria* in Europe, or *Calidris canutus* and *Arenaria interpres* across the high Arctic. These species likely experienced severe contractions of their ranges into very few areas of refugia, and quick post-glacial expansions from those areas. Furthermore, some subspecies restricted to high latitudes likely experienced the main fragmentation and reduction of their populations during the interglacials, resulting in a very recent and shallow diversity in their current areas of "warm refugia" (Kraaijeveld & Nieboer, 2000), which was yet enough to originate the observed phenotypic variation in a short period of time.

When considered together, Chapter 1 and Chapter 2 provide a spatial and temporal confirmation of the mechanisms of intraspecific diversification in this group of birds during the glacial cycles. The fragmentation of the breeding ranges, especially during glacial periods, provided a favourable scenario for allopatric speciation. As these periods increased its duration and intensity, this process of diversification increased substantially, resulting in the different diversity and distribution patterns we find today. This likely applies to many other species of the Arctic fauna and flora. Certain areas of glacial refugia, like Beringia or the mountain ranges below the ice cover, strongly determined the diversity patterns across different Arctic taxa (Skrede *et al.*, 2006; Todisco *et al.*, 2012; Eidesen *et al.*, 2013; Kleckova *et al.*, 2015). This results in a recent diversification of the subspecies across an east-west axis, found across different taxa with varying degrees of dispersal ability: from plants (e. g. Eidesen *et al.*, 2013) to mammals (e. g. Jaarola & Searle, 2002; Flagstad & Røed, 2003; Zigouris *et al.*, 2013) and even migratory birds (e.g. Ploeger, 1968; Jones *et al.*, 2005; Pruett & Winker, 2008; Pujolar *et al.*, 2017). Moreover, our findings agree with previous studies highlighting that most of the intraspecific diversity in high-latitude bird species occurred during this period of glacial cycles (Weir & Schluter, 2004; Lovette, 2005; van Els *et al.*, 2012; Weir *et al.*, 2016).

Arctic shorebirds have shown to be very capable of coping with extreme climatic oscillations. However, current climate change represents a completely different scenario than the glacial periods. Animal and plants species worldwide are experiencing a poleward shift due to the current changes in the global climate, and this trend is expected to continue and increase over the next decades. This also includes birds, in

which the northern and migratory species are considered among the most endangered. Our results in Chapter 3 agree with the displacement of the ranges of bird species towards higher latitudes, especially in northern species (Huntley *et al.*, 2008; Virkkala & Rajasärkkä, 2011; Barbet-Massin *et al.*, 2012). However, since many Arctic shorebirds species are already at the northernmost edges of the continents, we found that the process involves a loss of the southern part of their distributions more than an expansion to the north. This represents a major threat, especially for species confined to very high latitudes with very restricted distributions, while the species that inhabit temperate areas have greater margin of expansion. This process also shows a great asymmetry in geographic terms, as the Palearctic and Nearctic regions showed clearly different trends. In the Palearctic, the potential ranges of most species show significant reductions under all future climate change scenarios. On the other hand, in the Nearctic, the Canadian Archipelago provides such northern suitable areas for the species to maintain or even expand their ranges. But such possibility should be considered with great care, as this process is extremely dependant on the response of the ecosystems in the breeding and stopover sites, as well as on the phenology of the species (Meltofte *et al.*, 2007; McGowan *et al.*, 2011; Galbraith *et al.*, 2014; Alves *et al.*, 2019).

The changes in the breeding distribution of the Arctic shorebirds due to the current climate change could lead to new refugia, with all the implications seen in the first chapters. However, our results do not allow us to fully determine where the predicted areas of refugia will persist, or if the climate change will overwrite the diversity originated during glacial cycles, beyond the disappearance of certain species or subspecies in critical areas. Our results on the changes in the Arctic during the last 120,000 years show that the shorebirds have overcame other warm periods in the region recently, which likely contributed to establish their current diversity (Kraaijeveld & Nieboer, 2000). But as opposed to those periods, which developed over thousands of years, the current climate change is severely reducing the Arctic and altering its ecosystems in a few hundred years, or even decades. Furthermore, over the next century the climate of the planet will be analogue to past climates never experienced by current species (Burke *et al.*, 2018). The increased rate of the changes in the climate and ecosystems makes it difficult for the migratory species to adapt their phenology, diet and distribution in time (Crick, 2004; Newson *et al.*, 2009; Saino *et al.*, 2011). This is

already translating into severe population declines and habitat loss in Arctic shorebirds and other northern species (Gilg *et al.*, 2012; Lindström *et al.*, 2015; Stralberg *et al.*, 2015; Tayleur *et al.*, 2016).

In conclusion, this thesis shows that climatic changes have determined the recent diversification of this group of Arctic birds, splitting the breeding ranges during the glacial cycles of the Pleistocene. Our study links the spatial and temporal components of this climate-driven diversification, highlighting the different processes experienced in different regions and for different species. This integrative approach sheds light in the evolution of Arctic species during periods of climatic oscillations. Moreover, our results suggest that the current climate represents an unprecedented challenge for the survival of many of these species. Our work provides key insights on the potential response of the Arctic biodiversity to climate change and the differences between regions.

References

Alves, J. A., Gunnarsson, T. G., Sutherland, W. J., Potts, P. M., & Gill, J. A. (2019). Linking warming effects on phenology, demography and range expansion in a migratory bird population. *Ecology and Evolution*, (March 2018), 1–37.

Avise, J., & Walker, D. (1998). Pleistocene phylogeographic effects on avian populations and the speciation process. *Proceedings of the Royal Society B: Biological Sciences*, *265*, 457–463.

Barbet-Massin, M., Thuiller, W., & Jiguet, F. (2012). The fate of European breeding birds under climate, land-use and dispersal scenarios. *Global Change Biology*, *18*(3), 881–890.

Barisas, D. A. G., Amouret, J., Hallgrímsson, G. T., Summers, R. W., & Pálsson, S. (2015). A review of the subspecies status of the Icelandic Purple Sandpiper *Calidris maritima littoralis*. *Zoological Journal of the Linnean Society*, *175*(1), 211–221.

Buehler, D. M., & Baker, A. J. (2005). Population divergence times and historical demography in Red Knots and Dunlins. *Condor*, *107*, 497–513.

Buehler, D. M, Baker, A. J., & Piersma, T. (2006). Reconstructing palaeoflyways of the late Pleistocene and early Holocene red knot (*Calidris canutus*). *Ardea*, *94*(3), 485–498.

Burke, K. D., Williams, J. W., Otto-Bliesner, B. L., Haywood, A. M., Burke, K. D., Chandler, M. A., & Lunt, D. J. (2018). Pliocene and Eocene provide best analogs for near-future climates. *Proceedings of the National Academy of Sciences*, *115*(52), 13288–13293.

Cicero, C., & Johnson, N. K. (2006). The tempo of Avian diversification: Reply. *Evolution*, *60*(2), 413.

Cohen, K. M., & Gibbard, P. L. (2008). Global chronostratigraphical correlation table for the last 2.7 million years. *Episodes*, *31*(2), 243–247.

Crick, H. Q. P. (2004). Impact of climate change on birds. *Ibis*, *146*(Suppl. 1), 48–56.

Eidesen, P. B., Ehrich, D., Bakkestuen, V., Alsos, I. G., Gilg, O., Taberlet, P., & Brochmann, C. (2013). Genetic roadmap of the Arctic: Plant dispersal highways, traffic barriers and capitals of diversity. *New Phytologist*, *200*(3), 898–910.

EPICA community members. (2004). Eight glacial cycles from an Antarctic ice core. *Nature*, *429*, 623–628.

Flagstad, Ø., & Røed, K. H. (2003). Refugial origins of Reindeer (*Rangifer tarandus*) inferred from Mitochondrial DNA Sequences. *Evolution*, *57*(3), 658–670.

Friis, G., Aleixandre, P., Rodríguez-Estrella, R., Navarro-Sigüenza, A. G., & Milá, B. (2016). Rapid postglacial diversification and long-term stasis within the songbird genus *Junco*: phylogeographic and phylogenomic evidence. *Molecular Ecology*, *25*(24), 6175–6195.

Galbraith, H., DesRochers, D. W., Brown, S., & Reed, J. M. (2014). Predicting vulnerabilities of North American shorebirds to climate change. *PLoS ONE*, *9*(9), 21–23.

Garcia-moreno, J. (2004). Is there a universal mtDNA clock for birds? *Journal of Avian Biology*, *35*(6), 465–468.

Gilg, O., Kovacs, K. M., Aars, J., Fort, J., Gauthier, G., Grémillet, D., … Bollache, L. (2012). Climate change and the ecology and evolution of Arctic vertebrates. *Annals of the New York Academy of Sciences*, *1249*(1), 166–190.

Greenwood, J. G. (1986). Geographical variation and taxonomy of the Dunlin (*Calidris alpina*).

Bulletin of the British Ornithologists' Club, *106*, 43–42.

Hewitt, G. M. (1996). Some genetic consequences of ice ages, and their role in speciation. *Biological Journal of the Linnaean Society*, *58*(July), 247–276.

Hewitt, G. M. (1999). Post-glacial re-colonization of European biota. *Biological Journal of the Linnean Society*, *68*(1–2), 87–112.

Hewitt, G. M. (2000). The genetic legacy of the quaternary ice ages. *Nature*, *405*(6789), 907–913.

Huntley, B., Collingham, Y. C., Willis, S. G., & Green, R. E. (2008). Potential impacts of climatic change on European breeding birds. *PLoS ONE*, *3*(1).

Jaarola, M., & Searle, J. B. (2002). Phylogeography of field voles (*Microtus agrestis*) in Eurasia inferred from mitochondrial DNA sequences. *Molecular Ecology*, *11*, 2613–2621.

Johnson, N. K., & Cicero, C. (2004). New mitochondrial DNA data affirm the importance of Pleistocene speciation in North American birds. *Evolution*, *58*(5), 1122–1130.

Jones, K. L., Krapu, G. L., Brandt, D. A., & Ashley, M. V. (2005). Population genetic structure in migratory Sandhill Cranes and the role of Pleistocene glaciations. *Molecular Ecology*, *14*(9), 2645–2657.

Jouzel, J., Cattani, O., Dreyfus, G., Falourd, S., Hoffmann, G., Nouet, J., … Schilt, A. (2007). Orbital and Millennial Antarctic Climate Variability over the past 800,000 years. *Science*, *317*(5839), 793–796.

Jukema, J., van Rhijn, J. G., & Piersma, T. (2015). Geographic variation in morphometrics, molt, and migration suggests ongoing subspeciation in Pacific Golden-Plovers (*Pluvialis fulva*). *The Auk*, *132*(3), 647–656.

Kleckova, I., Cesanek, M., Fric, Z., & Pellissier, L. (2015). Diversification of the cold-adapted butterfly genus Oeneis related to Holarctic biogeography and climatic niche shifts. *Molecular Phylogenetics and Evolution*, *92*, 255–265.

Klicka, J., & Zink, R. M. (1997). The Importance of Recent Ice Ages in Speciation: A Failed Paradigm. *Science*, *277*(5332), 1666–1669.

Kraaijeveld, K., & Nieboer, E. N. (2000). Late Quaternary paleogeography and evolution of Arctic-breeding waders. *Ardea*, *88*(2), 193–205.

Leblanc, N. M., Stewart, D. T., Pálsson, S., Elderkin, M. F., Mittelhauser, G., Mockford, S., … Mallory, M. L. (2017). Population structure of Purple Sandpipers (*Calidris maritima*) as revealed by mitochondrial DNA and microsatellites. *Ecology and Evolution*, (7), 3225–3242.

Lindström, Å., Green, M., Husby, M., Kålås, J. A., & Lehikoinen, A. (2015). Large-scale monitoring of waders on their boreal and arctic breeding grounds in Northern Europe. *Ardea*, *103*(1), 3–15.

Lisiecki, L. E., & Raymo, M. E. (2005). A Pliocene-Pleistocene stack of 57 globally distributed benthic δ 18O records. *Paleoceanography*, *20*(1), 1–17.

Lovette, I. J. (2004). Mitochondrial dating and mixed support for the “2% rule” in birds. *The Auk*, *121*(1), 1–6.

Lovette, Irby J. (2005). Glacial cycles and the tempo of avian speciation. *Trends in Ecology and Evolution*, *20*(2), 57–59.

Maley, J. M., & Winker, K. (2010). Diversification at high latitudes: Speciation of buntings in the genus *Plectrophenax* inferred from mitochondrial and nuclear markers. *Molecular Ecology*,

19(4), 785–797.

McGowan, C. P., Hines, J. E., Nichols, J. D., Lyons, J. E., Smith, D. R., Kalasz, K. S., … Kendall, W. (2011). Demographic consequences of migratory stopover: linking Red Knot survival to Horseshoe Crab spawning abundance. *Ecosphere*, *2*(6).

Meltofte, H., Piersma, T., Boyd, H., McCaffery, B., Ganter, B., Golovnyuk, V. V., … Wennerberg, L. (2007). *Effects of Climate Variation on The Breeding Ecology of Arctic Shorebirds*. *Meddelelser Om Gronland Bioscience* (Vol. 59).

Mengel, R.M. (1964) The probable history ofspecies formation in some northern wood warblers (*Parulidae*). *Living Bird* 3 (4), 9–43.

Milá, B., McCormack, J. E., Castañeda, G., Wayne, R. K., & Smith, T. B. (2007). Recent postglacial range expansion drives the rapid diversification of a songbird lineage in the genus *Junco*. *Proceedings of the Royal Society B: Biological Sciences*, *274*(1626), 2653–2660.

Milá, B., Smith, T. B., & Wayne, R. K. (2006). Postglacial Population Expansion Drives the Evolution of Long-Distance Migration in a Songbird. *Evolution*, *60*(11), 2403–2409.

Nabholz, B., Lanfear, R., & Fuchs, J. (2016). Body mass-corrected molecular rate for bird mitochondrial DNA. *Molecular Ecology*, 4438–4449.

Newson, S. E., Mendes, S., Crick, H. Q. P., Dulvy, N. K., Houghton, J. D. R., Hays, G. C., … Robinson, R. A. (2009). Indicators of the impact of climate change on migratory species. *Endangered Species Research*, *7*(2), 101–113.

Ottvall, R., Höglund, J., Bensch, S., & Larsson, K. (2005). Population differentiation in the Redshank (*Tringa totanus*) as revealed by mitochondrial DNA and amplified fragment length polymorphism markers. *Conservation Genetics*, *6*(3), 321–331.

Pacheco, M. A., Battistuzzi, F. U., Lentino, M., Aguilar, R. F., Kumar, S., & Escalante, A. A. (2011). Evolution of modern birds revealed by mitogenomics: Timing the radiation and origin of major orders. *Molecular Biology and Evolution*, *28*(6), 1927–1942.

Pereira, S. L., & Baker, A. J. (2006). A mitogenomic timescale for birds detects variable phylogenetic rates of molecular evolution and refutes the standard molecular clock. *Molecular Biology and Evolution*, *23* (9), 1731-1740

Ploeger, P. L. (1968). Geographical differentation in arctic Anatidae as a result of isolation during the last glacial. *Ardea*, *56*(1–2), 4–155.

Pruett, C. L., & Winker, K. (2005). Biological impacts of climatic change on a Beringian endemic: Cryptic refugia in the establishment and differentiation of the Rock Sandpiper (*Calidris ptilocnemis*). *Climatic Change*, *68*(1–2), 219–240.

Pruett, C. L., & Winker, K. (2008). Evidence for cryptic northern refugia among high- and temperate-latitude species in Beringia. *Climatic Change*, *86*(1–2), 23–27.

Pujolar, J. M., Dalén, L., Hansen, M. M., & Madsen, J. (2017). Demographic inference from whole-genome and RAD sequencing data suggests alternating human impacts on goose populations since the last ice age. *Molecular Ecology*, *26*(22), 6270–6283.

Rand, A. L. (1948). Glaciation, An Isolating Factor in Speciation. *Evolution*, *2*(4), 314–321.

Rönkä, N., Kvist, L., Pakanen, V. M., Rönkä, A., Degtyaryev, V., Tomkovich, P., … Koivula, K. (2012). Phylogeography of the Temminck's Stint (*Calidris temminckii*): Historical vicariance but little present genetic structure in a regionally endangered Palearctic wader. *Diversity and Distributions*, *18*(7), 704–716.

Ruegg, K. C., Hijmans, R. J., & Moritz, C. (2006). Climate change and the origin of migratory pathways in the Swainson's Thrush. *Journal of Biogeography*, *33*, 1172–1182.

Ruegg, K. C., & Smith, T. B. (2002). Not as the crow flies: A historical explanation for circuitous migration in Swainson's Thrush (*Catharus ustulatus*). *Proceedings of the Royal Society B: Biological Sciences*, *269*(1498), 1375–1381.

Saino, N., Ambrosini, R., Rubolini, D., Von Hardenberg, J., Provenzale, A., Hüppop, K., … Sokolov, L. (2011). Climate warming, ecological mismatch at arrival and population decline in migratory birds. In *Proceedings of the Royal Society B: Biological Sciences, 278*, 835–842.

Skrede, I., Pernille Bronken Eidesen, Portela, R. P., & Brochmann, C. (2006). Refugia, differentiation and postglacial migration in arctic- alpine Eurasia, exemplified by the mountain avens (*Dryas octopetala* L.). *Molecular Ecology*, *15*, 1827–1840.

Stewart, J. R., & Dalén, L. (2008). Is the glacial refugium concept relevant for northern species? A comment on Pruett and Winker 2005. *Climatic Change*, *86*(1–2), 19–22.

Stralberg, D., Matsuoka, S. M., Hamann, A., Bayne, E. M., Sï¿½lymos, P., Schmiegelow, F. K. A., … Song, S. J. (2015). Projecting boreal bird responses to climate change: The signal exceeds the noise. *Ecological Applications*, *25*(1), 52–69.

Tayleur, C. M., Devictor, V., Gaüzère, P., Jonzén, N., Smith, H. G., & Lindström, Å. (2016). Regional variation in climate change winners and losers highlights the rapid loss of cold-dwelling species. *Diversity and Distributions*, *22*(4), 468–480.

Thies, L., Tomkovich, P., Remedios, N. dos, Lislevand, T., Pinchuk, P., Wallander, J., … Küpper, C. (2018). Population and Subspecies Differentiation in a High Latitude Breeding Wader, the Common Ringed Plover *Charadrius hiaticula*. *Ardea*, *106*(2), 163–176.

Todisco, V., Gratton, P., Zakharov, E. V., Wheat, C. W., Sbordoni, V., & Sperling, F. A. H. (2012). Mitochondrial phylogeography of the Holarctic *Parnassius phoebus* complex supports a recent refugial model for alpine butterflies. *Journal of Biogeography*, *39*(6), 1058–1072.

Trimbos, K. B., Doorenweerd, C., Kraaijeveld, K., Musters, C. J. M., Groen, N. M., Knijff, P., … De Snoo, G. R. (2014). Patterns in nuclear and mitochondrial DNA reveal historical and recent isolation in the Black-tailed Godwit (*Limosa limosa*). *PLoS ONE*, *9*(1).

van Els, P., Cicero, C., & Klicka, J. (2012). High latitudes and high genetic diversity: Phylogeography of a widespread boreal bird, the gray jay (*Perisoreus canadensis*). *Molecular Phylogenetics and Evolution*, *63*(2), 456–465.

Virkkala, R., & Rajasärkkä, A. (2011). Northward density shift of bird species in boreal protected areas due to climate change. *Boreal Environment Research*, *16*(supp. B), 2–13.

Weir, J. T., Haddrath, O., Robertson, H. A., Colbourne, R. M., & Baker, A. J. (2016). Explosive ice age diversification of kiwi. *Proceedings of the National Academy of Sciences*, *113*(38), 580–587.

Weir, J. T., & Schluter, D. (2004). Ice sheets promote speciation in boreal birds. *Proceedings of the Royal Society of London. Series B: Biological Sciences*, *271*(1551), 1881–1887.

Wenink, P., Baker, A., Rosner, H., & Tilanus, M. (1996). Global mitochondrial DNA phylogeography of holarctic breeding Dunlins (*Calidris alpina*). *Evolution*, *50*(1), 318–330.

Wenink, P. W., Baker, A. J., & Tilanus, M. G. (1994). Mitochondrial control-region sequences in two shorebird species, the Turnstone and the Dunlin, and their utility in population genetic studies. *Molecular Biology and Evolution*, *11*(1), 22–31.

Wennerberg, L., Klaassen, M., & Lindström, Å. (2002). Geographical variation and population

structure in the White-rumped Sandpiper *Calidris fuscicollis* as shown by morphology, mitochondrial DNA and carbon isotope ratios. *Oecologia*, *131*(3), 380–390.

Zigouris, J., Schaefer, J. A., Fortin, C., & Kyle, C. J. (2013). Phylogeography and post-glacial recolonization in wolverines (*Gulo gulo*) from across their circumpolar distribution. *PLoS ONE*, *8*(12), 1–13.

Zink, R. M., & Gardner, A. S. (2017). Glaciation as a migratory switch. *Science Advances*, *3*(9), e1603133.

Zink, R. M., & Klicka, J. (2006). The tempo of avian diversification: A comment on Johnson and Cicero. *Evolution*, *60*(2), 411–412.

Conclusions

1. The fragmentation of the breeding distribution of Arctic shorebirds during the glacial cycles promoted their current intraspecific diversity. Most of the species with described subspecies showed fragmented breeding ranges during glacial and/or interglacial periods. In contrast, the breeding ranges of almost all monotypic species remained continuous during both periods.

2. The species' distribution models and the fossil record support that the long-distance migratory behaviour was not interrupted during glacial periods. The migratory routes and the fragmentation of the breeding range could have acted together to reinforce and maintain the diversification between populations.

3. The calibration of the molecular clock rates for the mitochondrial genes in birds, the most comprehensive to date, contradicts the validity of the standard molecular clock or other generalized rates. Our results provide reliable rate estimations for each mitochondrial gene in a large number of avian lineages, which allows to better estimate divergence times and phylogeographic histories within and between bird species.

4. Genetic data supports a recent diversification within multiple Arctic shorebird species, especially over the Middle and Late Pleistocene, coinciding with longer and more intense glacial periods. Species with similar patterns of distribution, both now and during the LGM, show parallelism in their divergence time and degree of genetic differentiation.

5. Genetic and biogeographic data support a Pleistocene origin of the current diversity within the Arctic shorebird species. Together, they provide a spatial and temporal mechanism of diversification based on climate-driven allopatric differentiation. Fragmentation of the breeding range during glacial cycles favoured the diversification of subspecies, especially when these cycles increased in amplitude and duration.

6. Due to climate change, the breeding ranges of the Arctic shorebirds are expected to displace northwards over the next decades. However, many species are already restricted to the northernmost available territories, and they will experience the most severe range reductions as the southern margin of their distribution is lost.

7. The proportion of Arctic shorebird species experiencing severe range reduction is greater in the Palearctic than in the Nearctic, given the availability of high-latitude territories that could become suitable in the future. However, this relies heavily on the ability of the ecosystems and associated communities to colonize those territories in time.

8. The current climate change is altering the Arctic much faster than in previous climatic oscillations, which greatly challenges the possibilities of the species to quickly adapt to the new scenario and threatens their conservation. Following the current trend, the climate of the Arctic could transform beyond what the Arctic species have experienced in their evolutionary history.

9. Climate has played a key role in the diversification of Arctic shorebirds and other Arctic species during the Pleistocene, by promoting the differentiation of isolated populations during unsuitable periods. Current climate change can lead to a new scenario of reduced and fragmented populations that would deeply affect the diversity and conservation of the Arctic species.

Appendix 1: Species' distribution maps (present and LGM)

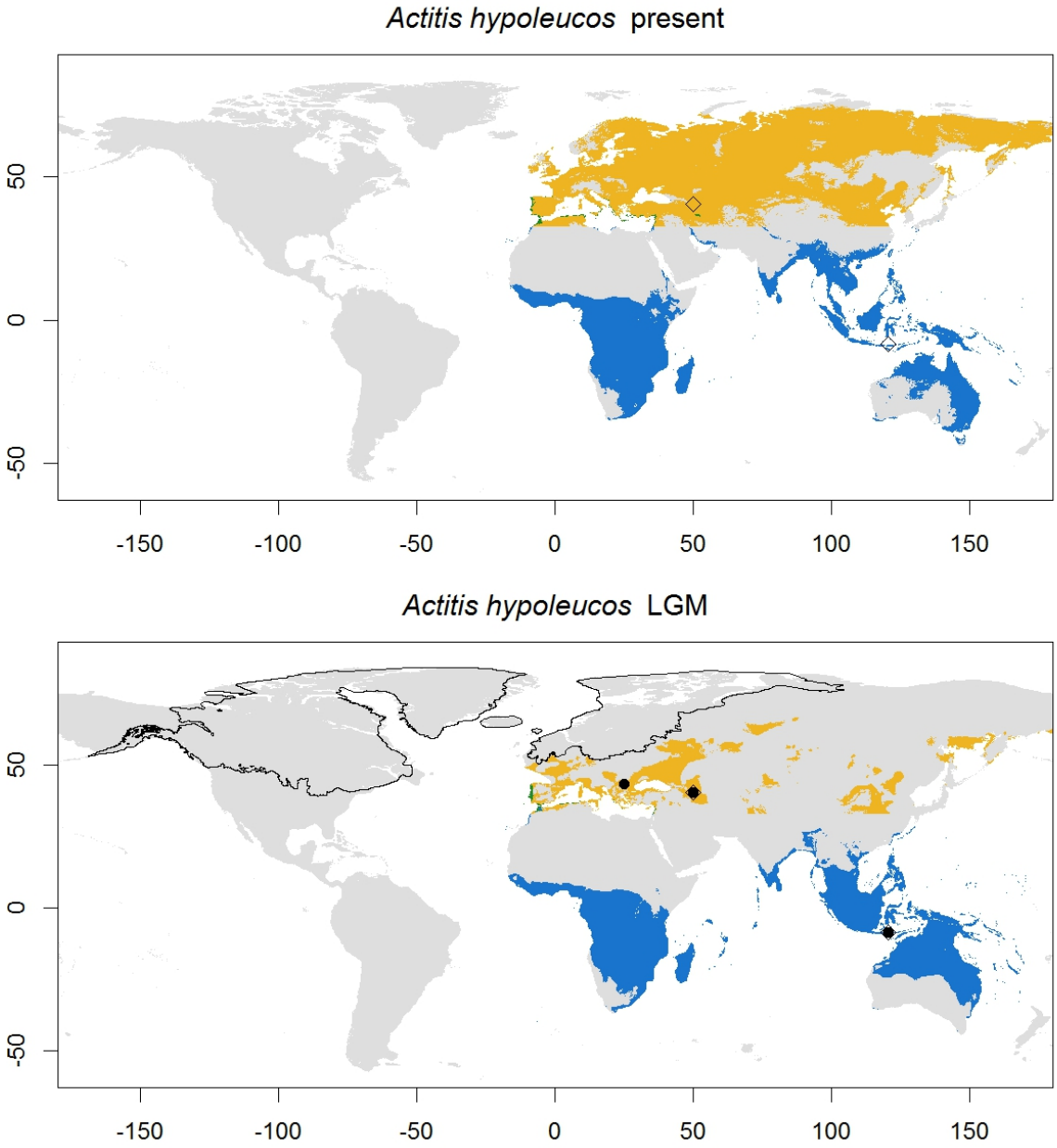

Map 1: Common Sandpiper (*Actitis hypoleucos*) predicted distributions for the breeding (yellow) and wintering (blue) ranges, and their overlap (green), in the present and the LGM. Dots represent fossil localities for the species in the Pleistocene, diamonds represent fossil localities both in the Pleistocene and the Holocene. Black line represents the extension of the main ice sheets during the LGM, simplified from Ehlers *et al*. (2011).

Common Sandpiper, *Actitis hypoleucos* (map 1). Breeding distribution is widespread across the Palearctic, from the Iberian Peninsula to Kamchatka, reaching the Arctic latitudes in Scandinavia and Siberia. No variation described. The SDM for the present returned a range that fits the distribution range (del Hoyo *et al*., 2018), with slight over predictions at the northern part. LGM hindcast shows a major range reduction, with just

low latitude patches (between 30°N and 50°N), mostly in the Mediterranean region, central and eastern Europe and eastern Asia. The wintering range covers most of Africa (except the Sahara Desert), Madagascar, southern Asia, New Guinea and Australia. The SDM fits this wintering range, failing to predict presence only in the Arabian Peninsula. In the LGM, the wintering range remains fairly stable, with slight reductions on the northern and southern margins, although still present in the Sahel region. This species is classified under scenario C.

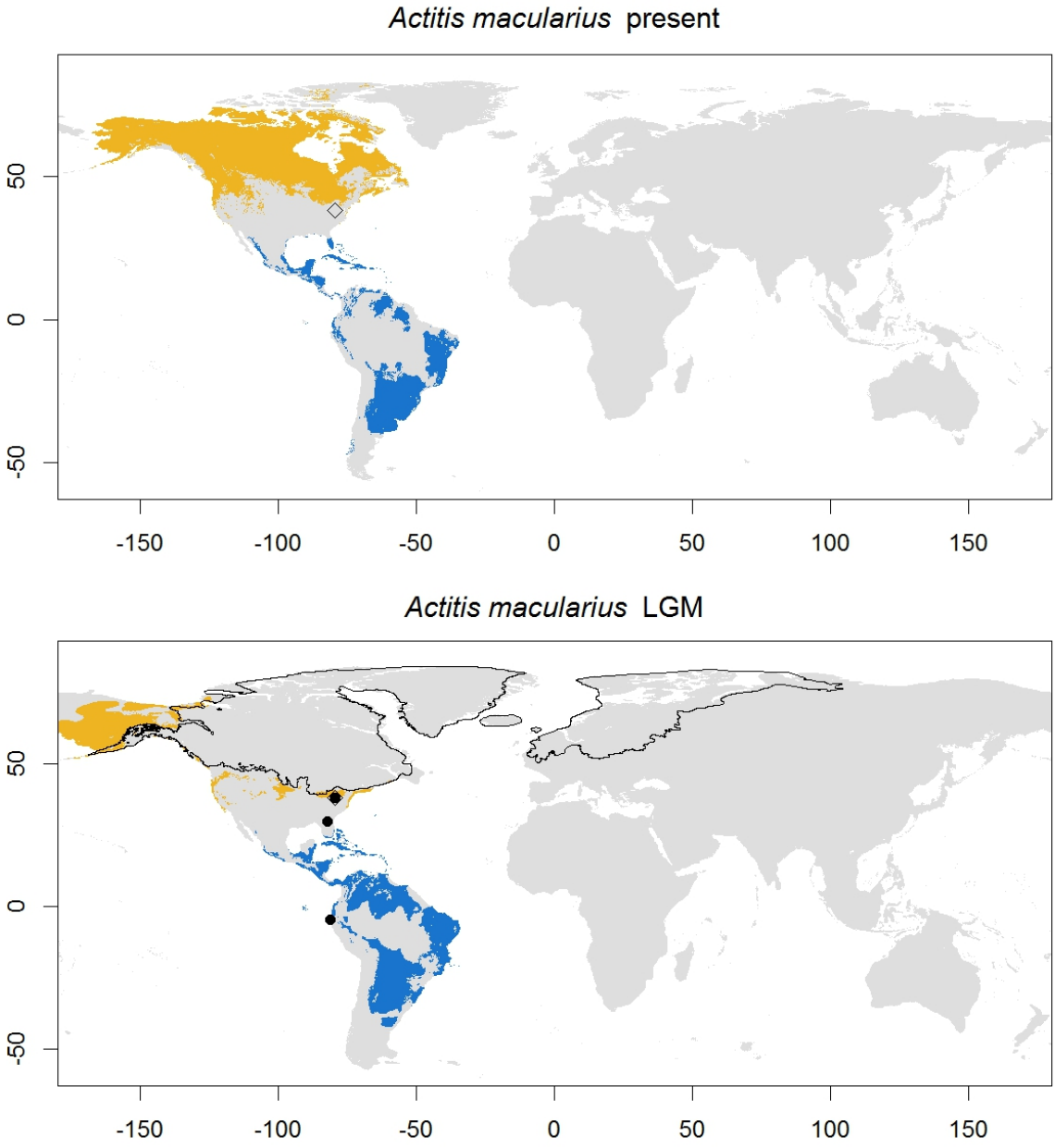

Map 2: Spotted Sandpiper (*Actitis macularius*) predicted distribution. Caption as in map 1.

Spotted Sandpiper, *Actitis macularius* (map 2). Breeds in temperate and artic areas in North America, from Alaska to the Labrador Peninsula (del Hoyo *et al*., 2018). No subspecies (*A. m. rava* not considered as valid). The SDM fits the known current range, with some under-predictions at lower latitudes and over-predictions at the Canadian Arctic. LGM models show a split of the range into two main areas: a large one in Beringia, and a group of smaller ones at around 40°N in what is now the USA. Wintering distribution covers from southern USA to the north of Argentina and Chile. The models from the present return a wintering predicted distribution similar to the real one, although not as a continuous extent. Models for the LGM show very little variation in the wintering range between past and present. This species is classified under scenario C.

Ruddy Turnstone, *Arenaria interpres* (map 3). Circumpolar coastal species, only absent in south and southeast Greenland and between Labrador Peninsula and Yukon. Two recognized subspecies, *A. i. interpres*, distributed across the Palearctic, northwest Alaska, north Canadian Arctic and Greenland; and *A. i. morinella*, in east Alaska and most of the Canadian Arctic (del Hoyo *et al*., 2018). Our SDM fits well the breeding distribution of the species, only over-predicting in some parts of Canada, Svalbard and some small regions in central Asia. The LGM model predicts a disappearance of all the current breeding range of *A. i. morinella*, with the closest predicted areas located in southern latitudes in inland territories of North America (therefore unlikely). The remaining range of the species is very fragmented, with large predicted areas in Beringia, northeast Siberia and Kamchatka, and north central Asia. Smaller predicted areas appear in central Europe and both eastern and western coasts of Greenland. The wintering distribution extends from Europe and North America to South America, the whole African coastline, south Asia and Oceania. The SDM for the wintering fits the known range, but also predicts large inland areas. In the LGM the wintering range remains stable, with reduction of the northern and southern parts of the distribution, especially in southern Asia and North America. This species is classified under scenario C.

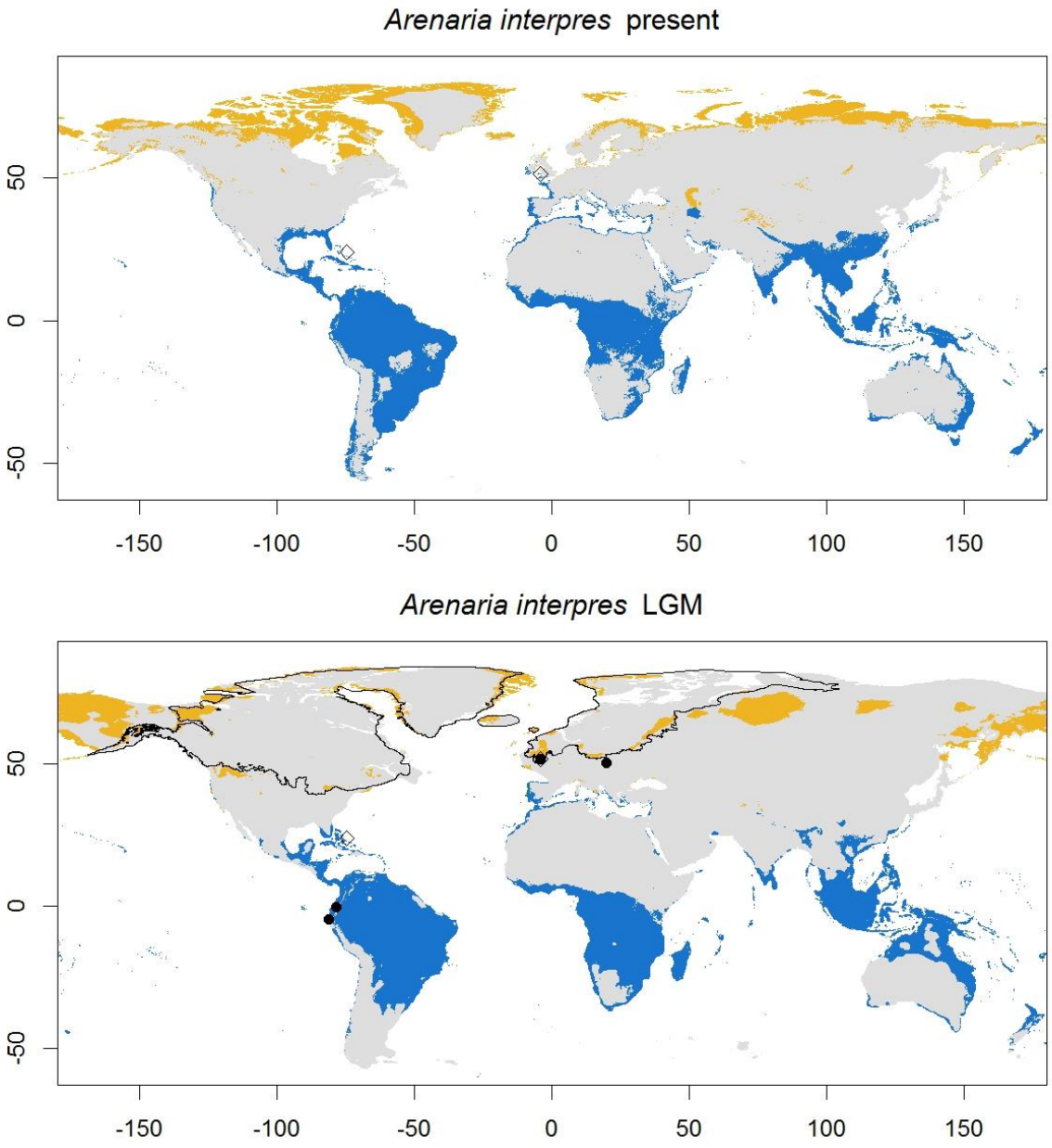

Map 3: Ruddy Turnstone (*Arenaria interpres*) predicted distribution. Caption as in map 1.

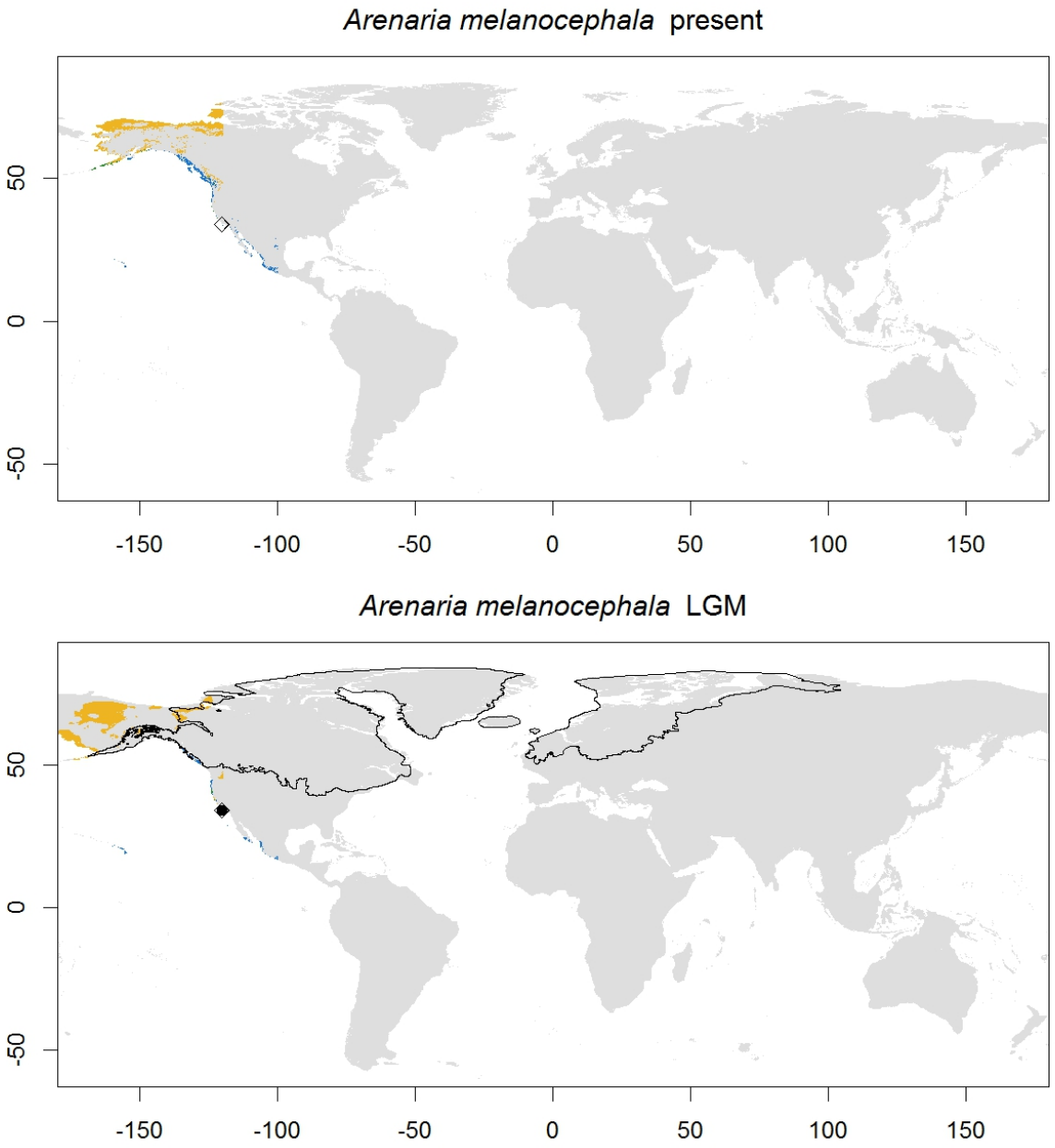

Map 4: Black Turnstone (*Arenaria melanocephala*) predicted distribution. Caption as in map 1.

Black Turnstone, *Arenaria melanocephala* (map 4). Coastal species breeding in the east coast of Alaska and Aleutian Islands. No variation described. The current SDM model over-predicts in north Alaska, Yukon and Banks Island. In the LGM, the model predicts the species to maintain a similar breeding range in the emerged lands of Beringia, as well as north Alaska. The current wintering range, along the western coast of North America, is well predicted by the SDM model for the present, although with a smaller extent size. The models show no major changes in the wintering range during the LGM. This species is classified under scenario A.

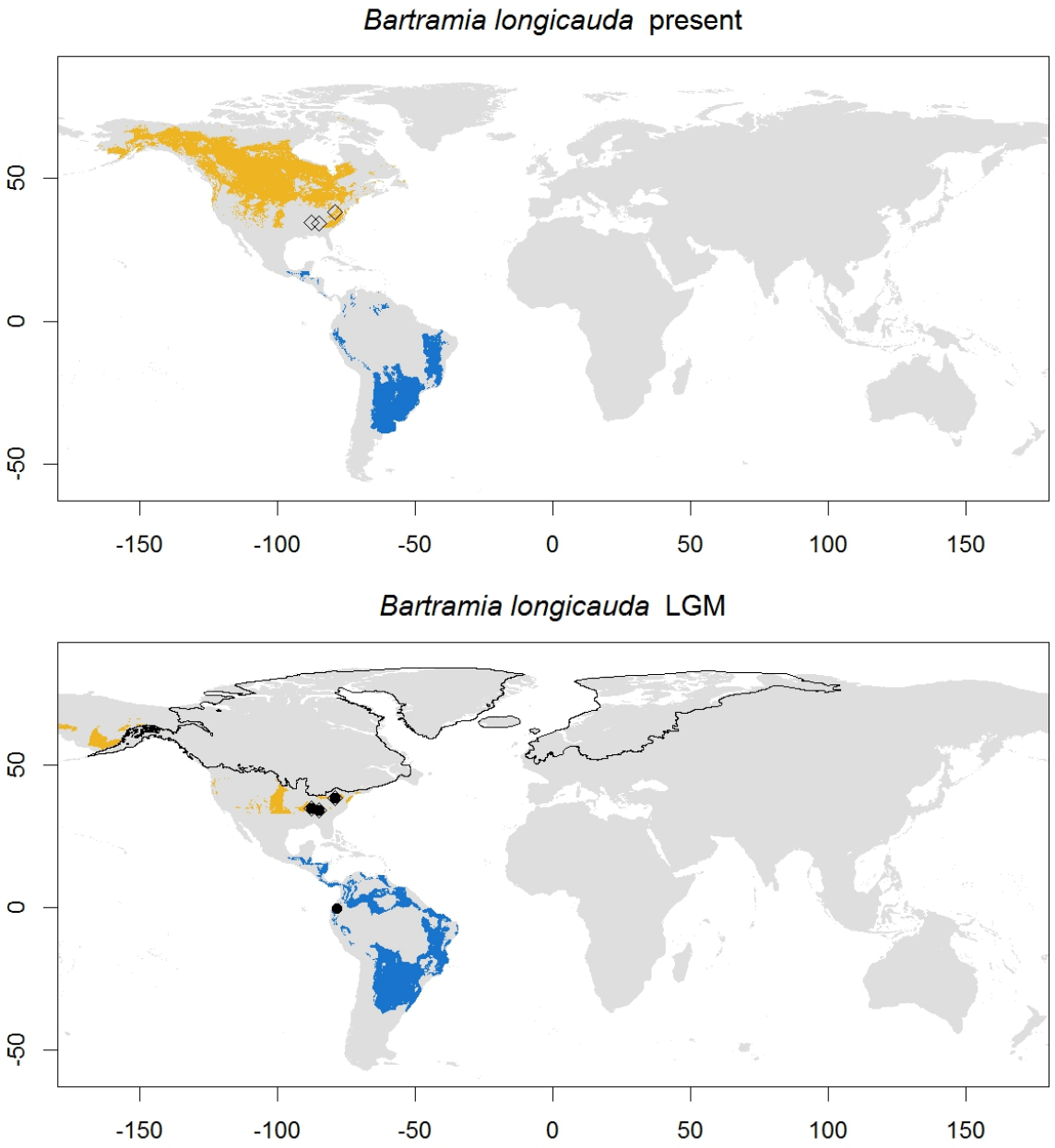

Map 5: Upland Sandpiper (*Bartramia longicauda*) predicted distribution. Caption as in map 1.

Upland Sandpiper, *Bartramia longicauda* (map 5). Monotypic species breeding in two main separated areas: temperate region of central North America, and subarctic region in central Alaska, Yukon and British Columbia. The current SDM returns a continuous breeding distribution, with over-predictions around the Hudson Bay, Labrador Peninsula, Manitoba, Alberta and Northwest Territories. The models predict a significant reduction in the breeding range during the LGM, with predicted presence only in two separated regions: one in southern Beringia, and the other at lower latitudes (30°-40°N) in inland North America. The wintering distribution is in South America, covering Bolivia, Paraguay, south Brazil and northern half or Argentina (del Hoyo *et al*., 2018). Our model

fits this range, but also shows some over-predictions in the northern part of South America, up to Central America. No major changes are predicted in the wintering distribution during the LGM. This species is classified under scenario D.

Sharp-tailed Sandpiper, *Calidris acuminata* (map 6). Monotypic Arctic species that breeds in north-eastern coast of Siberia, between the Lena and Kolyma rivers. The model predicts a slightly wider breeding range, reaching from Taymyr to the north of Chukotka. During the LGM, a series of sparse areas of potential breeding refugia are predicted in Beringia, Kamchatka and central Siberia. The wintering range of the species covers all the coast of Australia as well inland areas specially in the eastern part of the continent. It is also distributed in New Guinea and New Zealand. Our models predict the wintering distribution in Australia, although with over predictions inland and under predictions in the east coast. It also fails to predict the presence in New Guinea and New Zealand. The LGM model shows that the wintering range would have remained stable during the glacial period. This species is classified under scenario A

Sanderling, *Calidris alba* (map 7). Breeding distribution across the Arctic, although non-continuous. It is present across the Palearctic in Svalbard, Severnaya Zemlya Island, Taymyr Peninsula, the mouth of Lena River and New Siberian Islands, and from northern Alaska to British Columbia, northern Canada, Ellesmere Island and the coast of Greenland near it, as well as a small area in the eastern coast. There a two recognized subspecies: *C. a. alba* that occurs in the areas of eastern Greenland, Ellesmere, Svalbard and Taymyr; while *C. a. rubidus* breeds in Alaska and Canada, and likely in the Lena River delta and New Siberian Islands. Our SDM over-predicts the breeding range in northern Fennoscandia, northern Greenland and some parts of the Siberian coast, but overall fits the fragmented distribution of the species. For the LGM it predicts major breeding range reduction for *C. a. alba* in the Canadian high Arctic and Greenland, but a larger suitable area southern from Taymyr. This predicted breeding area extends north and contacts with the potential distribution of *C. a. rubidus* in northeast Siberia and Beringia. The Canadian populations of these subspecies seem to disappear due to the advance of the ice, and only a small predicted area in western North America remains. The species spends the wintering season along the coasts of North America, South America, western Europe, Africa, southeast Asia and Oceania. This range is well predicted by the model,

with over-predictions in inland areas, and is not predicted to have experienced major changes during the LGM. This species is classified under scenario D.

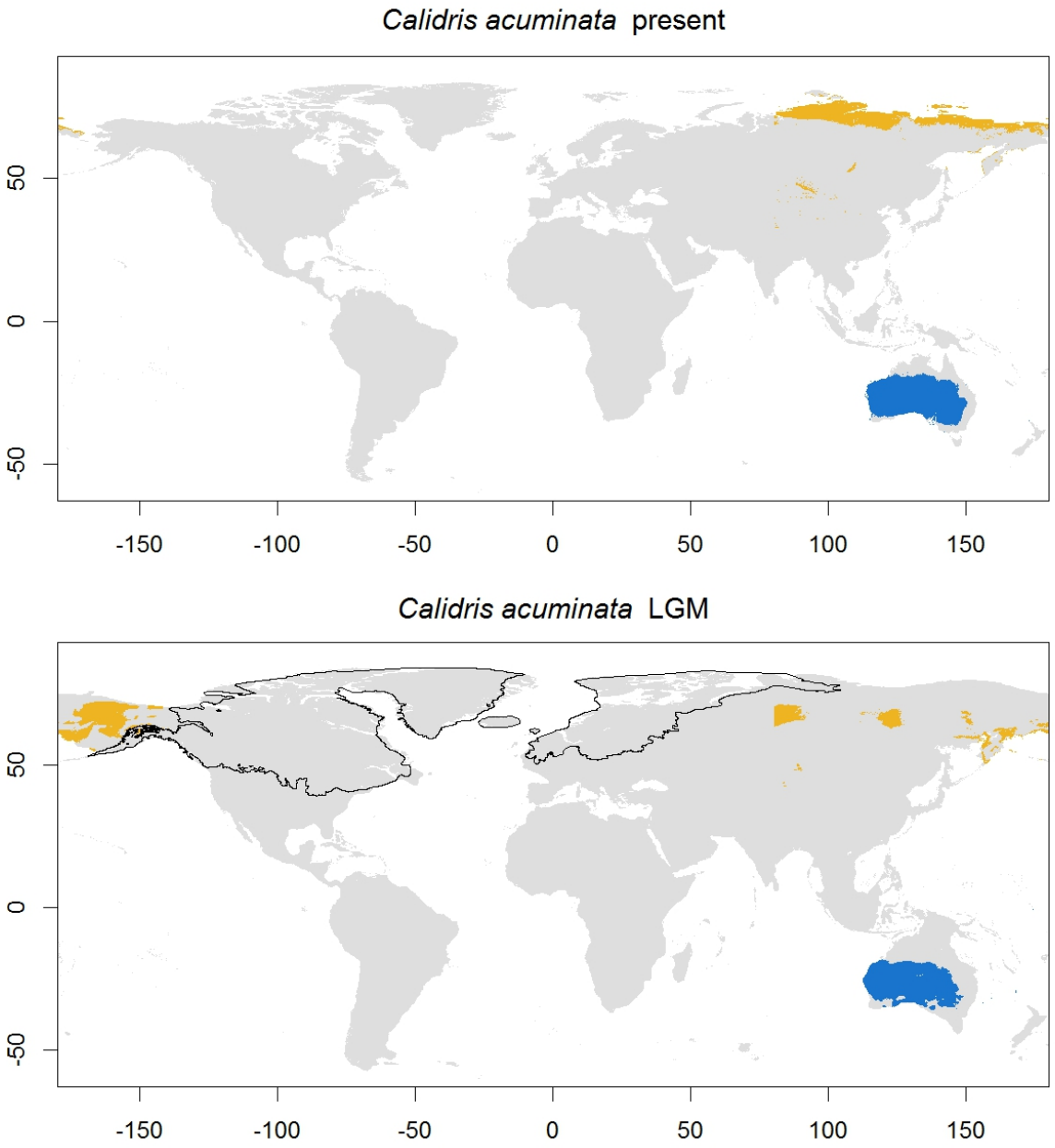

Map 6: Sharp-tailed Sandpiper (*Calidris acuminata*) predicted distribution. Caption as in map 1.

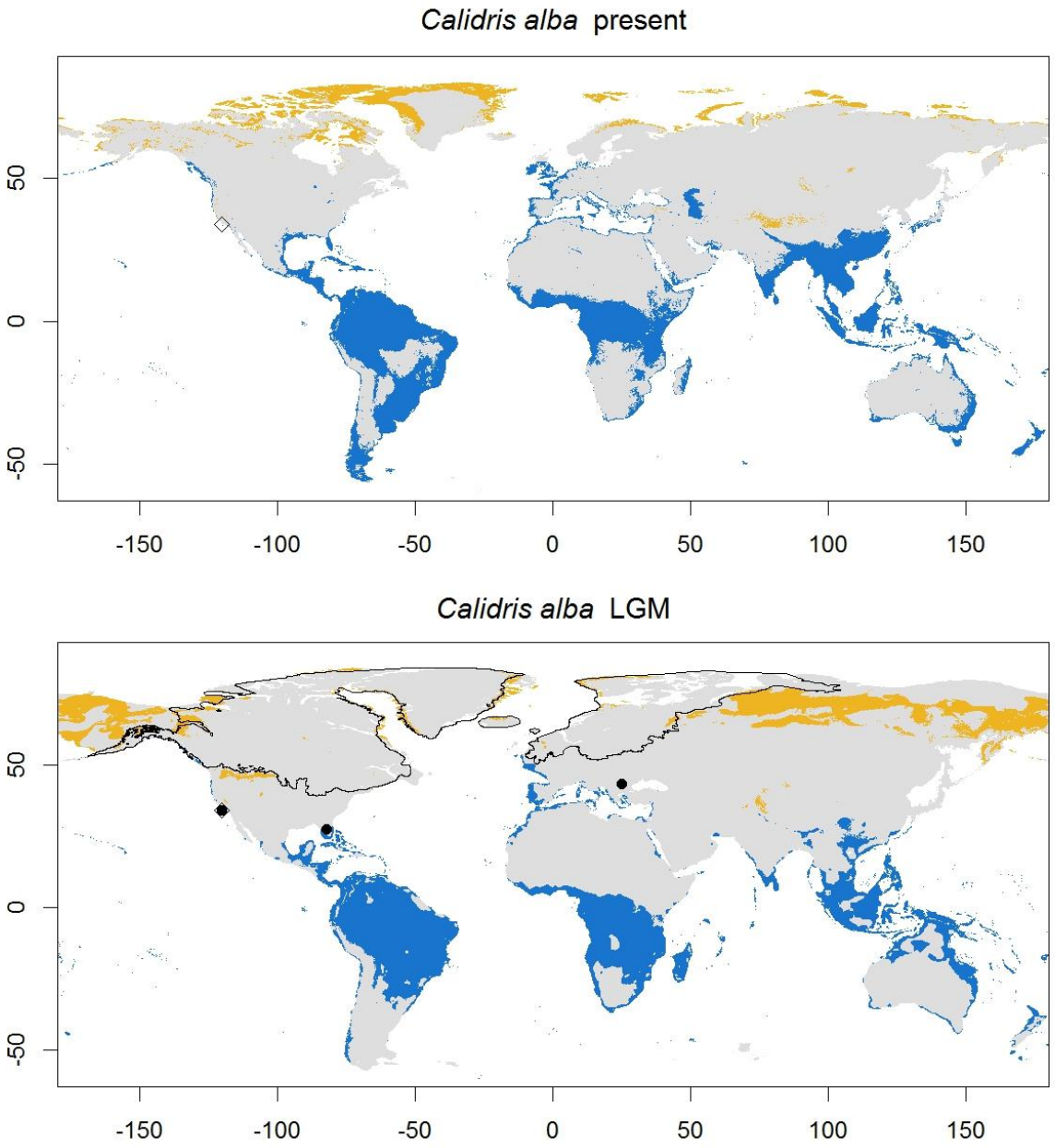

Map 7: Sanderling (*Calidris alba*) predicted distribution. Caption as in map 1.

Dunlin, *Calidris alpina* (map 8). An Arctic and temperate breeding species. Continuous breeding distribution from Britain to Siberia and Kamchatka; and in the Nearctic in Alaska, Beaufort Sea coast and central Canada to Nunavut and Newfoundland. It is absent from Arctic Canadian islands. It breeds in southern and eastern Greenland as well as Iceland. Up to ten subspecies recognized based on morphology (Engelmoer and Roselaar, 1998), but only five main DNA genetic lineages (Buehler & Baker, 2005; Marthinsen *et al*., 2007; Miller *et al*., 2015): *C. a. alpina* in the western Palearctic, *C. a. centralis* in Siberia overlapping in eastern Siberia with *C. a. sakhalina*. *C. a. pacifica*

occurs in Alaska and *C. a. hudsonia* in northern Canada to Newfoundland. Phenotypic variation supports ten subspecies that include (sensu Engelmoer and Roselaar 1998): *C. a. arctica* breeds in east Greenland; *C. a. schinzii* breeds in Iceland, the Faeroes and British islands, western Europe, the Baltic, south Scandinavia and south and southeast Greenland; *C. a. alpina* breeds in nothern Fennoscandia; *C. a. centralis* breeds in central Siberia from the Taymyr peninsula east to the Indigirka river; *C. a. actites* breeds on north Sakhalin island; *C. a. kistchinski* breeds on the southwest part of the Koryak highland, the northeast coast of the Ochotsk sea, the Kamchatka peninsula and the northern Kuril islands; *C. a. sakhalina* breeds on Wrangel Island, the Chukotka Peninsula and at Anadyr*; C. a. arcticola* breeds north of the Brooks range in Alaska; *C. a. pacifica* breeds in Alaska south of 65°N; and *C. a. hudsonia* breeds in the Northwest Territories of Canada. The SDM covers all the species' breeding distribution, over-predicting in central and southern parts of Europe and Asia. During the LGM, the model predicts major breeding range reductions for almost every genetic subspecies: *C. a. hudsonia* disappearing from the Canadian Arctic, *C. a. centralis* would have been reduced to an area in northern Asia near Taymyr, *C. a. alpina* restricted to a series of isolated refugia in central and eastern Europe, and *C. a. shakalina* being displaced towards Kamchatka and Beringia, where it overlaps with *C. a. pacifica*. Very small available areas are predicted in the ranges of the morphological subspecies *C. a. arctica* and *C. a. schinzii*. The wintering range is entirely located in the northern hemisphere, across coastal areas of North America, south and central Europe, north Africa and south Asia. Our SDM fits this distribution but over-predicts in areas of South America and central Africa. The LGM is predicted to have displaced this wintering range towards the equator, expanding to areas in the Southern Hemisphere in America and Africa. This species is classified under scenario C.

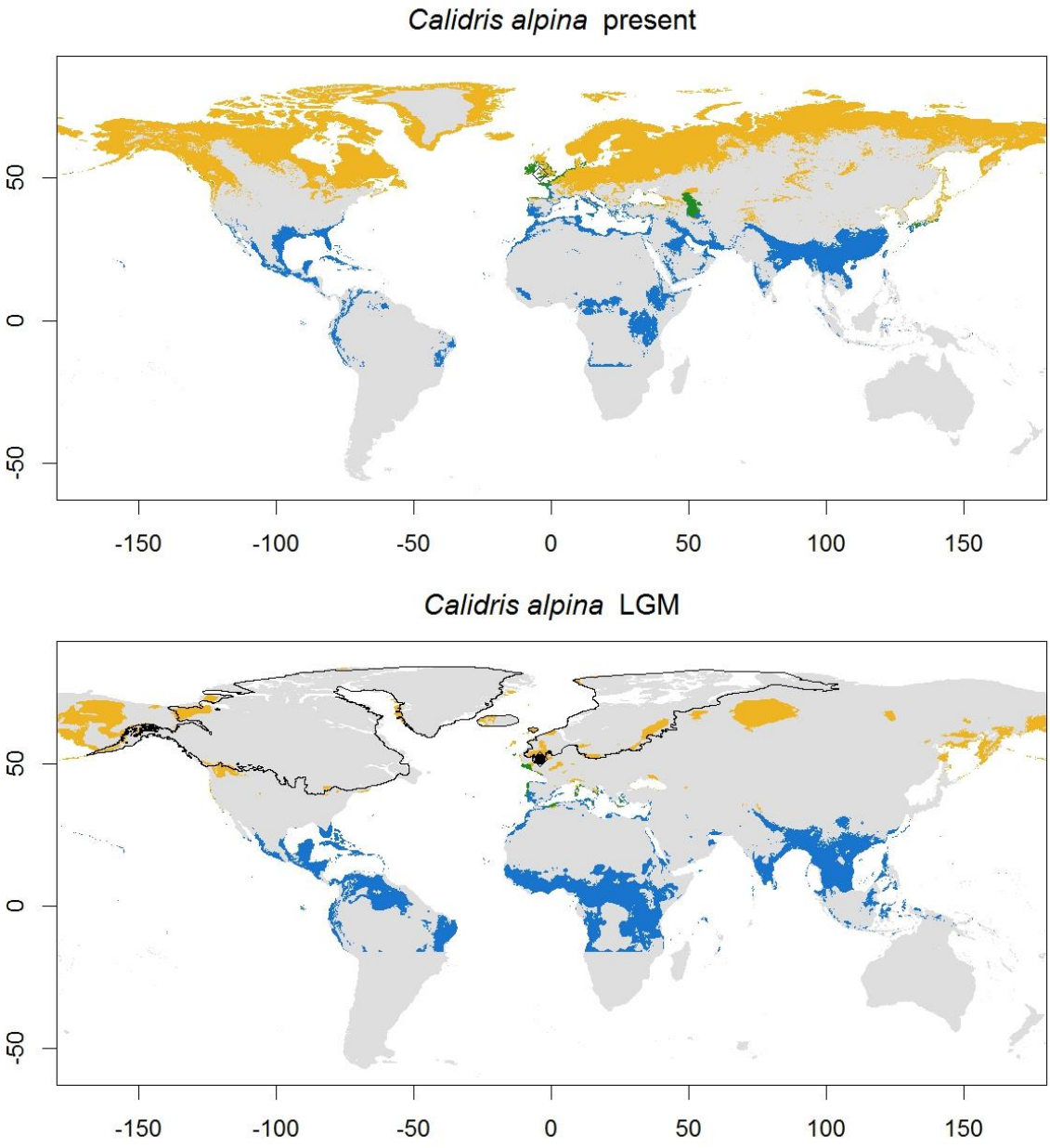

Map 8: Dunlin (*Calidris alpina*) predicted distribution. Caption as in map 1.

Baird's Sandpiper, *Calidris bairdii* (map 9). A monotypic species that mainly occurs in Alaska and the Canadian high Arctic up to Ellesmere Island, and in the Chukotka peninsula in Siberia. The current model fits the breeding distribution, over-predicting only in Newfoundland. LGM model predicts a reduction of this range in the Canadian high Arctic, concentrating most of the breeding distribution of the species in Beringia, with only small predicted areas in central and eastern North America. The wintering range is located in the southern part of South America and some areas in Central

America, as it is also predicted by the current SDM. This wintering range is not predicted to have experienced significant changes during the LGM. This species is classified under scenario A.

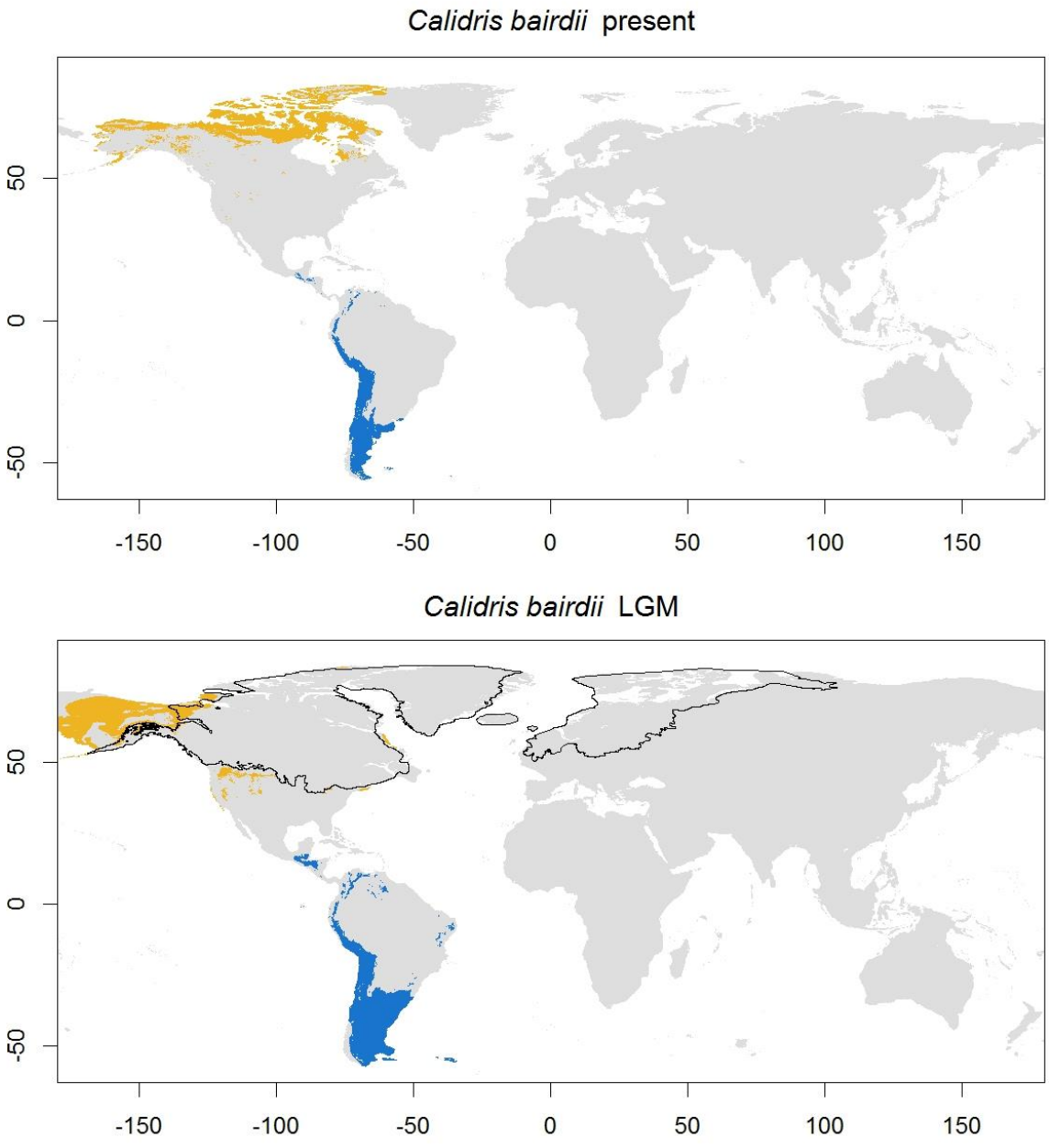

Map 9: Baird´s Sandpiper (*Calidris bairdii*) predicted distribution. Caption as in map 1.

Red knot, *Calidris canutus* (map 10). Arctic species with a fragmented breeding distribution, corresponding to several subspecies not connected between them. Five

subspecies are currently recognized based on morphology (Engelmoer & Roselaar 1998): *C. c. canutus* breeds in Northern Taymyr; *C. c. islandica* shows a wider distribution, breeding in northeast Canada to Ellesmere, most of the northern and eastern coast of Greenland, and Svalbard; *C. c. rufa* breeds in low Arctic Canada and Victoria and Prince Patrick islands limiting with *C. a. islandica* in Prince of Wales island; *C. c. rogersi* breeds in New Siberian Islands; *C. c. roselaari* breeds in Wrangel island and Beringia, including the Chukotka peninsula and the western Alaskan populations likely belong to this subspecies. From the genetic point of view these subspecies are genetically very similar (Baker *et al*., 1994; Buehler & Baker, 2005), but clearly distinguishable phenotypically. The SDM successfully predicts all the breeding areas where the species occurs, but there are also some over-predictions, which may suggest that the species could occur in many more areas than where it actually does. Over-predictions return a continuous breeding distribution from Fennoscandia to Chukotka and Alaska to Greenland, Iceland and Svalbard islands where it does not breed. The model also over-predicts the species in the boreal forests of north America and southern Alaska to Newfoundland, and central Asia as well as Kamchatka. The model for the LGM predict a wide continuous breeding distribution from east Europe to Beringia and Alaska, with no distinguishable areas associated with the fragments of the current distribution. The subspecies *C. c. islandica* is predicted to have lost most or all of its range in the Canadian high Arctic, but remained in suitable areas in Greenland and Svalbard. The range of *C. c. rufa* is restricted to small coastal areas around the Labrador Peninsula. Some predictions at lower latitudes (40°N - 50°N) in eastern North America and western Europe are close to current wintering areas. Other wintering areas include most of the coast of North America, South America, India, Australia, New Zealand and the west coast of Africa. Most of these areas are well predicted by the SDM, with over-predictions inlands in equatorial Africa and the east coast, as well as in Indochina and southeast China. This predicted wintering distribution shifted slightly towards the equator during the LGM. This species is classified under scenario B.

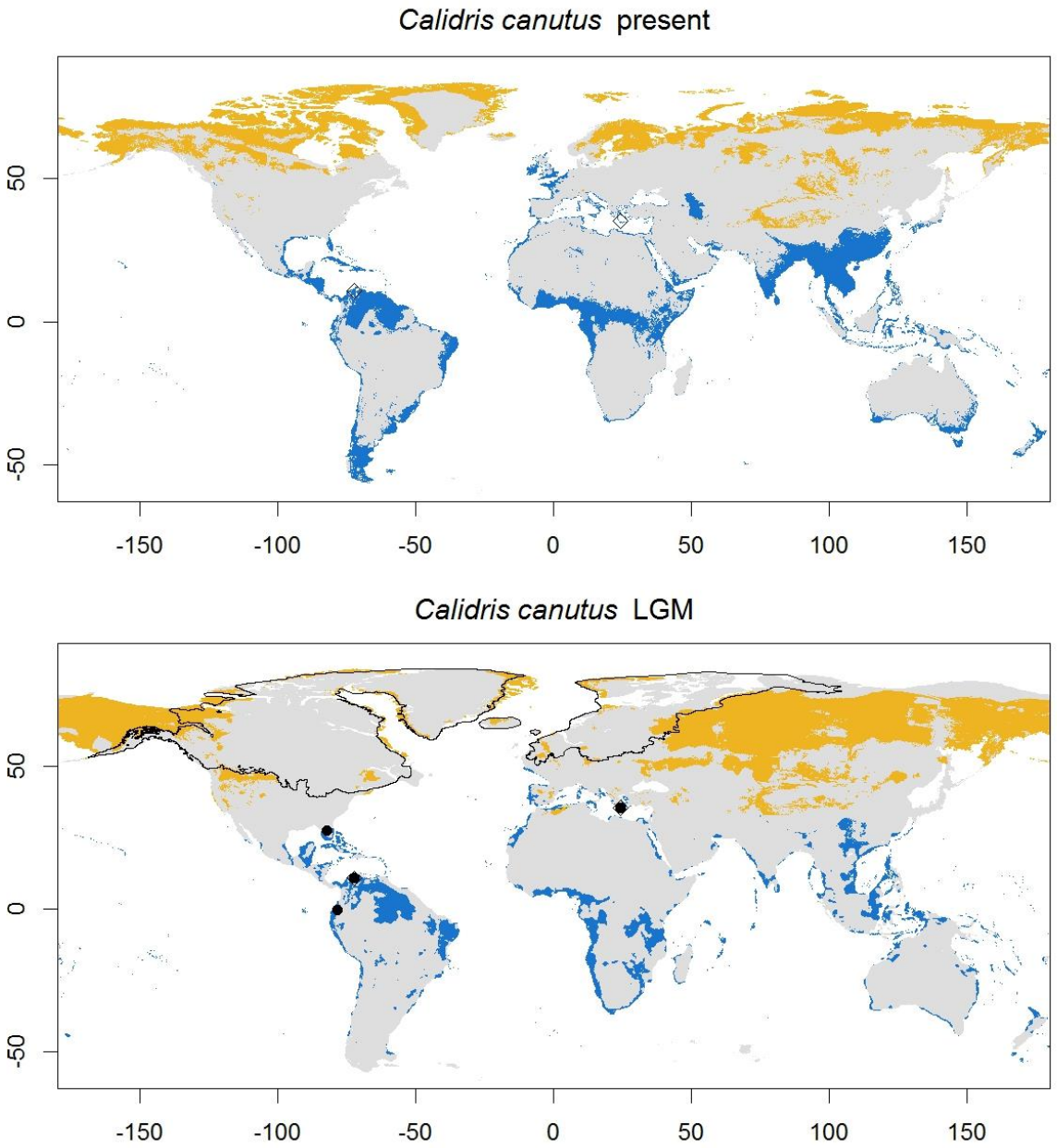

Map 10: Red Knot (*Calidris canutus*) predicted distribution. Caption as in map 1.

Broad-billed Sandpiper, *Calidris falcinellus* (map 11). Palearctic species, breeding distribution is in Scandinavia and northwest Russia, the Taymyr Peninsula and the deltas of the rivers Lena and Kolyma (del Hoyo *et al*., 2018). Two subspecies recognized, *C. f. falcinellus* in the Scandinavian part, and *C. f. sibirica* in the Siberian areas. The SDM predicts a potential breeding range that is almost continuous from the British Islands and north France to northeast Siberia, without any major gaps. Under the LGM

conditions, the model predicts a series of breeding areas across northern Siberia, reaching east to Kamchatka, and also an isolated area in western Europe. The wintering range consist of isolated coastal areas in east Africa, the Arabian Peninsula, India, Myanmar, Indonesia, New Guinea and the north of Australia. This is well predicted by our model, over-predicting in Madagascar. During the LGM, the predicted wintering range remained stable. This species is classified under scenario D

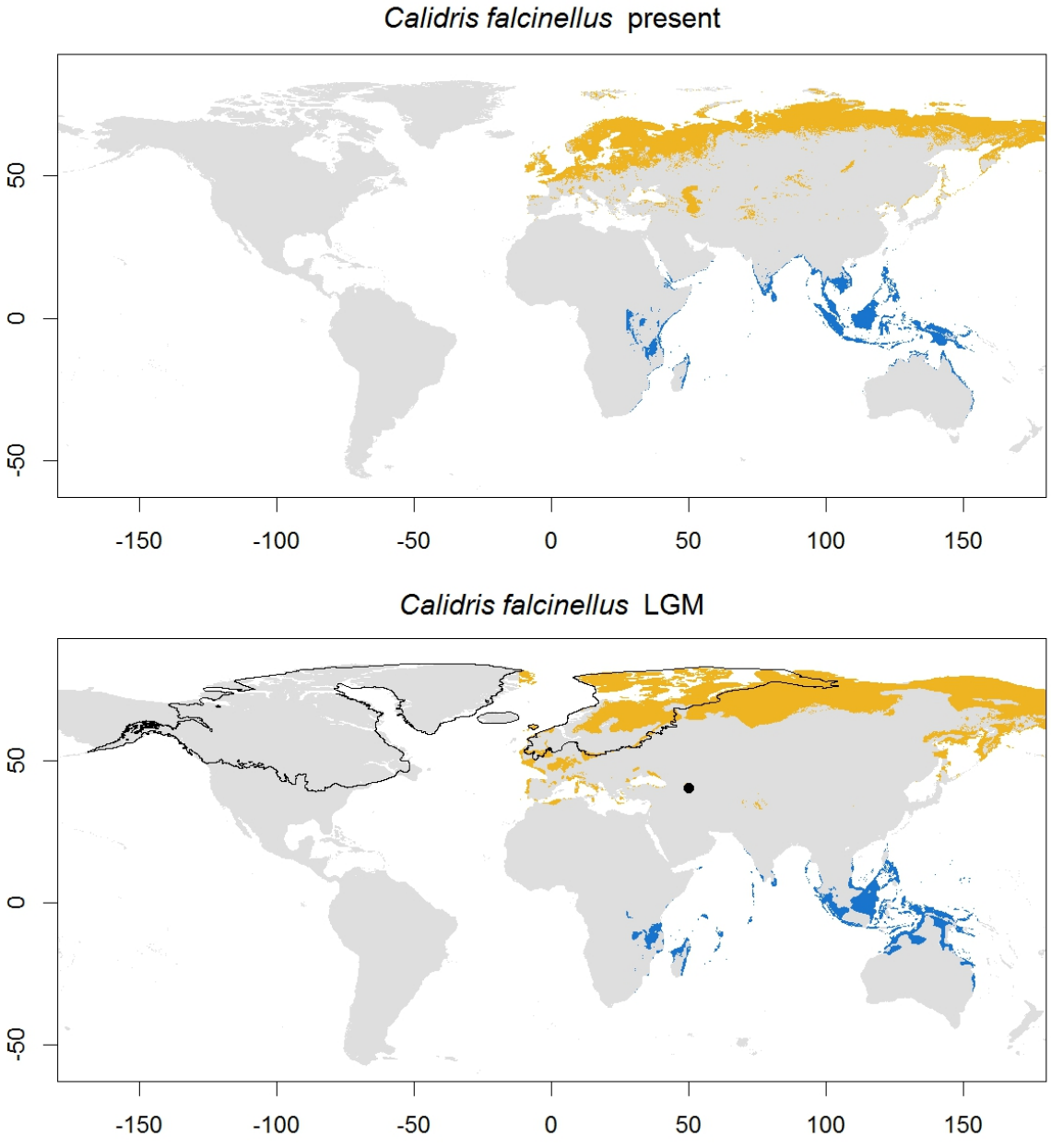

Map 11: Broad-billed Sandpiper (*Calidris falcinellus*) predicted distribution. Caption as in map 1.

Curlew Sandpiper, *Calidris ferruginea* (map 12). Arctic species breeding from the Obi River in west Siberia eastwards to the Chukotka peninsula (del Hoyo *et al.*, 2018). No variation described. The current SDM model fits well the breeding distribution of the species, over-predicting slightly to the west into Yuzhny island and south to Kamtchatka and Shakalin island. The LGM model shows two clearly separated breeding areas, one in northwest Siberia, between the Ural Mountains and southern Taymyr, and the other one in northeast Siberia and Kamchatka. The wintering range extends through most of eastern and southern Africa, from Ethiopia to South Africa; below the Sahara from Ethiopia to Mali; and the western and northern coasts of the continent. It is also present in coastal areas of Madagascar, the Arabian Peninsula, south Asia, Indochina, Indonesia, New Guinea and Australia. The SDM predicts well most of this wintering range, with over-predictions in inland territories of central Africa and south Asia. The LGM model predicts a slight reduction of the northern part of the non- breeding range, with no major changes in the other areas. This species is classified under scenario C.

White-rumped Sandpiper, *Calidris fuscicollis* (map 13). Breeds in the Arctic in Alaska and north Canada islands reaching Baffin Island in the East. It shows a distribution gap the north of Yukon. The SDM over-predicts the breeding range of the species in the north up to Ellesmere Island, and under-predicts the range in the south, failing to predict the species in continental Canada, north Alaska and the southern half of Baffin Island. In the LGM model, most of its breeding range in the high Canadian Arctic is predicted to disappear, with very few coastal localities remaining. Most of the predicted breeding range during the LGM is in the area of Beringia and Alaska, with some areas in southern latitudes. The wintering distribution covers the south and southeast coast of South America, from south Brazil to Patagonia; and the Falkland Islands. All this range is predicted by the SDM, which also predicts areas along the west coast of South America. During the LGM, the models predict a reduction of the southern part of the wintering distribution, and the emergence of potential areas in tropical regions in the western part of the continent. This species is classified under scenario A.

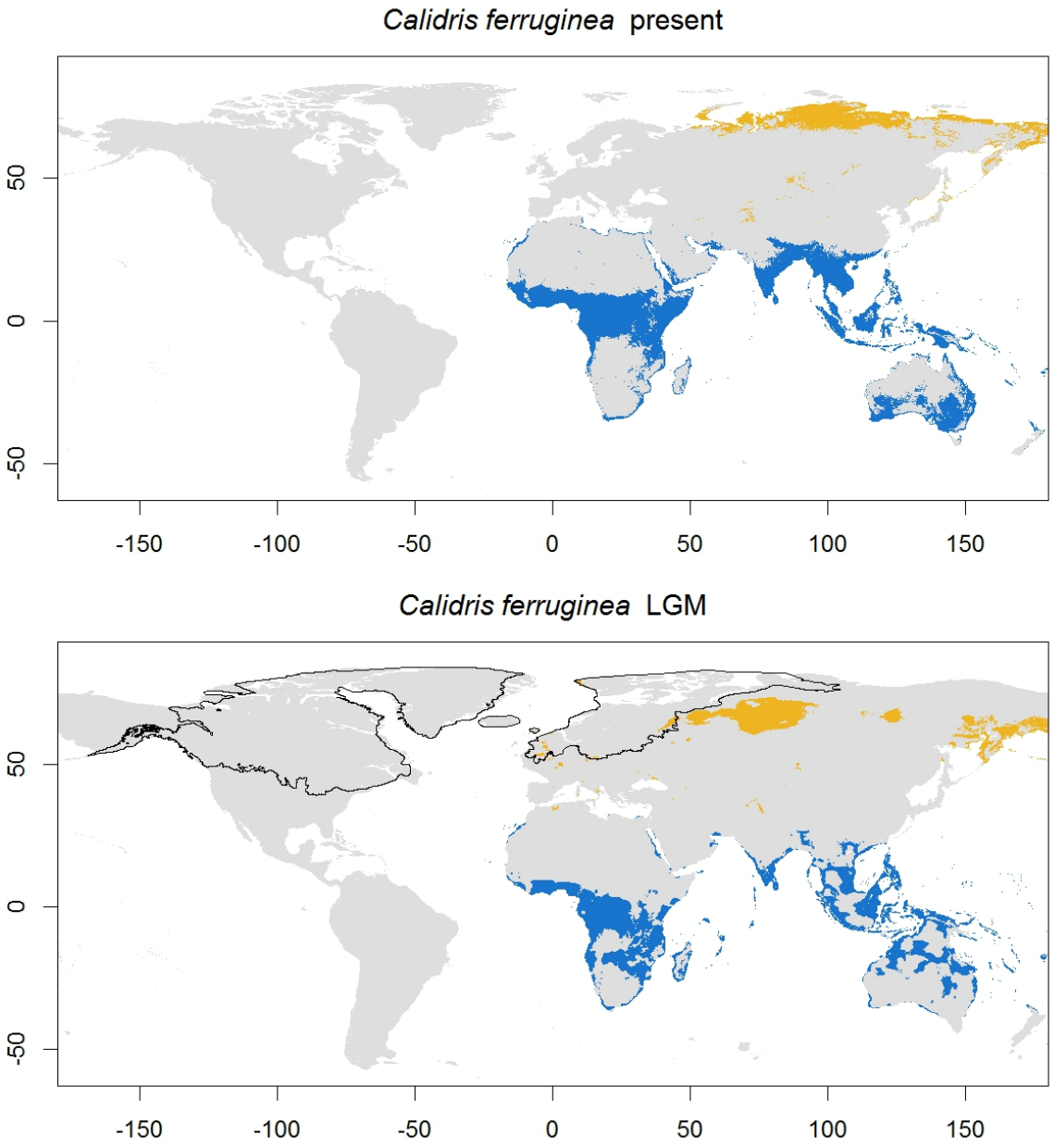

Map 12: Curlew Sandpiper (*Calidris ferruginea*) predicted distribution. Caption as in map 1.

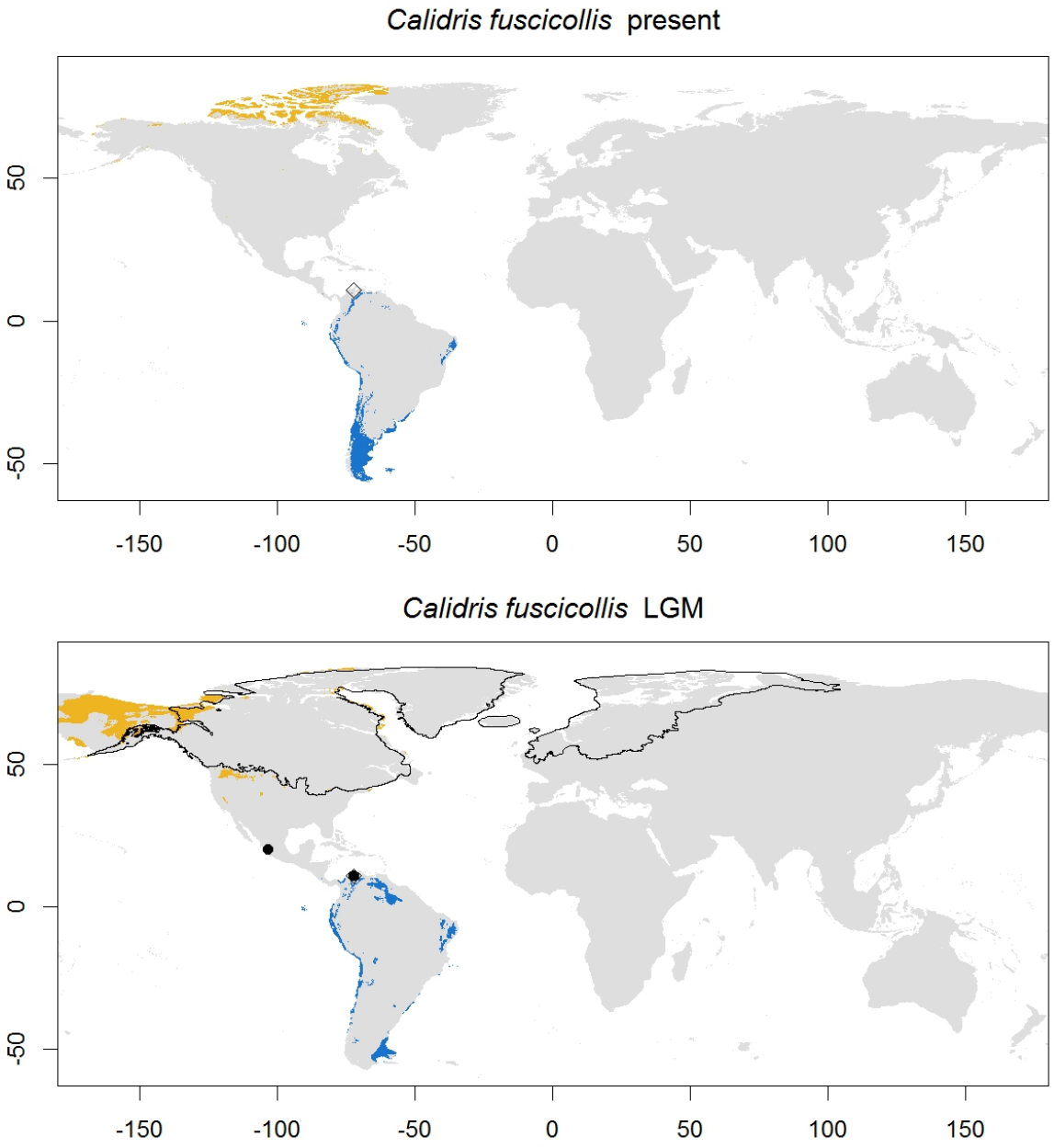

Map 13: White-rumped Sandpiper (*Calidris fuscicollis*) predicted distribution. Caption as in map 1.

Stilt Sandpiper, *Calidris himantopus* (map 14). Breeding distribution is almost continuous from Wainwrights in north Alaska to Melbourne and Victoria islands, with a separated breeding population in west Hudson Bay (del Hoyo *et al.,* 2018). The species is monotypic. The SDM fits the species' current breeding distribution, but under-predicts the Hudson Bay population, and shows over-predictions in the Canadian high Arctic up to Ellesmere Island where it does not occur. The LGM model predicts a loss of the breeding range in the Canadian Arctic, with populations only in the northern part of Beringia. The wintering range covers most of Central America and the northern and

central parts of South America, as well as the Caribbean Islands. This is well predicted by the SDM model for current conditions, and has a similar prediction during the LGM. This species is classified under scenario A

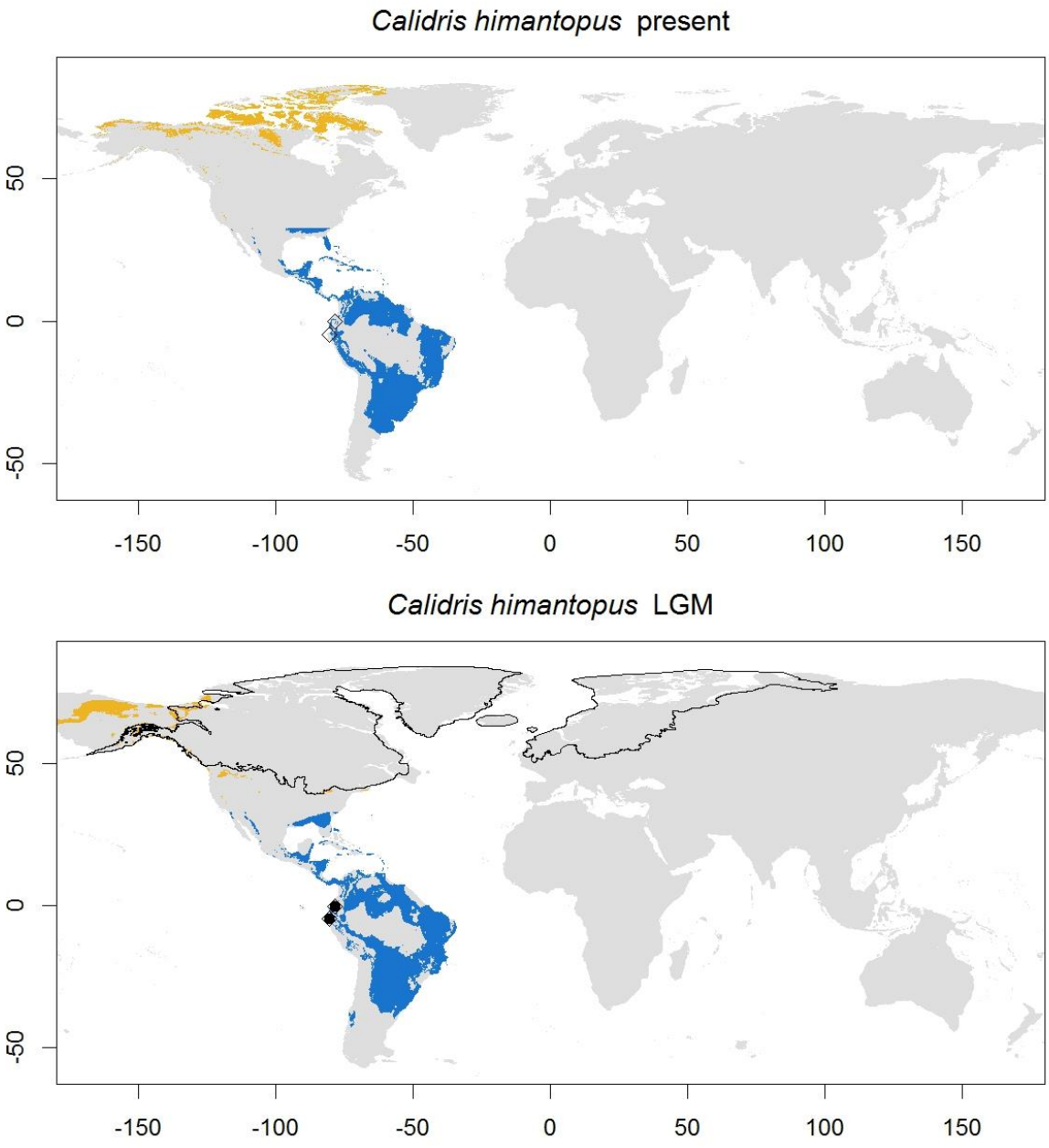

Map 14: Stilt Sandpiper (*Calidris himantopus*) predicted distribution. Caption as in map 1.

Purple Sandpiper, *Calidris maritima* (map 15). Arctic species breeding in Taymyr, Novaya Zemlya, Franz Joseph Land, Scandinavia, Iceland, Svalbard, Greenland, Baffin and Ellesmere Islands and locally in other islands of Nunavut. Despite considerable geographical variation in size, and the proposal of some subspecies (e.g. Engelmoer & Roselar, 1998; Barisas *et al*., 2015), none have been yet recognized (del Hoyo *et al*., 2018). The model correctly predicts the breeding distribution of the species in all of the areas of its distribution, with a larger range in Nunavut and Greenland, and over-predictions in the coast of the East Siberian Sea, Chukotka Peninsula and Alaska. The LGM model shows remaining suitable breeding areas matching the current range in Iceland, Greenland, Svalbard and south of Taymyr. There are also predicted areas in western and central Europe near Scandinavia, and at lower latitudes in central North America. There is also a predicted breeding area around Beringia, from northeast Siberia to British Columbia and Yukon, that is probably an expansion of the over-prediction of the model for the present region The wintering range cover high latitudes very near the breeding range, distributed around local areas of western Europe, Scandinavia, Iceland, south of Greenland, east coast of USA and Newfoundland, therefore the model could not correctly perform and the results were discarded. This species is classified under scenario D.

Western Sandpiper, *Calidris mauri* (map 16). Breeds in the western and northern coast of Alaska, and the eastern tip of the Chukotka peninsula. No variation described. The SDM models covers its current breeding range, but also over-predicts in the northern parts of Yukon and Northwest Territories, as well as into British Columbia. During the LGM the predicted breeding range is restricted to Beringia. The wintering distribution covers the west coast of America, from California to Peru, and also some parts of the east coast, from New Jersey to French Guayana, including the Gulf of Mexico and the Caribbean Islands (del Hoyo *et al*., 2018). The model under the current conditions fits the wintering distribution of the species, although it does not predict the presence in the west coast of North America, and over-predicts to the south in eastern and western South America. During the LGM, the model predicts a similar wintering range, but with less available areas in North America. This species is classified under scenario A.

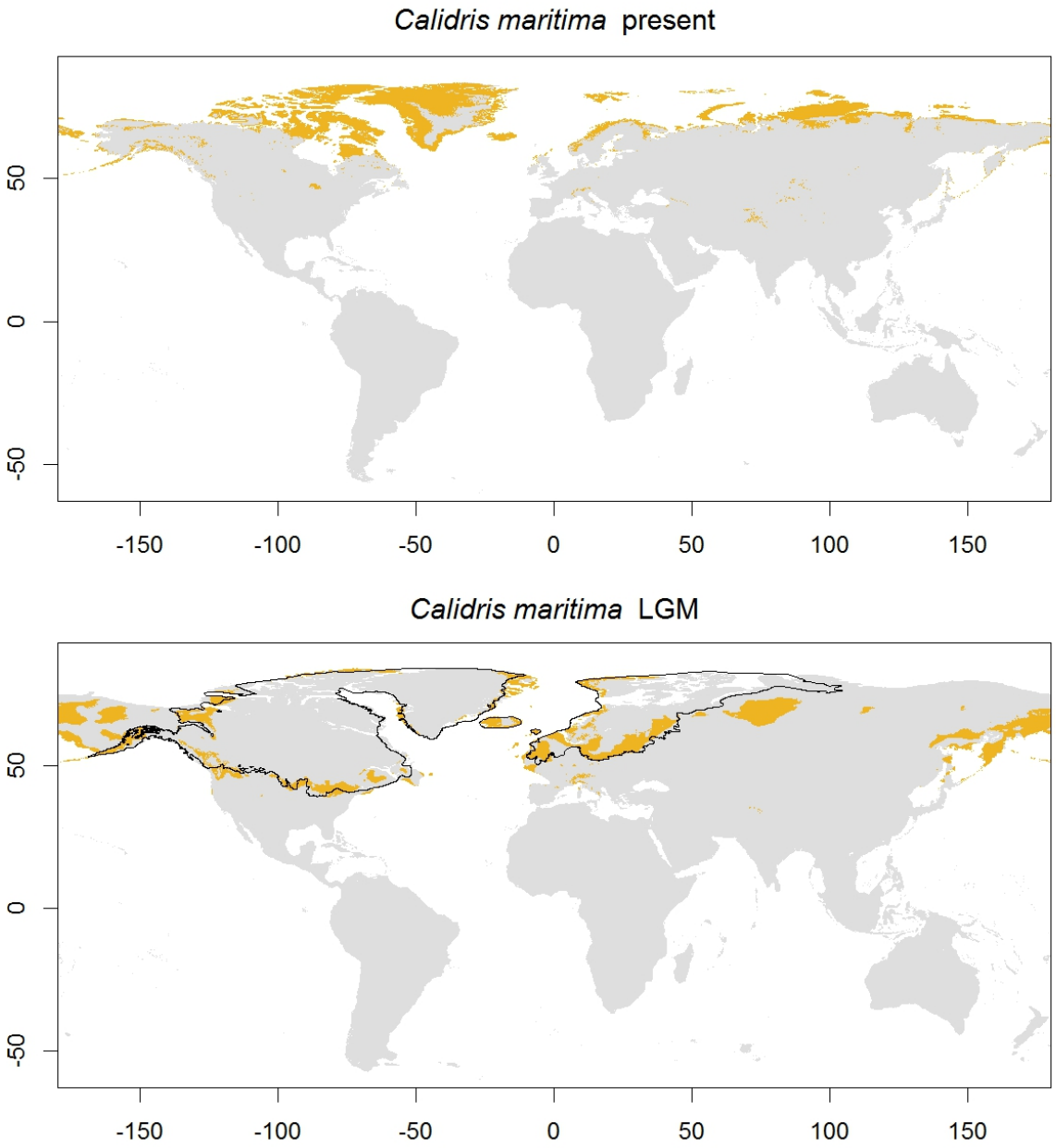

Map 15: Purple Sandpiper (*Calidris maritima*) predicted distribution. Caption as in map 1.

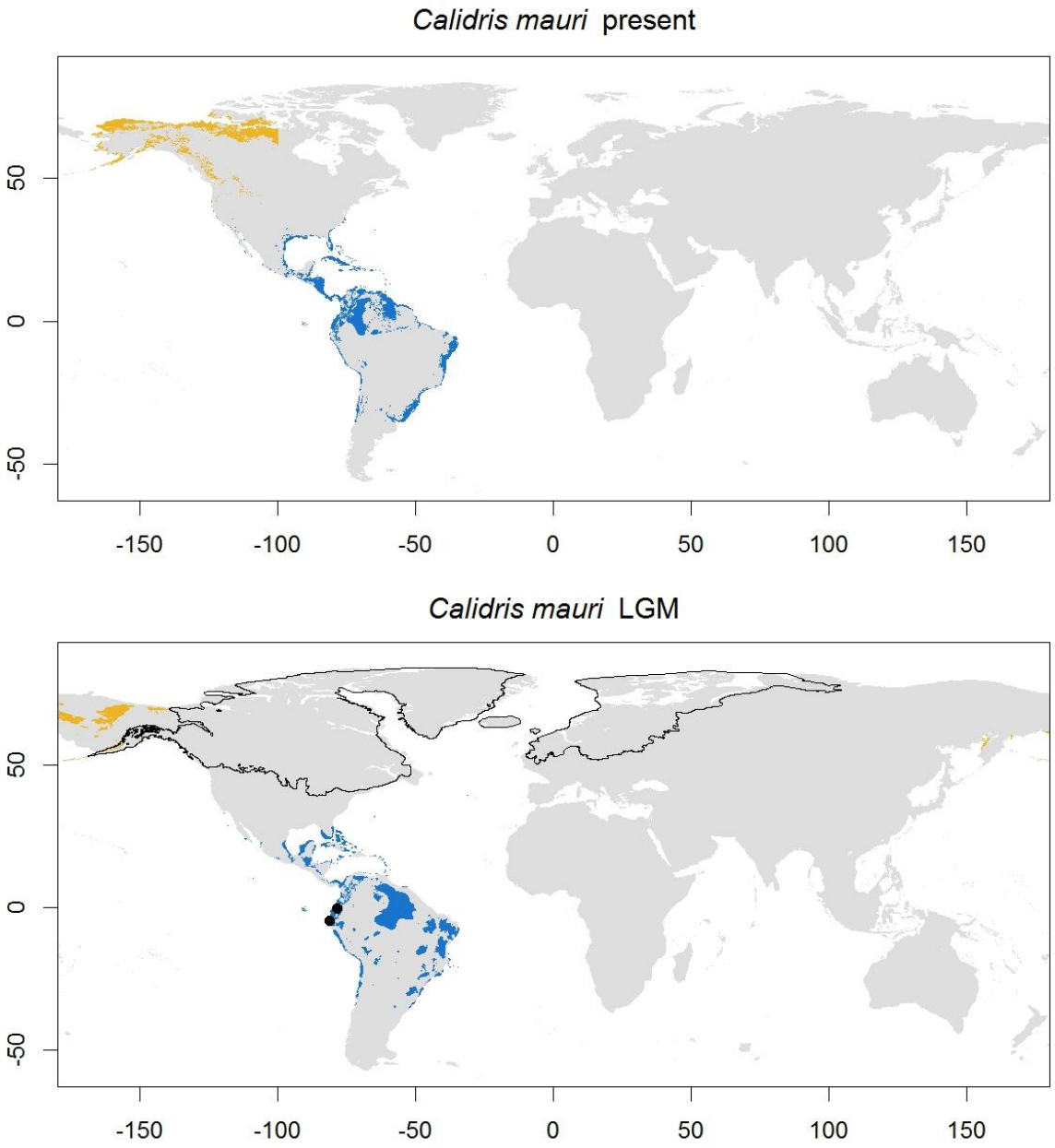

Map 16: Western Sandpiper (*Calidris mauri*) predicted distribution. Caption as in map 1.

Pectoral Sandpiper, *Calidris melanotos* (map 17). Monotypic species that breeds across north Siberia, from the Yamal Peninsula to Chukotka Peninsula, and in the Nearctic from east and north Alaska to the west of Hudson Bay, including Victoria, Banks Prince of Wales, Devon and Baffin Islands. The SDM model predicts all the breeding range of the species, with some over-predictions in south Alaska and part of British Columbia, and also in the north reaching Ellesmere Island, where it is not expected to breed (del Hoyo *et al*., 2018). The models for the LGM show a breeding distribution fragmented into three main areas: one in northwest Siberia, reaching the Ural Mountains; another in the north of north Siberia, probably between the Lena and Indigirka rivers; and a third area

covering northeast Siberia, Kamchatka, Beringia and Alaska. The species wintering range is in the southern half of South America, as well as in south-eastern Australia, Tasmania and New Zealand. The predictions from the model fit this wintering distribution well, with some predictions also in the northwest part of South America. During the LGM, the model predicts almost no change in the wintering range in Oceania, while in South America it shifts slightly towards the equator. This species is classified under scenario C.

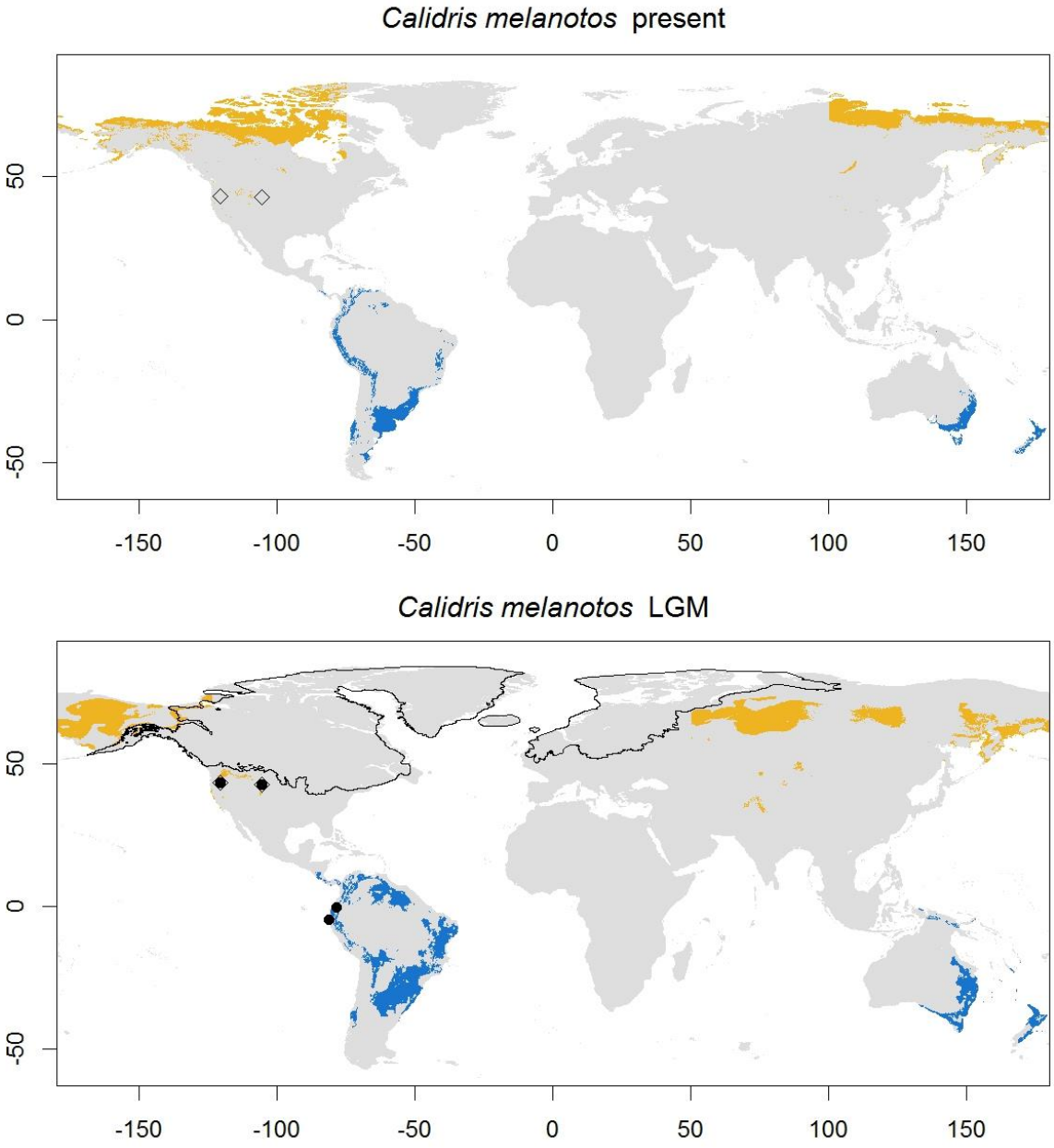

Map 17: Pectoral Sandpiper (*Calidris melanotos*) predicted distribution. Caption as in map 1.

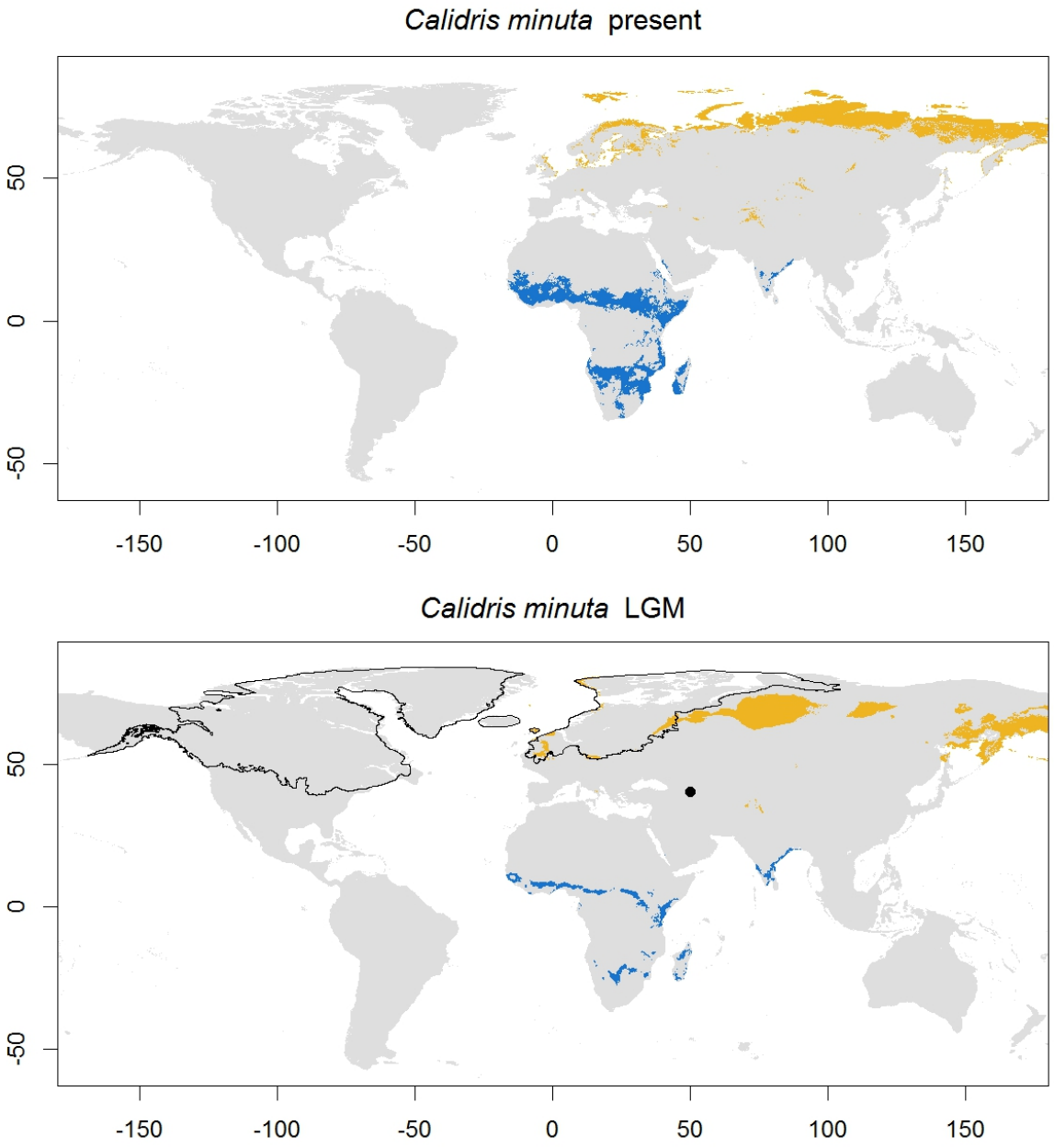

Map 18: Little Stint (*Calidris minuta*) predicted distribution. Caption as in map 1.

Little Stint, *Calidris minuta* (map 18). Arctic bird breeding in the Palearctic, from northern Fennoscandia to New Siberian Islands and the river Yana (del Hoyo *et al.*, 2018). No subspecies described. The SDM model fits the current breeding range well, over-predicting only in Svalbard and northwest Siberia. During the LGM, the model predicts a fragmentation of the breeding distribution, with several suitable areas: northwest Siberia (between Taymyr and the Ural Mountains), near the Lena and Yana rivers, Kamchatka and northeast Siberia, and some small localities in western Europe. The wintering distribution covers most of Africa below the Sahara, as well as the

northern coast; Madagascar, the Mediterranean basin, the Arabian Peninsula and south Asia, from Pakistan to Myanmar. The model under current conditions however only predicts the species' wintering range in some parts of central and southern Africa, as well as in Madagascar and some areas in India. Despite a reduction in available, the models do not predict latitudinal changes during the LGM in the wintering range. This species is classified under scenario C.

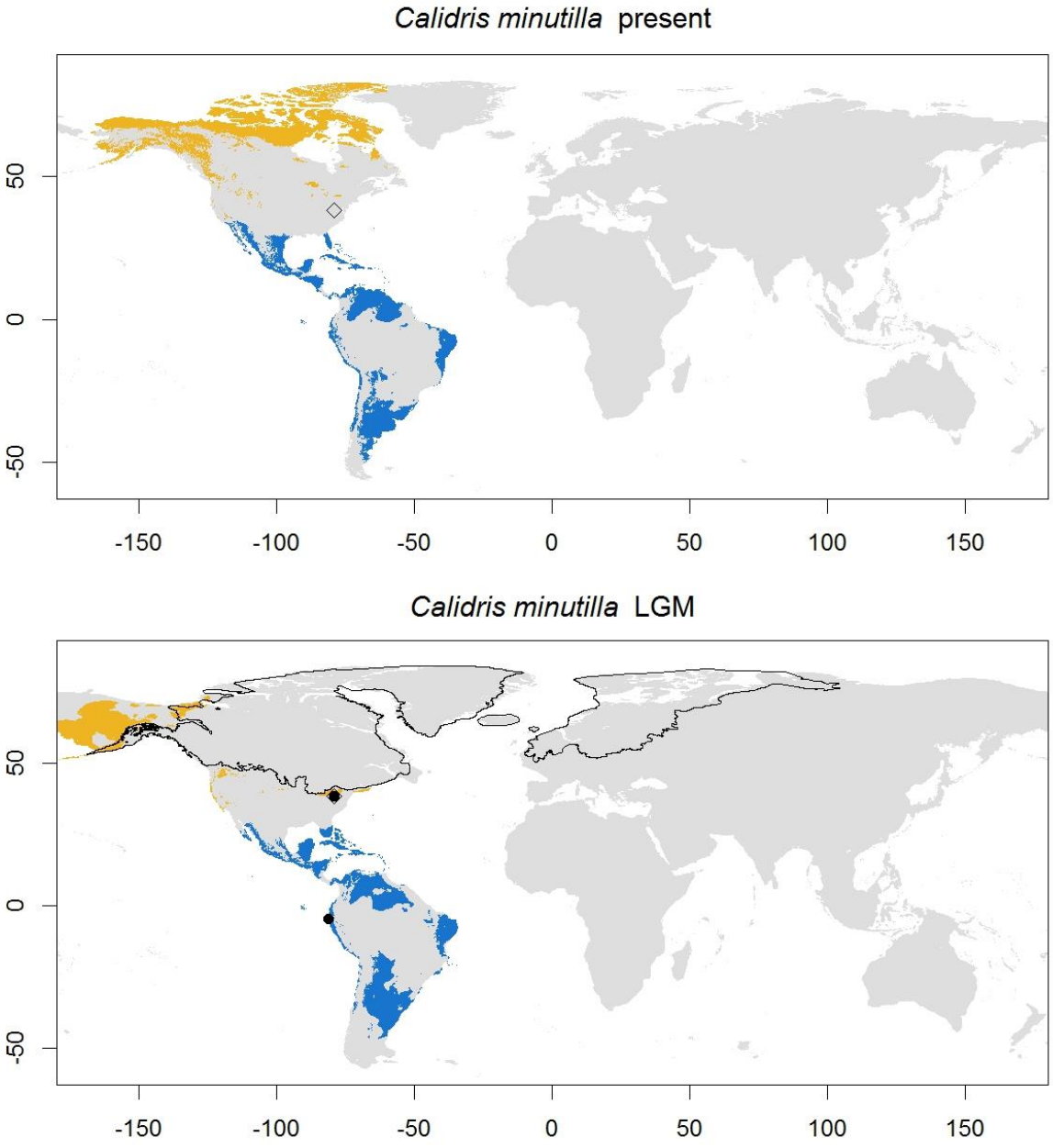

Map 19: Least Sandpiper (*Calidris minutilla*) predicted distribution. Caption as in map 1.

Least Sandpiper, *Calidris minutilla* (map 19). Monotypic species that breeds in the Nearctic, from Alaska and the Aleutian Islands, through north Canada to the Labrador Peninsula and Newfoundland. The SDM current model predicts the breeding range of the species in Alaska, but under-predicts in the southern part of the Canadian range, and over-predicts to the north though Nunavut up to Ellesmere Island. During the LGM, the species's breeding range is predicted in large areas in Beringia and northeast Alaska. The wintering range extends from the southern part of USA to the northern third of South America. The predictions from the model fit well the wintering distribution, and only over-predict in some southern areas in South America, around Argentina and Chile. The wintering range is not predicted to have suffered major changes during the LGM. This species is classified under scenario A.

Rock Sandpiper, *Calidris ptilocnemis* (map 20). Beringian species, breeding around the Bering Sea in west Alaska, the Aleutian Islands, St. Lawrence Island and Kamchatka. Four subspecies recognized (del Hoyo *et al*., 2018), although mitochondrial DNA analyses do not fully support the distinctiveness of all them (Pruett & Winker, 2005): *C. p. quarta* in south Kamchatka, *C. p. tschuktschorum* in Chukotka Peninsula, St. Lawrence and west Alaska, *C. p. couersi* in the Aleutian Islands and *C. p. ptilocnemis* in the smaller island of the Bering Sea. Our Model predicts the breeding range of the species in all of its current distribution, also expanding the potential breeding range to the north of Alaska and Yukon to Northwest Territories, in British Columbia and along the coast of the New Siberian Sea. The LGM model predicts that the species remained breeding in south and central Beringia during the glacial period. The restricted, high-latitude wintering range (along the coast from north California to south Alaska) did not allowed for a proper performance of the model and the results were discarded. This species is classified under scenario B.

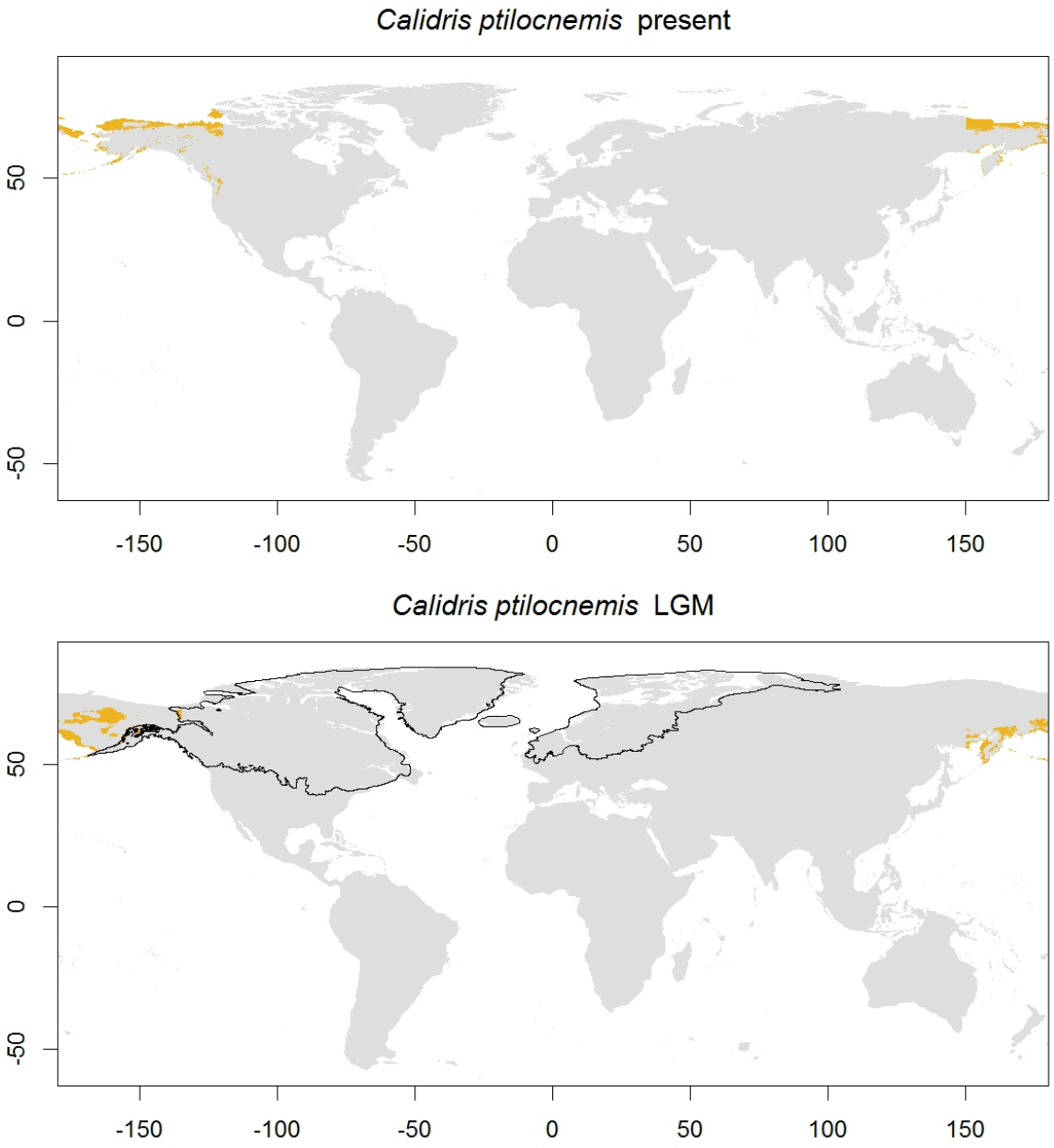

Map 20: Rock Sandpiper (*Calidris ptilocnemis*) predicted distribution. Caption as in map 1.

Ruff, *Calidris pugnax* (map 21). Breeds across all the Palearctic, from Scandinavia and Denmark to the Chukotka Peninsula through Siberia without described morphological variation. The model predicts the breeding range of the species well, over-predicting in north Taymyr, Novaya Zemlya and the British Islands (where it spends the winter). The species' breeding is predicted in areas of central and west Siberia and central Europe, as well as in east Siberia and Beringia during the LGM. The wintering range covers from sub-Saharan Africa to the south of the continent, south Asia, Indonesia and Philippines. There are also local wintering areas in west and southern Europe. Our model fits all the

wintering range except the areas in Europe, and also extends the prediction into Oceania. Overall the wintering range shows no significant change during the LGM. This species is classified under scenario A.

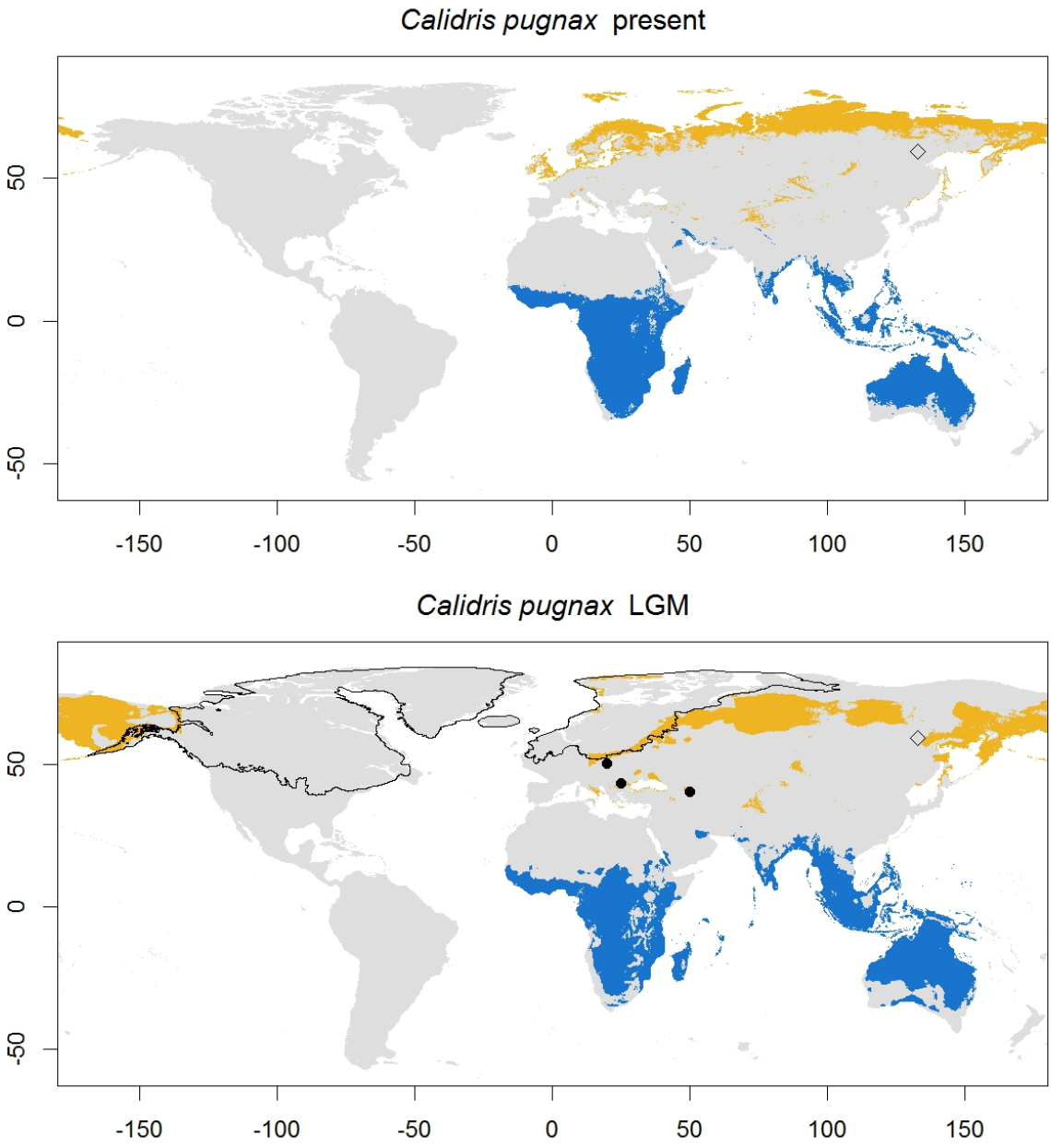

Map 21: Ruff (*Calidris pugnax*) predicted distribution. Caption as in map 1.

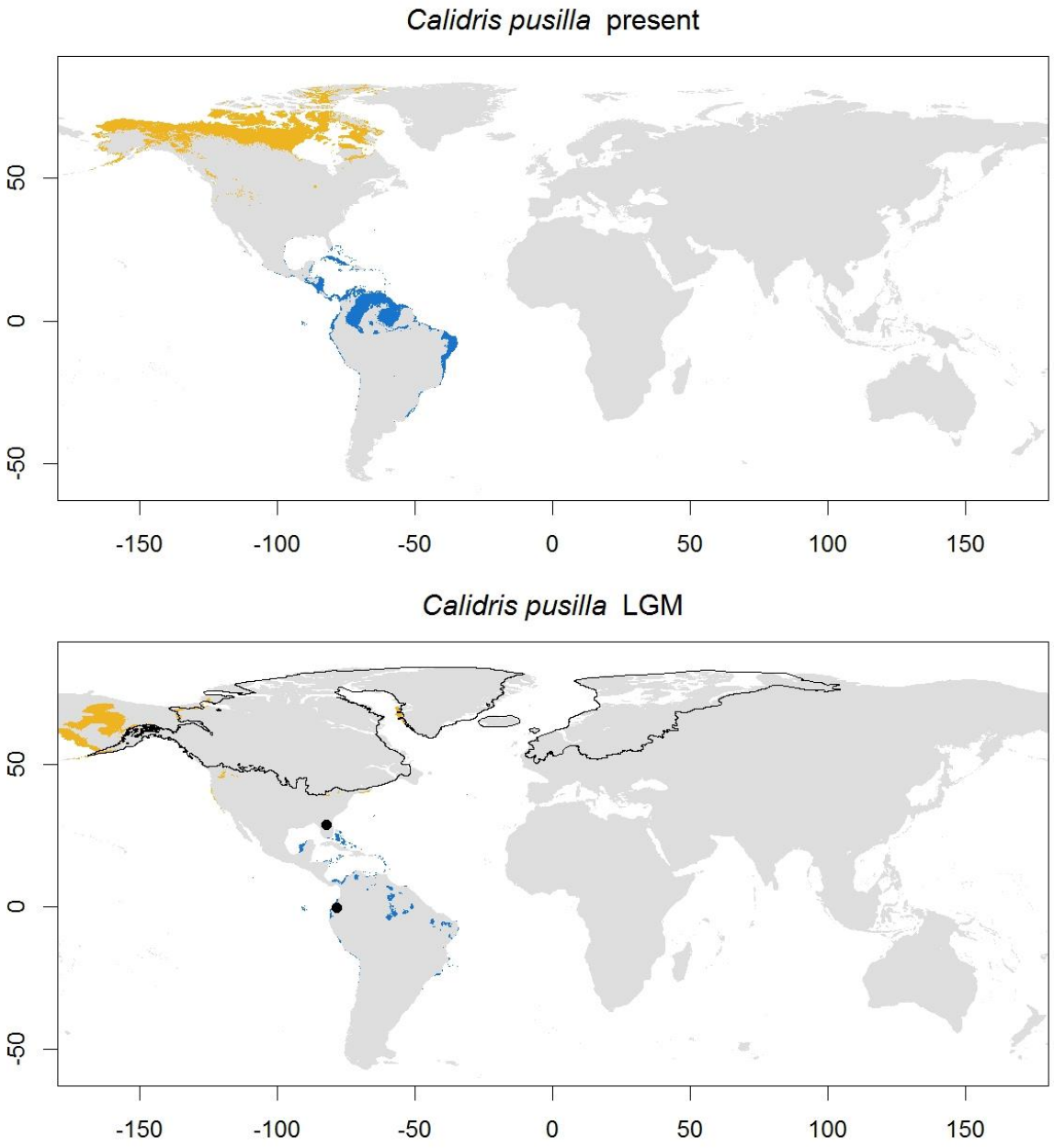

Map 22: Semipalmated Sandpiper (*Calidris pusilla*) predicted distribution. Caption as in map 1.

Semipalmated Sandpiper, *Calidris pusilla* (map 22). Nearctic species, breeding from west and north Alaska to the Labrador Peninsula, and recently expanded to Chukotka Peninsula (del Hoyo *et al*., 2018). The SDM model fits the breeding distribution range, with potential predicted areas in Ellesmere Island too. During the LGM, the model predicts a main breeding area in Beringia and Alaska. The wintering distribution covers coastal zones of the Caribbean and the northern part of South America. Our model correctly predicts this wintering range, with a reduction of available area extent during the LGM but no latitudinal shift. This species is classified under scenario A.

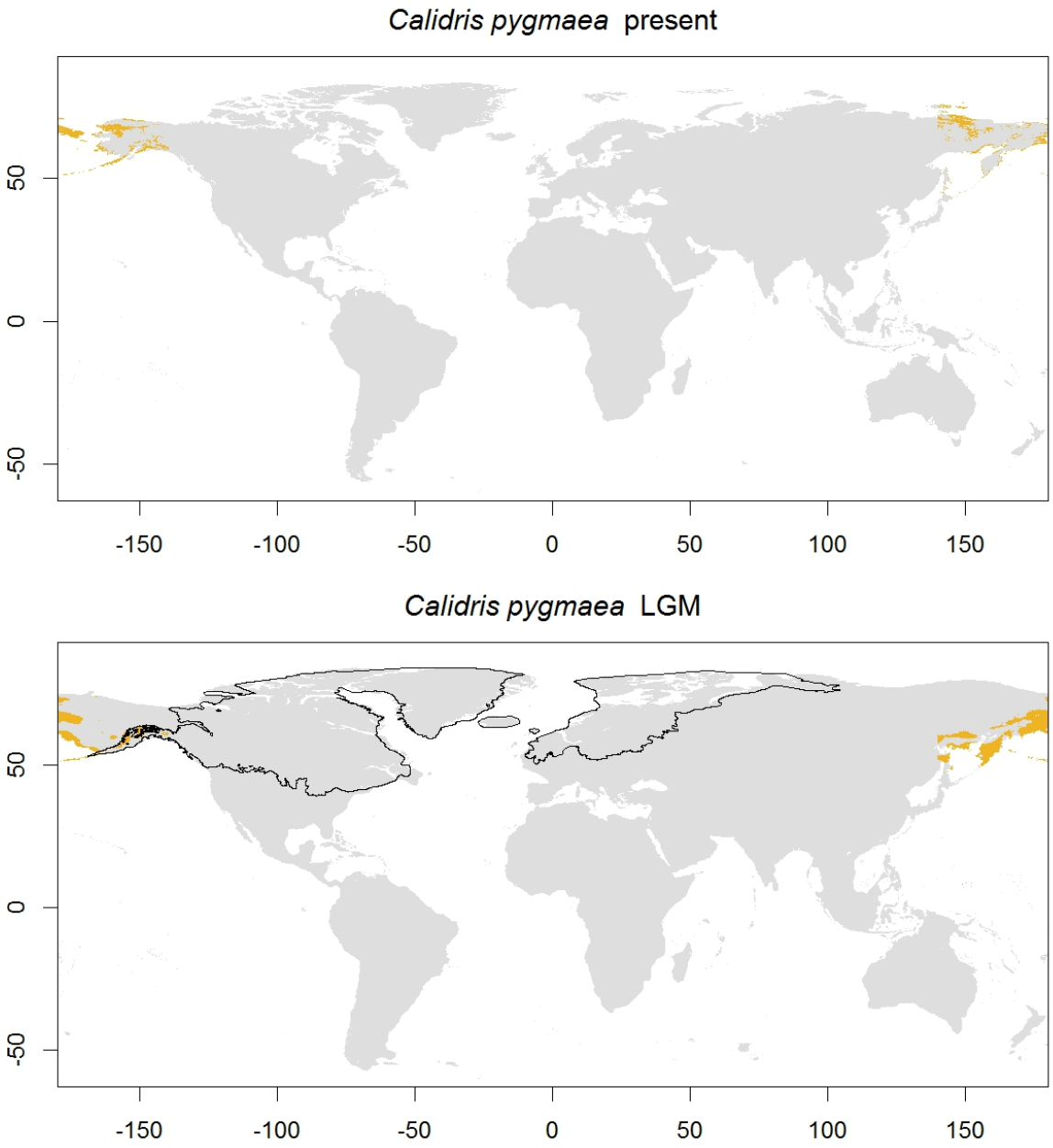

Map 23: Spoon-billed Sandpiper (*Calidris pygmaea*) predicted distribution. Caption as in map 1.

Spoon-billed Sandpiper, *Calidris pygmaea* (map 23). Critically endangered species with a small distribution reduced to the Chukotka Peninsula and northern Kamchatka. No subspecies described. The SDM predicts the breeding range of the species well, with potential areas also in the coast of the East Siberian Sea. During the LGM, the model predicts that the species displayed a similar breeding range, even extending into south Beringia. The full wintering range of the species is not well known (del Hoyo *et al*., 2018), and the available data cover an area too small to perform reliable models. This species is classified under scenario A.

Red-necked Stint, *Calidris ruficollis* (map 24). Fragmented breeding distribution, present in Taymyr, the Lena river delta and from the Kolyma River to the Chukotka Peninsula. No variation described. The SDM model returns a breeding distribution covering all those areas but as a continuous range. During the LGM is predicted to remain breeding at high latitudes in central and northwest Siberia, as well as in Beringia, with no clearly isolated regions. The wintering distribution covers from east India to southeast China, extending through Indonesia, New Guinea, Australia and New Zealand. This wintering range is predicted well by the model using current conditions, except for the southern coast of Australia and in New Zealand. For the LGM it shows a decrease in available area of the wintering distribution, but remaining in the same latitudes, except in Australia, where it only is predicted in the north. This species is classified under scenario A.

Buff-breasted Sandpiper, *Calidris subrufcollis* (map 25). Arctic species breeding in the north of Alaska and Northwest Territories, and in Nunavut. No variation described. The model correctly predicts the breeding distribution of the species, with some over-predictions in Ellesmere Island where it does not breed. During the LGM, the species is predicted to breed in Beringia, Alaska, and potentially in the coasts of the Beauffort Sea and the Baffin Bay. Potentially suitable breeding areas are also predicted in western North America. The wintering range is located in South America, between Paraguay, Uruguay, north Argentina and south Brazil. The model correctly predicts this wintering range, as well as other potential areas in the north of the continent. The prediction for the LGM shows a decrease in the current wintering range of the species, but an increase in extent of the over-predicted areas in the north. This species is classified under scenario A.

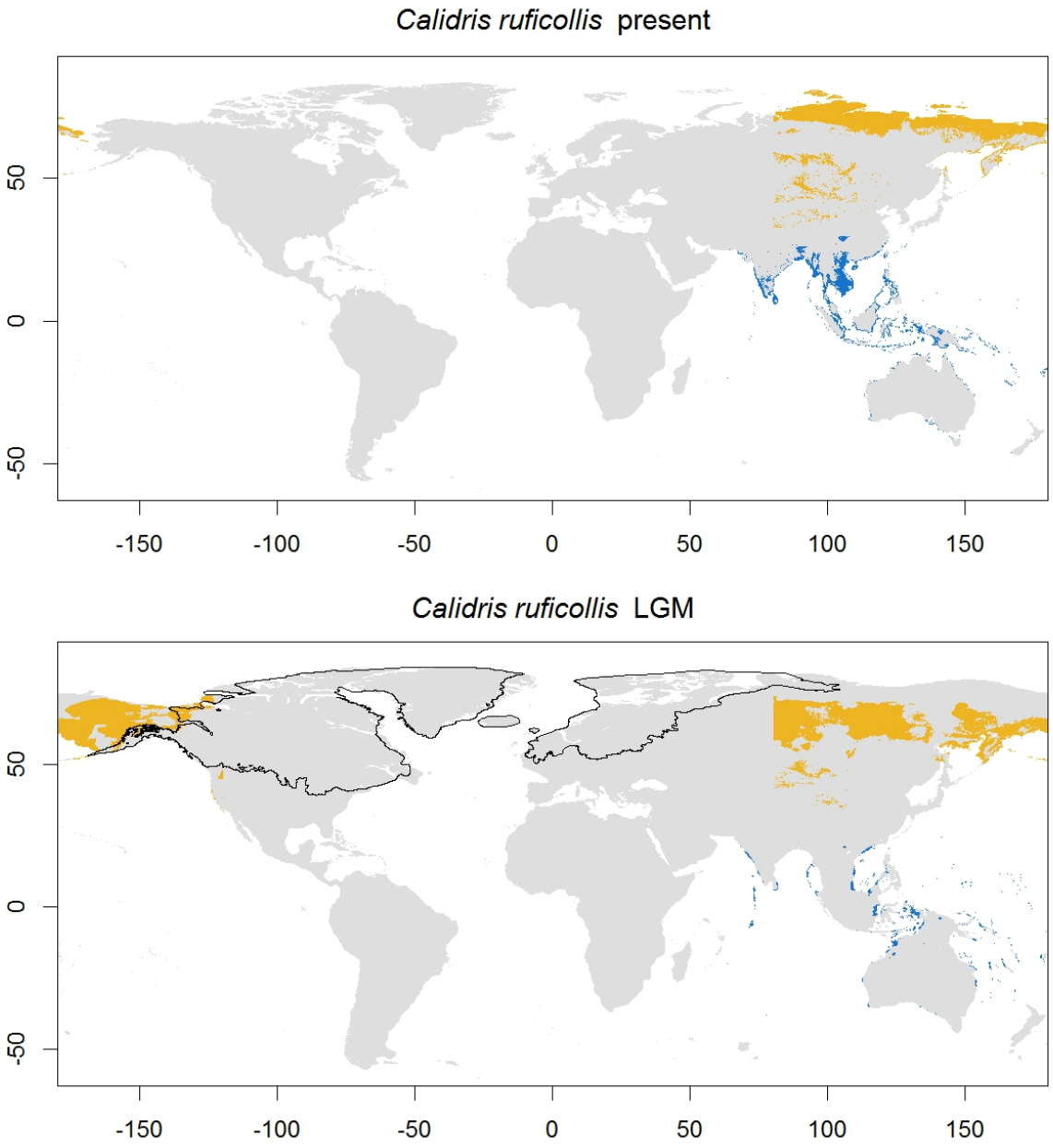

Map 23: Red-necked Sandpiper (*Calidris ruficollis*) predicted distribution. Caption as in map 1.

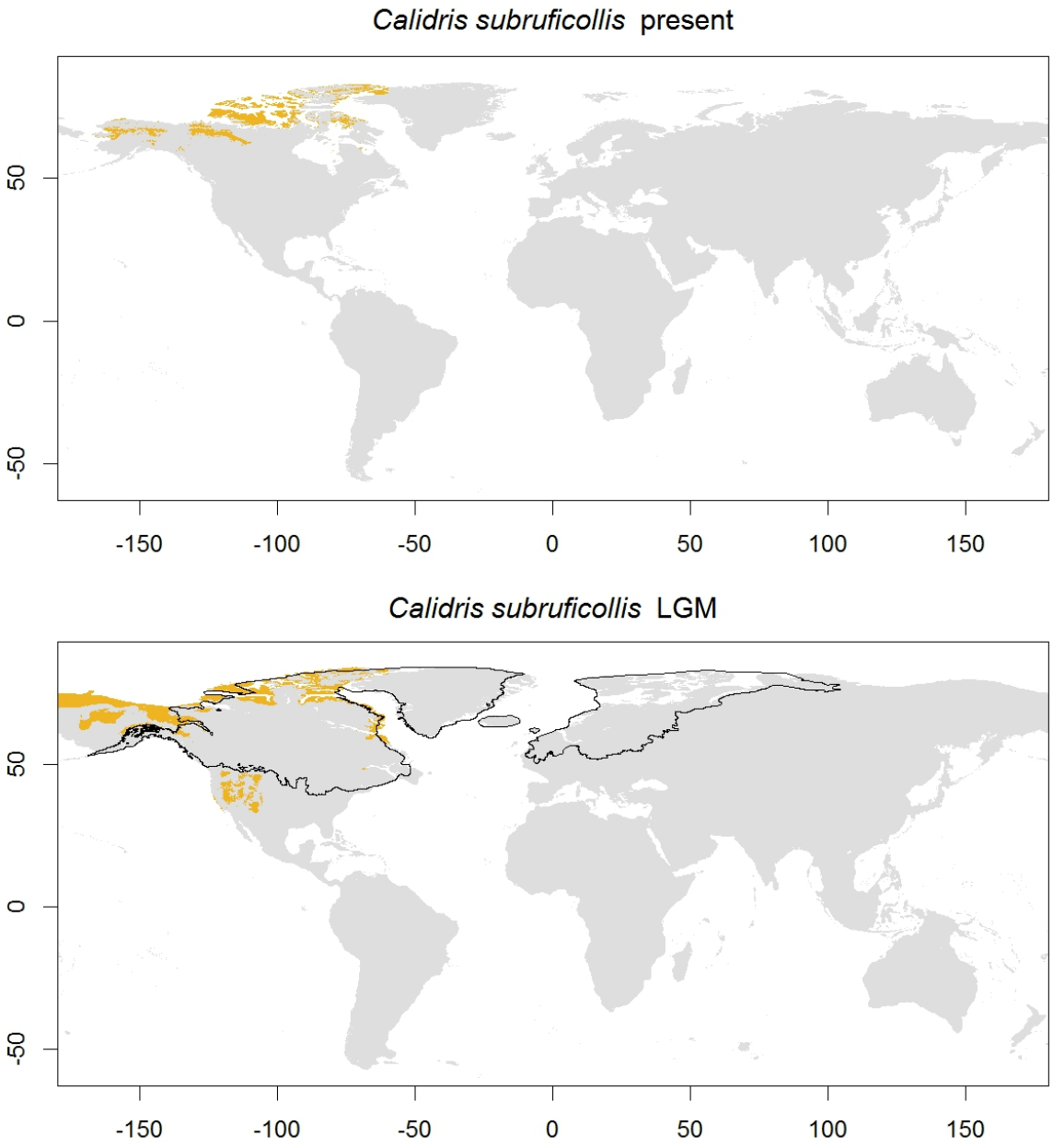

Map 25: Buff-breasted Sandpiper (*Calidris subruficollis*) predicted distribution. Caption as in map 1.

Temminck's Stint, *Calidris temminckii* (map 26). Breeds in the Palearctic, from Scandinavia to the Chukotka Peninsula in Siberia, including New Siberian Islands. It is absent in the northern part of Taymyr and in Novaya Zemlya. No variation described. Our SDM model covers all of the breeding distribution, predicting also in the northern part of Taymyr, Novaya Zemlya and Svalbard, as well as in some small areas of Kamchatka and around the Himalayas. The predictions in the British Island are congruent with occasional breeding there (del Hoyo *et al*., 2018). The LGM model predicts a similar but fragmented breeding distribution, with a large area between the Lena River and the Ural Mountains, further extending west in a narrow band towards

lower latitudes in central Europe; and another area in northwest Siberia and Beringia, reaching east to Alaska. Both areas are separated by a distribution gap between the Lena and Indigirka rivers. Wintering distribution is in the Mediterranean, around the Equator in Africa, and in India, Indochina and Indonesia. Except for the Mediterranean part of the range, the SDM fits the wintering distribution. During the LGM, the model predicts a similar wintering distribution but with a reduction in extent across the range. This species is classified under scenario A.

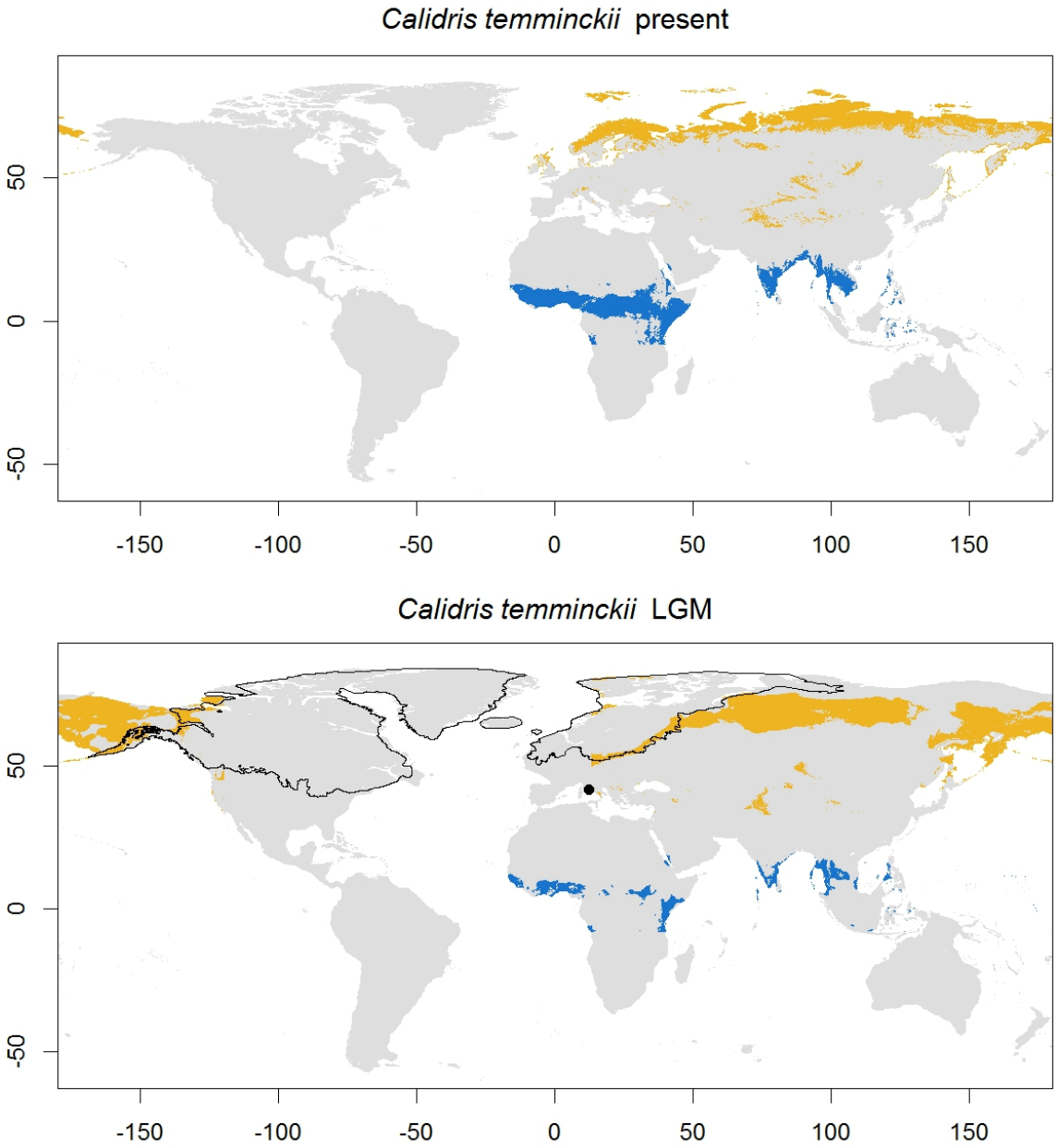

Map 26: Temminck's Stint (*Calidris temminckii*) predicted distribution. Caption as in map 1.

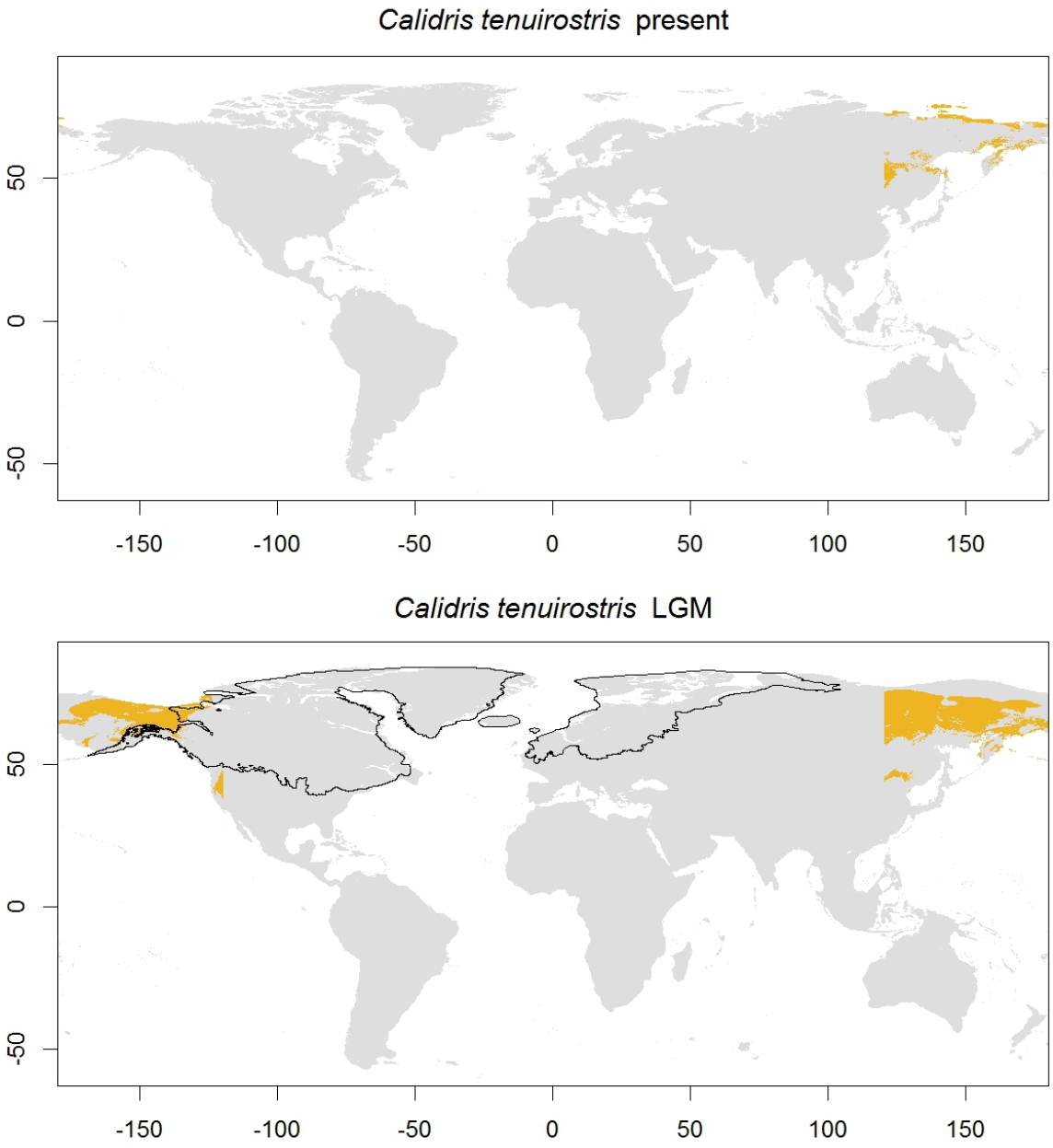

Map 27: Great Knot (*Calidris tenuirostris*) predicted distribution. Caption as in map 1.

Great Knot, *Calidris tenuirostris* (map 27). Endangered species restricted to northeast Siberia, between the Verkhoyansk Mountains and the Chukotka Peninsula. No variation described. Due to this restricted distribution, the current model only predicts the breeding distribution in the coastal areas of northeast Siberia, but it is difficult to evaluate this prediction since even the real breeding distribution is poorly known (del Hoyo *et al.*, 2018). Model for the LGM predicts suitable breeding areas between northeast Siberia and Alaska, including Beringia. The wintering range is very fragmented, with local areas of presence in the Arabian Peninsula, India, Myanmar and Australia, and the coast of Indonesia and New Guinea. The model for the present conditions covers

most of the wintering range, although with very few predicted areas in Australia and the Arabian Peninsula, and some over-prediction in Indochina and southeast China. The southernmost parts of the wintering distribution in Australia disappear in the model for the LGM conditions, as well as most of the areas in continental Asia, remaining mostly in the emerge land between the islands of Indonesia and New Guinea. This species is classified under scenario A.

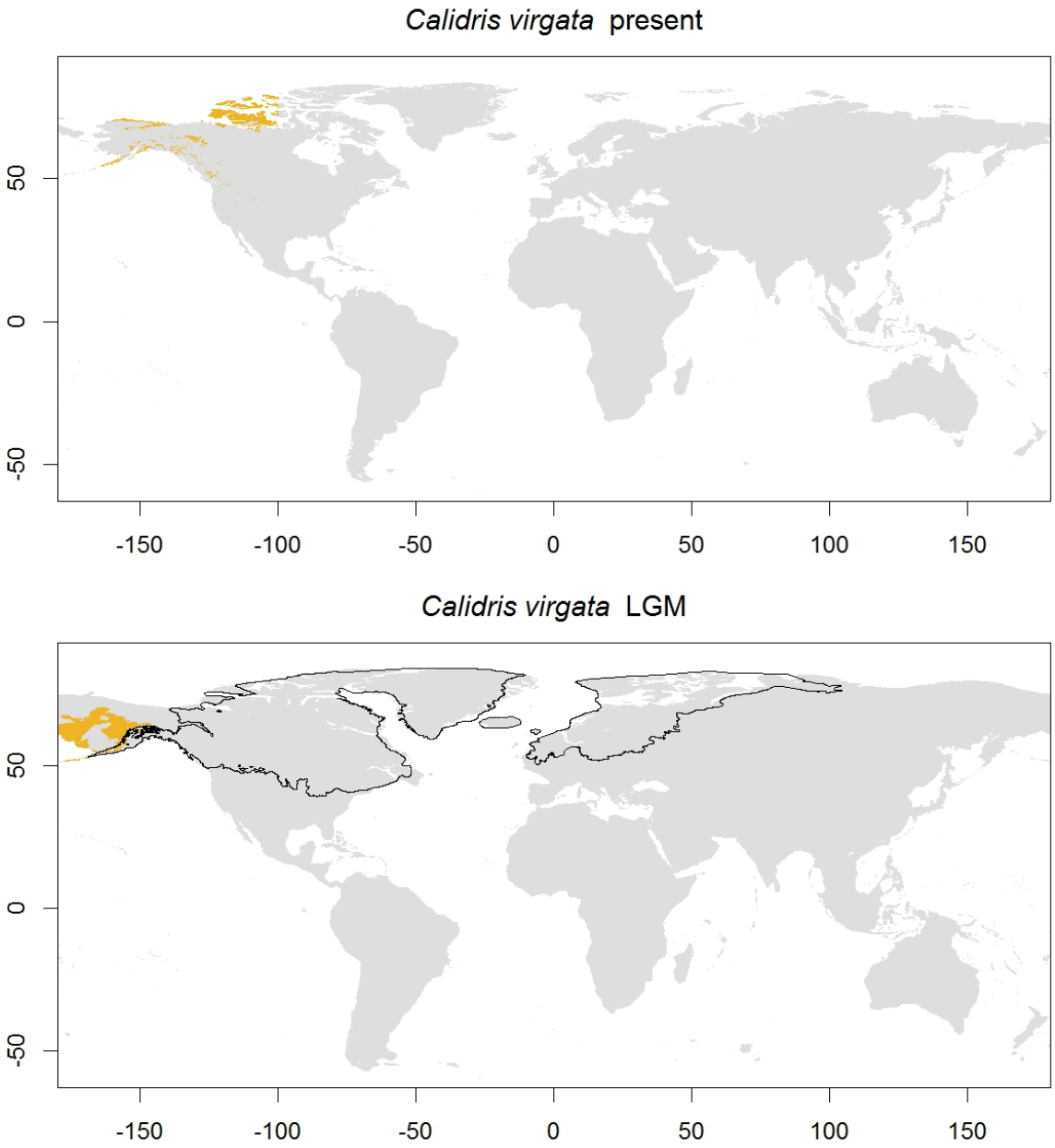

Map 28: Surfbird (*Calidris virgata*) predicted distribution. Caption as in map 1.

Surfbird, *Calidris virgata* (map 28). Breeding distribution restricted to in Alaska, with no described variation. Current SDM shows over-predictions on the Canadian Arctic islands (Victoria and Banks). The LGM models predict that the species' breeding was restricted in Beringia during the glacial period. The current wintering range is restricted to the coastal areas along the whole western coast of the American continent, which resulted in problematic results in the SDM and was discarded. This species is classified under scenario A.

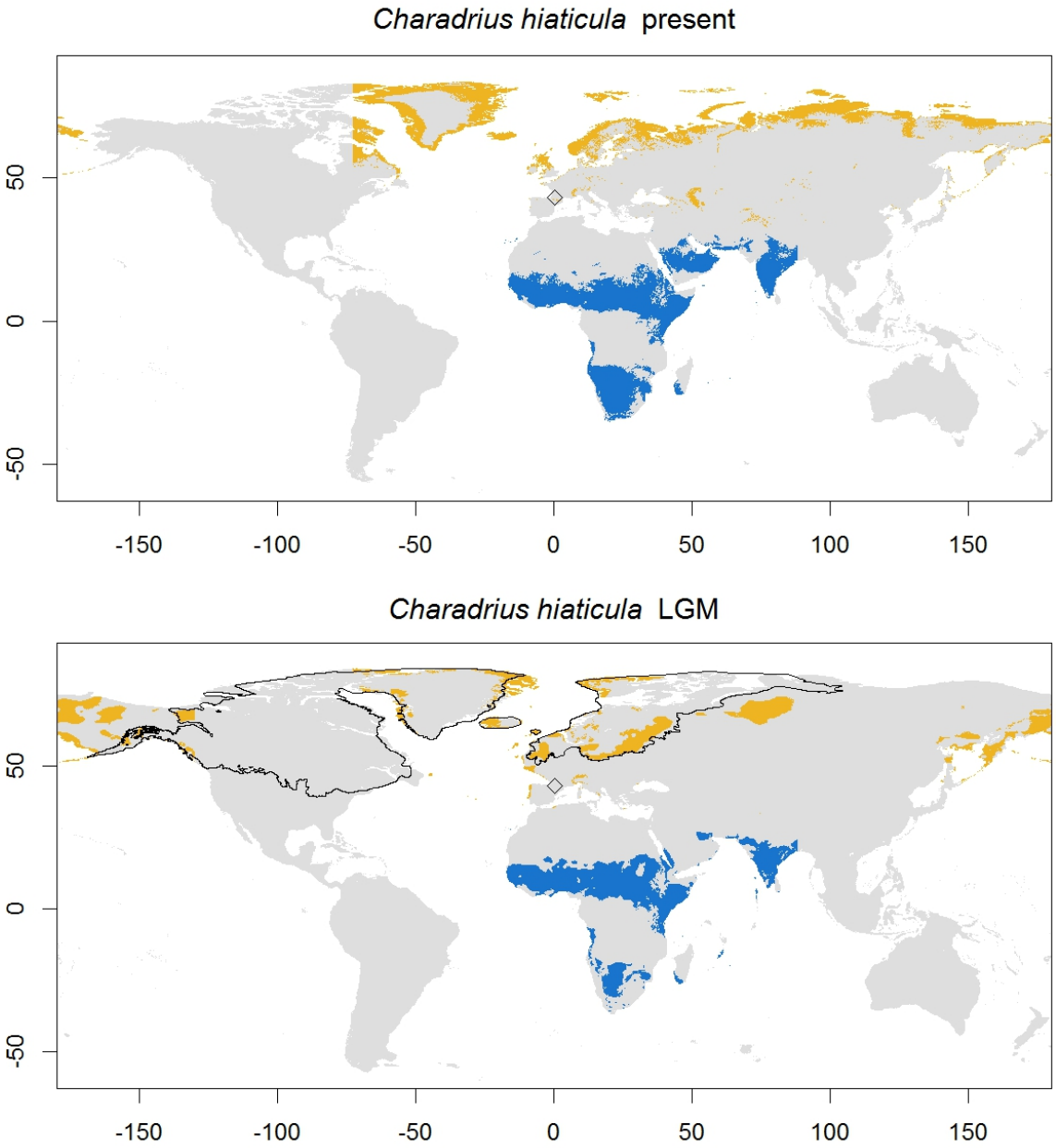

Map 29: Common Ringed Plover (*Charadrius hiaticula*) predicted distribution. Caption as in map 1.

Common Ringed Plover, *Charadrius hiaticula* (map 28). Arctic and temperate breeding species with three recognized subspecies based on the moult (Engelmoer & Roselaar, 1998). *C. h. psammodromus* breeds in northeast Canada (Ellesmere and Baffin Islands), Greenland, Svalbard, Iceland and Faeroes. *C. h. hiaticula* covers the south of Scandinavia, British Islands and northwest France. *C. h. tundrae* extends from northern Scandinavia to the Chukotka Peninsula, across all the north of Russia. All the breeding areas are predicted by our SDM, except for the distribution in France. During the LGM the model predicts a fragmented breeding distribution, although compatible with the persistence of the subspecies. *C. h. psammodromus* has suitable breeding predicted areas across most of its distribution in Greenland, Iceland and Svalbard. *C. h. hiaticula* is predicted to have suitable areas in western Europe, and also a large area in central and eastern Europe that could be assigned to either this subspecies or *C. h. tundrae*. This subspecies also is predicted to persist in northern Siberia near the river Ob, and also in northeast Siberia and Beringia. The wintering covers most of Africa (except the Sahara), Madagascar, southern and western Europe and south Asia. Most of this range is predicted by the SDM, except in Europe. The LGM is not predicted to have caused major changes in the wintering range. This species is classified under scenario C.

Piping Plover, *Charadrius melodus* (map 30). Subarctic and temperate breeding species with two subspecies based on genetic analyses (Miller *et al*., 2010). *C. m. melodus* breeds in the east coast of North America, up to Newfoundland; and *C. m. circumcinctus* extends over the Great Plains of central North America, between USA and Canada. The SDM however predicts a much larger potential breeding range, extending from Alaska and British Columbia on the west, to the Northwest Territories and Labrador Peninsula. However, breeding distribution of the species during the LGM is virtually inexistent. The wintering range, which covers most of the Gulf of Mexico and some Caribbean Islands, potentially remained stable during the LGM. This species is classified under scenario B.

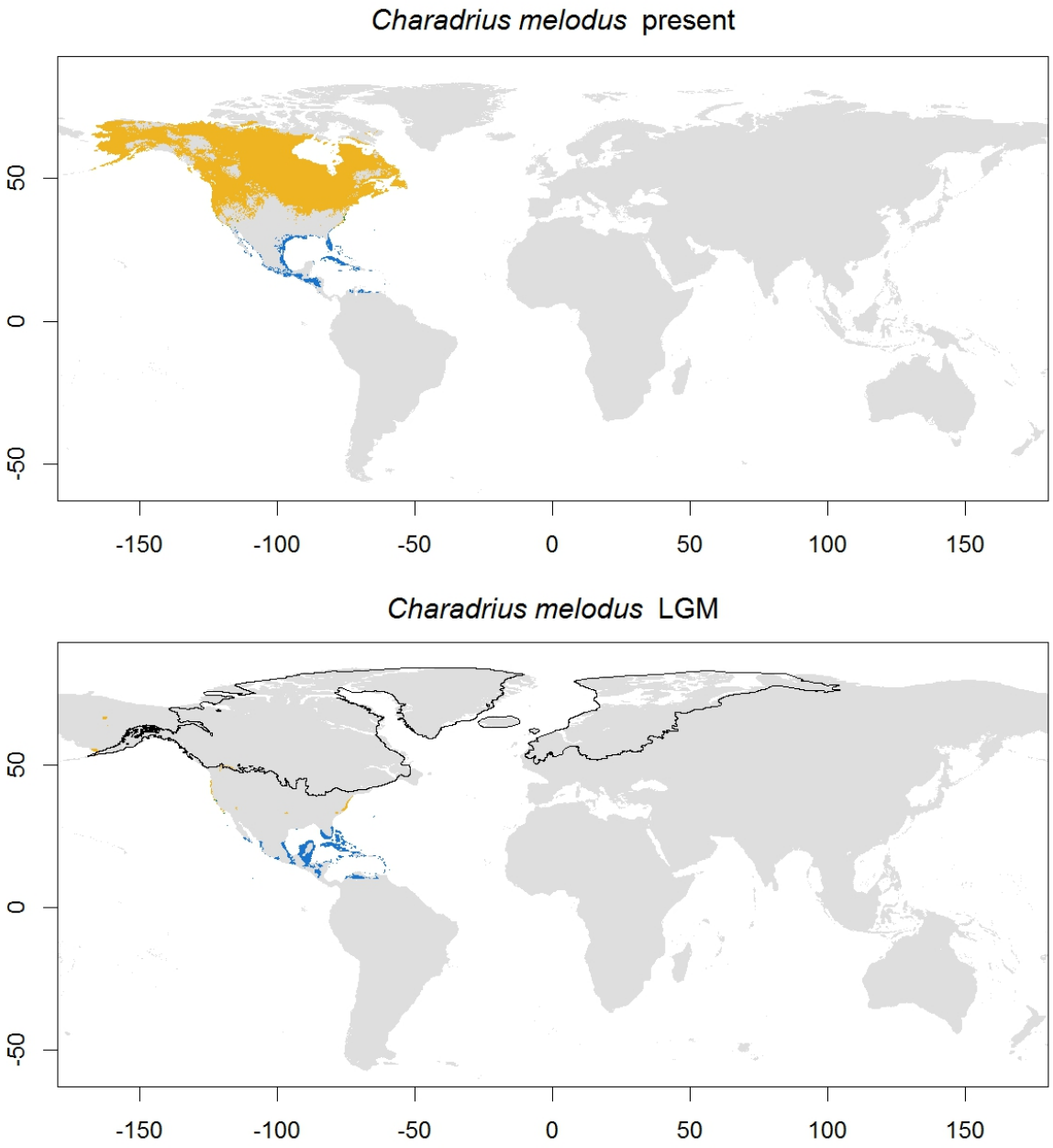

Map 30: Piping Plover (*Charadrius melodus*) predicted distribution. Caption as in map 1.

Lesser Sandplover, *Charadrius mongolus* (map 31). Arctic and subarctic species that also breeds in around the Himalayas and the Tibetan Plateau. Five described subspecies, with three of them (*C. m. palmirensis*, *C. m. atrifrons* and *C. m. schaeferi*) breeding in central Asia and the Tibetan Plateau. Of the other two, *C. m. mongolus* occupies some sparse areas the east of Russia, and *C. m. stegmanni* breeds across the Chukotka Peninsula and Kamchatka. Although the fragmented and sparse areas are very difficult to model with total accuracy, the SDM correctly predicts the breeding distribution of the species in the Tibetan Plateau and in northeast Siberia. There are some under

predictions in the breeding areas of eastern Russia, and some small over predicted areas in northern and central Siberia. During the LGM, the model predicts a much larger breeding distribution that potentially extended between central and eastern Siberia, and south into central Asia. The wintering range covers from south continental Asia to Australia and some parts of the African coast. The SDM does fit this wintering distribution well, and it is predicted to have remained stable during the LGM. This species is classified under scenario D.

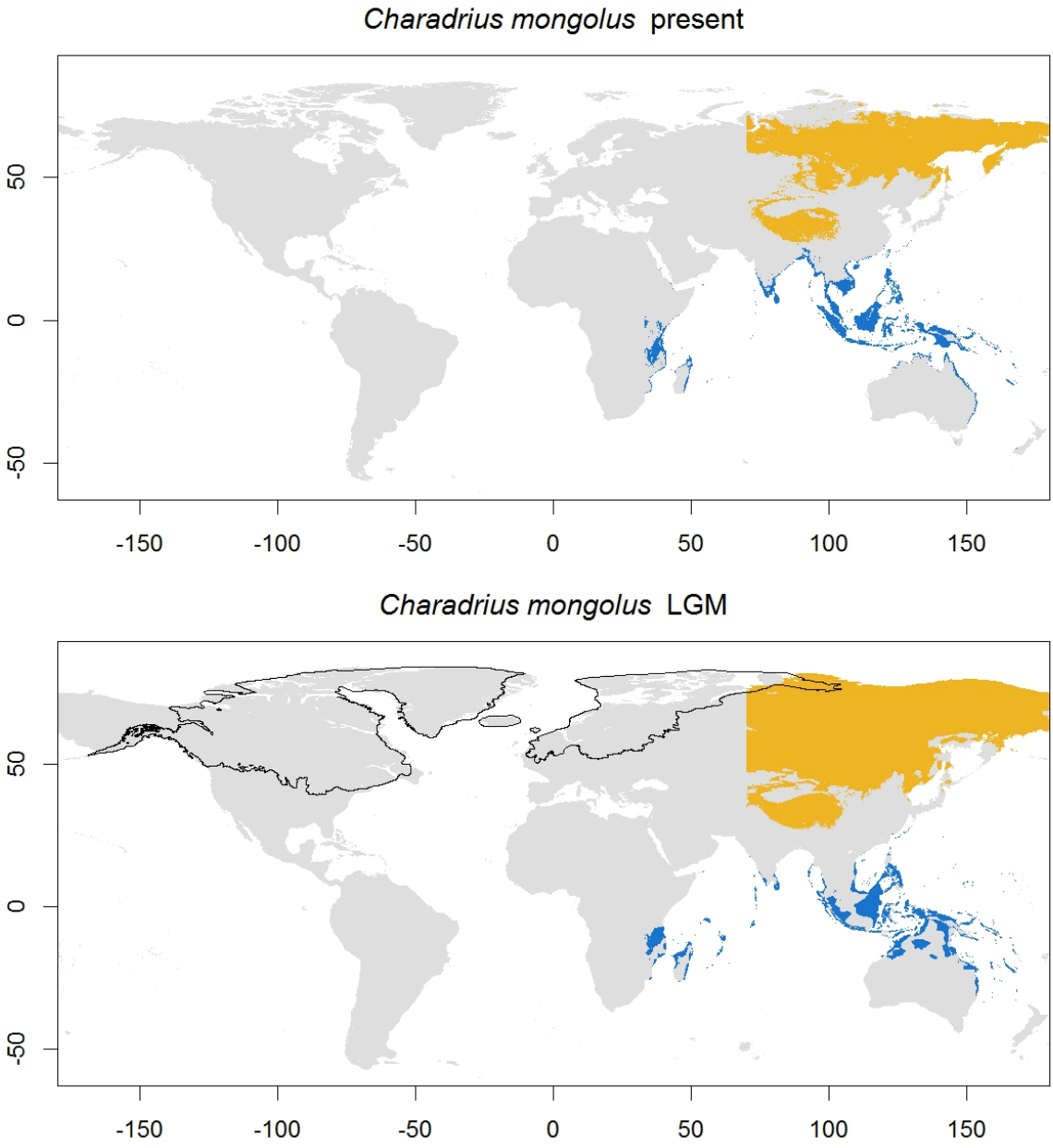

Map 31: Lesser Sandplover (*Charadrius mongolus*) predicted distribution. Caption as in map 1.

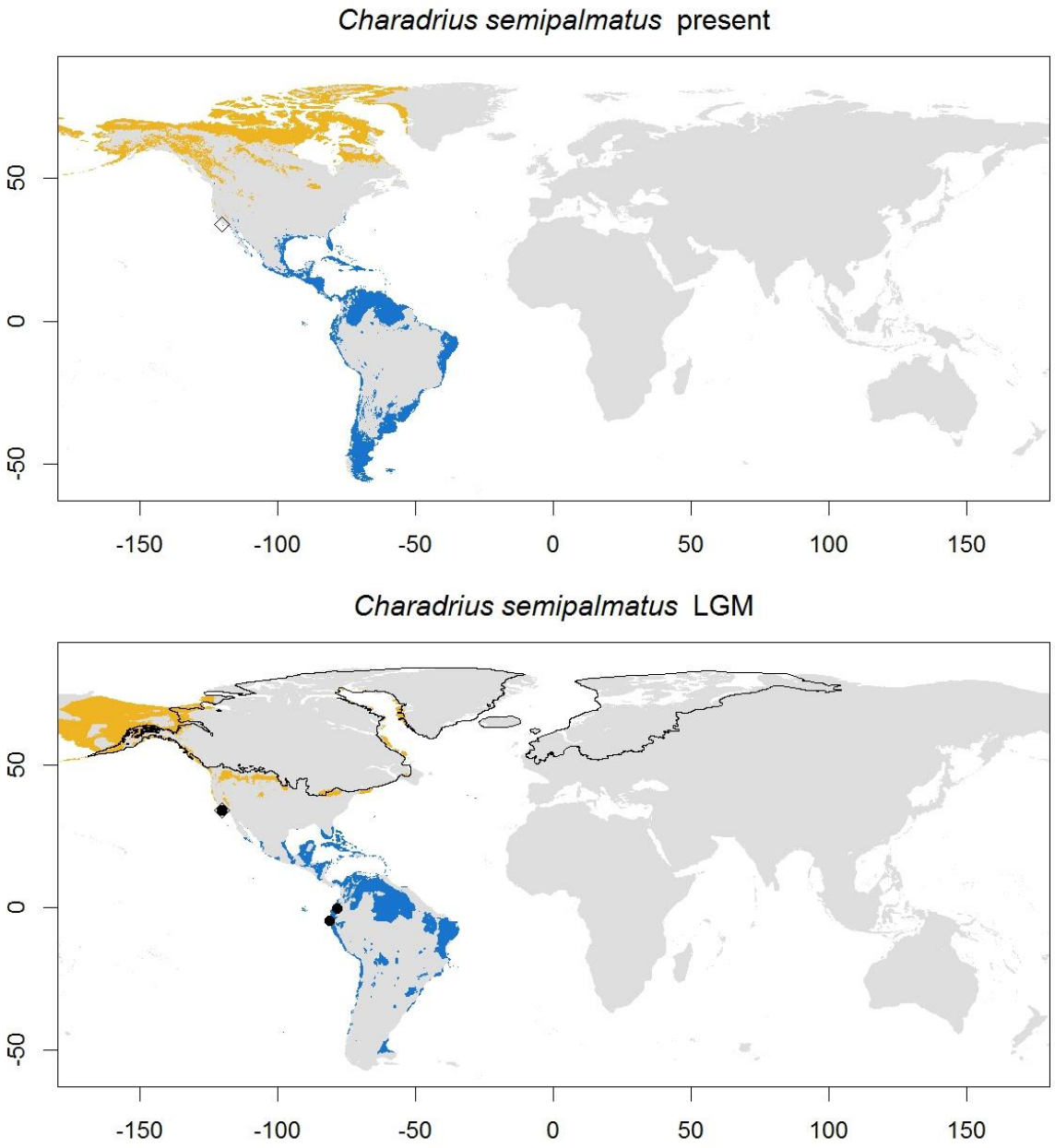

Map 32: Semipalmated Plover (*Charadrius semipalmatus*) predicted distribution. Caption as in map 1.

Semipalmated Plover, *Charadrius semipalmatus* (map 32). Nearctic species with no variation described. Breeding range covers from Alaska and the Aleutian Islands in the west, to Hudson Bay and Newfoundland in east. In the north reaches Baffin, Victoria and Bank Islands. The SDM fits well this breeding distribution, with over-predictions in the Chukotka and Labrador Peninsulas, Ellesmere Island and western Greenland. During the LGM, the species' breeding range is predicted mainly in Beringia and north Alaska, with some scarce predictions at lower latitudes in North America and east of Labrador Peninsula. The wintering range extends along the east and west coast of North America, Central America and most of South America, as well as in the Caribbean. The model

under current conditions predicts all those wintering areas, and over-predicts in the southern tip of South America. This over-prediction disappears under the LGM conditions, but the rest of the wintering range is predicted to remain stable, except for the northernmost parts in North America. This species is classified under scenario A.

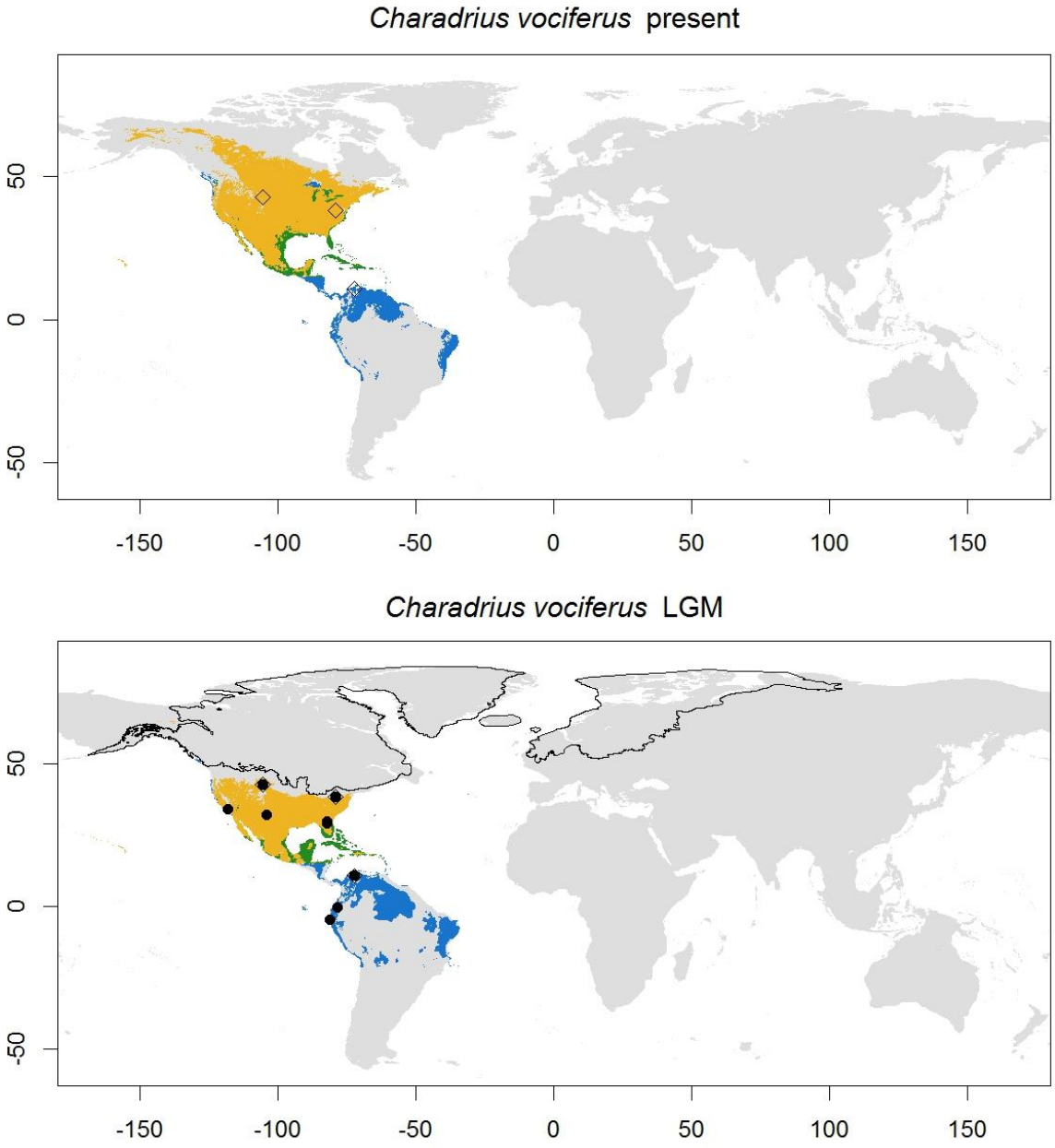

Map 33: Killdeer (*Charadrius vociferus*) predicted distribution. Caption as in map 1.

Killdeer, *Charadrius vociferus* (map 33). Subarctic and temperate species that breeds though most of central North America and up to the Hudson Bay, British Columbia and east Alaska. It is also resident year-round in the southern half of North America, the

Caribbean and the coast of Peru, and Ecuador. There are three recognized subspecies (del Hoyo *et al*., 2018), two of which are non-migratory: *C. v. ternomoniatus*, in the Caribbean, and *C. v. peruvianus*, in Ecuador and Peru. The other subspecies, *C. v. vociferus*, occupies the remainder of the range. The SDM predicts well most of the breeding range in temperate areas, but with a smaller extension in British Columbia and Alaska. The species' breeding range is predicted exclusively in lower latitudes during the LGM, occupying the southern areas of North America as well as Central America and the Caribbean. All of those predicted breeding areas correspond to where the species is resident today. The wintering range, from the east and west coasts of North America to the northern half of South America, is well predicted by our model, and the LGM model shows a similar wintering distribution, with no major changes. This species is classified under scenario A.

Eurasian Sotterel, *Eudromias morinellus* (map 34). Monotypic species breeding across the Palearctic in northern Britain, Scandinavia, some areas of central Asia, and in northern Siberia from the Ural Mountains and Novaya Zemlya to the Chukotka Peninsula and even northwest Alaska. Our model correctly predicts the breeding range, with some over-predictions in Svalbard and New Siberian Islands. During the LGM the model predicts suitable breeding areas at high latitudes (>50° N) in northeast Siberia, and a separated area covers most of central and eastern Siberia and extends to and central and western Europe. The wintering range is very fragmented and covers most of the southern coast of the Mediterranean, and also the east of the Arabian Peninsula. The SDM returns a prediction similar to the current wintering range, with potential areas also in the south of Europe. In the LGM model the wintering range is fragmented and restricted to the south of the Mediterranean, which highly resembles the current wintering distribution of the species in the present. This species is classified under scenario D.

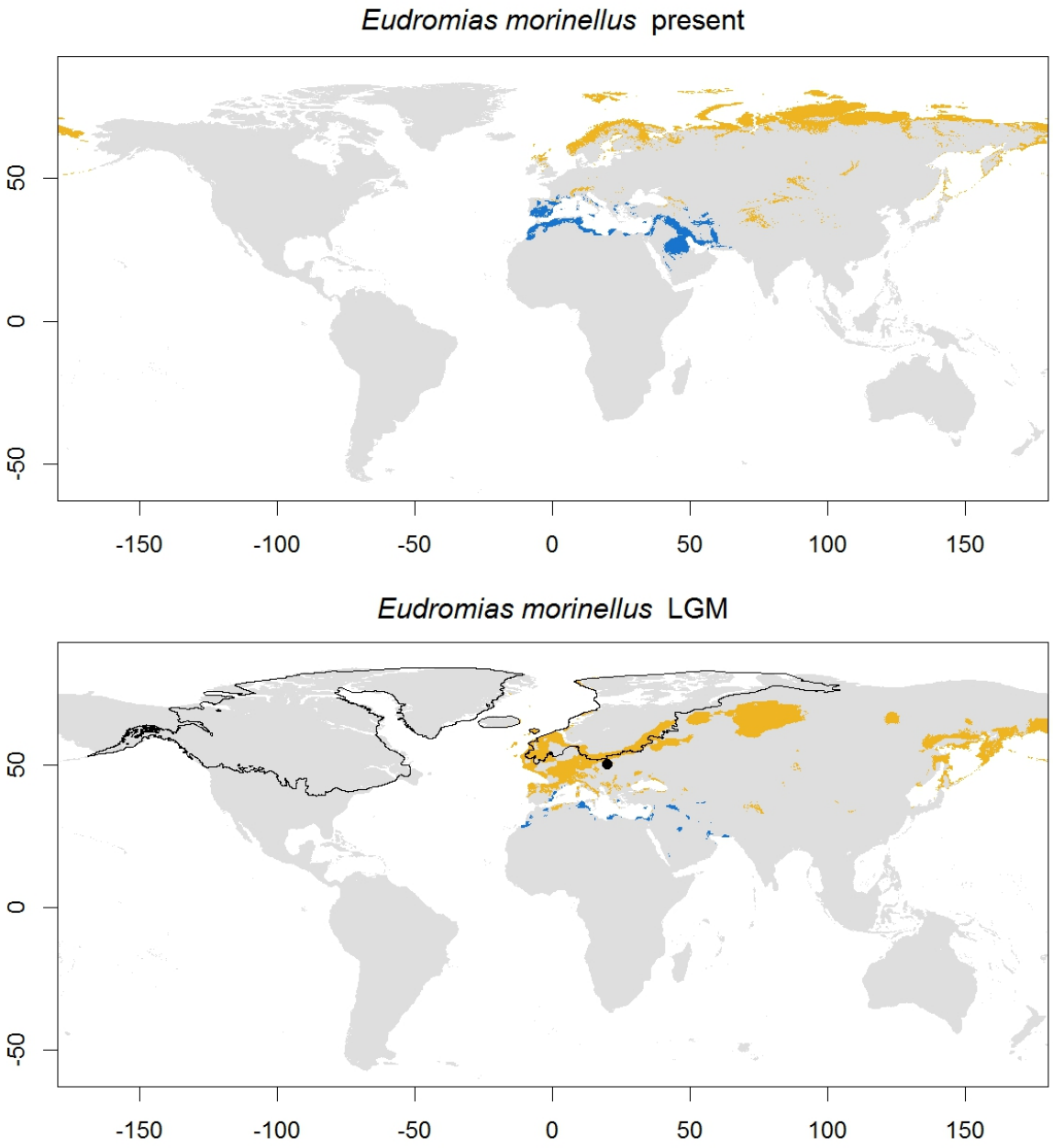

Map 34: Eurasian Dotterel (*Eudromias morinellus*) predicted distribution. Caption as in map 1.

Wilson's Snipe, *Gallinago delicata* (map 35). Monotypic species that breeds from Alaska and the Aleutian Islands to the Labrador Peninsula and Newfoundland, reaching the Northwest Territories on the north. It is resident all year in the northwest of the USA. Breeding range is well predicted by the SDM. The LGM model predicts two main breeding areas for the species, one in Beringia and the other at lower latitudes in North America, similar to the area where the species is resident in the present. A coastal area in British Columbia connects both predicted breeding areas. The wintering range covers the southern half of North America, (overlapping with the southwest part of the

breeding distribution), Central America, the Caribbean, Colombia and Venezuela. The model under current conditions fits that wintering area well, even the overlapping part with the breeding distribution. This predicted wintering range showed no major changes in the LGM. This species is classified under scenario C

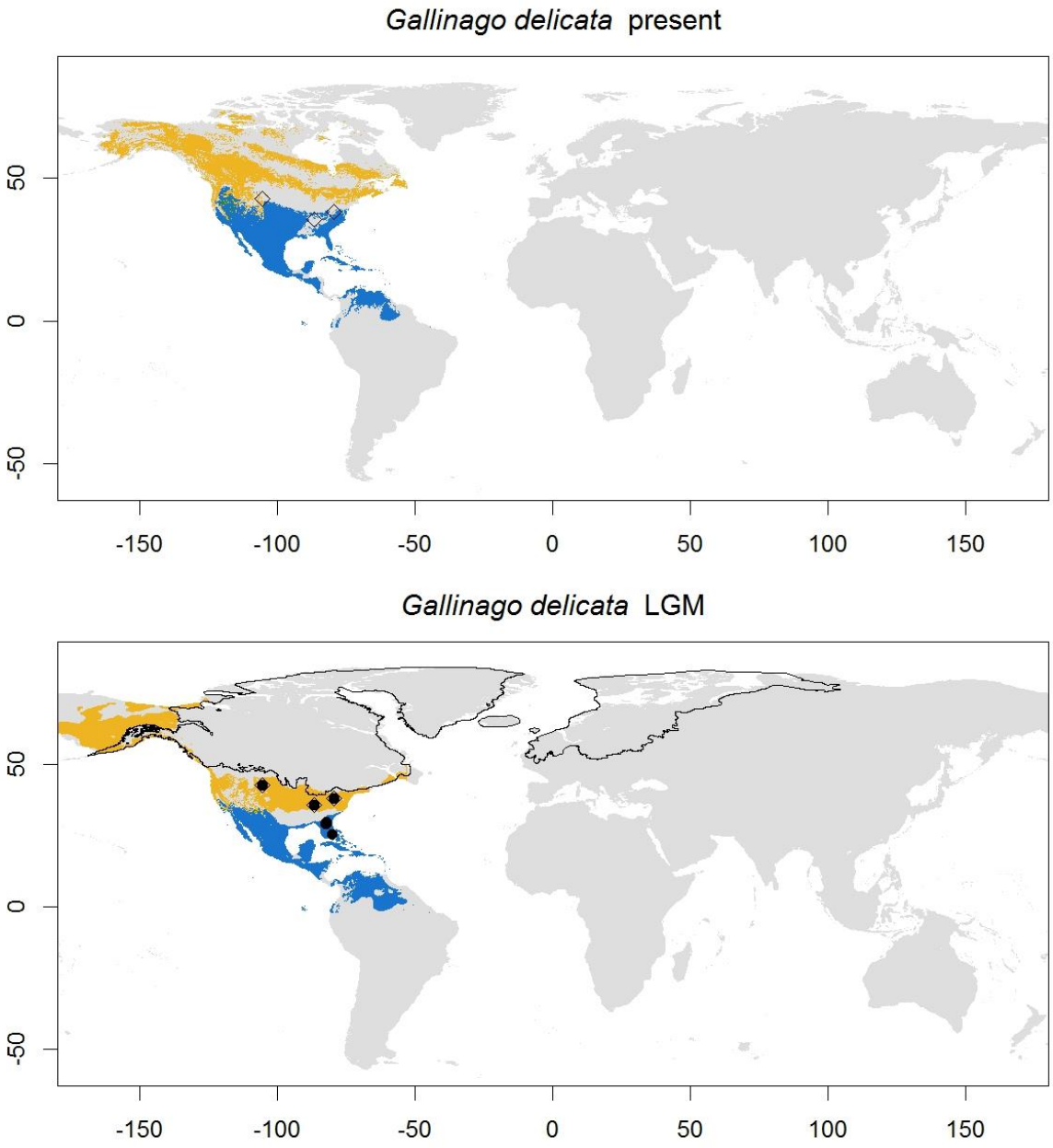

Map 35: Wilson's Snipe (*Gallinago delicata*) predicted distribution. Caption as in map 1.

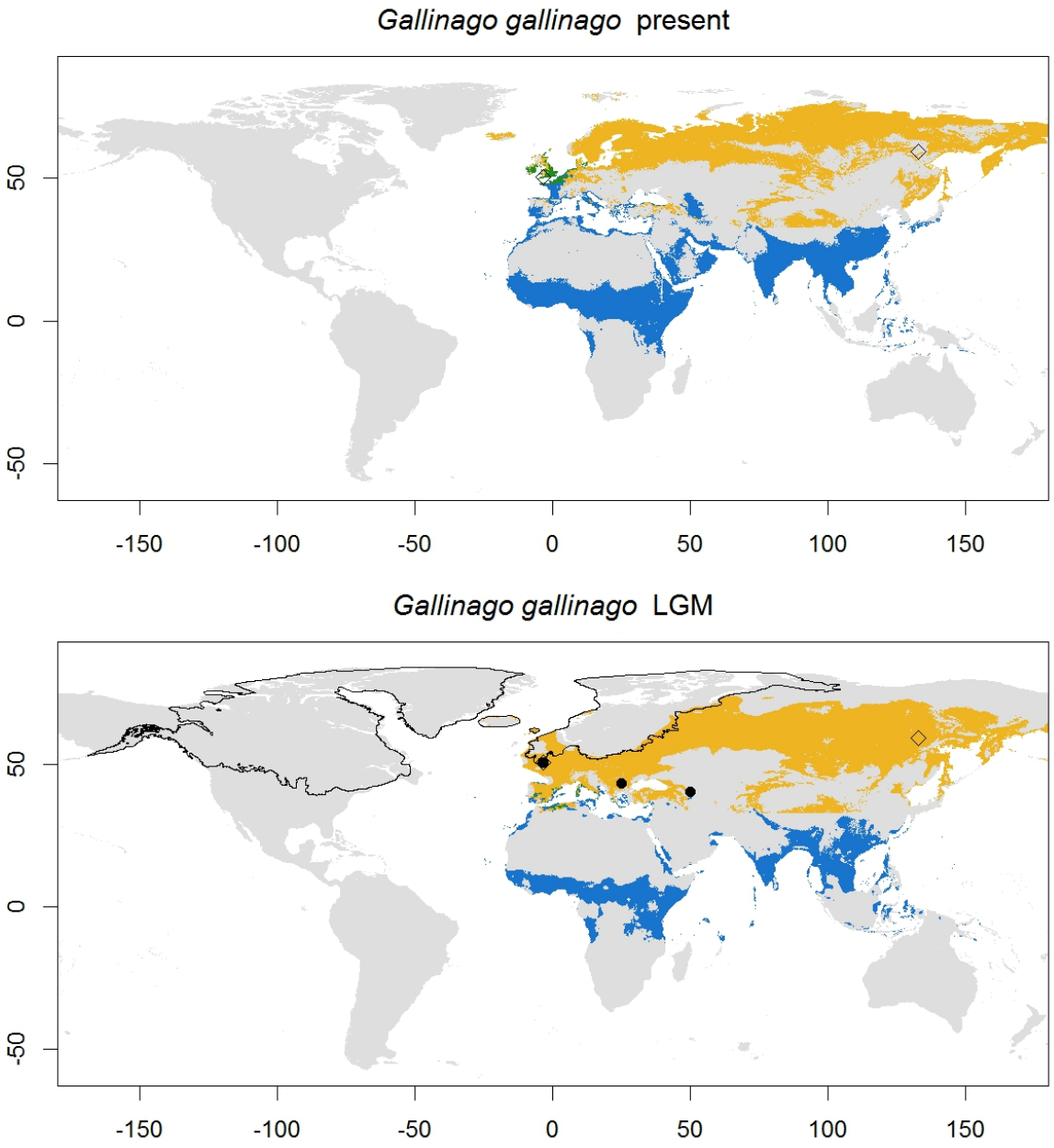

Map 36: Common Snipe (*Gallinago gallinago*) predicted distribution. Caption as in map 1.

Common Snipe, *Gallinago gallinago* (map 36). Palearctic species that breeds from Arctic to temperate areas. The breeding distribution is continuous and very wide, covering from Iceland and western Europe (where it is resident) to northeast Siberia and Kamchatka, between 30° N to 70° N. Two species are recognized, *G. g. faeroeensis* in Iceland and Faeroes, and *G. g. gallinago* in the remainder of the range. The prediction of the model for the present fits the known breeding distribution of the species. During the LGM the breeding range is predicted as a continuous area from east Siberia to western Europe. The breeding range of *G. g. faeroeensis* remained stable with predicted

available areas in some parts of Iceland and the Faeroes Islands, which due to changes in the coastline due to sea-level drop, are closer to the predicted areas in Britain and northwest France, where the species is now resident all year. The wintering distribution of the species is located in the Mediterranean, central and the south of Asia. The model for the present predicts the wintering range well, even the overlap with the breeding range in western Europe and the British Islands. Most of this wintering range is conserved in the model under the LGM conditions, decreasing only the overlap area in Europe, where it is predicted only as breeding area. This species is classified under scenario D.

Great Snipe, *Gallinago media* (map 37). Arctic and temperate species breeding in the western Palearctic, from Scandinavia to western Russia near the Yenisei River (del Hoyo *et al*., 2018). No described subspecies. The SDM under-predicts the southern part of the breeding range in favour of the Arctic distribution. Also, it does not predict the range to abruptly stop in western Russia, and instead extends the prediction to the East reaching northeast Siberia. The LGM model show a reduction of all the breeding range, with the species predicted in a series of localities across southern and western Europe and western Asia. The wintering range covers most of sub-Saharan Africa. The model for the present predicts that wintering distribution correctly, over-predicting a little to the south and in Madagascar, bur overall showing a good fit. During the LGM the species is predicted to be present in a similar wintering range, although with less available areas, mostly at lower latitudes in both hemispheres. This species is classified under scenario A.

Pintail Snipe, *Gallinago stenura* (map 38). The breeding range extends from the Ural Mountains to northeast Siberia, and also south to central Asia. No subspecies described. The SDM for the present predicts most of the breeding range of the species, but also over-predicts potential suitable areas in the western Palearctic. During the LGM, the species is predicted to have retained most of its breeding range in Asia, at slightly lower latitudes, and with an almost total reduction in northeast Siberia. The wintering range covers from southern continental Asia to southern Indonesia. The model fits that wintering distribution, and also predicts the species to potentially be present in New Guinea and Australia. During the LGM, the model predicts a reduction of the wintering

range in India and Indochina, and an increase in the emerged land between the Indonesian Islands. This species is classified under scenario A.

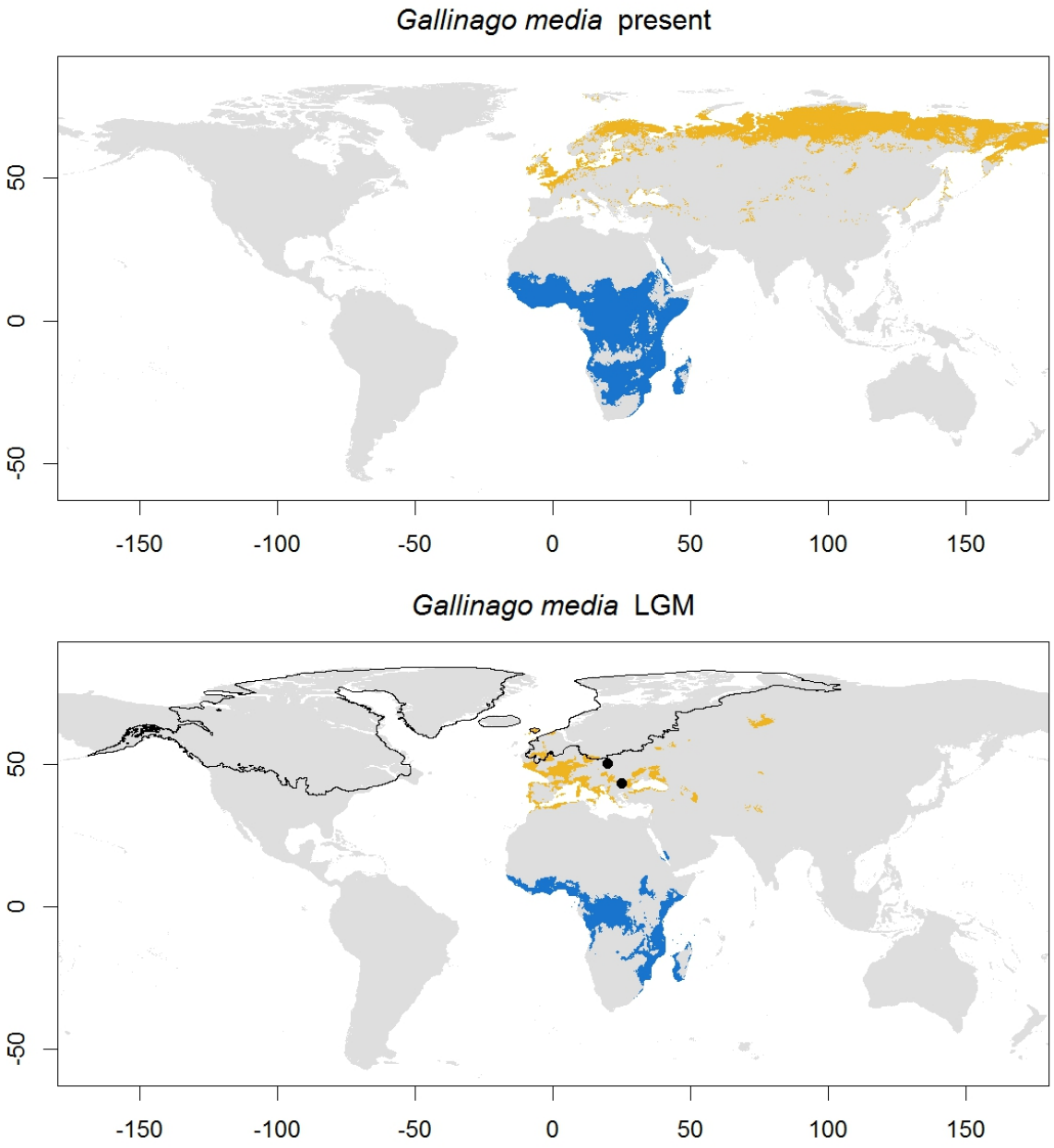

Map 37: Great Snipe (*Gallinago media*) predicted distribution. Caption as in map 1.

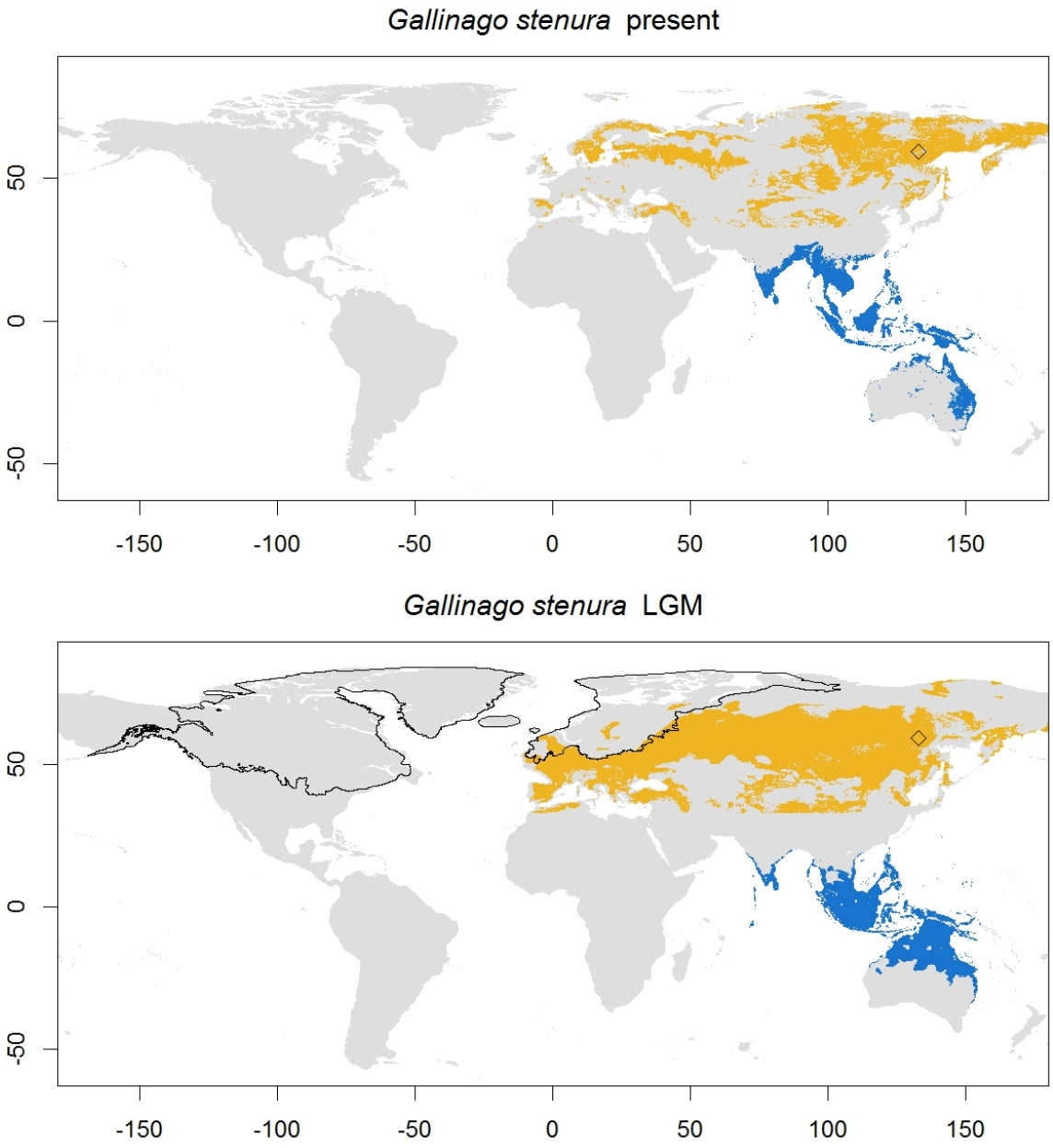

Map 38: Pintail Snipe (*Gallinago stenura*) predicted distribution. Caption as in map 1.

Eurasian Oystercatcher, *Haematopus ostralegus* (map 39). Arctic and temperate species with four subspecies recognized (del Hoyo *et al*., 2018), three of them breeding across the Palearctic: *H. o. ostralegus* in Iceland, Scandinavia and extreme northwest Russia, the British Islands and northwest France; *H. o. longipes* in western Russia up north to Siberia, and the Black, Caspian and Aral seas; and *H. o. osculans* in the coastal regions of east Asia, from northeast China to Kamchatka. There is a fourth subspecies,

H. o. finschi, which is endemic of New Zealand and its breeding distribution is not considered for the models. Due to the wide breeding range and the discontinuities of the distribution, the results of the model do not completely fit the breeding distribution of the species in all the areas. The model predicts the breeding range in western Europe, with some over-predictions in the south, and under-predicts in Iceland and parts of Scandinavia. It also over-predicts in central and northeast Asia, while under-predicting in the coastal regions of east Asia. However, the LGM model clearly shows three breeding areas, two in the western Palearctic and one in the eastern part, matching potential refugia for each of the subspecies. In the west, there is a predicted available area in southern Europe around the western Mediterranean, where *H. o. ostralegus* currently has some isolated breeding populations. The other predicted breeding area is around the Black and Caspian Seas, overlapping with the current distribution of *H. o. longipes*. Finally, a third available area is predicted in far east Asia, isolated from the other areas, similarly to the present isolation of *H. o. osculans* from the other two Palearctic species. The wintering range covers most of the coasts of the northern half of Africa, western Europe, the Arabian Peninsula and south Asia to the Korean Peninsula. The SDM fits this wintering distribution, even the parts in Europe where it overlaps with the breeding distribution, and it only over-predicts in some inland areas of Africa and Asia. The predicted wintering remained stable during the LGM period, only decreasing in the northern part of western Europe. This species is classified under scenario D.

Short-billed Dowitcher, *Limnodromus griseus* (map 40). Nearctic species with three subspecies recognized: *L. g. caurinus* breeding from south Alaska to northwest British Columbia, *L. g. hendersoni* in central Canada to south Nunavut and *L. g. griseus* in western Labrador. The model predicts the breeding range as continuous, without distribution gaps between subspecies. In the LGM model however the model shows isolated breeding areas in south Beringia, near the current range of *L. g. caurinus*, and at lower latitudes in the east and west of North America, but without a clear correlation with the subspecies. The wintering grounds extend along the east and west coasts of America, from California to Peru and from North Carolina to central Brazil, and the Caribbean Islands. The SDM fits this wintering distribution well. During the LGM, the

model predicts a reduction of the wintering range in North America, remaining similar in Central America and South America. This species is classified under scenario C.

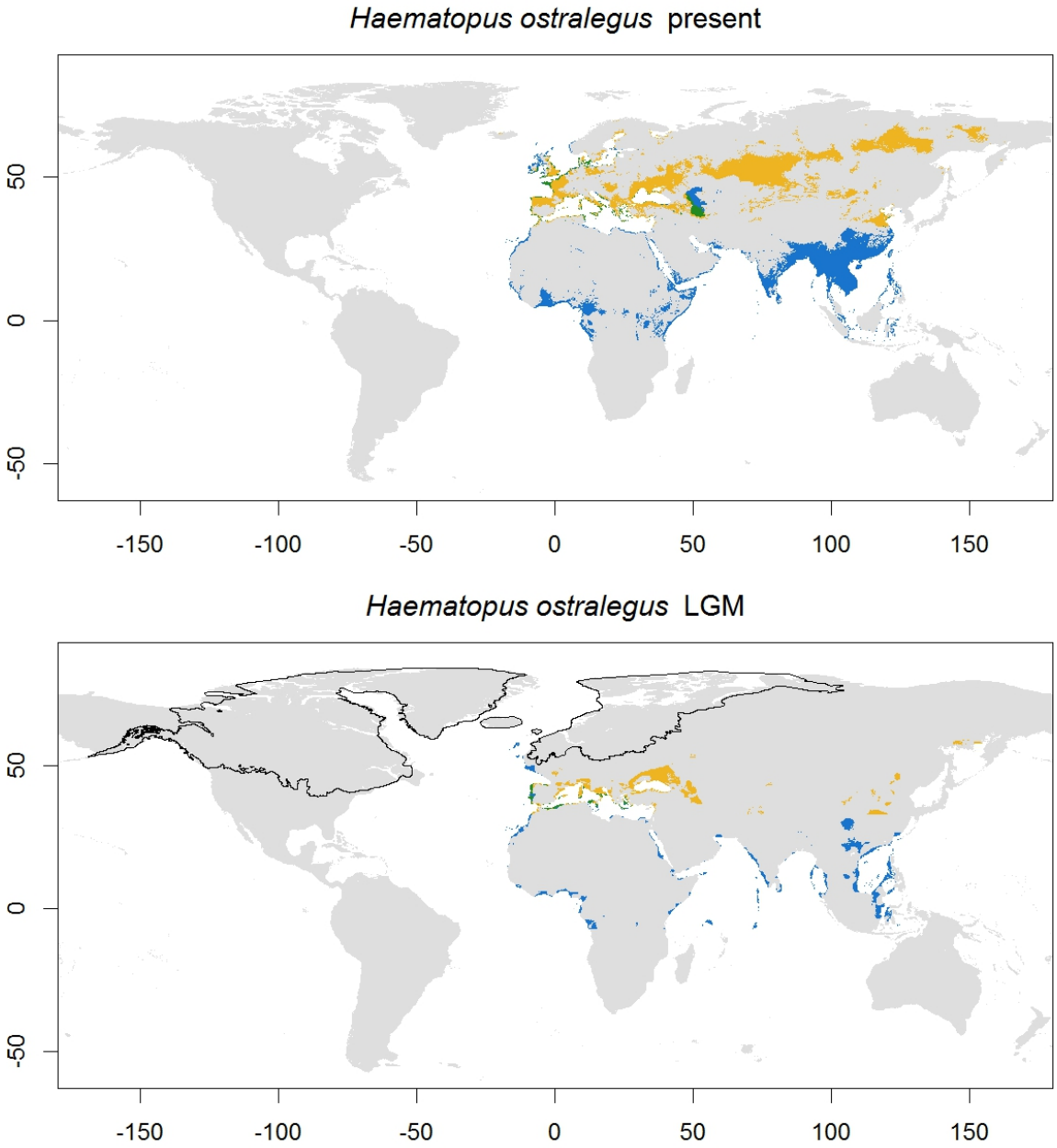

Map 39: Eurasian Oystercatcher (*Haematopus ostralegus*) predicted distribution. Caption as in map 1.

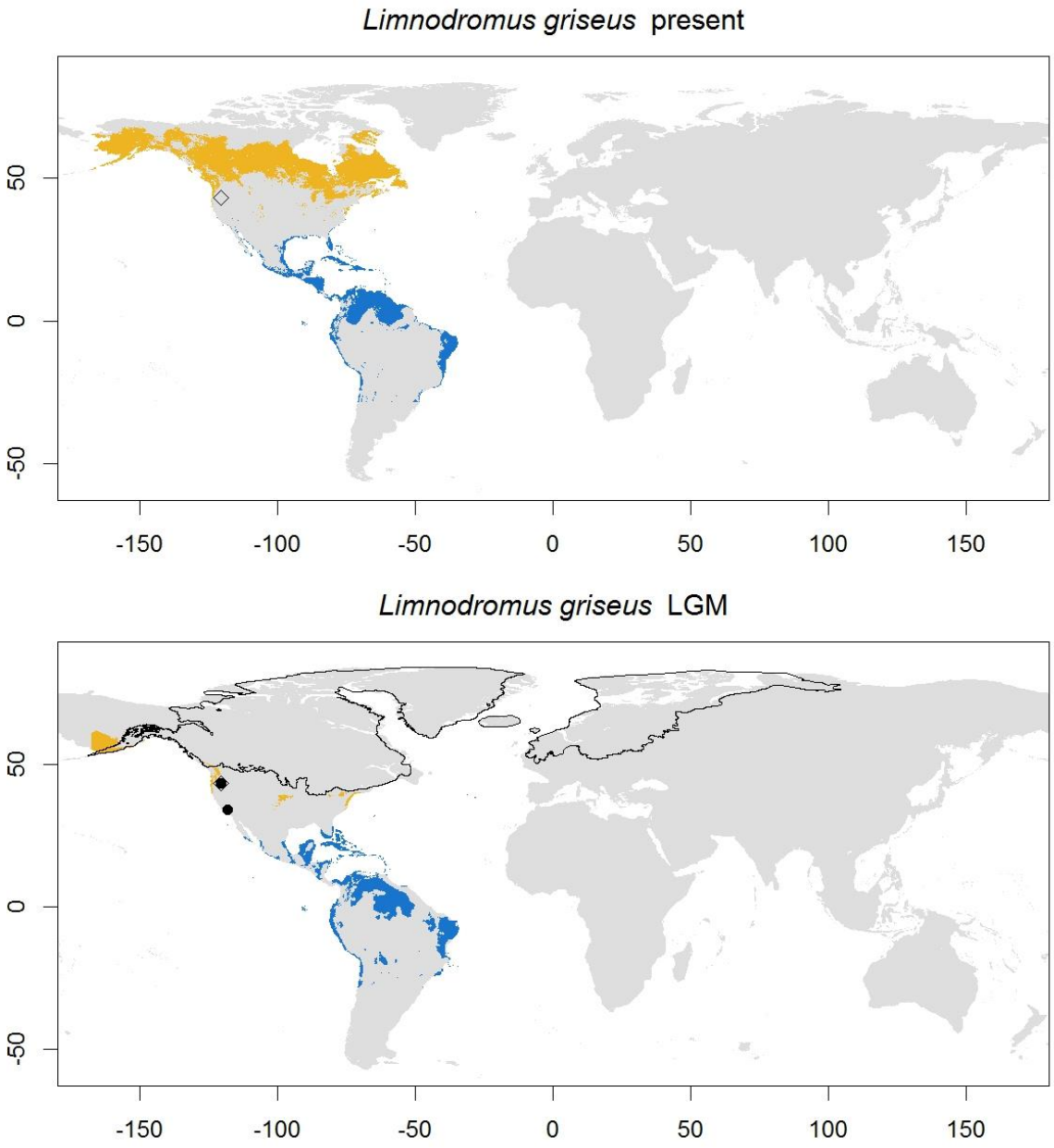

Map 40: Shot-billed Dowitcher (*Limnodromus griseus*) predicted distribution. Caption as in map 1.

Long-billed Dowitcher, *Limnodromus scolopaceus* (map 41). Monotypic species with breeding distribution in the Palearctic, from Yana River to Chukotka Peninsula, and in the Nearctic, in west and north Alaska and north Yukon. The SDM fits the breeding range of the species well, also extending the potential distribution into the Northwest Territories, Nunavut and Labrador Peninsula. The breeding distribution during the LGM is predicted to be greatly reduced, with the species remaining only in small areas of Beringia and the Sea of Okhotsk. The wintering range covers the southern part of USA and all of Mexico except for the Yucatan Peninsula. The SDM fit this wintering range

well, predicting also the presence in the Caribbean Islands and the north of South America. During the LGM, the predictions show a reduction in the northern part of the wintering range, and an increase in the south covering all of Central America and a larger area in the north of South America. This species is classified under scenario A.

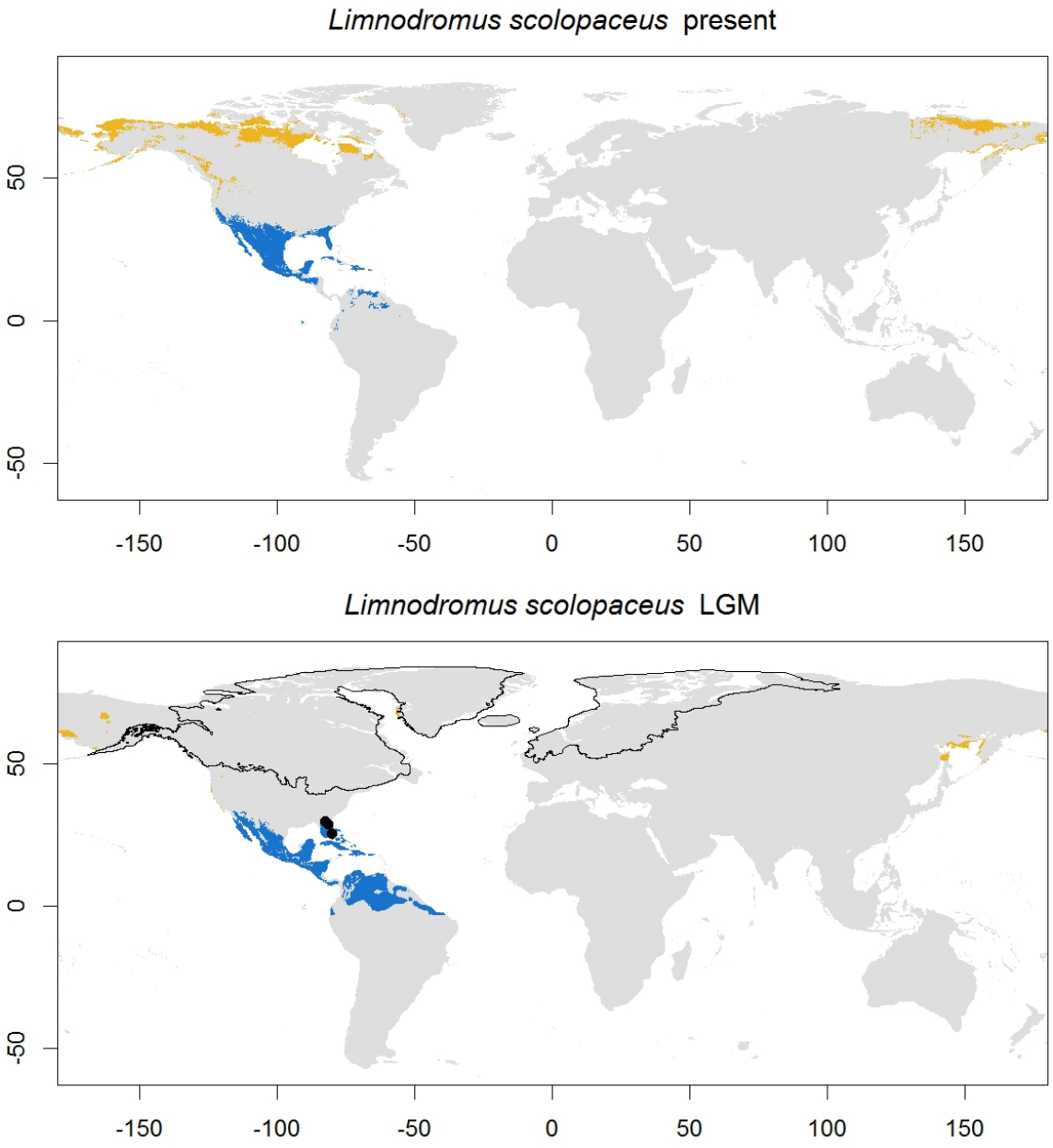

Map 41: Long-billed Dowitcher (*Limnodromus scolopaceus*) predicted distribution. Caption as in map 1.

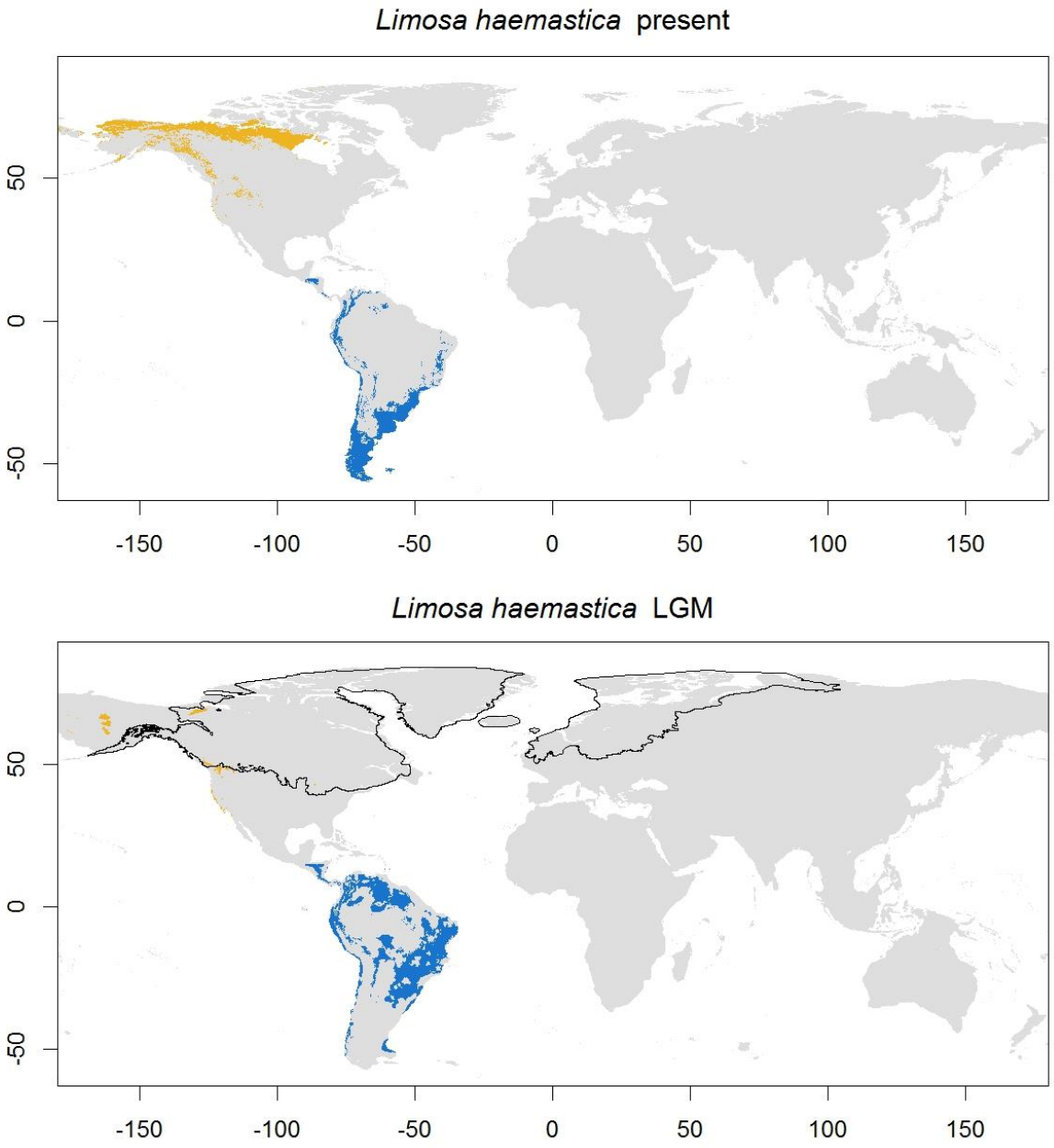

Map 42: Hudsonian Godwit (*Limosa haemastica*) predicted distribution. Caption as in map 1.

Hudsonian Godwit, *Limosa haemastica* (map 42). Nearctic breeder with a distribution fragmented into multiple isolated areas. It is present in west and south Alaska, north Yukon and Northwest Territories, northwest British Columbia, central Canada and the Hudson Bay. The predictions from the SDM cover most of the species' breeding range, but as a continuous range and with over-predictions of potential areas across Nunavut. The dispersion and small size of the patches of presence hinder the performance of the model and affect the accuracy of the predictions. The LGM model predicts only some small available breeding areas for the species in Beringia and northwest North America,

with a considerable breeding range reduction from the predicted present range. The wintering distribution extends across most of the southern cone of South America, especially in the east part of the continent. This wintering range is correctly predicted by the model, which also shows potential wintering areas in the west coast reaching up to Colombia. The LGM model shows a severe reduction of the available suitable wintering area in the southern part of the distribution, and predicts a wintering range that is very different from the present range, occupying large areas of east and north South America. This species is classified under scenario A.

Bar-tailed Godwit, *Limosa lapponica* (map 43). Arctic species breeding across the northern Palearctic, but with gaps in the distribution and isolated areas. Subspecies *L. l. lapponica* breeds in Scandinavia, *L. l. taymyrensis* extends between Yamal Peninsula and east of Taymyr Peninsula, *L. l. baueri* from the Lena River to Chukotka Peninsula, and *L. l. anadyrensis* in eastern Siberia. All of these breeding areas are predicted well by the model, although it also predicts in Novaya Zemlya and Svalbard. The LGM model shows four areas of breeding distribution that resemble the current distribution of subspecies: *L. l. lapponica* potentially distributed in some fragmented breeding areas in western Europe and the British Islands, similar to the current wintering range of the species; *L. l. taymyrensis* in a large breeding area between the Ural Mountains and the south of Taymyr, *L. l. baueri* in small breeding area in Siberia near the Lena River; and *L. l. anadyrensis* in northeast Siberia, Kamchatka and southern Beringia. The wintering distribution covers western Europe, west coast of Africa and from southern Asia to Australia and New Zealand. The model predicted well all this wintering range, with over-predictions in inland areas of central Africa and Indochina. During the LGM, the model predicts that most of the wintering distribution would have remained stable, with the exception of Europe, where the species is predicted to reduce its wintering range. This species is classified under scenario D.

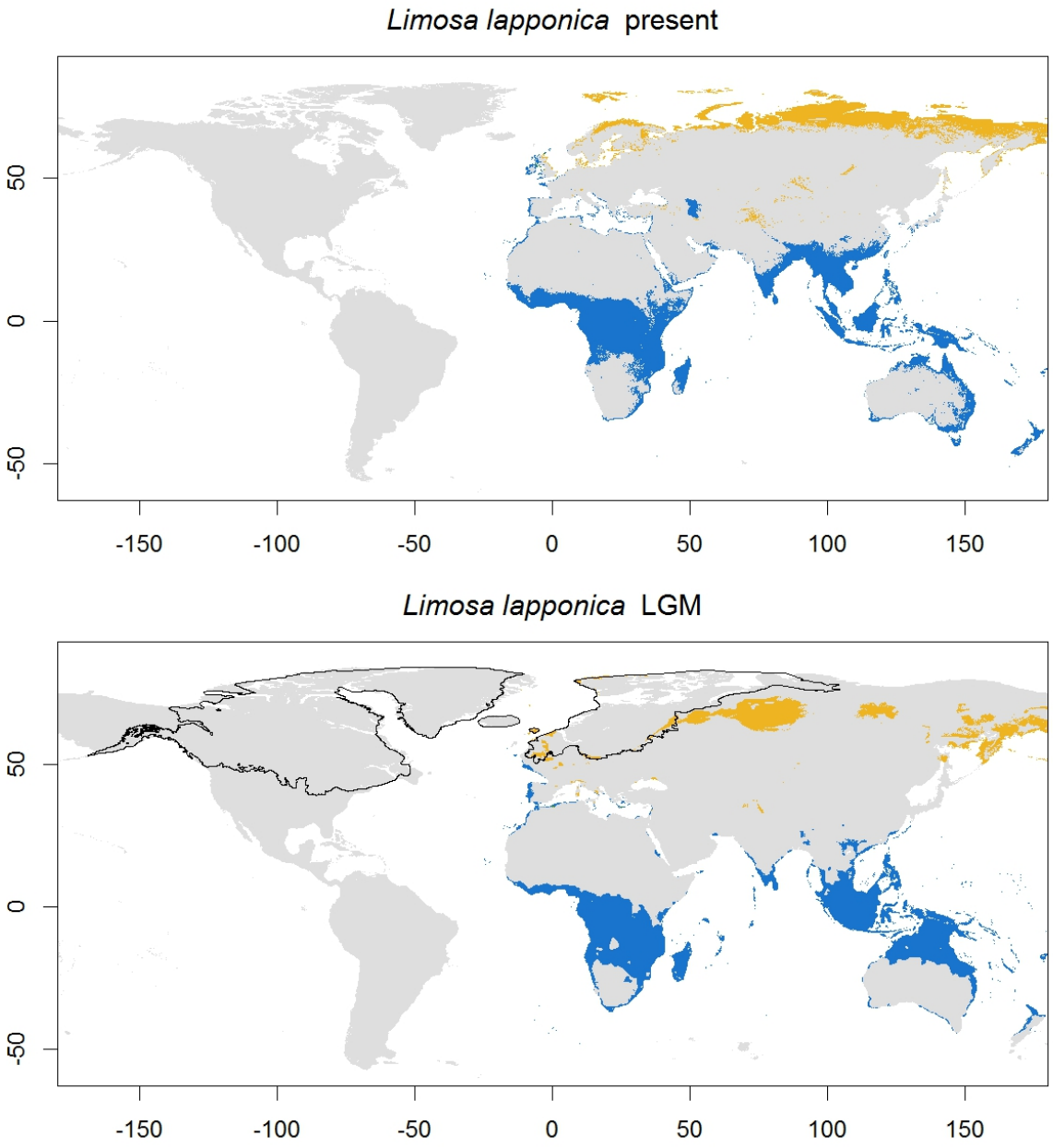

Map 42: Bar-tailed Godwit (*Limosa lapponica*) predicted distribution. Caption as in map 1.

Black-tailed Godwit, *Limosa limosa* (map 44). Subarctic to temperate species with a fragmented distribution across the Palearctic. Subspecies *L. l. limosa* breeds from western and central Europe and east Russia to the Yenisei River. *L. l. islandica* is in Iceland, Faeroes and Lofoten Islands. Subspecies *L. l. melanuroides* is isolated in breeding localities across far east Asia and northeast Siberia. The SDM covers the breeding range of the species in the western Palearctic, but over-predicts the breeding range into central Asia and southern Europe, and fails to predict the presence in Iceland and Siberia. The LGM model shows a series of small breeding areas distributed in the east and west regions of the Palearctic, with a large gap in between. The species winters

in the Mediterranean, south of the British Islands, sub-Saharan Africa, the Arabic Peninsula, and from south continental Asia to Australia. This wintering range is well predicted by our model, with predictions also in Madagascar and New Zealand. The northern part of the wintering range, especially in the Mediterranean, is reduced or disappears under the LGM, as well as in south Australia. In that period, most of the wintering range is predicted to be concentrated around inter-tropical Africa and in the emerged land between Asia and Australia. This species is classified under scenario D.

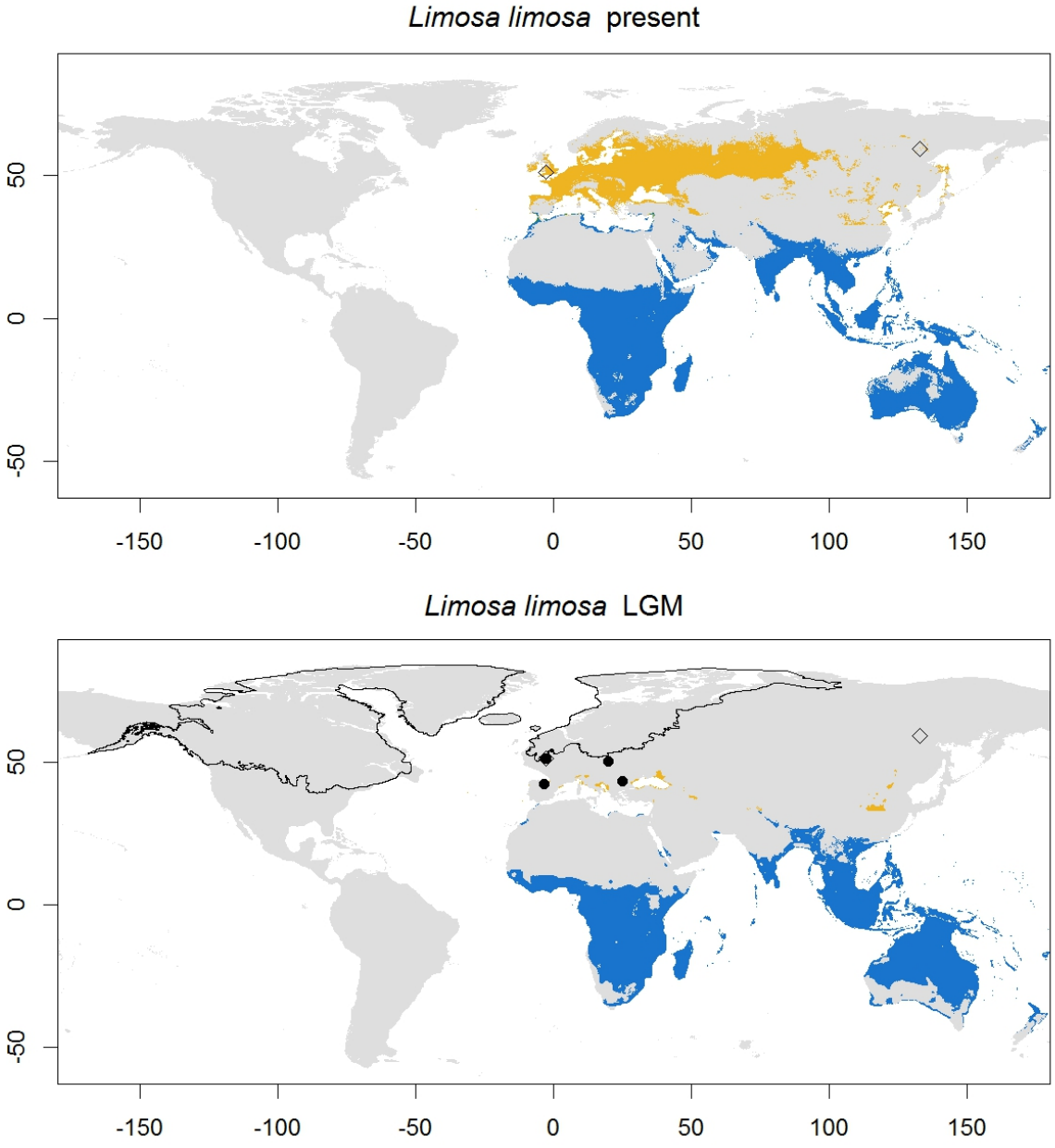

Map 44: Black-tailed Godwit (*Limosa limosa*) predicted distribution. Caption as in map 1.

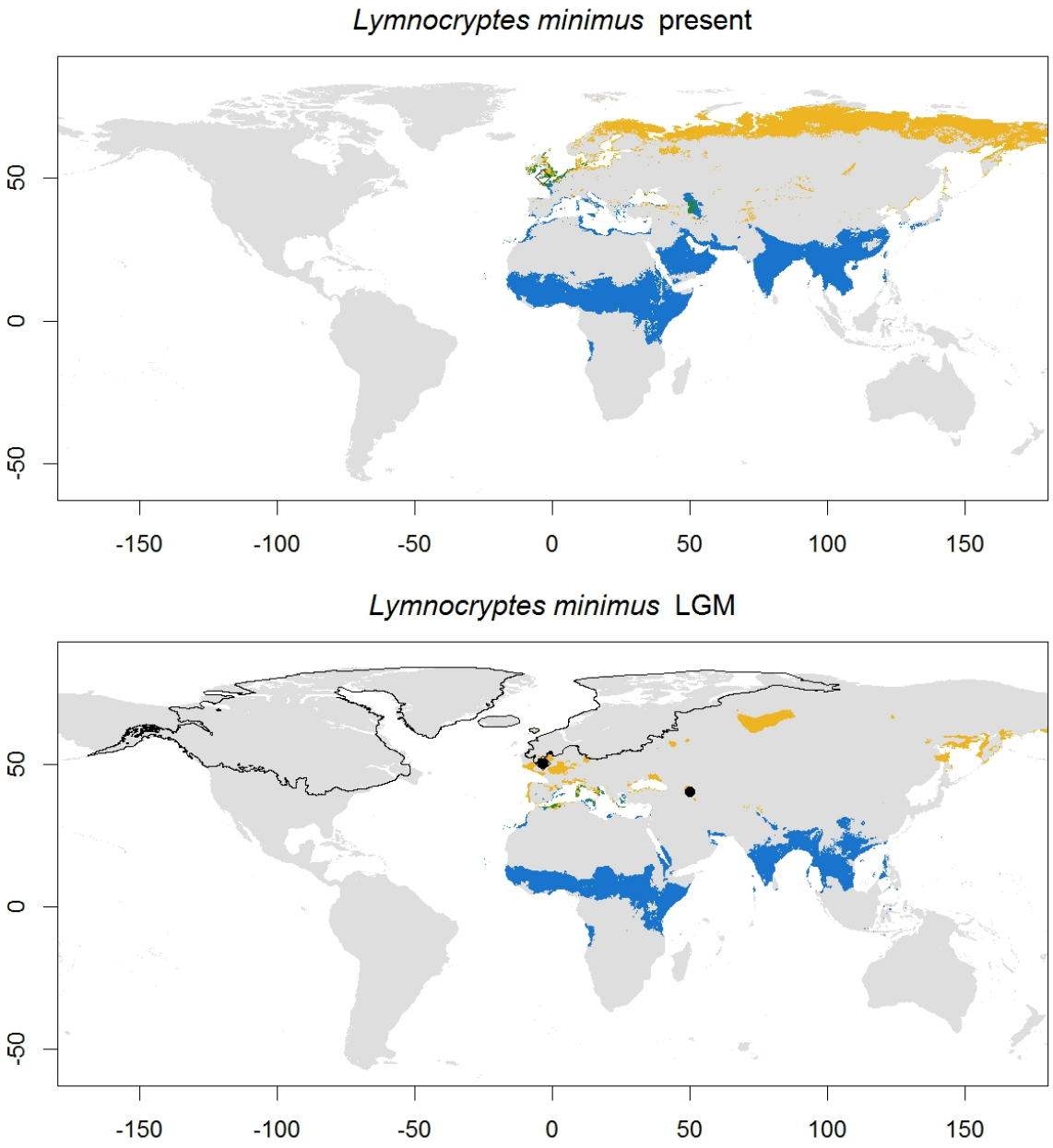

Map 45: Jack Snipe (*Lymnocryptes minimus*) predicted distribution. Caption as in map 1.

Jack Snipe, *Lymnocryptes minimus* (map 45). Monotypic species breeding in Arctic and subarctic latitudes of the Palearctic, from Scandinavia and west Russia to east Siberia. The predictions of the model cover all this breeding range, but also predict the species to reach higher latitudes in northern Russia (e.g. Taymyr, Novaya Zemlya) than its current breeding range suggest. It also under-predicts in the southern part of the breeding range. During the LGM, the model predicts that the species could have occupied suitable breeding areas in southwest Europe and around the Black Sea, in north Siberia near Taymyr, and in northeast Siberia and Kamchatka. The wintering range covers most of western Europe, sub-Saharan Africa and south of Asia. The model fits the

wintering distribution, and during the LGM no significant changes are predicted in this range, except for a decrease in Europe. This species is classified under scenario C.

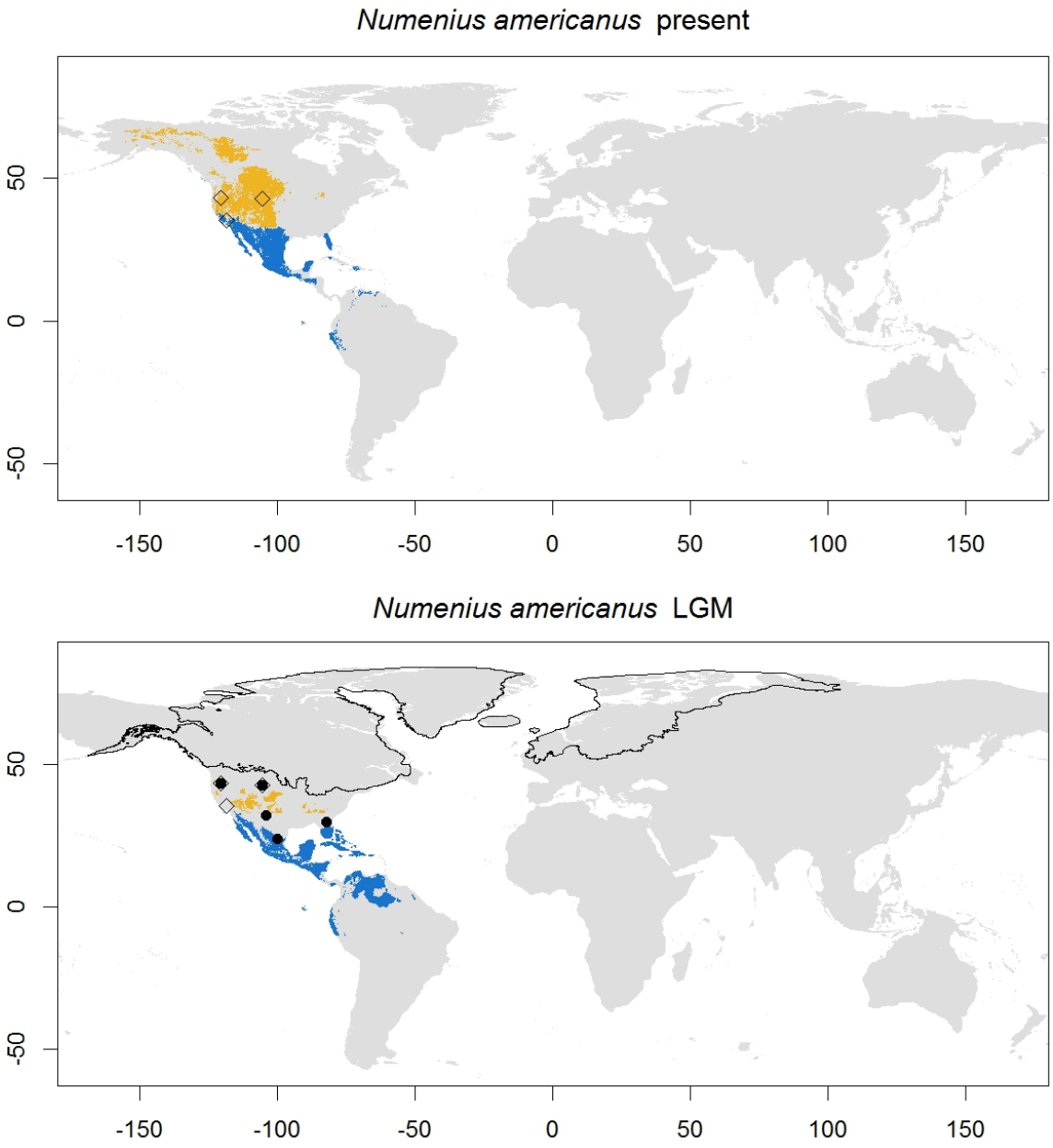

Map 46: Long-billed Curlew (*Numenius americanus*) predicted distribution. Caption as in map 1.

Long-billed Curlew, *Numenius americanus* (map 46). Subarctic and temperate species, breeds in the western half of USA and southwest Canada. Subspecies are not widely recognized. The model predicts all the breeding range correctly, and extends it to areas in Yukon and Alaska. During the LGM, the model predicts low latitude (30°N - 40°N) breeding areas in western North America. The wintering range covers from California to the south of Mexico. The predictions from the model fit that wintering distribution, and also predict suitable areas in Florida and Central America to north of South America. The

predicted wintering range of the species decreased in the northern part and increase towards Central America and South America during the LGM. This species is classified under scenario A.

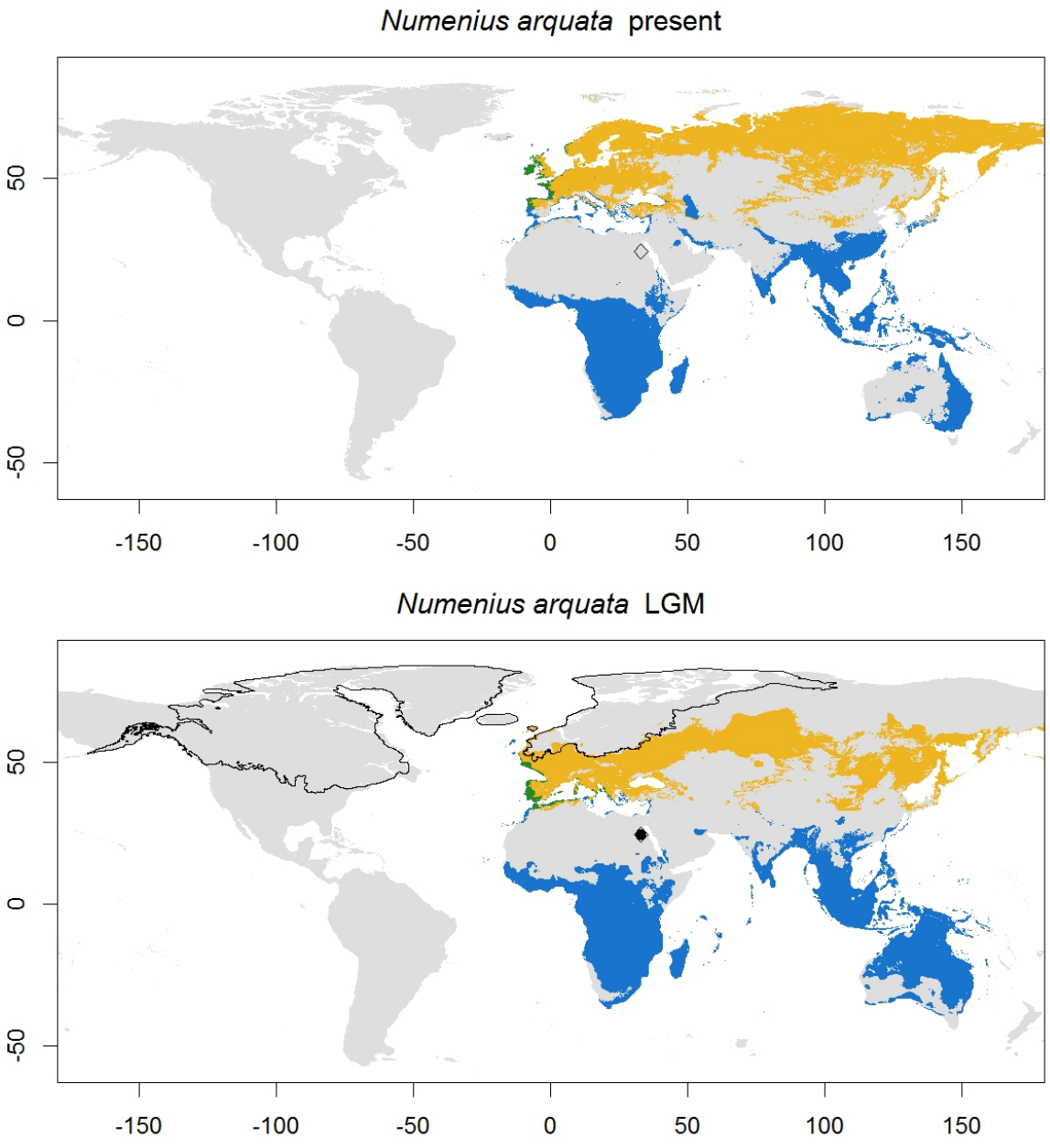

Map 47: Eurasian Curlew (*Numenius arquata*) predicted distribution. Caption as in map 1.

Eurasian Curlew, *Numenius arquata* (map 47). Palearctic species breeding from Scandinavia, the British Islands and western Europe to far east Asia, across Kazakhstan and south Russia. Three identified subspecies: *N. a. arquata* from western Europe to the

Ural Mountains, *N. a. suschkini* between the Urals and Kazakhstan, and *N. a. orientalis* from central Siberia to east Russia. The model predicts a more Arctic breeding distribution, also covering the Palearctic from East to West but at higher latitudes across Siberia to Chukotka and Kamchatka Peninsulas. The prediction in the western Palearctic does fit the breeding distribution correctly, over-predicting only in southern Europe. The LGM model resembles better the current lower-latitude breeding distribution, although the species is predicted to be absent in northern Europe and Scandinavia. As in the current breeding distribution, there is no recognizable separation between the areas of the subspecies during the LGM. The wintering distribution extends though west and southern Europe, Africa, all southern Asia and Indonesia. Our model's predictions fit that wintering distribution, also predicting potential areas in Australia. During the LGM, the wintering range of the species remained similar to the predictions for the present. This species is classified under scenario A.

Far Eastern Curlew, *Numenius madagascariensis* (map 48). Subarctic species, breeds in east Russia, reaching north to northeast Siberia and Kamchatka. No subspecies described. The model predicts the current breeding range correctly, and also some areas of potential breeding distribution in central Asia. According to the SDM, the species kept its current breeding range during the LGM. The wintering range covers the Philippines, Indonesia, New Guinea, Australia and New Zealand. All of these wintering areas are predicted by the model under current conditions, and no major changes are recovered under LGM conditions. This species is classified under scenario A.

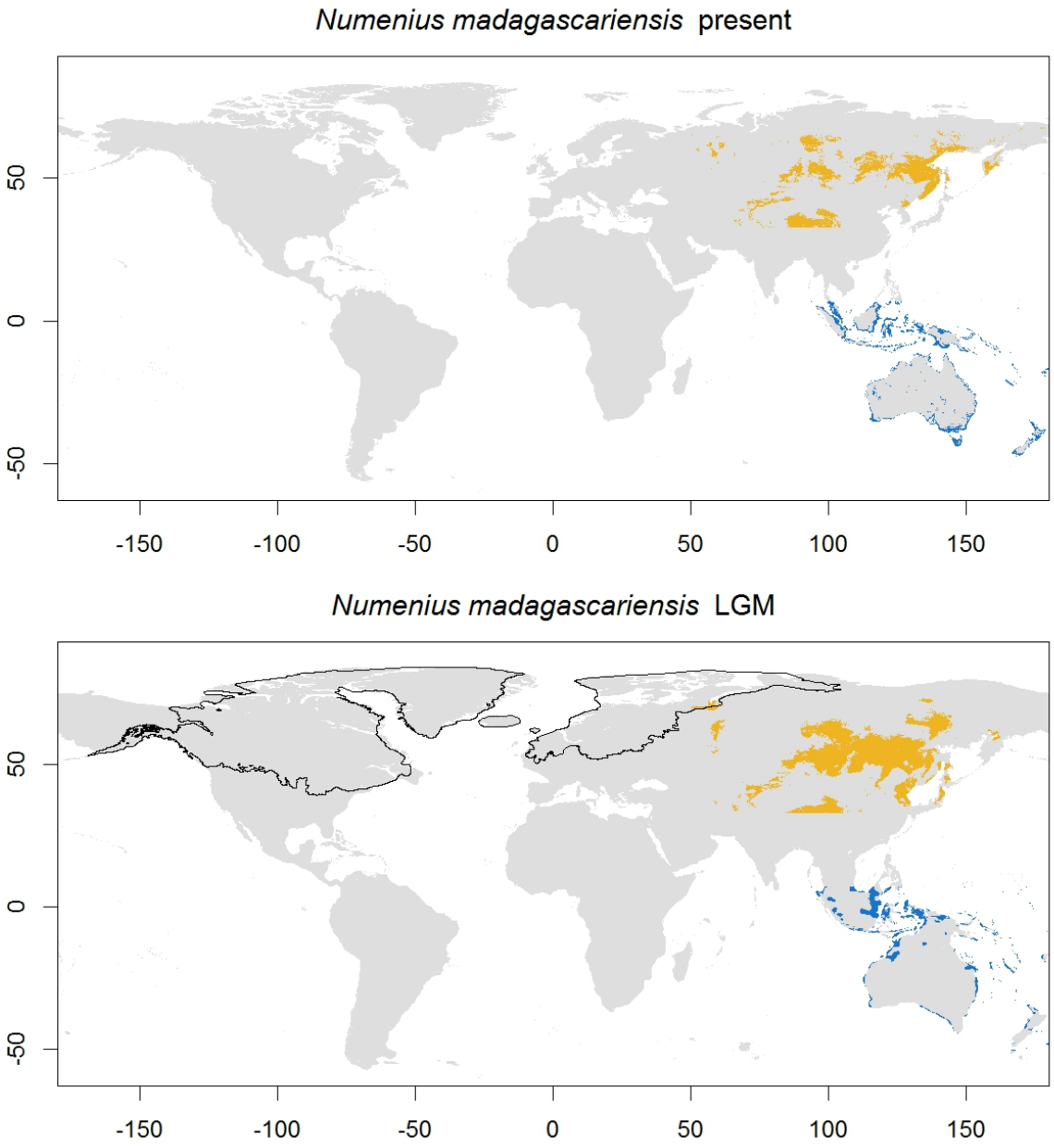

Map 48: Far Eastern Curlew (*Numenius madagascariensis*) predicted distribution. Caption as in map 1.

Little Curlew, *Numenius minutus* (map 49). Breeds in the eastern Palearctic, in a restricted range from the Kolyma River, west beyond the Lena River. No subspecies described. The model predicts not only the breeding distribution of the species, a much larger potential range under current conditions across the whole northern Palearctic. Aside from over predictions in central and western Palearctic, the LGM model predicts large suitable breeding areas in north and east Beringia, which suggest that the species would remained near its current breeding range during the glacial period. The species has its wintering grounds in north Australia, as it is well predicted by the model. During

the LGM, the species would have retained most of that wintering range, also expanding towards emerged land in Indonesia and New Guinea. This species is classified under scenario D.

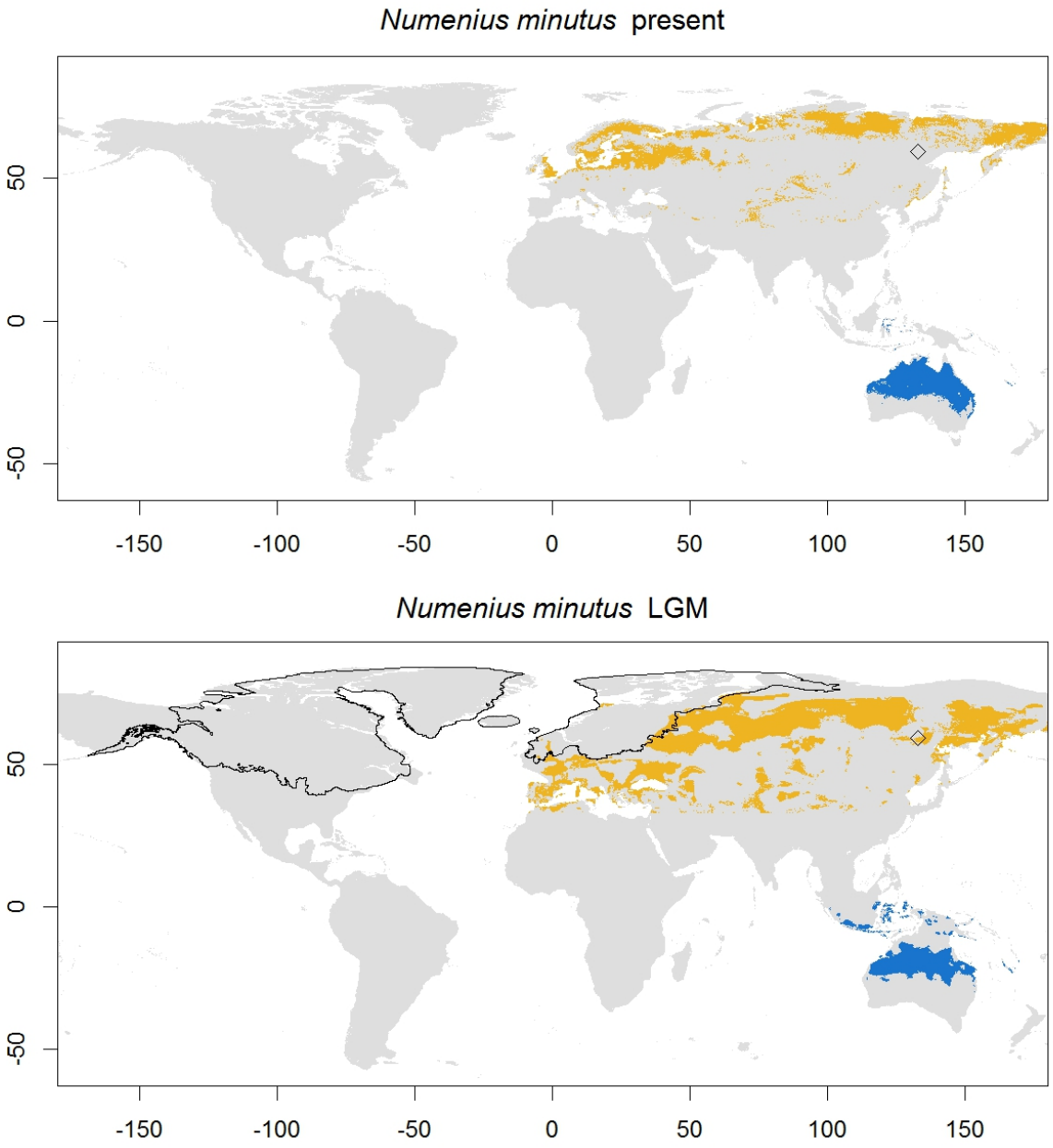

Map 49: Little Curlew (*Numenius minutus*) predicted distribution. Caption as in map 1.

Whimbrel, *Numenius phaeopus* (map 50). Arctic and subarctic species from the Nearctic and the Palearctic. The breeding range is fragmented into several separated

areas and covers Iceland, locally in Greenland, Faeroes and British Islands, Scandinavia and northwest Russia to the Yenisei River, several patches in north and northeast Siberia to Anadyr, Alaska and north of Yukon and Northwest Territories, and the western coast of the Hudson Bay. There are up to seven subspecies described (del Hoyo *et al*., 2018), but recent studies propose a separation of the Nearctic subspecies into its own species, the American whimbrel or Hudsonian Whimbrel, *Numenius hudsonicus* (Humphries *et al*., 2011; Sangster *et al*., 2011). The species of *N. hudsonicus* comprises the two Nearctic subspecies: *N. h. rufiventris* in Alaska and northwest Canada, and *N. h. hudsonicus* in the coast of the Hudson Bay. In the Palearctic, the subspecies *N. p. islandicus* breeds in Iceland and Greenland, *N. p. phaeopus* in Scandinavia, *N. p. alboaxilaris* in the north of the Caspian Sea, *N. p. rogachevae* in central Siberia and *N. p. variegatus* in east Siberia to Anadyr. The SDM predicts all the breeding range of the species, without gaps between populations, and over-predicting in central Europe, north Canada up to Ellesmere west Greenland, and Labrador Peninsula. The LGM model shows a fragmentation of the breeding distribution, with predicted breeding areas in the Palearctic in Iceland, west and south Europe, west Siberia between the Ural Mountains and south of Taymyr, and east Siberia and Kamchatka. The model also predicts potential breeding presence in Beringia, where *N. phaeopus* and *N. hudsonicus* would overlap. The wintering range extends from central North America to the southern tip of South America (except the east coast of the Southern Cone), most of Africa, the Iberian Peninsula, southern Asia and Oceania. Most of that wintering range is predicted by the SDM, although with over predictions in inland areas. During the LGM, the model predicts reductions of the northern and southern margins of the wintering distribution across all continents, maintaining most of its wintering range between the tropics. This species is classified under scenario D.

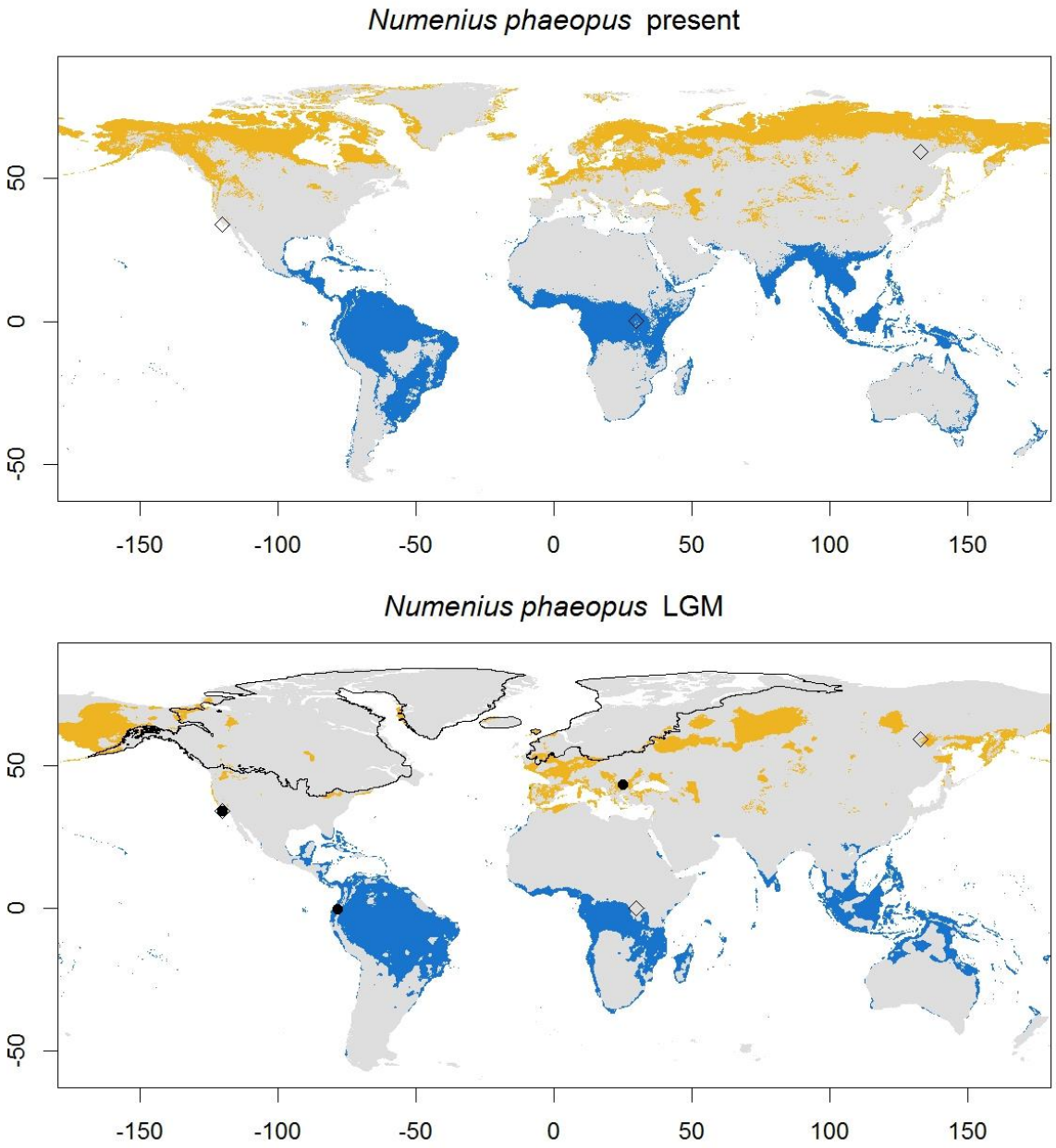

Map 50: Whimbrel (*Numenius phaeopus*) predicted distribution. Caption as in map 1.

Bristle-thighed Curlew, *Numenius tahitiensis* (map 51). Very restricted breeding distribution, just present in the delta of the Yukon River and Seward Peninsula. The SDM predicts breeding localities in the area, although very scarce. It was not possible to predict distinguishable breeding areas under the LGM conditions beyond isolated pixels in Beringia. Wintering range is located in island in the Pacific, and we were unable to successfully train a model to predict its distribution. This species is classified under scenario A.

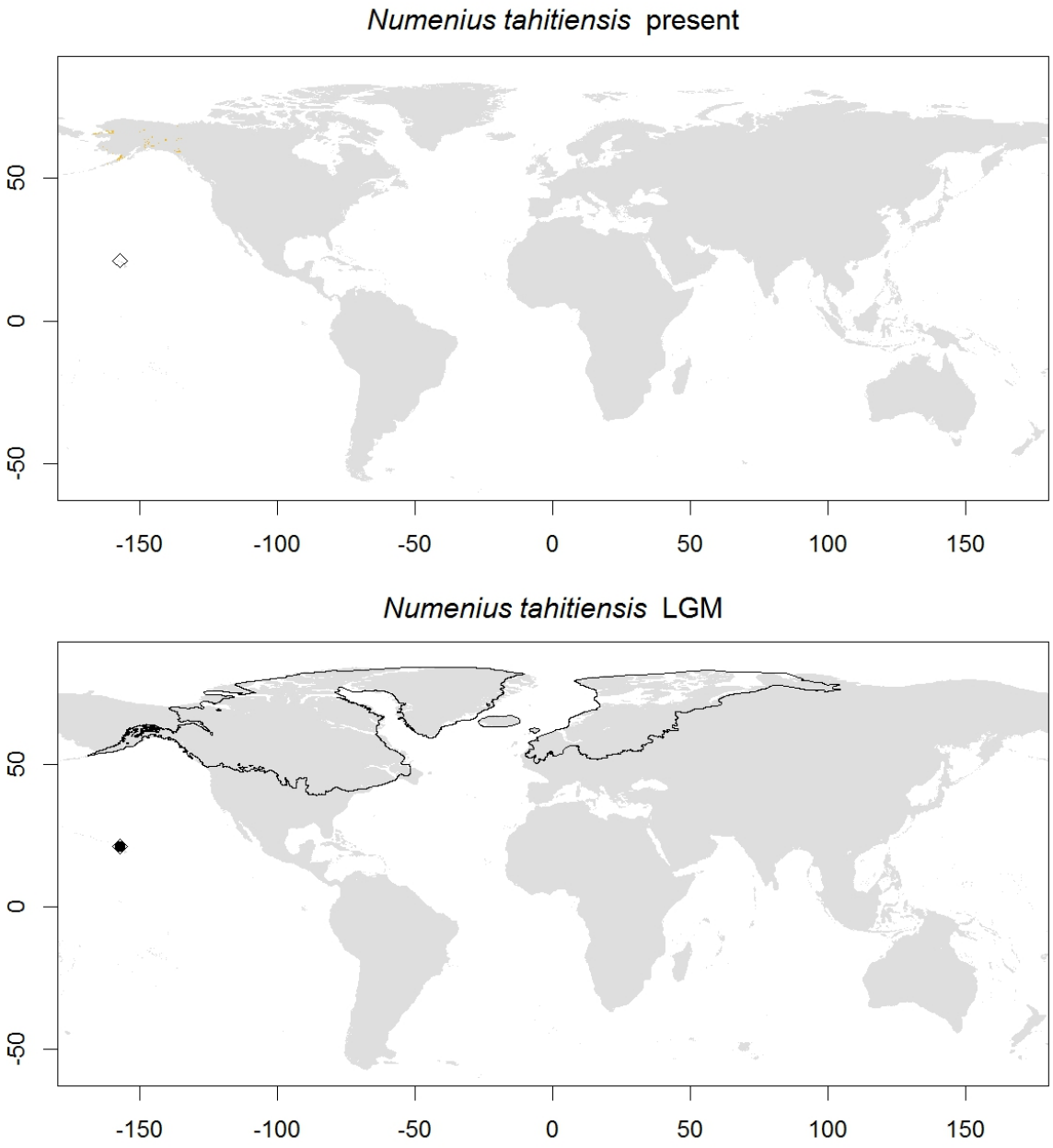

Map 51: Bristle-thighed Curlew (*Numenius tahitiensis*) predicted distribution. Caption as in map 1.

Red Phalarope, *Phalaropus fulicarius* (map 52). Monotypic Arctic breeder that extends from Taymyr to Chukotka Peninsula, from west Alaska to Labrador and Ellesmere Island, and also present in the west coast of Greenland, Svalbard, Novaya Zemlya and New Siberian Islands. The prediction from the SDM fits the breeding range of the species, also predicting in Iceland, north and east coast of Greenland and north Scandinavia. The model for the LGM returns a breeding distribution around eastern Siberia, Beringia and the coast of the Beaufort Sea. The breeding areas predicted in west Siberia and Europe are considered as probable over-predictions The wintering range is pelagic and was

therefore suitable to be included in the models. This species is classified under scenario A.

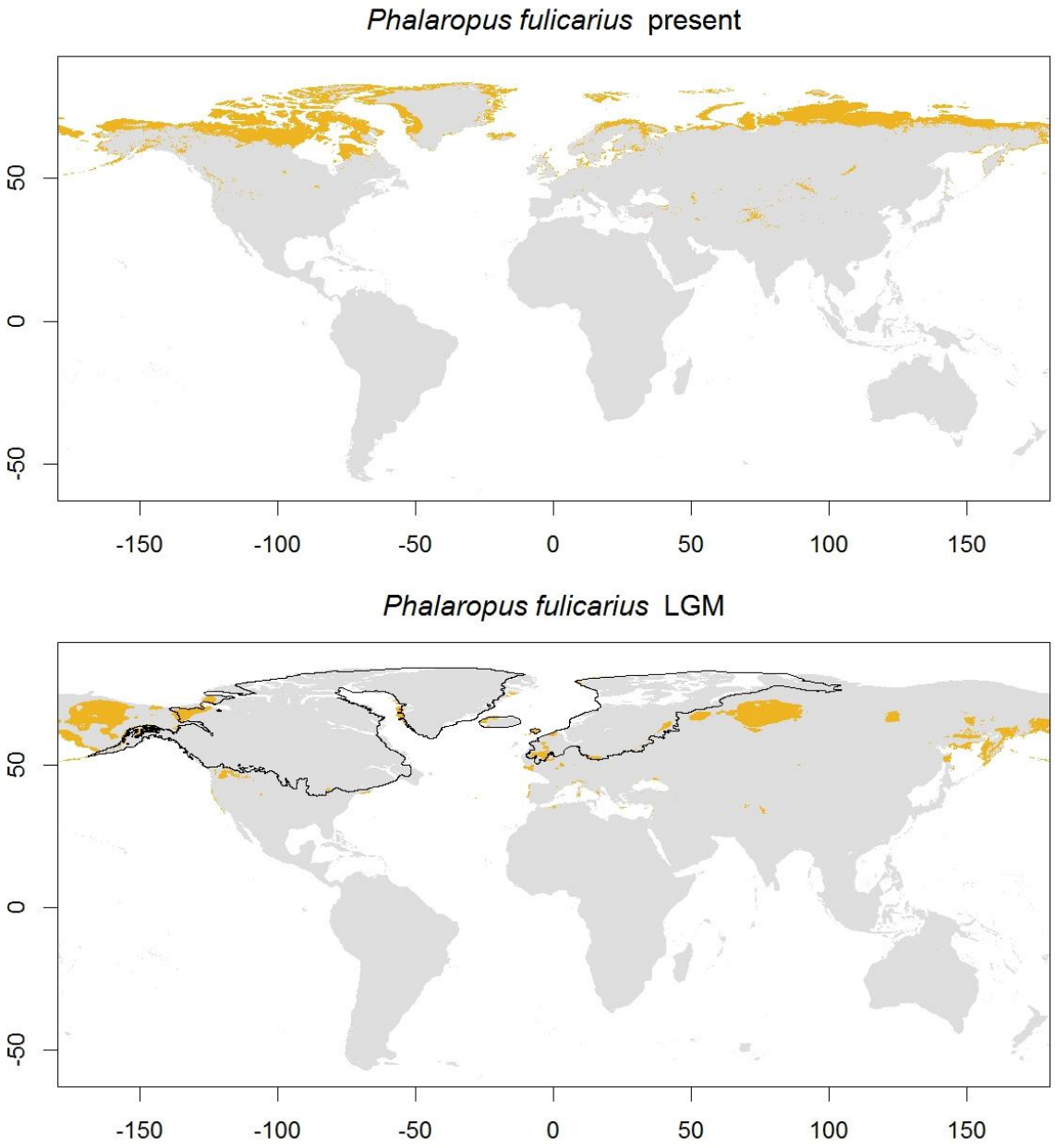

Map 52: Red Phalarope (*Phalaropus fulicarius*) predicted distribution. Caption as in map 1.

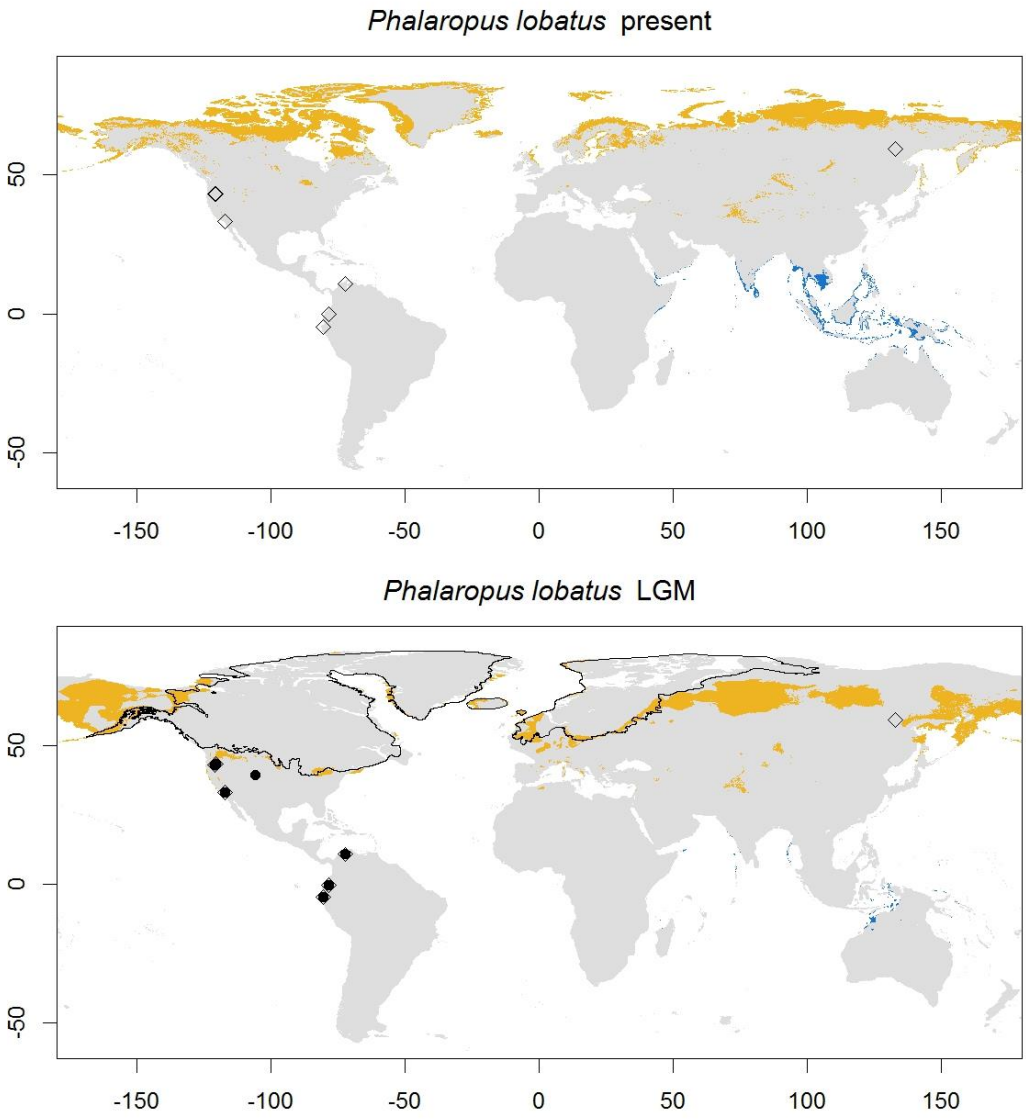

Map 53: Red-necked Phalarope (*Phalaropus lobatus*) predicted distribution. Caption as in map 1.

Red-necked Phalarope, *Phalaropus lobatus* (map 53). Circumpolar species that covers from Alaska to Labrador, including Baffin and Victoria Islands; south of Greenland, Iceland, British Islands, and from Scandinavia to east Siberia and Kamchatka. No variation described. The model fits all the breeding distribution of the species, over-predicting in the Canadian high Arctic, northern Greenland, Svalbard, Novaya Zemlya and Taymyr. During the LGM, the model shows isolated suitable breeding areas across the whole range. In Greenland and Iceland, the species retains most of its current range. In the western Palearctic, it is absent from Scandinavia, but potentially present across Europe, extending northeast to west and central Siberia, and also in northeast Siberia, Kamchatka and Beringia. In the Nearctic the model predicts breeding areas in north

Yukon and also around 40° N in North America. Most of the wintering range is pelagic in tropical oceanic regions, but the SDM managed to successfully predict the species wintering range in the coasts of the Arabian Peninsula, Indonesia and New Guinea, and also predicting coastal areas of India, Indochina and Australia, and failing to predict in the Pacific coast of America. The LGM wintering range is predicted in the same regions but considerably reduced. This species is classified under scenario C.

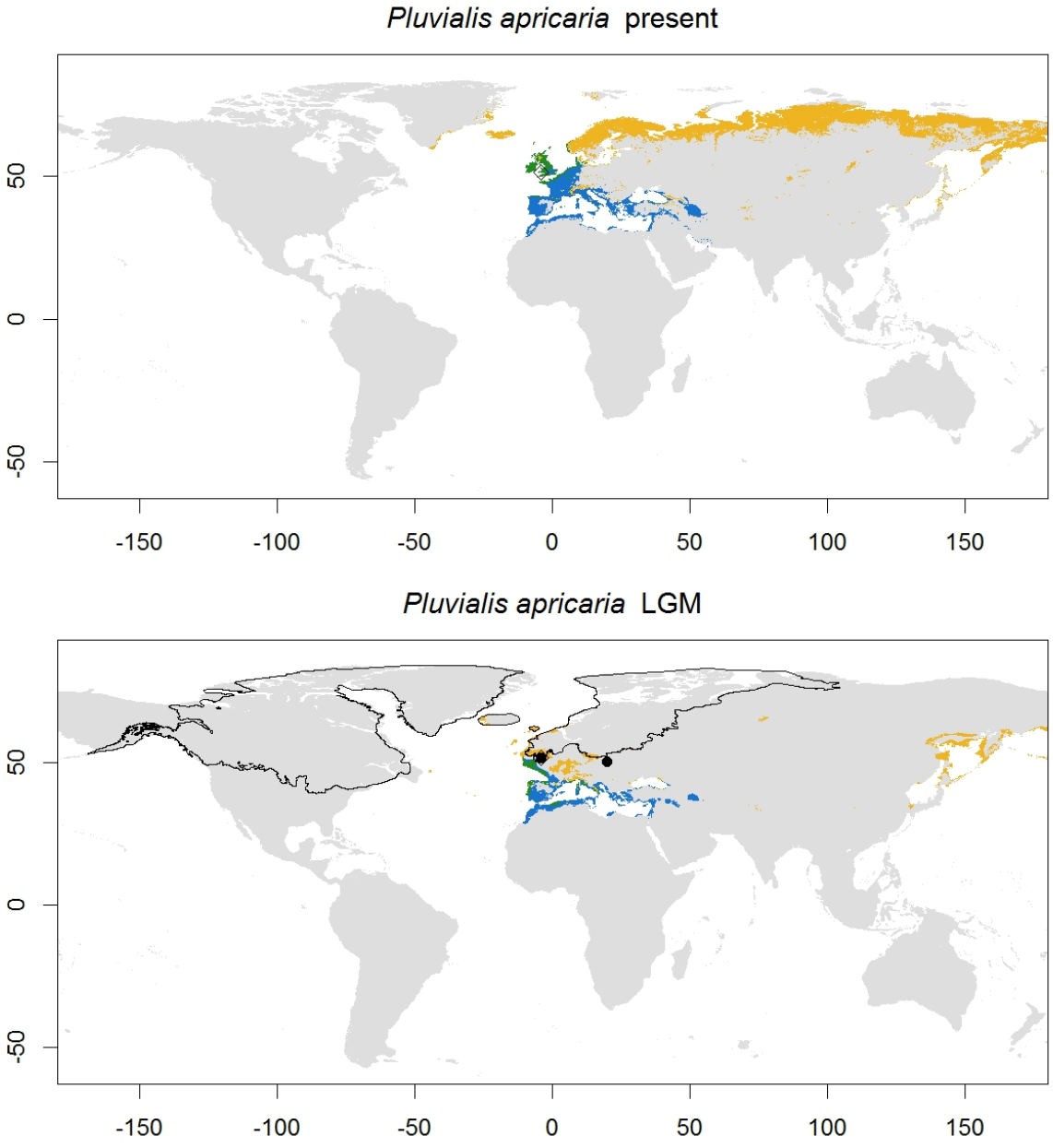

Map 54: Eurasian Golden Plover (*Pluvialis apricaria*) predicted distribution. Caption as in map 1.

Eurasian Golden Plover, *Pluvialis apricaria* (map 54). Breeding distribution from Scandinavia to Taymyr, and also in the British Islands, Faeroes, Iceland and east Greenland. The SDM covers this breeding range and extends the prediction to east

Siberia. Subspecies *P. a. altifrons* covers from Greenland to north Scandinavia, and *P. a. apricaria* the remainder of the continental breeding distribution, as well as the British Islands. The LGM model shows potentially suitable breeding areas in central and western Europe near the breeding range of *P. a. apricaria*, while Iceland and Faeroes retain most of the area currently inhabited by *P. a. altifrons*. The wintering range is very close to the breeding distribution, extending through the Mediterranean and western Europe. The model fits this wintering distribution well, even the overlap of breeding and wintering distributions in the British Islands, where the species is present all year. The wintering distribution remains stable in the LGM conditions, with still some overlap with the breeding distribution in the west of the continent. This species is classified under scenario C.

American Golden Plover, *Pluvialis dominica* (map 55). Nearctic species, breeds from Alaska to Baffin Island. The model predicts this breeding distribution, also reaching Labrador and Ellesmere Island. No variation described. During the LGM the species' breeding range is predicted in Beringia, although some predictions appeared in the east coast of the Canadian Arctic and in central North America. The wintering distribution is in south America, between south Brazil and north Argentina. The model predicts this wintering area, and includes some over-predictions in the east, west and north coasts of the northern part of South America. During the LGM the wintering range of the species is not predicted to change, except for increases in the extent of the over-predicted areas in the model for the present. This species is classified under scenario A.

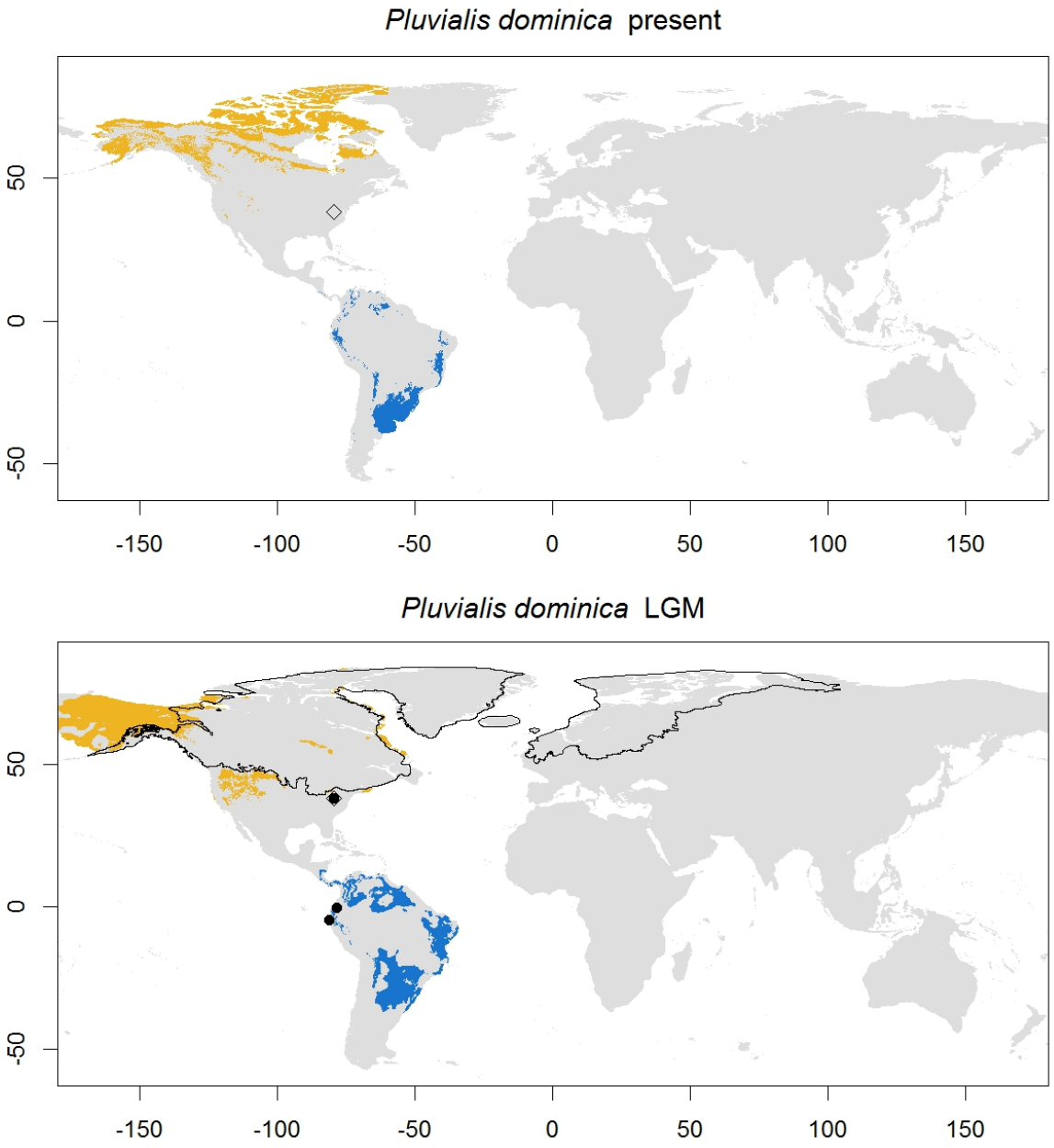

Map 55: American Golden Plover (*Pluvialis dominica*) predicted distribution. Caption as in map 1.

Pacific Golden Plover, *Pluvialis fulva* (map 56). Monotypic species, breeds in the north of the Palearctic from Yamal Peninsula to Chukotka and Kamchatka Peninsulas. The model fits the breeding distribution of the species, with an over-prediction in Novaya Zemlya. During the LGM, the model shows that the species retains most of its current breeding range, shifting slightly to the south. The predicted distribution during the glacial period however is not continuous, as a gap is predicted leaving the eastern part of the distribution isolated in northeast Siberia and Beringia. The wintering distribution is mainly in the south of Asia, Indonesia, Philippines, New Guinea, Australia and New

Zealand. All those wintering areas were predicted by the model. There is a small wintering area in east Africa, that the model fails to predict, although it does predict presence a little more to the south in Mozambique and Madagascar. Most of the wintering range remains unchained in the LGM model, except for decreases in New Zealand, south Australia and India. This species is classified under scenario C.

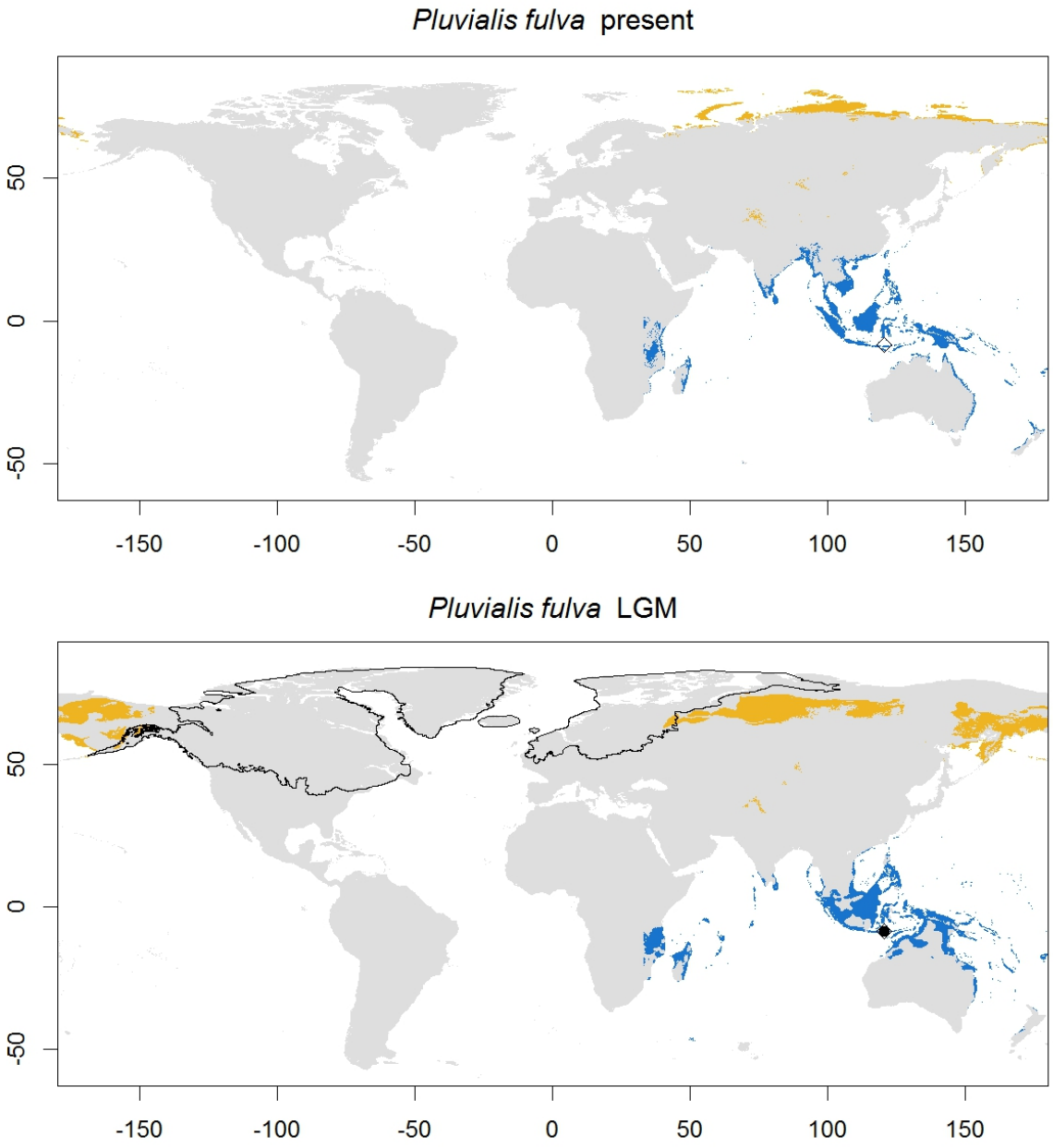

Map 56: Pacific Golden Plover (*Pluvialis fulva*) predicted distribution. Caption as in map 1.

Gray Plover, *Pluvialis squatarola* (map 57). Arctic species distributed along the Palearctic and the Nearctic. In the Palearctic it breeds from northwest Russia and Yamal

Peninsula to Chukotka Peninsula. In the Nearctic it covers east and north Alaska, and most of Nunavut including Victoria and Baffin Islands. Three subspecies recognized: *P. s. squatarola* breeding in the continental area of the Palearctic and Alaska, *P. s. tomkovichi* in Wrangel Island, and *P. s. cynosurae* in the coast and islands of the Canadian Arctic (del Hoyo *et al*., 2018). While the model under current conditions correctly predicts this breedingrange, it also over-predicts some areas where the species is not known to be present, such as Ellesmere Island, Greenland, Iceland, British Islands, Svalbard, northern Scandinavia and Novaya Zemlya. During the LGM the main predicted breeding areas are west Siberia, Kamchatka, Beringia, all of them within the range of *P. s. squatarola*. Very few breeding areas are predicted in central America or near the range of *P. s. cynosurae*. Predictions in western Palearctic and Iceland are likely over-predictions of the model with no informative value.

The species' wintering range extends across coastal areas of North America, Central America, the Caribbean, most of South America (except the southernmost part), Africa, southern and western Europe, southern Asia and Oceania. The model for the current conditions fit this wintering range, with over predictions in the southern tip of South America, New Zealand and inland areas of Africa and Asia. The model for the LGM shows a slight reduction of the northern and southern margins of the wintering range, but overall it remains stable. This species is classified under scenario C.

Eurasian Woodcock, *Scolopax rusticola* (map 58). Subarctic and temperate species breeding in the Palearctic, from the British Islands, western Europe and Scandinavia to east Russia and Japan. No variation described. The model predicts a similar breeding range, although over-predicting in the north across Siberia, and under-predicting in the southern part of the distribution, resulting in a more Arctic distribution than the current range. The model under the conditions of the LGM returns a predicted breeding range much more similar to the current range, except in Scandinavia and northern Europe, where the range of the species is predicted to decrease, and in the south of Europe, where the species shows a potential expansion during this period. The wintering range overlaps the breeding range in western Europe and British Islands, and also cover the Mediterranean, India, Thailand, Myanmar, the south of China, Taiwan, Korea and Japan. The SDM fits this wintering distribution, even predicting the areas of overlap between periods. Under the LGM conditions, the species' wintering range remain near the

breeding range in Europe, and expands southwards in Asia, towards Indonesia and Philippines. This species is classified under scenario A

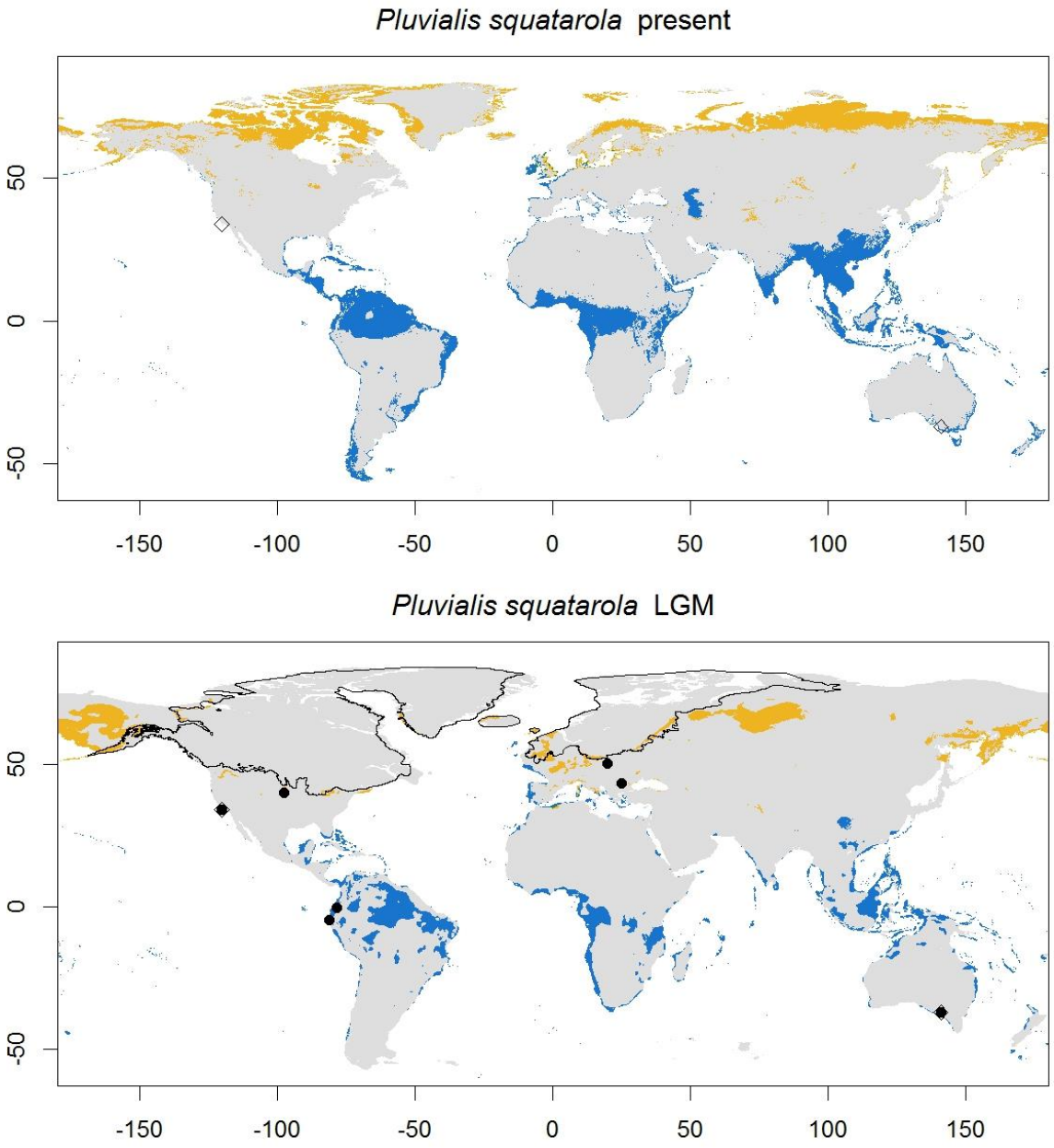

Map 57: Gray Plover (*Pluvialis squatarola*) predicted distribution. Caption as in map 1.

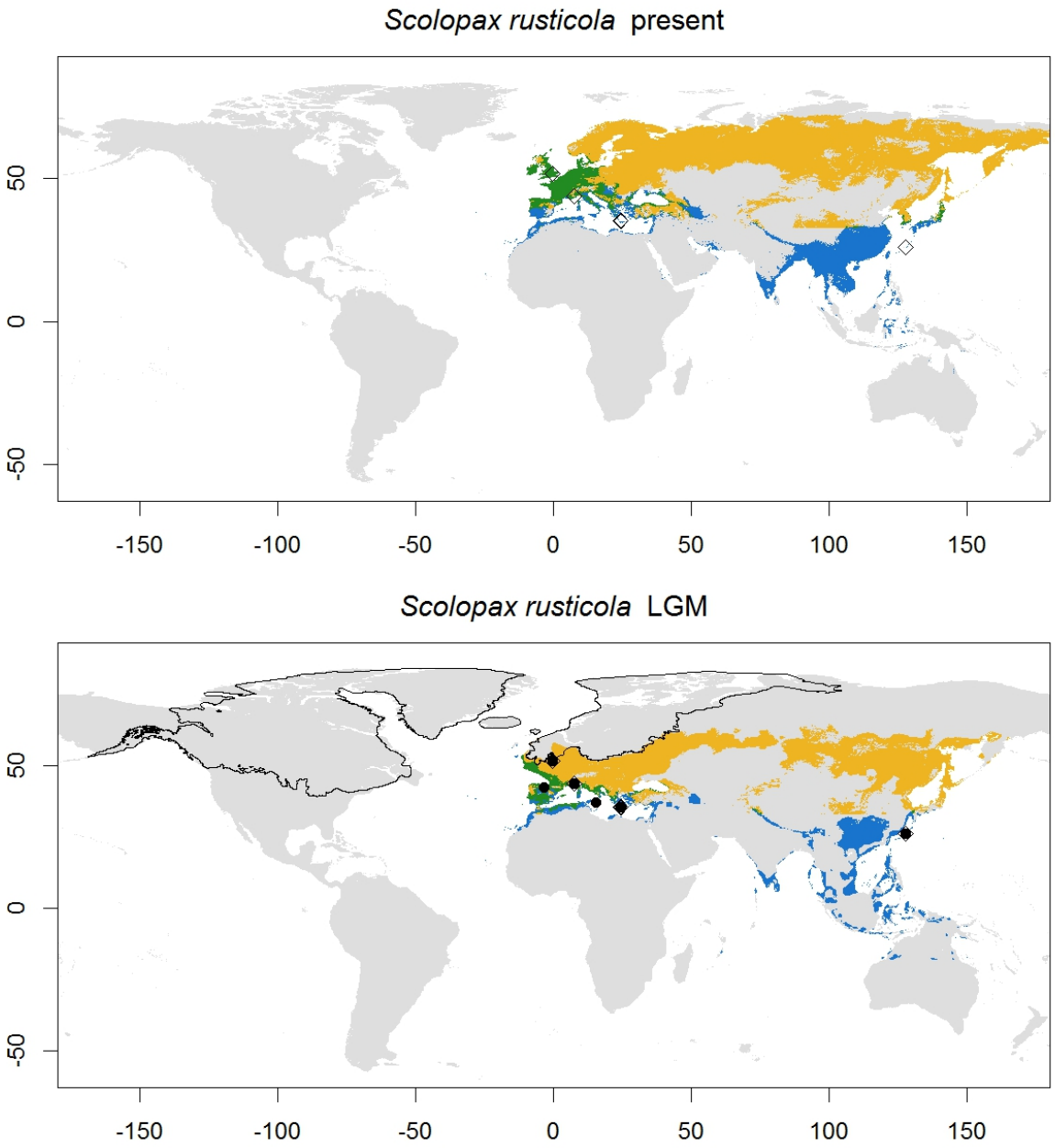

Map 58: Eurasian Woodcock (*Scolopax rusticola*) predicted distribution. Caption as in map 1.

Wilson's Phalarope, *Steganopus tricolor* (map 59). Subarctic species breeding from northwest USA to Alberta and British Columbia, and also around the Great Lakes. No subspecies. The SDM fits the current breeding range and also predicts areas in the Labrador Peninsula and Yukon. Although the LGM predicts a small suitable breeding area in Beringia, most of the distribution of the species is located between 30° N and 40° N across North America, where the species probably found suitable breeding areas during the glacial period. The wintering range covers the southern half of South America, reaching north to Ecuador in the west coast. The model partly predicts this wintering

range, under-predicting in some areas, and extends the prediction to the east coast and also into Central America. These over-predictions increase under the LGM conditions, with the species almost completely disappearing from the southern part of the wintering distribution. This species is classified under scenario A.

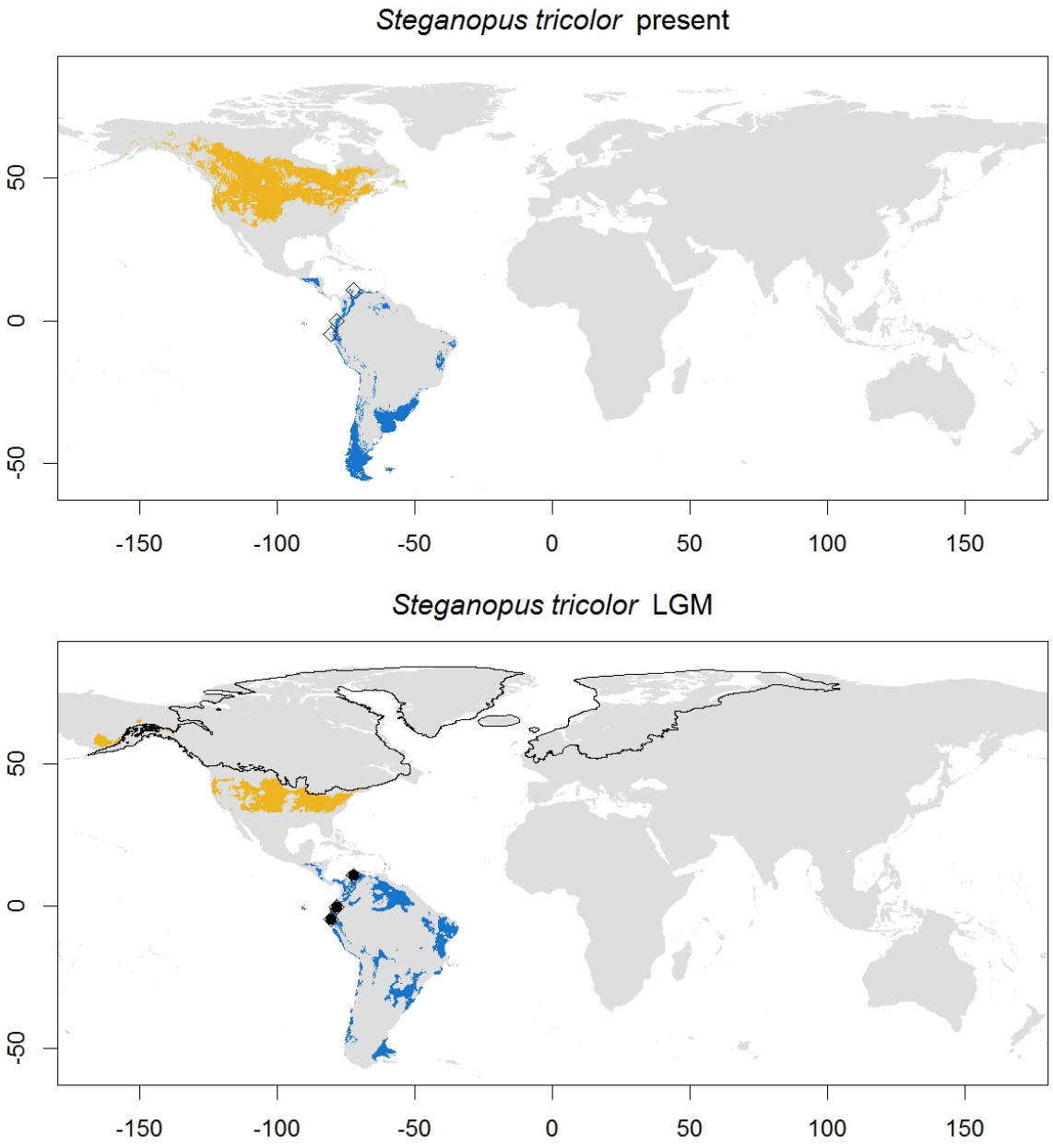

Map 59: Wilson's Phalarope (*Steganopus tricolor*) predicted distribution. Caption as in map 1.

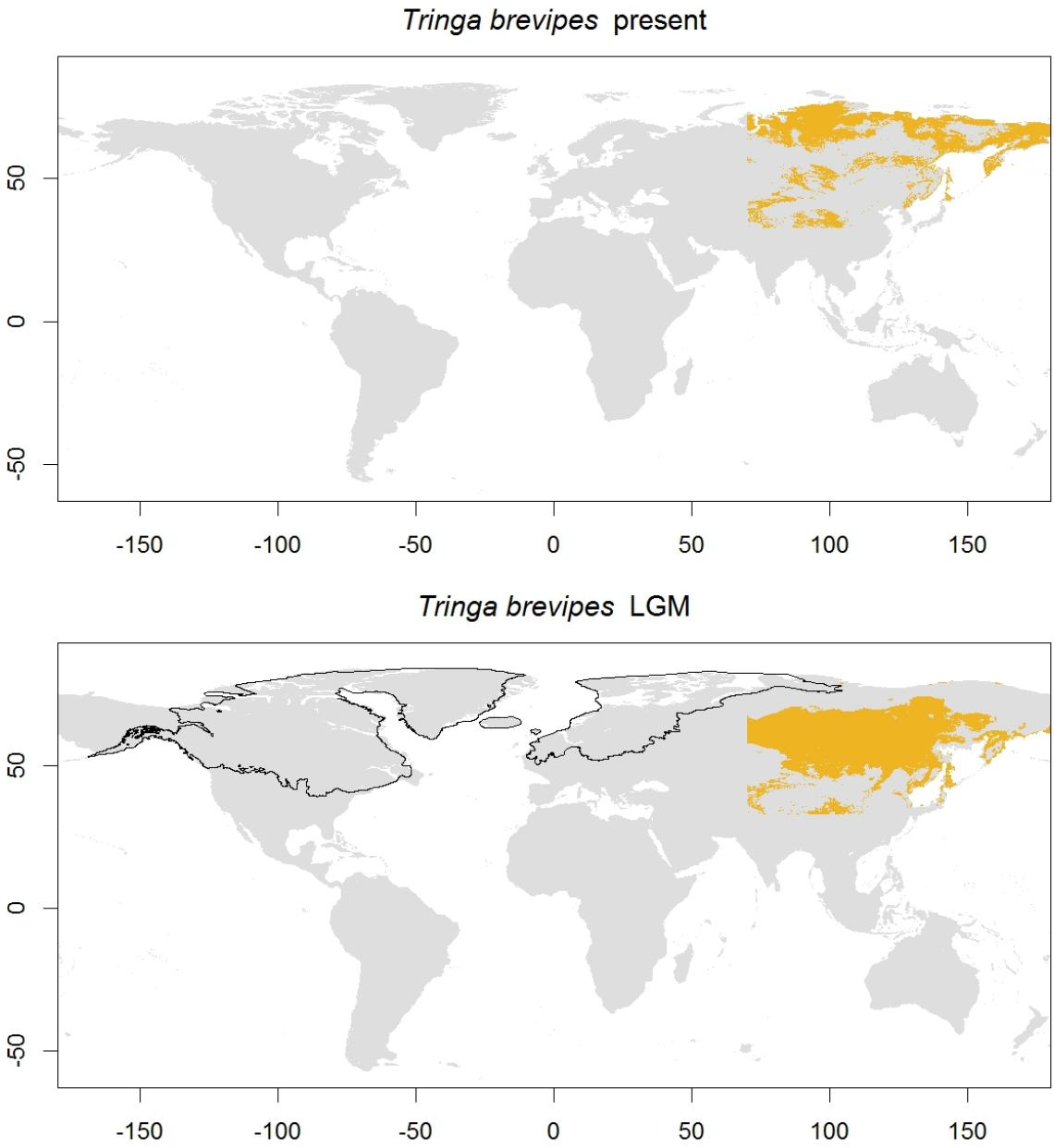

Map 60: Gray-tailed Tattler (*Tringa brevipes*) predicted distribution. Caption as in map 1.

Gray-tailed Tattler, *Tringa brevipes* (map 60). Monotypic species, breeds in northeast Siberia and Kamchatka, and also in south of Taymyr isolated from the rest of the distribution. The SDM predicts all the breeding distribution of the species but as a continuous range, over-predicting in the north of Taymyr and the northern coast of Siberia, as well as in some areas of central Asia. The breeding range is predicted at lower latitudes (between 40° N – 65° N) under the LGM conditions, but still covering a large area of Siberia, reaching Kamchatka in the east. The wintering range is distributed along the coast of Indonesia, New Guinea and Australia. The SDM fits this wintering range,

although with few predictions in Australia, and potential areas in Indochina. The wintering range, although with a smaller amount of available area, is predicted to remain stable under the LGM conditions. This species is classified under scenario B.

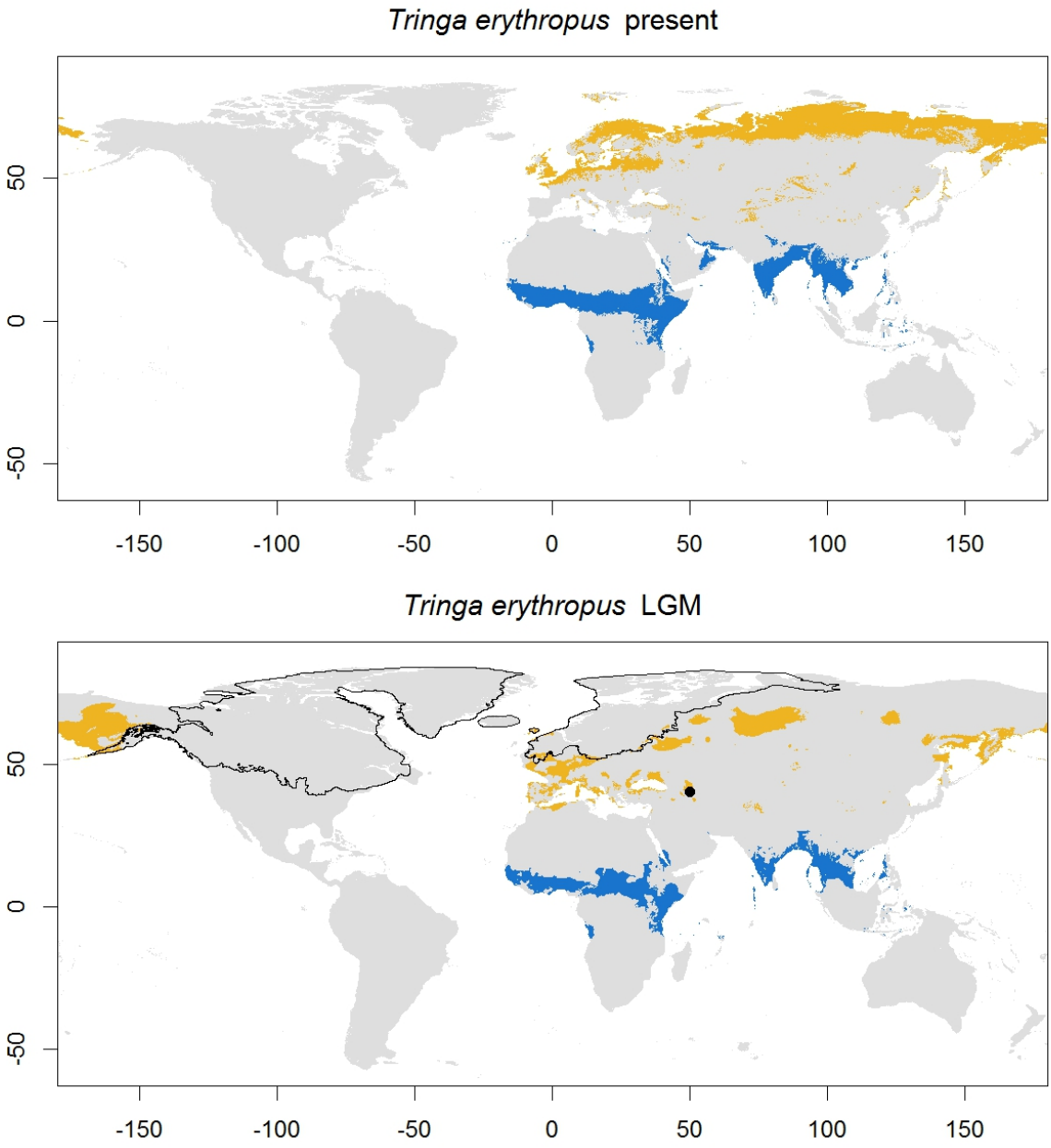

Map 61: Spotted Redshank (*Tringa erythropus*) predicted distribution. Caption as in map 1.

Spotted Redshank, *Tringa erythropus* (map 61). Palearctic species breeding from Scandinavia to northeast Siberia except in the north of Taymyr. No subspecies described. The SDM fits the breeding distribution of the species, with over-predictions in Svalbard, Novaya Zemlya, north of Taymyr, New Siberian Islands and Kamchatka Breeding range

predictions also extend to central Europe and the British Islands, coinciding with some areas where the species is present during the non – breeding season. The model under LGM conditions predicted disconnected breeding areas in western Europe and the Mediterranean coast (where the species is currently present during the winter), central Siberia, around the Kamchatka Peninsula and in Beringia. The wintering range covers most of south Asia, the Arabian Peninsula and sub-Saharan Africa and the northern Coast, and locally in south and west Europe. The model predicts all of these wintering areas except for those around the Mediterranean and Europe, which are actually predicted by the breeding model. The LGM model showed no significant changes in the wintering range during that period. This species is classified under scenario C.

Lesser Yellowlegs, *Tringa flavipes* (map 62). Monotypic species breeding in the Nearctic, from Alaska to central Canada and the Hudson Bay. The model under current conditions fits the breeding distribution of the species, over-predicting in south Nunavut, including Victoria and Baffin Islands. The LGM model predicts that the species' breeding distribution was restricted almost entirely to central Beringia. During the wintering season, the species is present in South America, Central America, the Caribbean and the south of North America. The model predicts all these wintering areas correctly, under-predicting in the Amazonian region and the Andes. During the LGM, the model predicts a reduction of the species wintering range in the northern and southern margins, remaining stable in Central America and the northern half of South America. This species is classified under scenario A.

Wood Sandpiper, *Tringa glareola* (map 63). Palearctic species breeding from the British Islands and Scandinavia to northeast Siberia and Kamchatka, not reaching the northernmost part of central Siberia. No variation described. Our model predicts all the breeding range of the species, and also over-predicts in central and western Europe, Taymyr, Chukotka Peninsula and north of Japan. During the LGM, the species' predicted breeding range covers wide range across the Palearctic, below 60° N in Siberia. In the western Palearctic, the breeding range is predicted in central Europe and the Mediterranean, matching areas where the species is currently wintering. The wintering range also covers most of Africa, Madagascar and from the south of Asia to Australia. All the wintering range is well predicted by the model, except for the Mediterranean small areas. Under LGM conditions, the model shows very little change in the predicted

wintering range of the species, decreasing mostly in the southern half of Africa but remaining stable overall. This species is classified under scenario A.

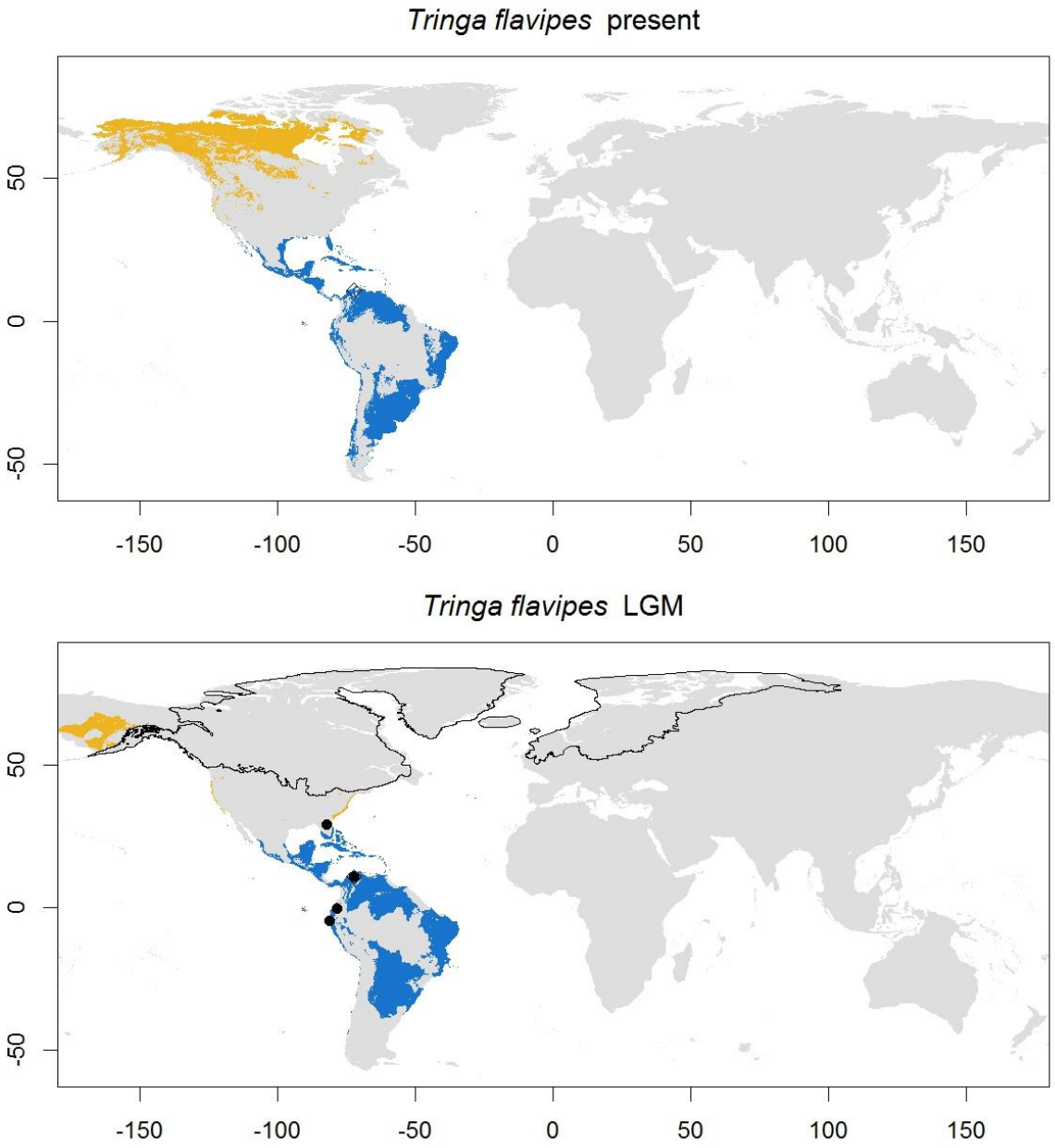

Map 62: Lesser Yellowlegs (*Tringa flavipes*) predicted distribution. Caption as in map 1.

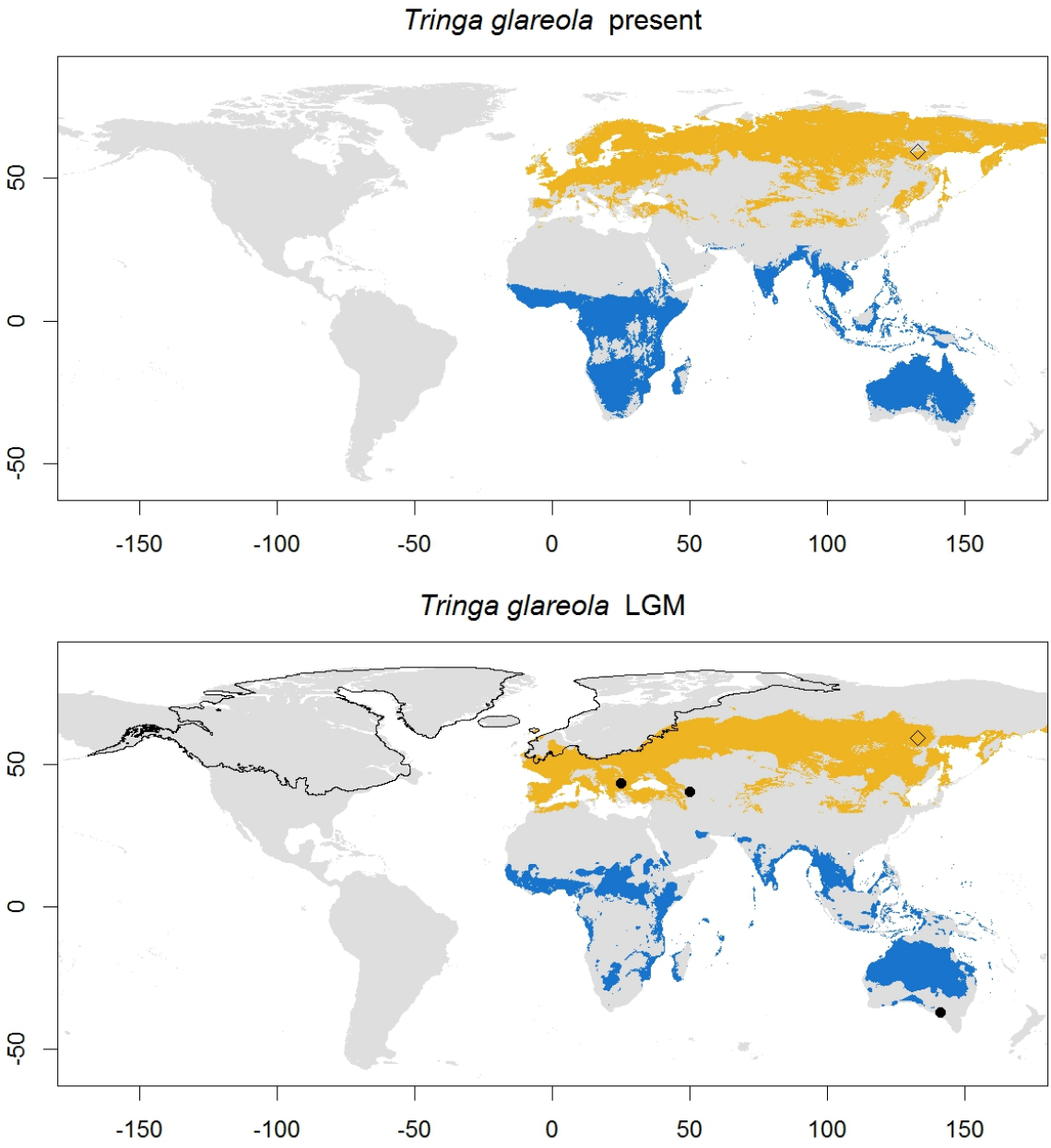

Map 63: Wood Sandpiper (*Tringa glareola*) predicted distribution. Caption as in map 1.

Wandering Tattler, *Tringa incana* (map 64). Arctic and subarctic species, the breeding grounds are across Alaska, part of British Columbia and Yukon, and the Chukotka Peninsula. No variation described. The SDM model fits the breeding distribution, but over-predicts in the northern part of Alaska and extends the potential breeding range towards the Northwest Territories, the north of Labrador and south of Baffin Island. During the LGM, the species breeding distribution is predicted in the area of Beringia, although some predictions recovered in central North America. The wintering range extends strictly along the west coast of America, from California to north Chile. Our

model, however, predicts the potential wintering range to extend further south, reaching Patagonia, and also along the east coast of Central America and South America to Brazil. The LGM model shows a reduction of the predicted wintering area in the southernmost part of South America, but remains overall stable especially in the area that fits the current distribution. This species is classified under scenario A.

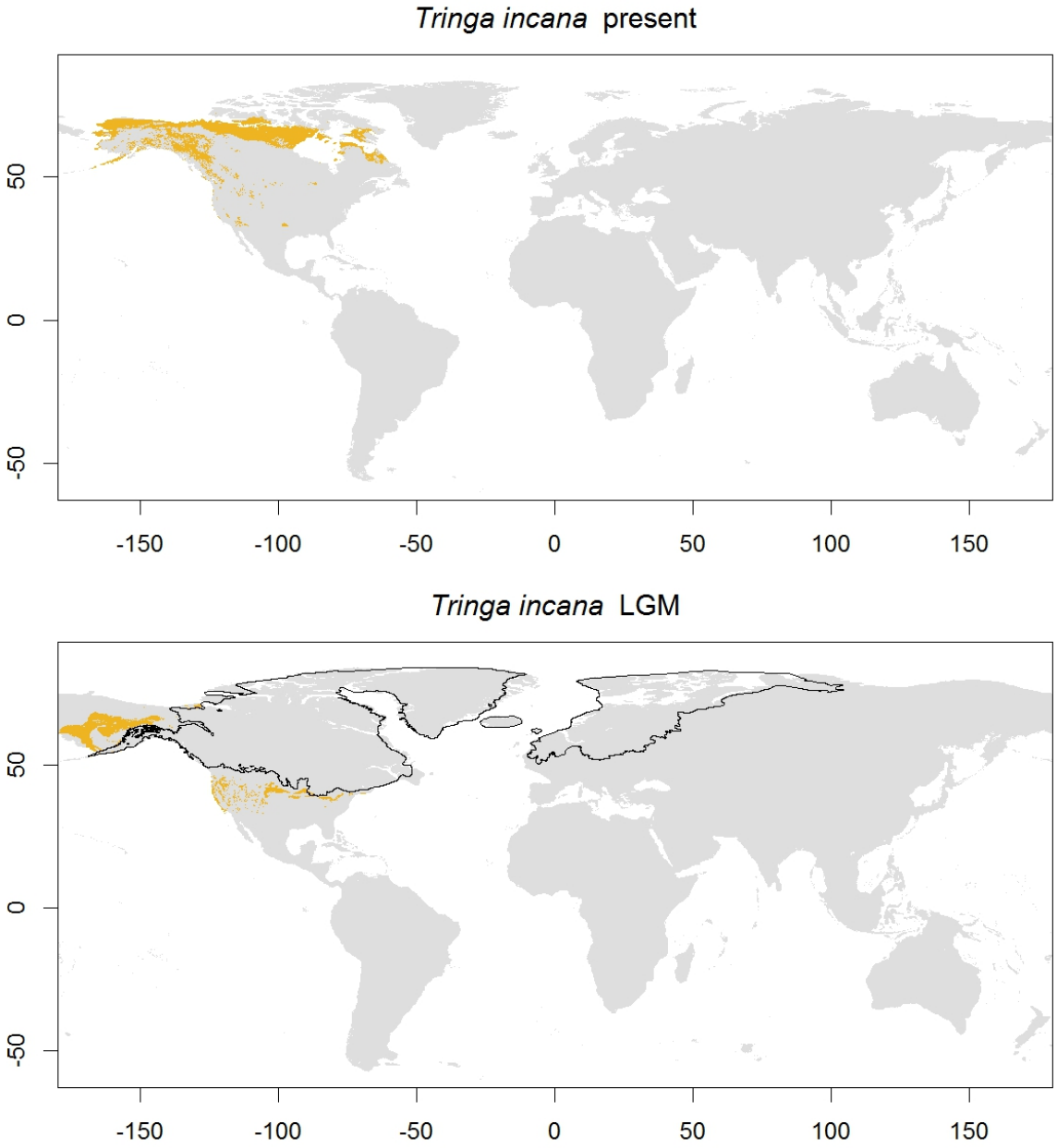

Map 64: Wandering Tattler (*Tringa incana*) predicted distribution. Caption as in map 1.

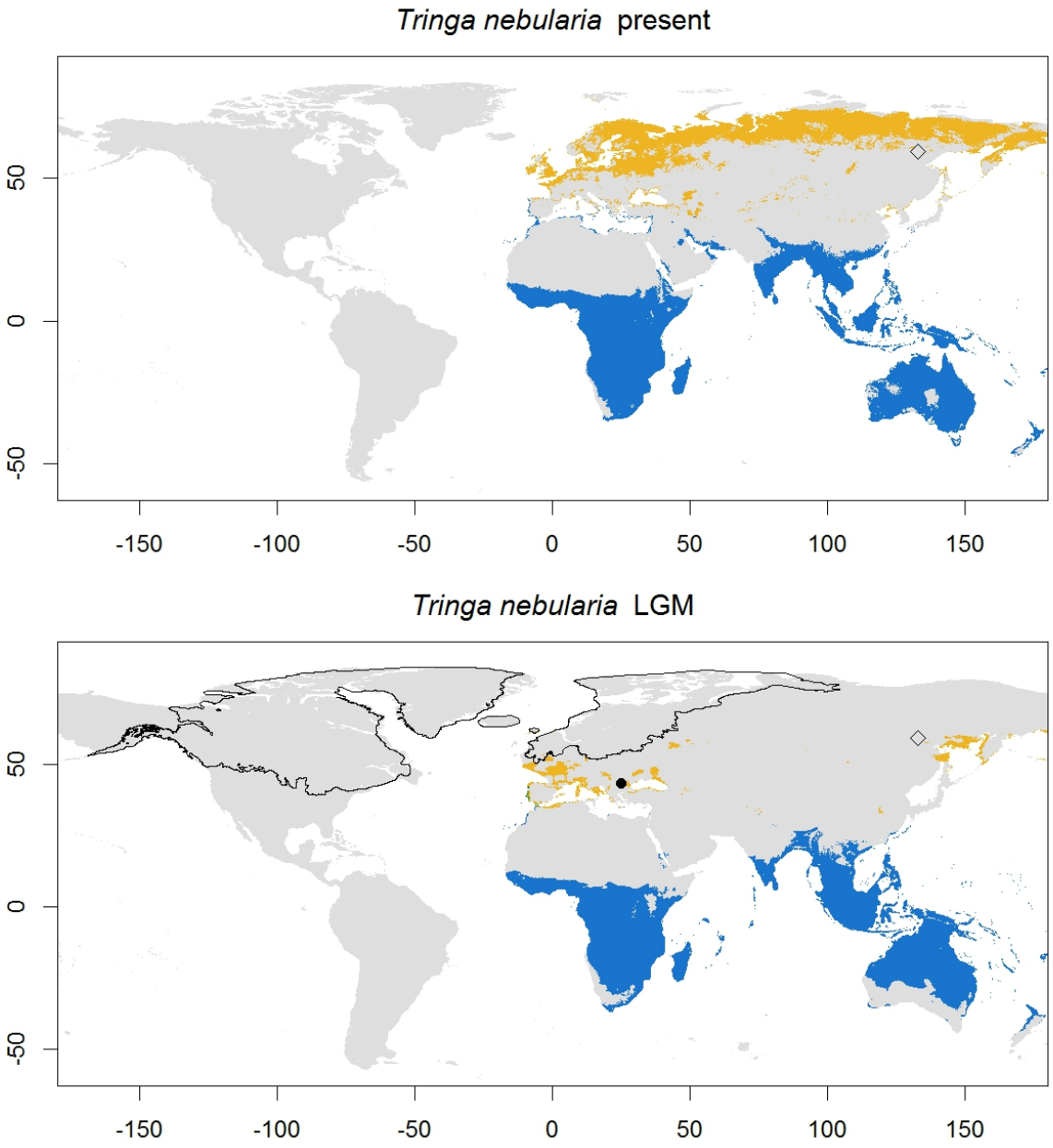

Map 65: Common Greenshank (*Tringa nebularia*) predicted distribution. Caption as in map 1.

Common Greenshank, *Tringa nebularia* (map 65). Palearctic species, its breeding distribution covers from the British Islands and Scandinavia to east Russia and Kamchatka. No subspecies described, and the race *glottoides* proposed for the eastern populations had not been accepted (del Hoyo *et al*., 2018). The SDM predicts a potential breeding range occupying higher latitudes in Siberia, reaching Taymyr and the East Siberian Sea, and under-predicts the southern part of the range in Asia. The LGM model shows two isolated breeding areas: one in the western Palearctic across west and south Europe and the Black Sea, and another in the eastern Palearctic around the Sea of

Okhotsk and Kamchatka. The wintering range covers western Europe, the Mediterranean region, all of sub-Saharan Africa, and from the south of Asia to Oceania. The model correctly predicts these wintering areas, and shows no significant changes under the LGM conditions. This species is classified under scenario C.

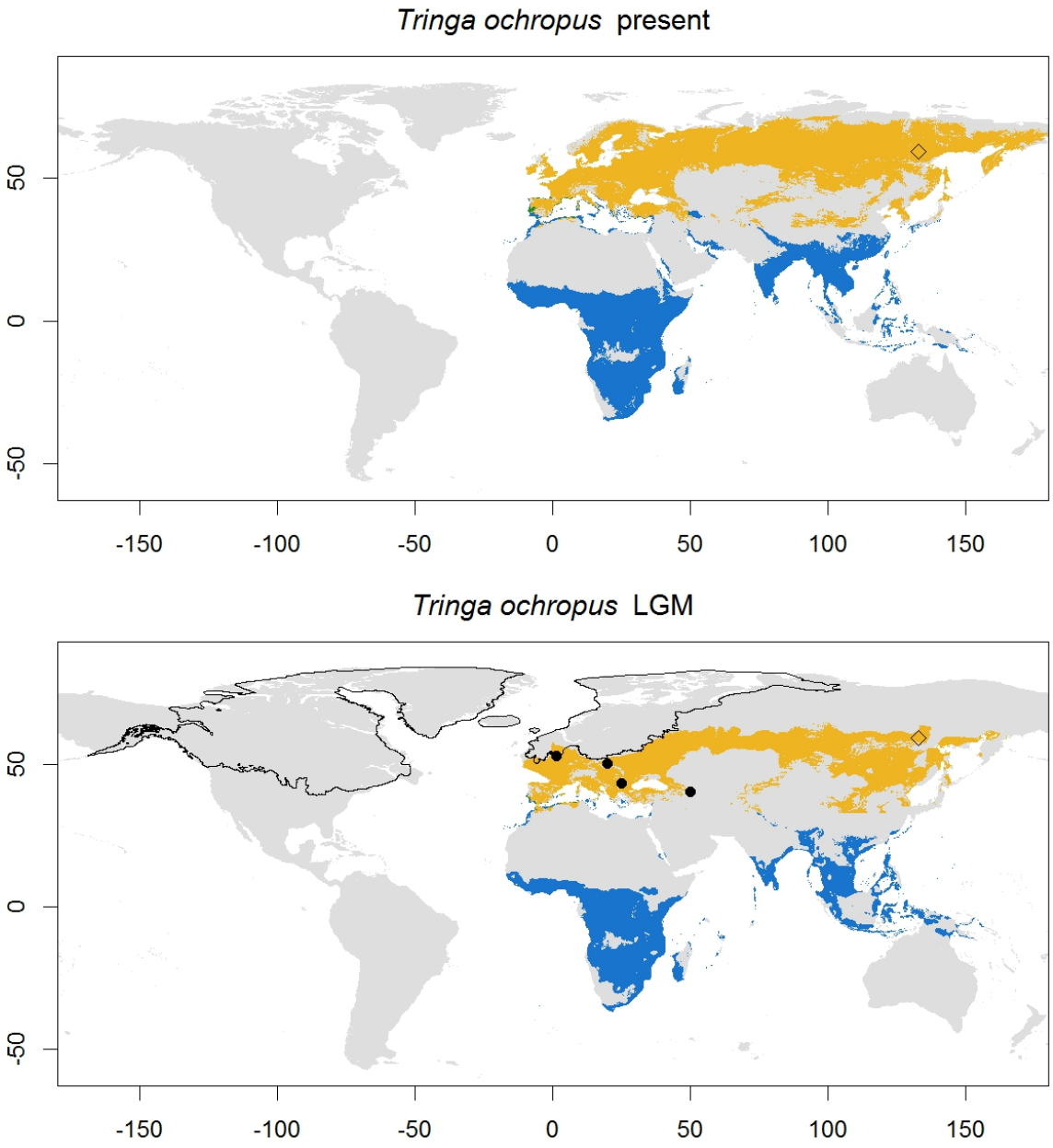

Map 66: Green Sandpiper (*Tringa ochropus*) predicted distribution. Caption as in map 1.

Green Sandpiper, *Tringa ochropus* (map 66). Monotypic species breeding in the Palearctic, from central Europe and Scandinavia to far east Russia across central Asia and south Siberia. The SDM covers all this breeding range and extends it in northeast

Siberia, and also predicts presence in western Europe and the British Islands, where the species occurs now during the wintering season. The LGM model predicts a decrease of the northern part of the breeding range, especially in the western Palearctic, but remaining overall stable during this period. The wintering range covers the mentioned parts of Europe, as well as the Mediterranean basin, sub-Saharan and inter-tropical Africa, south of Asia, Indonesia and Philippines. The model fits this wintering distribution, with over-predictions in Madagascar and New Guinea. Under the LGM conditions the wintering area decreases in the Mediterranean, which is occupied by predicted breeding distribution, but remains stable everywhere else, expanding into the emerged land between the islands of Indonesia. This species is classified under scenario A.

Solitary Sandpiper, *Tringa solitaria* (map 67). Nearctic species, breeding range covers from Alaska to the Labrador Peninsula across Yukon, British Columbia, Northwest Territories and south Canada. Two recognized species, *T. s. cinnamomea* in Alaska and northwest Canada, and *T. s. solitaria* in south Canada, from south British Columbia to Labrador Peninsula. The SDM fits well the breeding distribution of the species, although with less area predicted in west Alaska and central Canada. Under the LGM conditions, the SDM show a clear split of the breeding distribution, with a predicted area in Beringia near the current range of *T. s. cinnamomea*, another in the west coast of North America, reaching north up to British Columbia, and a third one in central north America at around 40°N, the latter two being a potentially southern refugia for *T. s. solitaria*. The wintering range covers the centre and north of South America, all of Central America, the Caribbean and the south of North America. This wintering range is also well predicted by the SDM, which shows a slight decrease in North America during the LGM period. This species is classified under scenario C.

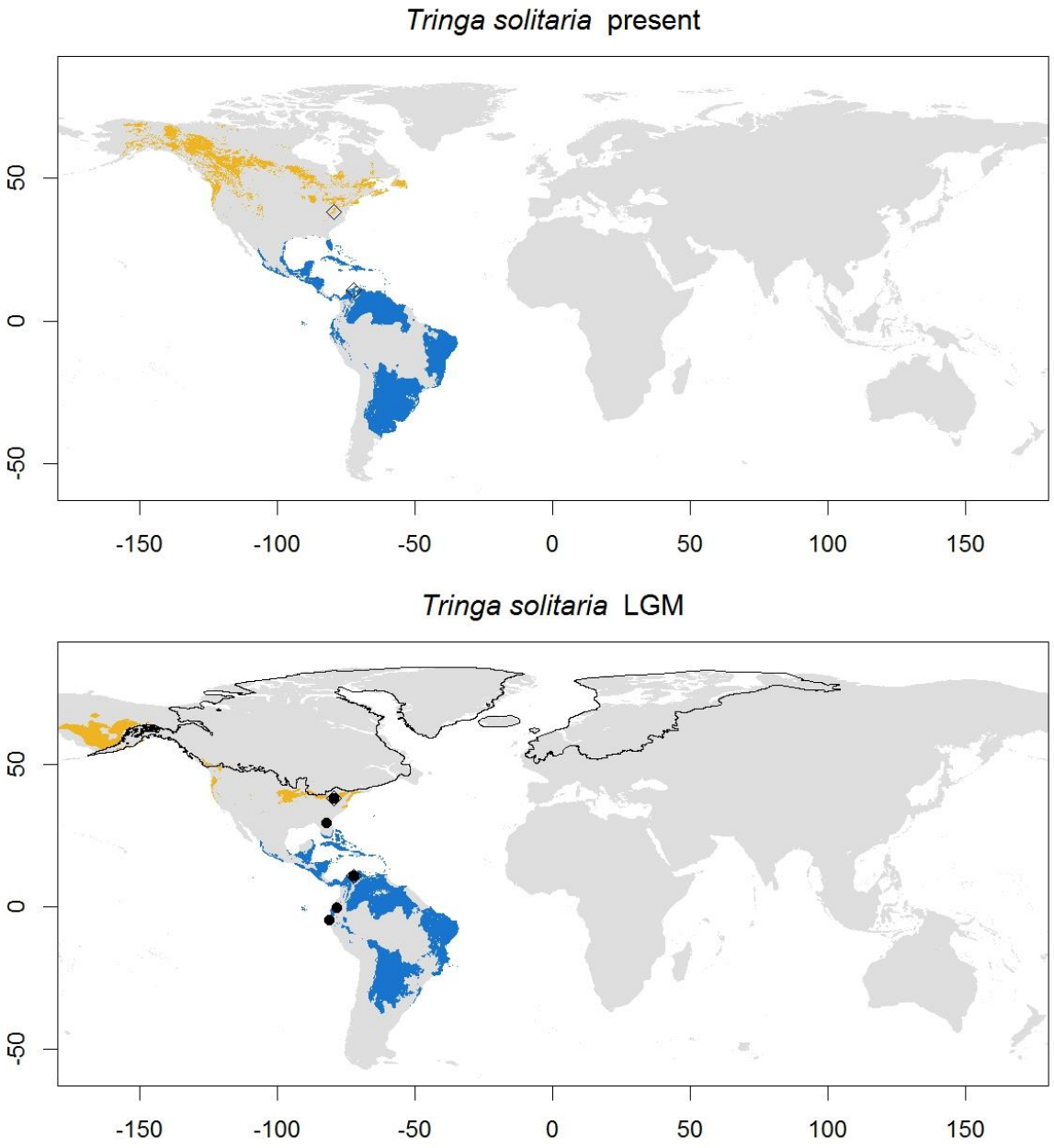

Map 67: Solitary Sandpiper (*Tringa solitaria*) predicted distribution. Caption as in map 1.

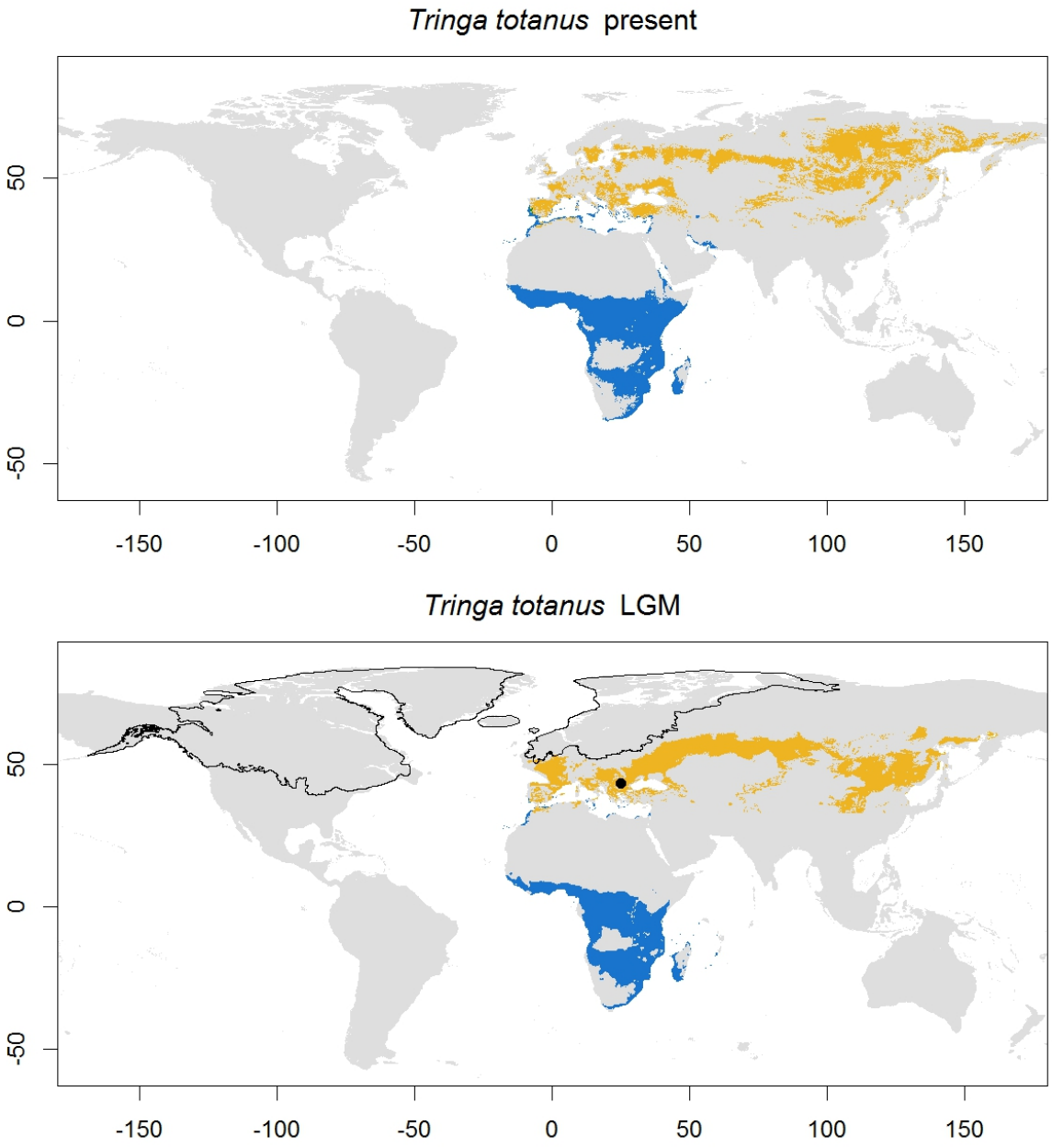

Map 68: Common Redshank (*Tringa totanus*) predicted distribution. Caption as in map 1.

Common Redshank, *Tringa totanus* (map 68). Breeds in Iceland, Scandinavia, all of Europe (being a resident all year in the south), south Russia, Kazakhstan, around the Tibetan Plateau in Mongolia and China, reaching east to Japan. Up to 6 described subspecies across the range (del Hoyo *et al*., 2018), with the main three being *T. t. robusta* in Iceland and Faeroes, *T. t. totanus* in Europe and the Mediterranean, and *T. t. ussuriensis* in south Siberia, Mongolia and north China. The distributions of the other three subspecies, *T. t. terrignotae* (northeast China), *T. t. craggi* (northwest China) and *T. t. eurhina* (north India) are all away from the Arctic and subarctic framework of the

study and are not included. The SDM predicts most of the breeding range of the species, although it fails to predict the species in Iceland, Faeroes and northern Scandinavia. It also predicts the potential breeding range to reach higher latitudes in east Siberia. The LGM model shows a reduction of the breeding range in northern Europe, concentrating around the Mediterranean, and extending east to the Sea of Japan and Sea of Okhotsk. No clear fragmentation is found during this period, although the range is much narrower from north to south. The breeding and wintering ranges are very close in Europe, with the species being resident all year round in the south. The wintering range also covers the north of Africa, as well as areas below the Sahara and around the Arabian Peninsula. The model predicts this wintering range, with low overlap with the breeding range in Europe and over predictions in the south of Africa and in Madagascar. The model predicts that the wintering distribution remained overall stable under the LGM conditions, with a reduction of the overlap between breeding and wintering in Europe. This species is classified under scenario A

Terek Sandpiper, *Xenus cinereus* (map 69). Monotypic species, breeds across the Palearctic from the Baltic Sea to northeast Siberia. The model predicts all of the breeding range, over-predicting in Scandinavia, western Europe and the Chukotka and Kamchatka Peninsulas. Under the LGM conditions, the model shows a decrease in the northern part of the breeding distribution, especially in the western Palearctic, where the over-predicted areas shift towards western Europe and the Mediterranean. Overall the breeding range would remain continuous across the Palearctic during this period, similar to the current distribution. The wintering range of the species is in the east coast of Africa, Madagascar, the Arabian Peninsula and from the south of Asia to Australia. The SDM's predictions fit this wintering distribution, also predicting inland areas in east Africa and Indochina. In the LGM model, the extent of suitable wintering areas decreases in continental Asia and the Arabian Peninsula, and increases in the emerged land between the Islands of Indonesia, Philippines and New Guinea. This species is classified under scenario A.

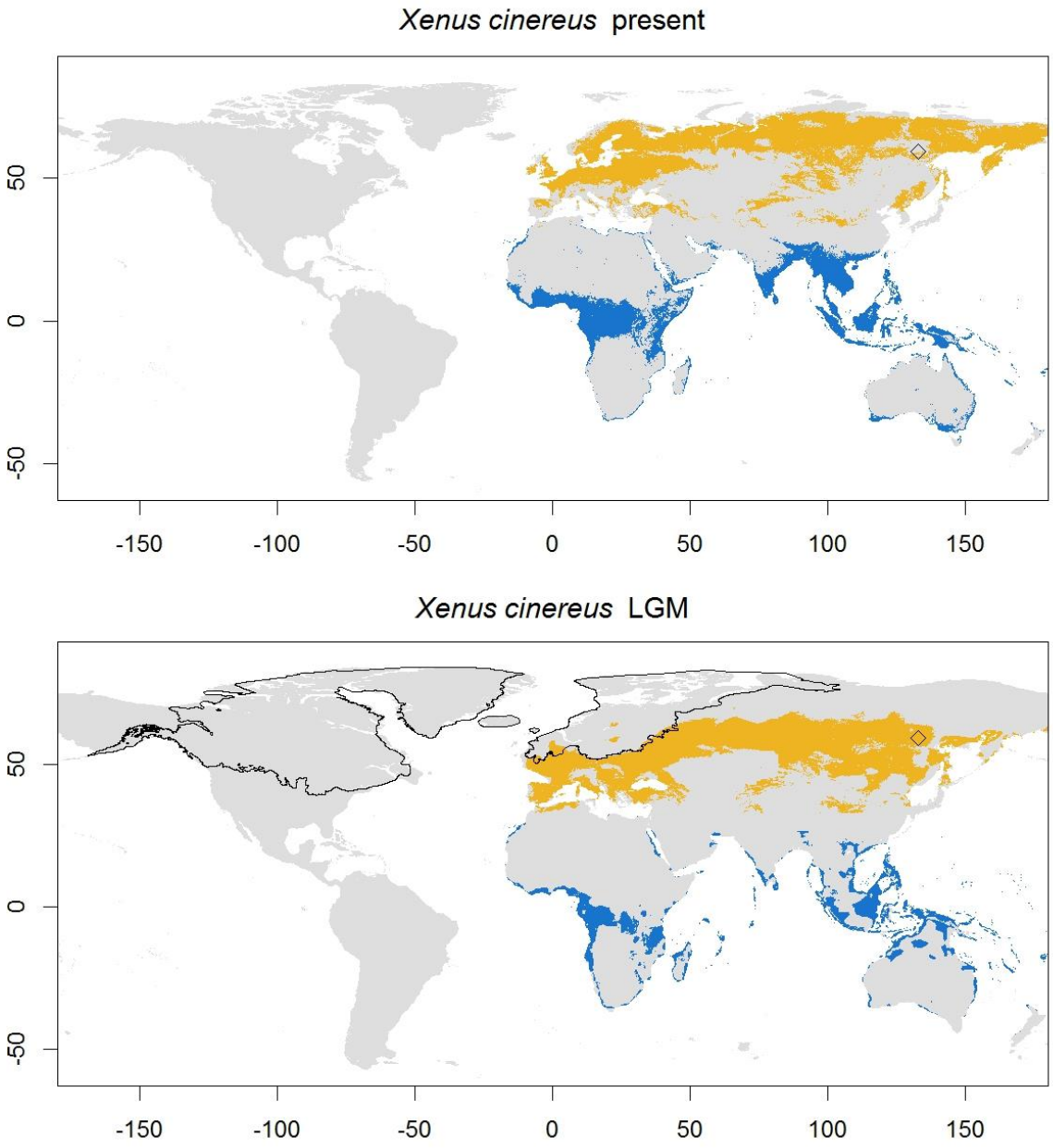

Map 69: Terek Sandpiper (*Xenus cinereus*) predicted distribution. Caption as in map 1.

References

Baker, A. J., Piersma, T., & Rosenmeier, L. (1994). Unraveling the intraspecific phylogeography of Knots *Calidris canutus*: a progress report on the search for genetic markers. *Journal of Ornithology*, *135*(4), 599–608.

Barisas, D. A. G., Amouret, J., Hallgrímsson, G. T., Summers, R. W., & Pálsson, S. (2015). A review of the subspecies status of the Icelandic Purple Sandpiper *Calidris maritima littoralis*. *Zoological Journal of the Linnean Society*, *175*(1), 211–221.

Buehler, D. M., & Baker, A. J. (2005). Population divergence times and historical demography in Red Knots and Dunlins. *Condor*, *107*, 497–513.

Ehlers, J., Gibbard, P. L., & Hughes, P. D. (Eds.). (2011). *Quaternary glaciations-extent and chronology: a closer look* (Vol. 15). Elsevier.

Engelmoer, M., & Roselaar, C. S. (1998). *Geographical variation in waders*. Springer Science & Business Media.

Humphries, E. M., & Winker, K. (2011). Discord reigns among nuclear, mitochondrial and phenotypic estimates of divergence in nine lineages of trans-Beringian birds. *Molecular Ecology*, *20*(3), 573–583.

Marthinsen, G., Wennerberg, L., & Lifjeld, J. T. (2007). Phylogeography and subspecies taxonomy of dunlins (*Calidris alpina*) in western Palearctic analyzed by DNA microsatellites and AFLP markers. *Biological Journal of the Linnean Society*, *92*, 713–726.

Miller, M. P., Haig, S. M., Gratto-Trevor, C. L., Mullins, T. D., Iller, M. A. R. K. P. M., Aig, S. U. M. H., … Ullins, T. H. D. M. (2010). Subspecies Status and Population Genetic Structure in Piping Plover (*Charadrius melodus*). *The Auk*, *127*(1), 57–71.

Miller, M. P., Haig, S. M., Mullins, T. D., Ruan, L., Casler, B., Dondua, A., … Lanctot, R. B. (2015). Intercontinental genetic structure and gene flow in Dunlin (*Calidris alpina*), a potential vector of avian influenza. *Evolutionary Applications*, *8*(2), 149–171.

Pruett, C. L., & Winker, K. (2005). Biological impacts of climatic change on a Beringian endemic: Cryptic refugia in the establishment and differentiation of the rock sandpiper (*Calidris ptilocnemis*). *Climatic Change*, *68*(1–2), 219–240.

Sangster, G., Collinson, J. M., Crochet, P. A., Knox, A. G., Parkin, D. T., & Votier, S. C. (2012). Taxonomic recommendations for British birds: eighth report. *Ibis, 154*(4), 874-883.

Appendix 2: supplementary tables

Monotypic species			
Scenario A	**Scenario B**	**Scenario C**	**Scenario D**
Arenaria melanocephala	*Tringa brevipes*	*Actitis hypoleucos*	*Bartramia longicauda*
Calidris acuminata		*Actitis macularius*	*Calidris maritima*
Calidris bairdii		*Calidris ferruginea*	*Eudromias morinellus*
Calidris fuscicollis		*Calidris melanotos*	*Numenius minutus*
Calidris himantopus		*Calidris minuta*	
Calidris mauri		*Gallinago delicata*	
Calidris minutilla		*Lymnocryptes minimus*	
Calidris pugnax		*Phalaropus lobatus*	
Calidris pusilla		*Pluvialis fulva*	
Calidris pygmaea		*Tringa erythropus*	
Calidris ruficollis		*Tringa nebularia*	
Calidris subruficollis			
Calidris temminckii			
Calidris tenuirostris			
Calidris virgata			
Charadrius semipalmatus			
Gallinago media			
Gallinago stenura			
Limnodromus scolopaceus			
Limosa haemastica			
Numenius americanus			
Numenius madagascariensis			
Numenius tahitiensis			
Phalaropus lobatus			
Pluvialis dominica			
Scolopax rusticola			
Steganopus tricolor			
Tringa flavipes			
Tringa glareola			
Tringa incana			
Tringa ochropus			
Xenus cinereus			

Species with described subspecies			
Scenario A	**Scenario B**	**Scenario C**	**Scenario D**
Charadrius vociferus	*Charadrius melodus*	*Arenaria interpres*	*Calidris alba*
Numenius arquata	*Calidris canutus*	*Calidris alpina*	*Calidris falcinellus*
Tringa totanus	*Calidris ptilocnemis*	*Charadrius hiaticula*	*Charadrius mongolus*
		Limnodromus griseus	*Gallinago gallinago*
		Pluvialis apricaria	*Haematopus ostralegus*
		Pluvialis squatarola	*Limosa lapponica*
		Tringa solitaria	*Limosa limosa*
			Numenius phaeopus

Table S1: Monotypic species and species with subspecies assigned to each of the four considered scenarios, represented in the schematic figure (A = no fragmentation of the breeding range, B = fragmentation only in the interglacial, C = fragmentation only during glacial period, D = fragmented breeding range in both periods).

Table S2: List of fossil records for the studied species. Records are ordered by country and locality, with its coordinates (latitude and longitude), minimum and maximum age (Mya), geological stage, source of the data [PB = Paleobiology Database (https://paleobiodb.org); WS = fosFARbase (http://www.wahre-staerke.com)] and the corresponding reference.

Locality		*Species*	Coordinates		Age (Mya)		Stage		Source	Reference
Country	**Site**		**Lat**	**Long**	**min**	**max**	**Upper**	**Lower**		
Australia	Blanche Cave, South Australia	*Pluvialis squatarola*	-37.0	140.8	0.01	0.13	NA	Late Pleistocene	PB	Reed & Bourne (2009)
Australia	Victoria Cave, South Australia	*Tringa glareola*	-37.0	140.8	0.13	0.78	NA	Middle Pleistocene	PB	Van Tets & Smith (1974)
Azerbaijan	Binagada asphalt lake	*Actitis hypoleucos*	40.5	49.8	0.01	0.13	NA	Late Pleistocene	PB	Gorobets & Yanenko (2018)
Azerbaijan	Binagada asphalt lake	*Calidris minuta*	40.5	49.8	0.10	0.13	NA	Late Pleistocene	PB	Gorobets & Yanenko (2018)
Azerbaijan	Binagada asphalt lake	*Calidris falcinellus*	40.5	49.8	0.10	0.13	NA	Late Pleistocene	PB	Gorobets & Yanenko (2018)
Azerbaijan	Binagada asphalt lake	*Calidris pugnax*	40.5	49.8	0.10	0.13	NA	Late Pleistocene	PB	Gorobets & Yanenko (2018)
Azerbaijan	Binagada asphalt lake	*Gallinago gallinago*	40.5	49.8	0.10	0.13	NA	Late Pleistocene	PB	Gorobets & Yanenko (2018)
Azerbaijan	Binagada asphalt lake	*Lymnocryptes minimus*	40.5	49.8	0.10	0.13	NA	Late Pleistocene	PB	Gorobets & Yanenko (2018)
Azerbaijan	Binagada asphalt lake	*Tringa erythropus*	40.5	49.8	0.10	0.13	NA	Late Pleistocene	PB	Gorobets & Yanenko (2018)
Azerbaijan	Binagada asphalt lake	*Tringa glareola*	40.5	49.8	0.10	0.13	NA	Late Pleistocene	PB	Gorobets & Yanenko (2018)
Azerbaijan	Binagada asphalt lake	*Tringa ochropus*	40.5	49.8	0.10	0.13	NA	Late Pleistocene	PB	Gorobets & Yanenko (2018)
Bahamas	Ficus Pit, San Salvador Island	*Arenaria interpres*	23.9	-74.6	0.00	0.13	Holocene	Late Pleistocene	PB	Olson *et al.* (1990)
Bulgaria	Devetashka Cave 3 km NW Devetaki, Lovech Region	*Actitis hypoleucos*	43.2	24.9	0.07	0.08	Upper Pleistocene	Upper Pleistocene	WS	Boev (2001)
Bulgaria	Devetashka Cave 3 km NW Devetaki, Lovech Region	*Calidris alba*	43.2	24.9	0.07	0.08	Upper Pleistocene	Upper Pleistocene	WS	Boev (2001)
Bulgaria	Devetashka Cave 3 km NW Devetaki, Lovech Region	*Gallinago gallinago*	43.2	24.9	0.07	0.08	Upper Pleistocene	Upper Pleistocene	WS	Boev (2001)

Bulgaria	Devetashka Cave 3 km NW Devetaki, Lovech Region	*Gallinago media*	43.2	24.9	0.07	0.08	Upper Pleistocene	Upper Pleistocene	WS	Boev (2001)
Bulgaria	Devetashka Cave 3 km NW Devetaki, Lovech Region	*Limosa limosa*	43.2	24.9	0.07	0.08	Upper Pleistocene	Upper Pleistocene	WS	Boev (2001)
Bulgaria	Devetashka Cave 3 km NW Devetaki, Lovech Region	*Numenius phaeopus*	43.2	24.9	0.07	0.08	Upper Pleistocene	Upper Pleistocene	WS	Boev (2001)
Bulgaria	Devetashka Cave 3 km NW Devetaki, Lovech Region	*Philomachus pugnax*	43.2	24.9	0.07	0.08	Upper Pleistocene	Upper Pleistocene	WS	Boev (2001)
Bulgaria	Devetashka Cave 3 km NW Devetaki, Lovech Region	*Pluvialis squatarola*	43.2	24.9	0.07	0.08	Upper Pleistocene	Upper Pleistocene	WS	Boev (2001)
Bulgaria	Devetashka Cave 3 km NW Devetaki, Lovech Region	*Tringa glareola*	43.2	24.9	0.07	0.08	Upper Pleistocene	Upper Pleistocene	WS	Boev (2001)
Bulgaria	Devetashka Cave 3 km NW Devetaki, Lovech Region	*Tringa nebularia*	43.2	24.9	0.07	0.08	Upper Pleistocene	Upper Pleistocene	WS	Boev (2001)
Bulgaria	Devetashka Cave 3 km NW Devetaki, Lovech Region	*Tringa ochropus*	43.2	24.9	0.07	0.08	Upper Pleistocene	Upper Pleistocene	WS	Boev (2001)
Bulgaria	Devetashka Cave 3 km NW Devetaki, Lovech Region	*Tringa totanus*	43.2	24.9	0.07	0.08	Upper Pleistocene	Upper Pleistocene	WS	Boev (2001)
Congo	Ishango	*Numenius phaeopus*	0.1	29.6	0.00	0.13	Holocene	Late Pleistocene	PB	Peters (1990)
Ecuador	La Carolina, Santa Elena Peninsula, near La Libertad	*Arenaria interpres*	-0.2	-78.5	0.02	0.12	Upper Pleistocene	Upper Pleistocene	WS	Campbell (1976)
Ecuador	La Carolina, Santa Elena Peninsula, near La Libertad	*Bartramia longicauda*	-0.2	-78.5	0.02	0.12	Upper Pleistocene	Upper Pleistocene	WS	Campbell (1976)
Ecuador	La Carolina, Santa Elena Peninsula, near La Libertad	*Calidris canutus*	-0.2	-78.5	0.02	0.12	Upper Pleistocene	Upper Pleistocene	WS	Campbell (1976)
Ecuador	La Carolina, Santa Elena Peninsula, near La Libertad	*Calidris mauri*	-0.2	-78.5	0.02	0.12	Upper Pleistocene	Upper Pleistocene	WS	Campbell (1976)
Ecuador	La Carolina, Santa Elena Peninsula, near La Libertad	*Calidris melanotos*	-0.2	-78.5	0.02	0.12	Upper Pleistocene	Upper Pleistocene	WS	Campbell (1976)
Ecuador	La Carolina, Santa Elena Peninsula, near La Libertad	*Calidris pusilla*	-0.2	-78.5	0.02	0.12	Upper Pleistocene	Upper Pleistocene	WS	Campbell (1976)
Ecuador	La Carolina, Santa Elena Peninsula, near La Libertad	*Charadrius semipalmatus*	-0.2	-78.5	0.02	0.12	Upper Pleistocene	Upper Pleistocene	WS	Campbell (1976)
Ecuador	La Carolina, Santa Elena Peninsula, near La Libertad	*Charadrius vociferus*	-0.2	-78.5	0.02	0.12	Upper Pleistocene	Upper Pleistocene	WS	Campbell (1976)

Ecuador	La Carolina, Santa Elena Peninsula, near La Libertad	*Numenius phaeopus*	-0.2	-78.5	0.02	0.12	Upper Pleistocene	Upper Pleistocene	WS	Campbell (1976)
Ecuador	La Carolina, Santa Elena Peninsula, near La Libertad	*Pluvialis dominica*	-0.2	-78.5	0.02	0.12	Upper Pleistocene	Upper Pleistocene	WS	Campbell (1976)
Ecuador	La Carolina, Santa Elena Peninsula, near La Libertad	*Pluvialis squatarola*	-0.2	-78.5	0.02	0.12	Upper Pleistocene	Upper Pleistocene	WS	Campbell (1976)
Ecuador	La Carolina, Santa Elena Peninsula, near La Libertad	*Tringa flavipes*	-0.2	-78.5	0.02	0.12	Upper Pleistocene	Upper Pleistocene	WS	Campbell (1976)
Ecuador	La Carolina, Santa Elena Peninsula, near La Libertad	*Tringa solitaria*	-0.2	-78.5	0.02	0.12	Upper Pleistocene	Upper Pleistocene	WS	Campbell (1976)
Ecuador	La Carolina, Santa Elena Peninsula, near La Libertad	*Calidris himantopus*	-0.2	-78.5	0.01	0.13	NA	Late Pleistocene	PB	Campbell (1976)
Ecuador	La Carolina, Santa Elena Peninsula, near La Libertad	*Phalaropus fulicarius*	-0.2	-78.5	0.01	0.13	NA	Late Pleistocene	PB	Campbell (1976)
Ecuador	La Carolina, Santa Elena Peninsula, near La Libertad	*Phalaropus lobatus*	-0.2	-78.5	0.01	0.13	NA	Late Pleistocene	PB	Campbell (1976)
Ecuador	La Carolina, Santa Elena Peninsula, near La Libertad	*Phalaropus tricolor*	-0.2	-78.5	0.01	0.13	NA	Late Pleistocene	PB	Campbell (1976)
Egypt	Kom Ombo, Upper Egypt	*Numenius arquata*	24.4	33.0	0.01	2.59	NA	Pleistocene	PB	Churcher (1974)
France	Cantet Cave, Espèche, Haute Pyrénées	*Charadrius hiaticula*	43.1	0.3	0.01	0.13	Upper Pleistocene	Upper Pleistocene	WS	Clot (1984)
Greece	Liko Cave bed A, Crete	*Scolopax rusticola*	35.4	24.3	0.01	0.13	NA	Late Pleistocene	PB	Wessie (1988)
Greece	Liko Cave bed A/B, Crete	*Scolopax rusticola*	35.4	24.3	0.01	0.13	NA	Late Pleistocene	PB	Wessie (1988)
Greece	Liko Cave bed B, Crete	*Scolopax rusticola*	35.4	24.3	0.01	0.13	NA	Late Pleistocene	PB	Wessie (1988)
Greece	Liko Cave bed C, Crete	*Scolopax rusticola*	35.4	24.3	0.01	0.13	NA	Late Pleistocene	PB	Wessie (1988)
Greece	Liko Cave bed C/D, Crete	*Scolopax rusticola*	35.4	24.3	0.01	0.13	NA	Late Pleistocene	PB	Wessie (1988)
Greece	Liko Cave bed D, Crete	*Scolopax rusticola*	35.4	24.3	0.01	0.13	NA	Late Pleistocene	PB	Wessie (1988)
Greece	Liko Cave bed Li-O, Crete	*Scolopax rusticola*	35.4	24.3	0.01	0.13	NA	Late Pleistocene	PB	Wessie (1988)
Greece	Liko Cave bed V, Crete	*Calidris canutus*	35.4	24.3	0.01	0.13	NA	Late Pleistocene	PB	Wessie (1988)
Greece	Liko Cave bed V, Crete	*Scolopax rusticola*	35.4	24.3	0.01	0.13	NA	Late Pleistocene	PB	Wessie (1988)
Indonesia	Lian Bua sector XI split 39	*Actitis hypoleucos*	-8.5	120.4	0.01	0.13	NA	Late Pleistocene	PB	Meijer *et al.* (2013)
Indonesia	Lian Bua sector XI split 41	*Actitis hypoleucos*	-8.5	120.4	0.01	0.13	NA	Late Pleistocene	PB	Meijer *et al.* (2013)
Indonesia	Lian Bua sector XI split 43	*Pluvialis fulva*	-8.5	120.4	0.01	0.13	NA	Late Pleistocene	PB	Meijer *et al.* (2013)
Indonesia	Lian Bua sector XI split 45	*Pluvialis fulva*	-8.5	120.4	0.01	0.13	NA	Late Pleistocene	PB	Meijer *et al.* (2013)

Indonesia	Lian Bua sector XI split 50	*Pluvialis fulva*	-8.5	120.4	0.01	0.13	NA	Late Pleistocene	PB	Meijer *et al.* (2013)
Italy	Malagrotta MIS9, Rome	*Calidris temminckii*	41.8	12.2	0.13	0.78	NA	Middle Pleistocene	PB	Cassoli *et al.* (1982)
Italy	Spinagallo Cave, Siracusa	*Scolopax rusticola*	37.0	15.2	0.13	0.78	NA	Middle Pleistocene	PB	Pavia (1999)
Japan	Minatogawa Fissure, Okinawa	*Scolopax rusticola*	26.1	127.8	0.01	0.13	NA	Late Pleistocene	PB	Matsuoka (2000)
Mexico	Cantera de Jocotepec, Chapala-Zacoalco, Jalisco	*Calidris fuscicollis*	20.3	-103.5	0.01	1.80	Upper Pleistocene	Lower Pleistocene	WS	Corona-Martinez (2002)
Mexico	Cueva de San Josecito, 8 km SE Aramberri, Zaragoza, Nuevo León	*Pluvialis sp.*	24.0	-99.9	0.01	0.13	Upper Pleistocene	Upper Pleistocene	WS	Arroyo-Cabrales & Johnson (1995)
Mexico	Cueva de San Josecito, 8 km SE Aramberri, Zaragoza, Nuevo León	*Numenius americanus*	24.0	-99.9	0.01	0.13	Upper Pleistocene	Upper Pleistocene	WS	Miller (1943)
Monaco	Grotte de l'Observatoire	*Scolopax rusticola*	43.7	7.4	0.01	0.78	Late Pleistocene	Middle Pleistocene	PB	Boule & Villeneuve (1927)
Morocco	Ahl al Oughlam (near Casablanca)	*Pluvialis sp.*	33.6	-7.6	2.50	2.50	Gelasian	Gelasian	WS	Mourer-Chauviré & Geraads (2010)
Peru	Talara Tar Seeps, Piura Department	*Actitis macularius*	-4.6	-81.1	0.01	0.01	Upper Pleistocene	Upper Pleistocene	WS	Campbell (1979)
Peru	Talara Tar Seeps, Piura Department	*Arenaria interpres*	-4.6	-81.1	0.01	0.01	Upper Pleistocene	Upper Pleistocene	WS	Campbell (1979)
Peru	Talara Tar Seeps, Piura Department	*Calidris mauri*	-4.6	-81.1	0.01	0.01	Upper Pleistocene	Upper Pleistocene	WS	Campbell (1979)
Peru	Talara Tar Seeps, Piura Department	*Calidris melanotos*	-4.6	-81.1	0.01	0.01	Upper Pleistocene	Upper Pleistocene	WS	Campbell (1979)
Peru	Talara Tar Seeps, Piura Department	*Calidris minutilla*	-4.6	-81.1	0.01	0.01	Upper Pleistocene	Upper Pleistocene	WS	Campbell (1979)
Peru	Talara Tar Seeps, Piura Department	*Charadrius semipalmatus*	-4.6	-81.1	0.01	0.01	Upper Pleistocene	Upper Pleistocene	WS	Campbell (1979)
Peru	Talara Tar Seeps, Piura Department	*Charadrius vociferus*	-4.6	-81.1	0.01	0.01	Upper Pleistocene	Upper Pleistocene	WS	Campbell (1979)
Peru	Talara Tar Seeps, Piura Department	*Pluvialis dominica*	-4.6	-81.1	0.01	0.01	Upper Pleistocene	Upper Pleistocene	WS	Campbell (1979)
Peru	Talara Tar Seeps, Piura Department	*Pluvialis squatarola*	-4.6	-81.1	0.01	0.01	Upper Pleistocene	Upper Pleistocene	WS	Campbell (1979)
Peru	Talara Tar Seeps, Piura Department	*Tringa flavipes*	-4.6	-81.1	0.01	0.01	Upper Pleistocene	Upper Pleistocene	WS	Campbell (1979)

Peru	Talara Tar Seeps, Piura Department	*Tringa solitaria*	-4.6	-81.1	0.01	0.01	Upper Pleistocene	Upper Pleistocene	WS	Campbell (1979)
Peru	Talara Tar Seeps, Piura Department	*Calidris himantopus*	-4.7	-80.5	0.01	0.13	NA	Late Pleistocene	PB	Campbell (1979)
Peru	Talara Tar Seeps, Piura Department	*Phalaropus lobatus*	-4.7	-80.5	0.01	0.13	NA	Late Pleistocene	PB	Campbell (1979)
Peru	Talara Tar Seeps, Piura Department	*Phalaropus tricolor*	-4.7	-80.5	0.01	0.13	NA	Late Pleistocene	PB	Campbell (1979)
Poland	Bisnik Cave fauna complex II, 50 km NE Kraków	*Gallinago media*	50.4	19.7	0.02	0.03	Upper Pleistocene	Upper Pleistocene	WS	Tomek *et al.* (2011)
Poland	Bisnik Cave fauna complex II, 50 km NE Kraków	*Gallinago media*	50.4	19.7	0.02	0.03	Upper Pleistocene	Upper Pleistocene	WS	Tomek *et al.* (2011)
Poland	Bisnik Cave fauna complex II, 50 km NE Kraków	*Limosa limosa*	50.4	19.7	0.02	0.03	Upper Pleistocene	Upper Pleistocene	WS	Tomek *et al.* (2011)
Poland	Bisnik Cave fauna complex II, 50 km NE Kraków	*Philomachus pugnax*	50.4	19.7	0.02	0.03	Upper Pleistocene	Upper Pleistocene	WS	Tomek *et al.* (2011)
Poland	Bisnik Cave fauna complex III, 50 km NE Kraków	*Arenaria interpres*	50.4	19.7	0.04	0.07	Upper Pleistocene	Upper Pleistocene	WS	Tomek *et al.* (2011)
Poland	Bisnik Cave fauna complex III, 50 km NE Kraków	*Philomachus pugnax*	50.4	19.7	0.04	0.07	Upper Pleistocene	Upper Pleistocene	WS	Tomek *et al.* (2011)
Poland	Bisnik Cave fauna complex IV, 50 km NE Kraków	*Philomachus pugnax*	50.4	19.7	0.05	0.08	Upper Pleistocene	Upper Pleistocene	WS	Tomek *et al.* (2011)
Poland	Bisnik Cave fauna complex IV, 50 km NE Kraków	*Pluvialis squatarola*	50.4	19.7	0.05	0.08	Upper Pleistocene	Upper Pleistocene	WS	Tomek *et al.* (2011)
Poland	Bisnik Cave fauna complex VI, 50 km NE Kraków	*Eudromias morinellus*	50.4	19.7	0.10	0.16	Upper Pleistocene	Middle Pleistocene	WS	Tomek *et al.* (2011)
Poland	Bisnik Cave fauna complex VI, 50 km NE Kraków	*Philomachus pugnax*	50.4	19.7	0.10	0.16	Upper Pleistocene	Middle Pleistocene	WS	Tomek *et al.* (2011)
Poland	Bisnik Cave fauna complex VI, 50 km NE Kraków	*Tringa ochropus*	50.4	19.7	0.10	0.16	Upper Pleistocene	Middle Pleistocene	WS	Tomek *et al.* (2011)
Poland	Bisnik Cave fauna complex VIII, 50 km NE Kraków	*Pluvialis apricaria*	50.4	19.7	0.16	0.23	Middle Pleistocene	Middle Pleistocene	WS	Tomek *et al.* (2011)
Russia	Dyuktai Cave	*Calidris pugnax*	59.3	132.6	0.01	0.02	Holocene	Late Pleistocene	PB	Zelenkov *et al.* (2008)
Russia	Dyuktai Cave	*Gallinago gallinago*	59.3	132.6	0.01	0.02	Holocene	Late Pleistocene	PB	Zelenkov *et al.* (2008)
Russia	Dyuktai Cave	*Gallinago stenura*	59.3	132.6	0.01	0.02	Holocene	Late Pleistocene	PB	Zelenkov *et al.* (2008)
Russia	Dyuktai Cave	*Limosa limosa*	59.3	132.6	0.01	0.02	Holocene	Late Pleistocene	PB	Zelenkov *et al.* (2008)

Russia	Dyuktai Cave	*Numenius minutus*	59.3	132.6	0.01	0.02	Holocene	Late Pleistocene	PB	Zelenkov *et al.* (2008)
Russia	Dyuktai Cave	*Numenius phaeopus*	59.3	132.6	0.01	0.02	Holocene	Late Pleistocene	PB	Zelenkov *et al.* (2008)
Russia	Dyuktai Cave	*Phalaropus fulicarius*	59.3	132.6	0.01	0.02	Holocene	Late Pleistocene	PB	Zelenkov *et al.* (2008)
Russia	Dyuktai Cave	*Phalaropus lobatus*	59.3	132.6	0.01	0.02	Holocene	Late Pleistocene	PB	Zelenkov *et al.* (2008)
Russia	Dyuktai Cave	*Pluvialis sp.*	59.3	132.6	0.01	0.02	Holocene	Late Pleistocene	PB	Zelenkov *et al.* (2008)
Russia	Dyuktai Cave	*Tringa glareola*	59.3	132.6	0.01	0.02	Holocene	Late Pleistocene	PB	Zelenkov *et al.* (2008)
Russia	Dyuktai Cave	*Tringa nebularia*	59.3	132.6	0.01	0.02	Holocene	Late Pleistocene	PB	Zelenkov *et al.* (2008)
Russia	Dyuktai Cave	*Tringa ochropus*	59.3	132.6	0.01	0.02	Holocene	Late Pleistocene	PB	Zelenkov *et al.* (2008)
Russia	Dyuktai Cave	*Xenus cinereus*	59.3	132.6	0.01	0.02	Holocene	Late Pleistocene	PB	Zelenkov *et al.* (2008)
Spain	Atapuerca TD6	*Scolopax rusticola*	42.4	-3.5	0.78	1.81	NA	Calabrian	PB	Sánchez-Marco (1999)
Spain	Gran Dolina TD 6-1+TD 6-2, Atapuerca, Burgos	*Limosa limosa*	42.3	-3.4	0.85	0.85	Lower Pleistocene	Lower Pleistocene	WS	Sánchez-Marco (1999)
U.K.	Bacon Hole, Wales	*Arenaria interpres*	51.6	-4.1	0.01	0.13	NA	Late Pleistocene	PB	Harrison (1987)
U.K.	Bacon Hole, Wales	*Calidris alpina*	51.6	-4.1	0.01	0.13	NA	Late Pleistocene	PB	Harrison (1987)
U.K.	Bacon Hole, Wales	*Pluvialis apricaria*	51.6	-4.1	0.01	0.13	NA	Late Pleistocene	PB	Harrison (1987)
U.K.	Chudleigh Gorge, Devon	*Gallinago gallinago*	50.6	-3.6	0.01	0.13	NA	Late Pleistocene	PB	Harrison (1980)
U.K.	Minchin Hole, Wales	*Calidris alpina*	51.6	-4.1	0.01	0.13	NA	Late Pleistocene	PB	Harrison (1987)
U.K.	Park Street, Roman Villa	*Scolopax rusticola*	51.7	-0.3	0.01	2.59	NA	Pleistocene	PB	Harrison (1980)
U.K.	Soldier's hole	*Limosa limosa*	51.3	-2.8	0.01	0.13	NA	Late Pleistocene	PB	Harrison (1987)
U.K.	Torbryan Cave, Devon	*Lymnocryptes minimus*	50.5	-3.5	0.01	0.13	NA	Late Pleistocene	PB	Harrison (1980)
U.K.	West Runton Freshwater Bed, Norfolk	*Tringa ochropus*	52.9	1.2	0.13	0.78	NA	Middle Pleistocene	PB	Harrison (1979)
U.S.A.	Bell Cave, Alabama	*Bartramia longicauda*	34.7	-87.8	0.01	0.13	NA	Late Pleistocene	PB	Parmalee(1992)
U.S.A.	Camp Cady, California	*Actitis sp.*	34.8	-117.0	0.01	0.13	NA	Late Pleistocene	PB	Jefferson (1987)
U.S.A.	Chick Bend Cave, Tennessee	*Gallinago delicata*	35.6	-86.8	0.01	0.13	NA	Late Pleistocene	PB	Parmalee & Klippel (1982)
U.S.A.	Clark´s Cave, Virginia	*Actitis macularius*	38.1	-79.7	0.01	0.13	NA	Late Pleistocene	PB	Guilday *et al.* (1977)
U.S.A.	Clark´s Cave, Virginia	*Gallinago delicata*	38.1	-79.7	0.01	0.13	NA	Late Pleistocene	PB	Guilday *et al.* (1977)
U.S.A.	Clark´s Cave, Virginia	*Pluvialis dominica*	38.1	-79.7	0.01	0.13	NA	Late Pleistocene	PB	Guilday *et al.* (1977)
U.S.A.	Clark´s Cave, Virginia	*Tringa solitaria*	38.1	-79.7	0.01	0.13	NA	Late Pleistocene	PB	Guilday *et al.* (1977)

U.S.A.	Fossil Lake, Oregon	*Calidris melanotos*	43.3	-120.5	0.01	0.13	NA	Late Pleistocene	PB	Elftman (1931)
U.S.A.	Fossil Lake, Oregon	*Limnodromus griseus*	43.3	-120.5	0.01	0.13	NA	Late Pleistocene	PB	Elftman (1931)
U.S.A.	Fossil Lake, Oregon	*Numenius americanus*	43.3	-120.5	0.01	0.13	NA	Late Pleistocene	PB	Elftman (1931)
U.S.A.	Fossil Lake, Oregon	*Phalaropus lobatus*	43.3	-120.5	0.01	0.13	NA	Late Pleistocene	PB	Elftman (1931)
U.S.A.	Ingleside Site No. 1, Texas	*Limnodromus sp.*	27.9	-97.2	0.01	0.13	NA	Late Pleistocene	PB	Feduccia (1973)
U.S.A.	Inglis 1A, Florida	*Gallinago delicata*	29.0	-82.7	0.78	1.81	NA	Calabrian	PB	Emslie (1998)
U.S.A.	Inglis 1C, Florida	*Gallinago delicata*	29.0	-82.7	0.30	1.80	NA	Irvingtonian	PB	Emslie (1998)
U.S.A.	Kingston Saltpeter Cave, Georgia	*Bartramia longicauda*	34.2	-84.9	0.01	0.13	NA	Late Pleistocene	PB	Steadman (2005)
U.S.A.	Little Box Elder Cave, Wyoming	*Calidris melanotos*	42.8	-105.7	0.01	0.13	NA	Late Pleistocene	PB	Emslie (1985)
U.S.A.	Little Box Elder Cave, Wyoming	*Charadrius vociferus*	42.8	-105.7	0.01	0.13	NA	Late Pleistocene	PB	Emslie (1985)
U.S.A.	Little Box Elder Cave, Wyoming	*Gallinago delicata*	42.8	-105.7	0.01	0.13	NA	Late Pleistocene	PB	Emslie (1985)
U.S.A.	Little Box Elder Cave, Wyoming	*Numenius americanus*	42.8	-105.7	0.01	0.13	NA	Late Pleistocene	PB	Emslie (1985)
U.S.A.	Manix Lake W19, California	*Phalaropus lobatus*	33.2	-117.3	0.01	0.13	NA	Late Pleistocene	PB	Howard (1955)
U.S.A.	Moomomi Dunes, Hawaii	*Numenius tahitiensis*	21.2	-157.2	0.01	0.13	NA	Late Pleistocene	PB	Olson & James (1991)
U.S.A.	Natural Chimneys, Virginia	*Bartramia longicauda*	38.4	-79.1	0.01	0.13	NA	Late Pleistocene	PB	Wetmore (1962)
U.S.A.	Natural Chimneys, Virginia	*Calidris minutilla*	38.4	-79.1	0.01	0.13	NA	Late Pleistocene	PB	Wetmore (1962)
U.S.A.	Natural Chimneys, Virginia	*Charadrius vociferus*	38.4	-79.1	0.01	0.13	NA	Late Pleistocene	PB	Wetmore (1962)
U.S.A.	Porcupine Cave, Colorado	*Phalaropus lobatus*	39.5	-105.8	0.30	1.80	NA	Irvingtonian	PB	Emslie (2004)
U.S.A.	Rancho La Brea, California	*Charadrius vociferus*	34.1	-118.3	0.01	0.30	NA	Rancholabrean	PB	Howard (1936)
U.S.A.	Rancho La Brea, California	*Limnodromus griseus*	34.1	-118.3	0.01	0.30	NA	Rancholabrean	PB	Howard (1936)
U.S.A.	Reddick 1A, Florida	*Charadrius vociferus*	29.1	-82.3	0.01	0.30	NA	Rancholabrean	PB	Emslie (1998)
U.S.A.	Reddick 1A, Florida	*Gallinago delicata*	29.1	-82.3	0.01	0.30	NA	Rancholabrean	PB	Emslie (1998)
U.S.A.	Reddick 1A, Florida	*Tringa flavipes*	29.1	-82.3	0.01	0.30	NA	Rancholabrean	PB	Emslie (1998)
U.S.A.	San Miguel Island V-10, California	*Calidris alba*	34.0	-120.3	0.01	0.13	NA	Late Pleistocene	PB	Guthrie (2005)
U.S.A.	San Miguel Island V-10, California	*Charadrius semipalmatus*	34.0	-120.3	0.01	0.13	NA	Late Pleistocene	PB	Guthrie (2005)

U.S.A.	San Miguel Island V-10, California	*Pluvialis squatarola*	34.0	-120.3	0.01	0.13	NA	Late Pleistocene	PB	Guthrie (2005)
U.S.A.	San Miguel Island V-11, California	*Numenius phaeopus*	34.0	-120.3	0.01	0.13	NA	Late Pleistocene	PB	Guthrie (2005)
U.S.A.	San Miguel Island V-16, California	*Charadrius semipalmatus*	34.0	-120.4	0.01	0.13	NA	Late Pleistocene	PB	Guthrie (2005)
U.S.A.	San Miguel Island V-16, California	*Numenius phaeopus*	34.0	-120.4	0.01	0.13	NA	Late Pleistocene	PB	Guthrie (2005)
U.S.A.	San Miguel Island V-16, California	*Phalaropus fulicarius*	34.0	-120.4	0.01	0.13	NA	Late Pleistocene	PB	Guthrie (2005)
U.S.A.	San Miguel Island V-16, California	*Pluvialis squatarola*	34.0	-120.4	0.01	0.13	NA	Late Pleistocene	PB	Guthrie (2005)
U.S.A.	San Miguel Island V-18, California	*Arenaria melanocephala*	34.0	-120.4	0.01	2.59	NA	Pleistocene	PB	Guthrie (2005)
U.S.A.	San Miguel Island V-6, California	*Arenaria melanocephala*	34.1	-120.4	0.01	0.13	NA	Late Pleistocene	PB	Guthrie (2005)
U.S.A.	San Miguel Island V-6, California	*Phalaropus fulicarius*	34.1	-120.4	0.01	0.13	NA	Late Pleistocene	PB	Guthrie (2005)
U.S.A.	San Miguel Island V-7, California	*Calidris alba*	34.1	-120.4	0.01	0.13	NA	Late Pleistocene	PB	Guthrie (2005)
U.S.A.	San Miguel Island V-7, California	*Phalaropus fulicarius*	34.1	-120.4	0.01	0.13	NA	Late Pleistocene	PB	Guthrie (2005)
U.S.A.	Silver Lake, Oregon	*Phalaropus lobatus*	43.1	-121.0	0.01	0.13	NA	Late Pleistocene	PB	Shufeldt (1891)
U.S.A..	Arredondo IIA, Alachua County, Florida	*Tringa solitaria*	29.6	-82.4	0.01	0.13	Upper Pleistocene	Upper Pleistocene	WS	Brodkorb (1959)
U.S.A..	Cutler Hammock Local Fauna, Dade County, Florida	*Gallinago delicata*	25.4	-80.2	0.01	0.13	Upper Pleistocene	Upper Pleistocene	WS	Emslie (1998)
U.S.A..	Cutler Hammock Local Fauna, Dade County, Florida	*Limnodromus scolopaceus*	25.4	-80.2	0.01	0.13	Upper Pleistocene	Upper Pleistocene	WS	Emslie (1998)
U.S.A..	Haile pit 11B (south of Haile), Alachua County, Florida	*Actitis macularius*	29.8	-82.1	0.01	0.13	Upper Pleistocene	Upper Pleistocene	WS	Emslie (1998)
U.S.A..	Haile pit 11B (south of Haile), Alachua County, Florida	*Charadrius vociferus*	29.8	-82.1	0.01	0.13	Upper Pleistocene	Upper Pleistocene	WS	Emslie (1998)
U.S.A..	Haile pit 11B (south of Haile), Alachua County, Florida	*Gallinago delicata*	29.8	-82.1	0.01	0.13	Upper Pleistocene	Upper Pleistocene	WS	Emslie (1998)

U.S.A..	Haile pit 11B (south of Haile), Alachua County, Florida	*Limnodromus sp.*	29.8	-82.1	0.01	0.13	Upper Pleistocene	Upper Pleistocene	WS	Emslie (1998)
U.S.A..	Haile pit 11B (south of Haile), Alachua County, Florida	*Numenius americanus*	29.8	-82.1	0.01	0.13	Upper Pleistocene	Upper Pleistocene	WS	Emslie (1998)
U.S.A..	Haile pit 16A (south of Haile), Alachua County, Florida	*Limnodromus scolopaceus*	29.7	-82.6	1.00	1.60	Lower Pleistocene	Lower Pleistocene	WS	Emslie (1998)
U.S.A..	Haile pit 7C (south of Haile), Alachua County, Florida	*Limnodromus scolopaceus*	29.7	-82.6	1.90	2.10	Gelasian	Gelasian	WS	Emslie (1998)
U.S.A..	Harris´ Pocket, Dry Cave, UTEP 6; Eddy County, New Mexico	*Charadrius vociferus*	32.0	-104.0	0.01	0.02	Upper Pleistocene	Upper Pleistocene	WS	Harris (1993)
U.S.A..	Harris´ Pocket, Dry Cave, UTEP 6; Eddy County, New Mexico	*Numenius americanus*	32.0	-104.0	0.01	0.02	Upper Pleistocene	Upper Pleistocene	WS	Harris (1993)
U.S.A..	Inglis 1A, Citrus County, Florida	*Gallinago delicata*	29.0	-82.7	1.90	2.00	Gelasian	Gelasian	WS	Emslie (1998)
U.S.A..	Inglis 1C, Citrus County, Florida	*Gallinago delicata*	29.0	-82.7	1.60	1.90	Lower Pleistocene	Gelasian	WS	Emslie (1998)
U.S.A..	McKittrick-Asphalto, Kern County, California	*Numenius americanus*	35.3	-118.5	0.01	0.13	Upper Pleistocene	Upper Pleistocene	WS	Miller (1935)
U.S.A..	Reddick IA+B, Marion County, Florida	*Gallinago delicata*	29.1	-82.3	0.01	0.13	Upper Pleistocene	Upper Pleistocene	WS	Emslie (1998)
U.S.A..	Richardson Road Shell Pit, Sarasota County, Florida	*Calidris alba*	27.4	-82.4	2.00	2.50	Gelasian	Gelasian	WS	Emslie (1998)
U.S.A..	Richardson Road Shell Pit, Sarasota County, Florida	*Calidris canutus*	27.4	-82.4	2.00	2.50	Gelasian	Gelasian	WS	Emslie (1998)
U.S.A..	Rock Springs, Orange County, Florida	*Limnodromus scolopaceus*	28.7	-81.5	0.01	0.13	Upper Pleistocene	Upper Pleistocene	WS	Emslie (1998)
U.S.A..	Sabertooth Cave, Lecanto 2A, Citrus County, Florida	*Calidris pusilla*	28.8	-82.2	0.01	0.13	Upper Pleistocene	Upper Pleistocene	WS	Emslie (1998)
U.S.A..	White Rock local fauna, Republic County, Kansas	*Pluvialis squatarola*	39.9	-97.7	1.80	2.20	Gelasian	Gelasian	WS	Eshelman (1975)
Venezuela	Mene de Inciarte Tar Seep, Zulia	*Calidris canutus*	10.8	-72.2	0.01	0.13	NA	Late Pleistocene	PB	Steadman *et al.* (2015)
Venezuela	Mene de Inciarte Tar Seep, Zulia	*Calidris fuscicollis*	10.8	-72.2	0.01	0.13	NA	Late Pleistocene	PB	Steadman *et al.* (2015)
Venezuela	Mene de Inciarte Tar Seep, Zulia	*Charadrius vociferus*	10.8	-72.2	0.01	0.13	NA	Late Pleistocene	PB	Steadman *et al.* (2015)

Venezuela	Mene de Inciarte Tar Seep, Zulia	*Phalaropus lobatus*	10.8	-72.2	0.01	0.13	NA	Late Pleistocene	PB	Steadman *et al.* (2015)
Venezuela	Mene de Inciarte Tar Seep, Zulia	*Phalaropus tricolor*	10.8	-72.2	0.01	0.13	NA	Late Pleistocene	PB	Steadman *et al.* (2015)
Venezuela	Mene de Inciarte Tar Seep, Zulia	*Tringa flavipes*	10.8	-72.2	0.01	0.13	NA	Late Pleistocene	PB	Steadman *et al.* (2015)
Venezuela	Mene de Inciarte Tar Seep, Zulia	*Tringa solitaria*	10.8	-72.2	0.01	0.13	NA	Late Pleistocene	PB	Steadman *et al.* (2015)

Bibliography:

Arroyo-Cabrales, J., & Johnson, E. (1995). A reappraisal of fossil vertebrates from San Josecito cave, Nuevo Leon, Mexico. *Ancient Peoples and Landscapes: Lubbock, Texas, Museum of Texas Tech University*, 217-231.

Boev, Z. (2001). Birds over the mammoths' head in Bulgaria. *The World of Elephants first International Congress, Rome,* 16-20.

Boule, M., & de Villeneuve, L. (1927). *La Grotte de l'Observatoire a Monaco: étude anthropologique*. Masson.

Brodkorb, P. (1959). *The Pleistocene avifauna of Arredondo, Florida*. University of Florida.

Campbell, K. E. (1976). The late Pleistocene avifauna of La Carolina, southwestern Ecuador. Collected papers in avian paleontology honoring the 90th birthday of Alexander Wetmore. *Smithsonian Contributions to Paleobiology, 27*, 155-168.

Campbell, K. E. (1979*). Non-passerine Pleistocene avifauna of the Talara Tar Seeps, northwestern Peru*. Royal Ontario Museum.

Cassoli, P. F., De Giuli, C., Radmilli, A. M., & Segre, A. G. (1982). Giacimento del paleolitico inferiore a Malagrotta (Roma). *Atti della XXIII Riunione Scientifica dell'Istituto Italiano di Preistoria e Protostoria, 23*, 531-549.

Churcher, C. S. (1974). Relationships of the late Pleistocene vertebrate fauna from Kom Ombo, Upper Egypt. *Annals of the Geological Surveys in Egypt, 4*.

Clot, A., Brochet, G., Chaline, J., Desse, G., Evin, J., Granier, J., ... & Rage, J. C. (1984). Faune de la grotte préhistorique du bois du Cantet (Espèche, Hautes-Pyrénées, France). *Munibe, 36*(3).

Corona-Martinez, E. (2002). The Pleistocene bird record of México. *Acta Zoologica Cracovia, 45*, 293-306.

Elftman, H. O. (1931). Pleistocene mammals of Fossil Lake, Oregon. *American Museum novitates, 481*.

Emslie, S. D. (1985). The late Pleistocene (Rancholabrean) avifauna of Little Box Elder Cave, Wyoming. *Rocky Mountain Geology, 23*(2), 63-82.

Emslie, S. D. (1998). Avian community, climate, and sea-level changes in the Plio-Pleistocene of the Florida Peninsula. *Ornithological Monographs*, 1-113.

Emslie, S. D. (2004). *The early and middle Pleistocene avifauna from Porcupine Cave. Biodiversity Response to Climate Change in the Middle Pleistocene: The Porcupine Cave Fauna from Colorado* (A. Barnosky, Ed.). University of California Press, Berkeley, 127-140.

Eshelman, R. E. (1975). Geology and Paleontology of the Early Pleistocene (Late Blancan) White Rock Fauna from North-Central Kansas. *Claude W. Hibbard Memorial Volume IV*.

Feduccia, A. (1973). Fossil Birds from the Late Pleistocene Ingleside Fauna, San Patricio County, Texas. *The Condor, 75*(2), 243-244.

Gorobets, L. V., & Yanenko, V. O. (2018). Late Pleistocene Birds from Binagada (Azerbaijan) in Collection of the National Museum of Natural History (Kyiv, Ukraine). *Vestnik zoologii, 52*(1), 31-36.

Guilday, J. E., Parmalee, P. W., & Hamilton, H. W. (1977). The Clark's Cave bone deposit and the late Pleistocene paleoecology of the central Appalachian Mountains of Virginia. *Bulletin of Carnegie Museum of Natural History, 2.*

Guthrie, D. A. (2005). Distribution and provenance of fossil avifauna on San Miguel Island. In *Proceedings of the Sixth California Islands Symposium. National Park Service Technical Publication CHIS-05-01. Institute for Wildlife Studies, Arcata* 35-42.

Harris, A. H. (1993). Quarternary vertebrates of New Mexico. Bulletin 2. *New Mexico Museum of Natural History and Science*, 179-198.

Harrison, C. J. O. (1979). Birds of the Cromer Forest bed series of the East Anglian Pleistocene. *Transactions of the Norfolk and Norwich Naturalists' Society, 24*, 277-286.

Harrison, C. J. O. (1980). A re-examination of British Devensian and earlier Holocene bird bones in the British Museum (Natural History). *Journal of Archaeological Science, 7*(1), 53-68.

Harrison, C. J. O. (1987). Pleistocene and prehistoric birds of south-west Britain. *Proceedings of the University of Bristol Spelaeological Society, 18*(1), 81-104.

Howard, H. (1936). Further studies upon the birds of the Pleistocene of Rancho La Brea. *The Condor, 38*(1), 32-36.

Howard, H. (1955). *Fossil birds from Manix Lake, California*. US Government Printing Office.

Jefferson, G. T. (1987). *The Camp Cady local fauna: paleoenvironment of the Lake Manix basin*. San Bernardino County Museum.

Matsuoka, H. (2000). The Late Pleistocene Fossil Birds of the Central and Southern Ryukyu Islands, and their Zoogeographical Implications for the Recent Avifauna of the Archipelago. *Tropics, 10*(1), 165-188.

Meijer, H. J., Sutikna, T., Saptomo, E. W., Awe, R. D., Jatmiko, Wasisto, S., ... & Tocheri, M. W. (2013). Late Pleistocene-Holocene non-Passerine Avifauna of Liang Bua (Flores, Indonesia). *Journal of Vertebrate Paleontology, 33*(4), 877-894.

Miller, L. (1935). A second avifauna from the McKittrick Pleistocene. *The Condor, 37*(2), 72-79.

Miller, L. (1943). *The Pleistocene birds of San Josecito Cavern, Mexico*. University of California Press.

Mourer-Chauviré, C., & Geraads, D. (2010). The upper Pliocene avifauna of Ahl al Oughlam, Morocco. Systematics and biogeography. *Records of the Australian Museum, 62*(1), 157-184.

Olson, S. L., & James, H. F. (1991). *Descriptions of thirty-two new species of birds from the Hawaiian Islands, Part 1: Non-Passeriformes*. Smithsonian Institution, Washington DC.

Olson, S. L., Pregill, G. K., & Hilgartner, W. B. (1990). *Studies on fossil and extant vertebrates from San Salvador (Watling's) Island, Bahamas*. Smithsonian Contributions to Zoology.

Parmalee, P. W. (1992). A late Pleistocene avifauna from northwestern Alabama. *Natural History Museum of Los Angeles County Science Series, 36*, 307-318.

Parmalee, P. W., & Klippel, W. E. (1982). Evidence of a boreal avifauna in middle Tennessee during the late Pleistocene. *The Auk, 99*(2), 365-368.

Pavia, M. (1999). The Middle Pleistocene avifauna of the Spinagallo Cave (Sicily, Italy): preliminary report. *Smithsonian Contributions to Paleobiology, 89*, 125-127.

Peters, J. (1990). Late Pleistocene Hunter-gatherers at Ishango (Eastern-Zaire). *Revue de paléobiologie*, (1), 73-112.

Reed, E. H., & Bourne, S. J. (2009). Pleistocene fossil vertebrate sites of the south east region of South Australia II. *Transactions of the Royal Society of South Australia, 133*(1), 30-40.

Sánchez-Marco, A. (1999). Implications of the avian fauna for paleoecology in the Early Pleistocene of the Iberian Peninsula. *Journal of Human Evolution, 37*(3-4), 375-388.

Shufeldt, R. W. (1891). *On a collection of fossil birds from the Equus beds of Oregon*. Essex Institute.

Steadman, D. W. (2005). Late Pleistocene birds from Kingston Saltpeter Cave, southern Appalachian Mountains, Georgia. *Bulletin of the Florida Museum of Natural History, 45*(4), 231-248.

Steadman, D. W., Oswald, J. A., & Rincón, A. D. (2015). The diversity and biogeography of late Pleistocene birds from the lowland Neotropics. *Quaternary Research, 83*(3), 555-564.

Tomek, T., Bocheński, Z. M., Socha, P., & Stefaniak, K. (2011). Continuous 300.000-year fossil record: changes in the ornithofauna of Biśnik Cave, Poland. *Palaeontologia Electronica, 15*(1), 1-20.

Van Tets, G. F., & Smith, M. J. (1974). Small fossil vertebrates from Victoria Cave, Naracoorte, South Australia. III. Birds (Aves). *Transactions of the Royal Society of South Australia, 97*(4), 185-198

Weesie, P. D. (1988). The quaternary avifauna of Crete, Greece. *Palaeovertebrata 18*, 1-94

Wetmore, A. (1962). *Notes on fossil and subfossil birds*. Smithsonian Miscellaneous Collections.

Zelenkov, N. V., Kurochkin, E. N., Karhu, A. A., & Ballmann, P. (2008). Birds of the Late Pleistocene and Holocene from the Palaeolithic Djuktai Cave site of Yakutia, Eastern Siberia. *Oryctos, 7*, 213-222.

Appendix 3: Genbank accession numbers for the mitochondrial genomes (Chapter 2)

Species	Accesion number
Abrornis inornata(Phylloscopus)	NC_024726
Acanthis flammea	NC_027285
Acanthisitta chloris	AY325307
Accipiter gentilis	NC_011818
Accipiter gularis	KX585864 / EU583261
Accipiter nisus	NC_025580
Accipiter soloensis	KJ680303
Accipiter virgatus	NC_026082
Aceros corrugatus	HM755883
Aceros waldeni	NC_015085
Acridotheres cristatellus	NC_015613
Acridotheres tristis (Sturnus)	NC_015195
Acrocephalus scirpaceus	NC_010227
Acryllium vulturinum	NC_014180
Aegithalos bonvaloti	NC_024267
Aegithalos caudatus	KF951088
Aegithalos concinnus	KF951092
Aegithalos fuliginosus	NC_024266
Aegithalos glaucogularis	NC_024268
Aegotheles cristatus	NC_011718
Aegypius monachus	KF682364
Aepyornis hildebrandti	KJ749824
Aethopyga gouldiae	NC_027241
Agapornis roseicollis	NC_011708
Agelaius phoeniceus	NC_018801
Aix galericulata	NC_023969
Akialoa obscura	NC_031349
Alauda arvensis	NC_020425
Alectoris chukar	NC_020585
Alectura lathami	NC_007227
Amaurornis akool	NC_023982
Amaurornis phoenicurus	NC_024593
Amazilia versicolor	NC_024156
Amazona barbadensis	JX524615
Amazona ochrocephala	NC_027840
Amblyramphus holosericeus	NC_018802
Anas acuta	NC_024631
Anas chathamica	KF562761
Anas clypeata	NC_028346
Anas crecca	NC_022452
Anas formosa	NC_015482
Anas platyrhynchos	NC_009684
Anas poecilorhyncha	NC_022418
Anhinga rufa	GU071055
Anomalopteryx didiformis	NC_002779
Anser albifrons	NC_004539
Anser anser	NC_011196
Anser cygnoides	NC_023832
Anser fabalis	NC_016922
Anser indicus	NC_025654
Anseranas semipalmata	NC_005933
Anthornis melanura	KC545408
Anthropoides paradiseus	NC_020572
Anthropoides virgo	NC_020573
Anthus hodgsoni	KX189345
Anthus novaeseelandiae	NC_029137
Aphrodroma brevirostris	NC_007174
Aptenodytes forsteri	NC_027938
Apteryx australis	KU695537
Apteryx haastii	NC_002782
Apteryx owenii	NC_013806
Apus apus	NC_008540
Aquila chrysaetos	NC_024087
Ara ararauna	NC_029319
Ara glaucogularis	NC_026029
Ara militaris	NC_027839
Aratinga (Psittaccara) mitrata	JX215256
Arborophila ardens	NC_022683
Arborophila brunneopectus	NC_022684
Arborophila gingica	FJ752425
Arborophila rufipectus	NC_012453
Arborophila rufogularis	NC_020584
Archilochus colubris	NC_010094

Ardea cinerea	NC_025900
Ardea intermedia	NC_025918
Ardea modesta	NC_025916
Ardea novaehollandiae	NC_008551
Ardea purpurea	NC_025919
Ardeola bacchus	NC_025921
Arenaria interpres	NC_003712
Argusianus argus	JQ713768
Arremon aurantiirostris	NC_027731
Asio flammeus	NC_027606
Athene brama	KF961185
Aythya americana	NC_000877
Aythya ferina	NC_024602
Aythya fuligula	NC_024595
Babax lanceolatus	KR818090
Balaeniceps rex	GU071053
Balearica pavonina	NC_020570
Balearica regulorum	NC_020569
Bambusicola fytchii	NC_020583
Bambusicola thoracica	NC_011816
Bombycilla cedrorum	KJ909187
Botaurus stellaris	NC_025923
Branta bernicla	KJ680301
Branta canadensis	NC_007011
Brotogeris cyanoptera	NC_015530
Bubo blakistoni	LC099103
Bubo bubo	AB918148
Bubo flavipes	LC099100
Bubulcus ibis	NC_025917
Bucorvus leadbeateri	NC_015199
Buteo buteo	NC_003128
Buteo hemilasius	NC_029377
Buteo lagopus	NC_029189
Butorides striata	NC_025922
Bycanistes brevis	NC_015201
Cacatua moluccensis	NC_020592
Cacatua pastinator	JF414240
Cairina moschata	NC_010965
Callaeas cinereus	NC_031350
Callipepla squamata	NC_029340
Calliphlox amethystina	NC_030286
Caloperdix oculeus	NC_024619
Calyptorhynchus baudinii	NC_020594
Calyptorhynchus lathami	NC_020593
Calyptorhynchus latirostris	NC_020595
Campephilus guatemalensis	NC_028020
Campephilus imperialis	KU158198
Campylorhynchus brunneicapillus	NC_029482
Campylorhynchus zonatus	NC_022840
Caprimulgus indicus	NC_025773
Cardinalis cardinalis	NC_025618
Carduelis (Spinus) psaltria	NC_025627
Carduelis (Spinus) spinus	NC_015198
Carduelis pinus	NC_025619
Carduelis sinica	NC_015196
Carpodacus erythrinus	NC_025597
Carpodacus roseus	NC_025607
Casuarius casuarius	NC_002778
Cathartes aura	NC_007628
Cecropis daurica	NC_024107
Centropus sinensis	KT947122
Ceryle rudis	NC_024280
Chaetura pelagica	NC_028545
Chalcophaps indica	HM746789
Chlorophanes spiza	NC_025606
Chroicocephalus ridibundus	NC_025649
Chrysolampis mosquitus	NC_025786
Chrysolophus amherstiae	NC_020590
Chrysolophus pictus	NC_014576
Chrysomus cyanopus	NC_018813
Chrysomus icterocephalus	NC_018799
Chrysomus ruficapillus	NC_018796
Chrysomus thilius	NC_018807
Chrysomus xanthophthalmus	NC_018798
Ciconia boyciana	NC_002196
Ciconia ciconia	NC_002197
Ciconia nigra	NC_023946
Cnemotriccus fuscatus	NC_007975
Coccothraustes coccothraustes	NC_025614
Colinus virginianus	NC_024620
Columba janthina	KM926619
Columba livia	NC_013978

Copsychus saularis	NC_030603
Coracopsis vasa	NC_027841
Corvus brachyrhynchos	NC_026461
Corvus cornix	NC_024698
Corvus frugilegus	NC_002069
Corvus hawaiiensis	NC_026783
Corvus macrorhynchos	NC_027173
Corvus moriorum	NC_031518
Corvus splendens	NC_024607
Coturnicops exquisitus	NC_012143
Coturnix chinensis	NC_004575
Coturnix japonica	NC_003408
Crax daubentoni	NC_024617
Crax rubra	NC_024618
Crossoptilon auritum	NC_015897
Crossoptilon crossoptilon	NC_016679
Crossoptilon harmani	NC_026547
Crossoptilon mantchuricum	NC_026548
Crotophaga ani	HM746794
Cuculus poliocephalus	NC_028414
Curaeus curaeus	NC_018808
Cyanistes cyanus	KX388472
Cyanopica cyanus	NC_015824
Cyanoptila cyanomelana	NC_015232
Cygnus atratus	NC_012843
Cygnus columbianus	NC_017604
Cygnus cygnus	NC_027095
Cygnus olor	NC_027096
Dendrocopos leucotos	NC_029862
Dendrocopos major	NC_028174
Dendrocygna javanica	NC_012844
Deroptyus accipitrinus	KM611476
Dinornis giganteus	NC_002672
Diomedea chrysostoma	AP009193
Dives dives	NC_018800
Dromaius novaehollandiae	NC_002784
Dryocopus pileatus	NC_008546
Dupetor flavicollis	NC_024575
Eclectus roratus	NC_027842
Ectopistes migratorius	KC489473
Egretta eulophotes	NC_009736
Egretta garzetta	NC_023981
Egretta sacra	NC_025920

Emberiza (Schoeniclus) elegans	NC_030368
Emberiza (Schoeniclus) rustica	NC_024924
Emberiza (Schoeniclus) spodocephala	NC_021445
Emberiza aureola (Schoeniclus aureolus)	NC_022150
Emberiza chrysophrys	NC_015233
Emberiza cioides	NC_024524
Emberiza jankowskii	NC_027251
Emberiza pusilla	NC_021408
Emberiza rutila	NC_024925
Emberiza tristrami	NC_015234
Emeus crassus	NC_002673
Eophona migratoria	NC_031374
Eopsaltria australis	NC_019665
Eopsaltria georgiana	NC_027230
Eopsaltria griseogularis	NC_027229
Epthianura albifrons	NC_019664
Eremopsaltria mongolica	NC_025616
Eudocimus ruber	NC_027504
Eudromia elegans	NC_002772
Eudynamys taitensis	NC_011709
Eudyptes chrysocome	NC_008138
Eudyptula minor	NC_004538
Eulabeornis castaneoventris	NC_025501
Euphagus cyanocephalus	NC_018827
Eupsittula pertinax	NC_015197
Eurynorhynchus pygmeus	NC_027496
Eurystomus orientalis	NC_011716
Falco cherrug	NC_026715
Falco columbarius	NC_025579
Falco naumanni	NC_029846
Falco peregrinus	NC_000878
Falco rusticolus	NC_029359
Falco sparverius	NC_008547
Falco tinnunculus	NC_011307
Ficedula zanthopygia	NC_015802
Fidecula albicollis	NC_021621
Florisuga fusca	NC_030287
Florisuga mellivora	NC_027455
Forpus modestus	HM755882
Forpus passerinus	NC_027843

Francolinus pintadeanus	NC_011817
Fregata sp.	AP009192
Fringilla coelebs	NC_025599
Fringilla montifringilla	NC_024048
Fringilla polatzeki	NC_031157
Fringilla teydea	KU705760
Fulica atra	NC_025500
Gallicolumba luzonica	HM746790
Gallicrex cinerea	NC_028408
Gallinula chloropus	NC_015236
Gallirallus australis	KF425525
Gallirallus okinawae	NC_012140
Gallirallus philippensis	NC_025507
Gallus gallus	NC_001323
Gallus lafayetii	NC_007239
Gallus sonneratii	NC_007240
Gallus varius	NC_007238
Garrulax affinis	NC_029402
Garrulax canorus	NC_020429
Garrulax cineraceus	NC_024553
Garrulax ocellatus	NC_027657
Garrulax perspicillatus	NC_026068
Garrulax poecilorhynchus	NC_028082
Garrulax sannio	NC_028186
Garrulus glandarius	NC_015810
Gavia pacifica	NC_008139
Gavia stellata	NC_007007
Geococcyx californianus	NC_011711
Geopelia striata	HM746791
Geospiza fortis	KM891730
Geotrygon violacea	NC_015207
Gerygone igata	NC_029139
Glaucidium brodiei	KP684122
Gnorimopsar chopi	NC_018795
Gorsachius goisagi	NC_028194
Gorsachius magnificus	NC_028193
Gorsachius melanolophus	NC_028195
Goura cristata	LN589994
Goura scheepmakeri	NC_027947
Goura victoria	LN589993
Gracula religiosa	NC_015898
Grus americana	NC_020576
Grus antigone	NC_020581
Grus canadensis	NC_020582
Grus carunculatus	NC_020571
Grus grus	NC_020577
Grus japonensis	NC_020575
Grus leucogeranus	NC_020574
Grus monacha	NC_020578
Grus nigricollis	NC_020579
Grus rubicunda	NC_020580
Grus vipio	NC_021368
Gymnomystax mexicanus	NC_018812
Haematopus ater	NC_003713
Haemorhous cassinii	NC_025613
Haemorhous mexicanus	NC_025610
Halcyon coromanda	NC_028177
Halcyon pileata	NC_024198
Halcyon smyrnensis	KT965614
Heliodoxa aurescens	NC_030285
Heliornis fulica	NC_025499
Hemignathus flavus	NC_025608
Hemignathus parvus	NC_025622
Hemignathus stejnegeri	NC_025624
Hemignathus virens	KM078788
Hemiphaga novaeseelandiae	NC_013244
Henicorhina leucosticta	NC_024673
Hesperiphona vespertina	NC_025600
Heteralocha acutirostris	NC_031351
Hieraaetus fasciatus	NC_029188
Himatione sanguinea	NC_025602
Hirundo rustica	KX398931
Hyliota flavigaster	NC_024868
Hylocharis cyanus	NC_027453
Ichthyaetus relictus	NC_023777
Icterus mesomelas	JX516068
Ithaginis cruentus	NC_018033
Ixobrychus cinnamomeus	NC_015077
Ixobrychus eurhythmus	NC_025924
Ixobrychus sinensis	NC_025925
Jacana jacana	NC_024069
Jacana spinosa	NC_024068
Lampropsar tanagrinus	JX516057
Lanius cristatus	NC_028333
Lanius isabellinus	NC_027655
Lanius schach	NC_030604

Lanius sphenocercus	KU884610
Lanius tephronotus	NC_021105
Larus brunnicephalus	NC_018548
Larus crassirostris	NC_025556
Larus dominicanus	NC_007006
Larus vegae	NC_029383
Leiothrix argentauris	NC_015114
Leiothrix lutea	NC_020427
Lepidothrix coronata	KJ909196
Leptotila verreauxi	NC_015190
Leucocarbo (Phalacrocorax) chalconotus	GU071054
Leucosticte arctoa	NC_025615
Leucosticte brandti	NC_025604
Lewinia muelleri	NC_025502
Lonchura punctulata	NC_028036
Lonchura striata	NC_029475
Lophophanes dichrous	KX388477
Lophophorus lhuysii	NC_013979
Lophophorus sclateri	NC_020589
Lophura ignita	NC_010781
Lophura nycthemera	NC_012895
Lophura swinhoii	NC_023779
Loxia curvirostra	NC_025623
Loxops caeruleirostris	NC_025605
Loxops coccineus	NC_025612
Loxops mana	NC_025598
Luscinia calliope	NC_015074
Luscinia cyanura	NC_026067
Lyrurus tetrix	NC_024554
Machlolophus spilonotus	KX388476
Macroagelaius imthurni	NC_018810
Malurus melanocephalus	NC_024873
Mareca (Anas) falcata	NC_023352
Megalurus pryeri	NC_029151
Megalurus punctatus	NC_029138
Melamprosops phaeosoma	NC_025617
Meleagris gallopavo	NC_010195
Meleagris ocellata	KU094576
Melophus lathami	KX702277
Melopsittacus undulatus	NC_009134
Menura novaehollandiae	NC_007883
Mergus squamatus	NC_016723
Micrastur gilvicollis	NC_008548
Minla ignotincta	NC_030588
Mionectes oleagineus	NC_024682
Moho braccatus	NC_031348
Mohoua novaeseelandiae	KC545409
Molothrus aeneus	NC_018806
Molothrus badius	NC_018811
Montifringilla adamsi	NC_025913
Montifringilla nivalis	NC_025911
Montifringilla ruficollis	NC_022815
Montifringilla taczanowskii	NC_025914
Morus serrator	GU071056
Motacilla alba	NC_029229
Motacilla cinerea	NC_027933
Motacilla lugens	NC_029703
Mullerornis agilis	KJ749825
Myadestes myadestinus	NC_031352
Myiopsitta monachus	NC_027844
Nannopterum brasilianus	NC_029758
Neophema chrysogaster	NC_019804
Nesopsar nigerrimus	NC_018794
Nestor notabilis	NC_027845
Netta rufina	NC_024922
Ninox novaeseelandiae	NC_005932
Ninox scutulata	NC_029384
Nipponia nippon	NC_008132
Nisaetus alboniger	NC_007599
Nisaetus nipalensis	NC_007598
Notiomystis cincta	NC_029140
Nucifraga columbiana	NC_022839
Numenius phaeopus	NC_030507
Numida meleagris	NC_006382
Nyctibius grandis	EU344977
Nyctibius griseus	HM746792
Nycticorax nycticorax	NC_015807
Nymphicus hollandicus	NC_015192
Oedistoma iliolophum (iliolophus)	NC_024865
Oreomystis bairdi	NC_025628
Oreopsar bolivianus	NC_018797
Oreotrochilus melanogaster	NC_027454
Oriolus chinensis	NC_020424

Orthopsittaca manilata	NC_029161
Otis tarda	NC_014046
Otus bakkamoena	NC_028163
Otus scops	NC_028162
Pachyplichas yaldwyni	KX369036
Padda oryzivora	NC_028441
Pandion haliaetus	NC_008550
Paradoxornis fulvifrons	NC_028436
Paradoxornis nipalensis	NC_028437
Paradoxornis webbianus	NC_024539
Paroreomyza montana	NC_025601
Parus major	NC_026293
Parus monticolus	NC_028187
Parus venustulus	NC_026701
Passer ammodendri	NC_029344
Passer domesticus	NC_025611
Passer montanus	NC_024821
Pavo cristatus	NC_024533
Pavo muticus	NC_012897
Pelagodroma marina	KC875856
Pelecanus conspicillatus	DQ780883
Penelopides panini	NC_015087
Perdix dauurica	NC_020588
Perdix hodgsoniae	NC_023940
Pericrocotus ethologus	NC_024257
Periparus ater	NC_026223
Petroica australis	NC_029141
Petroica boodang	NC_019666
Petroica goodenovii	NC_019667
Petroica macrocephala	NC_029142
Petroica phoenicea	NC_019668
Phaethon lepturus	NC_027275
Phaethon rubricauda	NC_007979
Phaethornis hispidus	KP853098
Phaethornis malaris	NC_030288
Phalacrocorax carbo	NC_027267
Phalcoboenus australis	KP064202
Phasianus colchicus	NC_015526
Phasianus versicolor	NC_010778
Philesturnus carunculatus	NC_029143
Phodilus badius	NC_023787
Phoebastria albatrus	NC_026190
Phoebastria immutabilis	NC_026189
Phoebastria nigripes	NC_026188
Phoenicopterus roseus	NC_010089
Phoenicopterus ruber	NC_027934
Phoenicurus auroreus	NC_026066
Pica pica	NC_015200
Picathartes gymnocephalus	KJ909200
Picoides pubescens	NC_027936
Pinguinus impennis	NC_031347
Pinicola enucleator	NC_025609
Pipile pipile	KU221053
Pitta nympha	NC_027067
Platalea leucorodia	NC_012772
Platalea minor	NC_010962
Podiceps cristatus	NC_008140
Podoces hendersoni	NC_014879
Poecile atricapilla	NC_024867
Poecile montanus	KX388479
Poecile palustris	NC_026911
Polyplectron bicalcaratum	NC_012900
Polyplectron germaini	NC_023264
Polyplectron napoleonis	NC_024615
Pomatorhinus ruficollis	NC_029769
Poospiza cabanisi	NC_028038
Poospiza lateralis	NC_028039
Poospiza thoracica	NC_028037
Porphyrio hochstetteri	NC_010092
Porphyrio porphyrio	NC_025508
Primolius couloni	NC_025742
Primolius maracana	NC_029322
Prioniturus luconensis	NC_027846
Procellaria cinerea	AP009191
Progne chalybea	NC_020605
Prosthemadera novaeseelandiae	NC_029144
Prunella montanella	NC_027284
Prunella strophiata	KU975800
Psephotellus pulcherrimus	NC_031358
Pseudoleistes guirahuro	NC_018809
Pseudoleistes virescens	NC_018805
Pseudonestor xanthophrys	NC_025630
Pseudopodoces humilis	NC_014341
Psittacara acuticaudatus	NC_020325
Psittacara brevipes	NC_021764

Psittacara rubritorquis	NC_026042
Psittacus erithacus	NC_027847 / KM611474
Psittirostra psittacea	NC_031353
Psittrichas fulgidus	NC_027848
Pterocnemia pennata	NC_002783
Pteroglossus azara	NC_008549
Ptilopachus petrosus	NC_024616
Pucrasia macrolopha	NC_020587
Pycnonotus melanicterus	NC_024730
Pycnonotus sinensis	NC_013838
Pycnonotus taivanus	NC_013483
Pycnonotus xanthorrhous	KX129905
Pygoscelis adeliae	NC_021137
Pygoscelis antarcticus	NC_021474
Pyrgilauda blanfordi	NC_025912
Pyrgilauda davidiana	NC_025915
Pyrrhocorax graculus	NC_025927
Pyrrhocorax pyrrhocorax	NC_025926
Pyrrhula pyrrhula	NC_025625
Pyrrhura rupicola	NC_028404
Quiscalus quiscula	NC_018803
Rallina eurizonoides	NC_012142
Recurvirostra avosetta	NC_027420
Regulus calendula	NC_024866
Regulus regulus	NC_029837
Remiz consobrinus	NC_021641
Rhea americana	NC_000846
Rhipidura fuliginosa	NC_029145
Rhynchopsitta terrisi	NC_021771
Rhynchortyx cinctus	KJ914547
Rhynochetos jubatus	NC_010091
Sagittarius serpentarius	NC_023788
Sasia ochracea	NC_028019
Saundersilarus saundersi	NC_017601
Sceloglaux albifacies	KX098448
Scolopax rusticola	NC_025521
Scytalopus magellanicus	KJ909189
Serinus albogularis	NC_025595
Serinus canaria	NC_023375
Serinus dorsostriatus	NC_025621
Sitta carolinensis	NC_024870
Smithornis sharpei	NC_000879
Spheniscus demersus	NC_022817
Spilornis cheela	NC_015887
Spizixos semitorques	NC_029321
Stachyris ruficeps	NC_030771
Stercorarius maccormicki	NC_026125
Sternula albifrons	NC_028176
Streptopelia chinensis	NC_026459
Streptopelia decaocto	KX372273
Streptopelia orientalis	NC_031447
Strigops habroptilus	NC_005931
Strix leptogrammica	KC953095
Struthio camelus	NC_002785
Sturnus cineraceus	NC_015237
Sturnus nigricollis	NC_020423
Sturnus sericeus	NC_014455
Sturnus vulgaris	NC_029360
Sylvia atricapilla	NC_010228
Sylvia crassirostris	NC_010229
Sylviparus modestus	NC_026793
Synthliboramphus antiquus	NC_007978
Synthliboramphus wumizusume	NC_029328
Syrmaticus ellioti	NC_010771
Syrmaticus humiae	NC_010774
Syrmaticus reevesii	NC_010770
Syrmaticus soemmerringi	NC_010767
Tachybaptus novaehollandiae	NC_010095
Tachybaptus ruficollis	NC_024594
Tachycineta albilinea	NC_020601
Tachycineta albiventer	NC_020602
Tachycineta bicolor	NC_020596
Tachycineta cyaneoviridis	NC_020599
Tachycineta euchrysea	NC_020598
Tachycineta leucorrhoa	NC_020603
Tachycineta meyeni	NC_020604
Tachycineta stolzmanni	NC_020600
Tachycineta thalassina	NC_020597
Tadorna ferruginea	NC_024640
Tadorna tadorna	NC_024750
Taeniopygia guttata	NC_007897
Tanygnathus lucionensis	KM611480
Tetraogallus himalayensis	NC_027279

Tetraogallus tibetanus	NC_023939
Tetraophasis obscurus	NC_018034
Tetraophasis szechenyii	NC_020613
Tetrastes bonasia	NC_020591
Tetrastes sewerzowi	NC_025318
Thalassarche melanophrys	NC_007172
Thamnophilus nigrocinereus	KJ909192
Thraupis episcopus	NC_025596
Threskiornis aethiopicus	NC_013146
Tinamus guttatus	NC_027260
Tinamus major	NC_002781
Todiramphus sanctus	NC_011712
Tragopan caboti	NC_013619
Tragopan temminckii	NC_020586
Traversia lyalli	KX369034
Tregellasia capito	NC_027231
Tregellasia leucops	NC_024871
Tringa erythropus	NC_030585
Trogon viridis	NC_011714
Turdus eunomus	NC_028273
Turdus hortulorum	NC_024552
Turdus merula	NC_028188
Turdus migratorius	NC_024872
Turdus naumanni	KJ834096
Turdus philomelos	NC_029147
Turdus rufiventris	NC_028179
Turnagra capensis	NC_028336
Turtur tympanistria	HM746793
Tyto alba	EU410491
Tyto longimembris	KP893332
Upupa epops	NC_028178
Uragus sibiricus	NC_025594
Urocissa erythrorhyncha	NC_020426
Vanellus cinereus	NC_025514
Vanellus vanellus	NC_025637
Vestiaria coccinea	NC_025620
Vidua chalybeata	NC_000880
Vireo olivaceus	NC_024869
Xanthopsar flavus	NC_018804
Xenicus gilviventris	KX369033
Xenicus longipes	KX369035
Yuhina diademata	NC_029462
Zenaida auriculata	NC_015203
Zoothera dauma	KT340629
Zosterops erythropleurus	NC_027942
Zosterops japonicus	KT601061
Zosterops lateralis	NC_029146

Appendix 4: Accession numbers for shorebird species' mitocondrial DNA data (Chapter 2)

Arenaria interpres

Barcode of Life	Locality
BISE200-08	Sweden, Oland
BISE323-08	Sweden, Oland
BON092-06	Norway, Finnmark
BON222-07	Norway, Finnmark
BOTW060-04	US, Florida
BROM274-06	Canada, Nunavut
BROM276-06	Norway, Finnmark
BROM277-06	Russia, Krasnoyarsk
BROM711-07	US, Alaska
HCBR177-04	Canada, Nunavut
KBPBU194-06	Russia, Chukot
KBPBU195-06	Russia, Magadan
KBPBU196-06	Russia, Promorsky Krai
KBPBU197-06	Russia, Kamchatka Krai
SWEBI026-11	Sweden, Oeland

Calidris alpina

GenBank	Locality
L06721 - L06755	See Wenink et al. (1993)
KP205178 - KP205271	See Miller et al. (2015)

Calidris canutus

Barcode of Life	GenBank	Locality
BROM307-06		Argentina, Tierra del Fuego
BROM310-06		Australia, Queensland
BROM308-06		Australia, W Australia
BROM309-06		Australia, W Australia
BROM311-06		Canada, Nunavut
BROM312-06		Canada, Nunavut
TZBNA133-03	AY666343	Canada, Quebec
BOTW061-04	DQ432799	US, Florida
BROM319-06		US, Florida
BROM314-06		Netherlands, Friesland
BROM315-06		Netherlands, Friesland

BON373-07	GU571299	Norway, Troms
BON374-07	GU571300	Norway, Troms
BROM316-06		New Zaeland, North Auckland
KBPBU218-06	GQ481436	Russia, Chukot
KBPBU219-06	GQ481437	Russia, Chukot
BROM317-06		Russia, Krasnoyarsk
BROM318-06		Russia, Krasnoyarsk
KBPBU220-06	GQ481435	Russia, Magadan
BISE180-08	GU571779	Sweden
BISE378-08	GU571778	Sweden, Ostergotland

Calidris ptilocnemis

GenBank	**Subspecies**
AY156153 - AY156154	*quarta*
AY156101 - AY156105	*couersi*
AY156233 - AY156237	*couersi*
AY156247 - AY156251	*tschuktschorum*
AY156154 - AY156258	*tschuktschorum*
AY156137 - AY156141	*tschuktschorum*
AY156143	*tschuktschorum*
AY156252 - AY156253	*tschuktschorum*
AY156143 - AY156147	*ptilocnemis*
AY156148 - AY156152	*ptilocnemis*

Charadrius hiaticula

Barcode of Life	**GenBank**	**Locality**
BISE201-08	GU571812	Sweden, Oland
BISE327-08	GU571811	Sweden, Oland
BOTW173-04	DQ432843	UK, Suffolk
GBIR5698-15	KF946637	Netherlands
BOTW300-05	DQ432844	Iceland, Sudurnes, Keflavik
BROM640-07		Iceland, Sudurnes, Keflavik
BROM735-07		Iceland, Sudurnes, Keflavik
BROM639-07		South Africa, Western Cape
BON022-06	GU571330	Norway, Finnmark
BON218-07	GU571331	Norway, Finnmark
BROM491-07		Russia, Chukot Autonomus Okrug
BROM667-07		Finland, Lapland
BROM668-07		Russia, Yamal-Nenets
BROM879-08		Russia, Chukot Autonomus Okrug

Limosa limosa

Barcode of Life	GenBank	Subspecies
	JQ657321	*islandica*
	JQ657320	*Islándica*
	JQ657319	*Islándica*
	JQ657318	*limosa*
	JQ657317	*limosa*
	JQ657316	*limosa*
	JQ657315	*limosa*
	JQ657314	*limosa*
	JQ657313	*limosa*
	JQ657312	*limosa*
	JQ657311	*limosa*
	JQ657310	*limosa*
	JQ657309	*limosa*
	JQ657308	*limosa*
	JQ657307	*limosa*
	JQ657306	*limosa*
	JQ657305	*limosa*
	JQ657304	*limosa*
	JQ657303	*limosa*
	JQ657302	*limosa*
	JQ657301	*limosa*
	JQ657300	*limosa*
	JQ657299	*limosa*
	JQ657298	*limosa*
	JQ657297	*limosa*
	JQ657296	*limosa*
	JQ657295	*limosa*
	JQ657294	*limosa*
	JQ657293	*limosa*
	JQ657292	*limosa*
	JQ657291	*limosa*
	JQ657290	*limosa*
	JQ657289	*limosa*
	JQ657288	*limosa*
	JQ657287	*limosa*
	JQ657286	*limosa*
	JQ657285	*limosa*
	JQ657284	*limosa*
	JQ657283	*limosa*
	JQ657282	*limosa*

	JQ657281	*limosa*
	JQ657280	*limosa*
	JQ657279	*limosa*
	JQ657278	*limosa*
	JQ657277	*limosa*
	JQ657276	*limosa*
	JQ657275	*limosa*
	JQ657274	*limosa*
	JQ657273	*limosa*
	JQ657272	*limosa*
	JQ657271	*limosa*
	JQ657270	*limosa*
	JQ657269	*limosa*
	JQ657268	*limosa*
	JQ657322	*melanuroides*
BROM195-06		*islandica*
BROM196-06		*islandica*
BROM203-06		*limosa*
BROM204-06		*limosa*
BROM215-06		*melanuroides*
BROM248-06		*melanuroides*
BROM817-07		*limosa*
BROM818-07		*limosa*
BROM819-07	KF009544	*islandica*
BROM820-07		*melanuroides*
BROM821-07	KF009543	*melanuroides*
BROM822-07		*melanuroides*
BROM823-07		*melanuroides*
BROM905-08		*islandica*
BROM906-08		*melanuroides*
BROM907-08		*melanuroides*
KBPBU152-06	GQ482065	*melanuroides*
KBPBU779-06	GQ482064	*melanuroides*
KBPBU780-06	GQ482062	*melanuroides*
KKB290-05	GQ482063	*melanuroides*
KKB728-05	GQ482066	*melanuroides*
SWEBI020-11		*limosa*

Pluvialis apricaria

Barcode of Life	GenBank	Region
GBIR5699-15	KF946832	Netherlands
GBIR5700-15	KF946831	Netherlands
BROM586-07		Finland, Lapland
BROM832-07		Finland, Lapland
BON214-07	GU571580	Norway, Finnmark
BON220-07	GU571581	Norway, Finnmark
KBPBU168-06	GQ482505	Russia, Murmansk
KBPBU169-06	GQ482507	Russia, Murmansk
BROM656-07		Russia, Yamal-Nenets Autonomous Okrug
KBPBU170-06	GQ482506	Russia, Yamal-Nenets Autonomous Okrug
KBPBU171-06	GQ482504	Russia, Yamal-Nenets Autonomous Okrug
BISE481-08	GU572050	Sweden
BISE482-08	GU572049	Sweden
BOTW044-04	JN801365	Sweden, Lappland
BISE038-07	GU572051	Sweden, Stockholm
BROM609-07		Netherlands, Friesland
BROM831-07		Germany, Schleswig-Holstein

Pluvialis dominica

Barcode of Life	GenBank	Region
KB606-04	DQ433964	Canada, Manitoba
KB607-04	DQ433963	Canada, Manitoba
KB608-04	DQ433962	Canada, Manitoba
BROM554-07		Canada, Nunavut
BROM595-07		Canada, Nunavut
BROM608-07		Canada, Nunavut
BROM702-07		Canada, Nunavut
BROM833-07		Canada, Ontario
BROM549-07		US, Alaska
BBB603-13	KM896538	Brazil
KAARG440-07	FJ028119	Argentina
BROM548-07		Argentina, Chubut
TZB136-03	AY666317	US, Texas

Pluvialis fulva

Barcode of Life	GenBank	Region
BROM606-07		Russia, Chukot Autonomous Okrug
BROM834-07		Russia, Chukot Autonomous Okrug
KBPBU165-06	GQ482509	Russia, Magadan

KBPBU166-06	GQ482508	Russia, Magadan
KBPBU167-06	GQ482510	Russia, Sakha-Yakutia
GBIR5346-13	JX297482	-
BROM598-07		Australia, W Australia
CDAMH084-05	DQ433122	Singapore
GBIR475-07	EF515745	South Korea
KBBI090-07		South Korea, Seoul-si
SIBHI003-11	JF498890	US, Hawaii
SIBHI004-11	JF498889	US, Hawaii
SIBHI077-11	JF498888	US, Hawaii
BOTW045-04	DQ433123	US, Johnston Atoll

Pluvialis squatarola

Barcode of Life	**GenBank**	**Region**	**Barcode of Life**
GBIR5702-15	KF946834	Netherlands?	squatarola NET1
GBIR5703-15	KF946833	Netherlands?	squatarola NET2
TZB154-03	AY666203	Canada, Alberta	squatarola CAN1
BROM441-06		Canada, Nunavut	squatarola CAN2
BROM615-07		Canada, Ontario	squatarola CAN3
KBPBU161-06	GQ482514	Russia, Chukot Autonomous Okrug	squatarola RUS1
KBPBU162-06	GQ482511	Russia, Chukot Autonomous Okrug	squatarola RUS2
BROM440-06		Russia, Krasnoyarsk Krai	squatarola RUS3
BROM584-07		Russia, Krasnoyarsk Krai	squatarola RUS4
BROM837-07		Russia, Krasnoyarsk Krai	squatarola RUS5
KBPBU164-06	GQ482513	Russia, Magadan	squatarola RUS6
KBPBU163-06	GQ482512	Russia, Sakha-Yakutia	squatarola RUS7
BISE390-08	GU572052	Sweden, Stockholm	squatarola SWE1
BROM442-06		Netherlands	squatarola NET3
BROM601-07		Australia, W Australia	squatarola aus
BROM839-07		Brazil	squatarola bra
BROM579-07		Guinea-Bissau	squatarola guin1
BROM836-07		Guinea-Bissau	squatarola guin2
GBIR474-07	EF515746	South Korea	squatarola kor1
KBBI181-07		South Korea, Gangwon	squatarola kor2
BOTW046-04	DQ433124	US, Florida	squatarola flo1
BROM665-07		US, Florida	squatarola flo2
BROM838-07		US, Florida	squatarola flo3
BROM840-07		US, Georgia	squatarola flo4
TZB145-03	AY666202	US, Texas	squatarola tex

References

Miller, M. P., Haig, S. M., Mullins, T. D., Ruan, L., Casler, B., Dondua, A., … Lanctot, R. B. (2015). Intercontinental genetic structure and gene flow in Dunlin (*Calidris alpina*), a potential vector of avian influenza. *Evolutionary Applications, 8*(2), 149–171. https://doi.org/10.1111/eva.12239

Wenink, P. W., Baker, A. J., & Tilanus, M. G. (1993). Hypervariable-control-region sequences reveal global population structuring in a long-distance migrant shorebird, the Dunlin (*Calidris alpina*). *Proceedings of the National Academy of Sciences of the United States of America, 90*(1), 94–98. https://doi.org/10.1073/pnas.90.1.94

Appendix 5: mtDNA molecular clock substitution rates estimations

Orders	12S	16S	ATP8	ATP6	COX1	COX2	COX3	CYTB	ND1	ND2	ND3	ND4	ND4L	ND5	ND6
Accipitriformes	0.0011	0.0004	0.0026	0.0023	0.0013	0.0011	0.0009	0.0012	0.0018	0.0023	0.0016	0.0018	0.0014	0.0015	0.0026
Anseriformes	0.001	0.0004	0.0025	0.0021	0.0013	0.0011	0.0011	0.0013	0.0017	0.002	0.0016	0.0017	0.0015	0.0016	0.0026
Apodiformes	0.0012	0.0005	0.0026	0.0021	0.0013	0.0011	0.0011	0.0013	0.0017	0.0022	0.0016	0.0018	0.0015	0.0018	0.0023
Bucerotiformes	0.0013	0.0006	0.0028	0.0021	0.0012	0.0011	0.0011	0.0013	0.0016	0.0022	0.0015	0.0018	0.0015	0.0019	0.0025
Caprimulgiformes	0.0013	0.0006	0.0028	0.002	0.001	0.001	0.0009	0.0011	0.0016	0.002	0.0014	0.0015	0.0015	0.0016	0.0022
Charadriiformes	0.0011	0.0005	0.0027	0.0021	0.0013	0.0011	0.001	0.0014	0.0018	0.0022	0.0016	0.0018	0.0015	0.0017	0.0023
Ciconiiformes	0.0009	0.0004	0.0028	0.002	0.0011	0.001	0.0011	0.0013	0.0016	0.0019	0.0015	0.0016	0.0015	0.0016	0.0027
Columbiformes	0.001	0.0006	0.0026	0.002	0.0012	0.0011	0.0011	0.0013	0.0016	0.0022	0.0015	0.0017	0.0015	0.0017	0.0024
Coraciiformes	0.0011	0.0005	0.0026	0.002	0.0013	0.0011	0.001	0.0014	0.0017	0.0023	0.0016	0.0018	0.0015	0.0018	0.0022
Cuculiformes	0.0013	0.0005	0.0028	0.0022	0.0013	0.0012	0.0011	0.0015	0.0018	0.0024	0.0016	0.002	0.0016	0.002	0.0021
Falconiformes	0.0013	0.0005	0.0027	0.0021	0.0014	0.0012	0.0011	0.0014	0.0017	0.0023	0.0016	0.0018	0.0016	0.0017	0.0023
Galliformes	0.0011	0.0005	0.0026	0.0021	0.0013	0.0011	0.0011	0.0014	0.0017	0.0022	0.0016	0.0018	0.0015	0.0019	0.0023
Gaviiformes	0.0009	0.0006	0.0026	0.0019	0.0011	0.001	0.001	0.0011	0.0015	0.0019	0.0015	0.0015	0.0014	0.0014	0.002
Gruiformes	0.0013	0.0005	0.0028	0.0021	0.0013	0.0011	0.0011	0.0014	0.0018	0.0023	0.0016	0.0019	0.0015	0.0019	0.0023
Otidiformes	0.0007	0.0005	0.002	0.0014	0.0009	0.0008	0.0007	0.0009	0.0011	0.0017	0.0013	0.0014	0.0012	0.0013	0.0017
Paleognathae	0.0011	0.0004	0.0028	0.0021	0.0013	0.0011	0.0011	0.0013	0.0017	0.0023	0.0016	0.0017	0.0015	0.0017	0.0026
Passeriformes	0.0008	0.0003	0.0025	0.0022	0.0013	0.0012	0.0011	0.0014	0.0018	0.0023	0.0017	0.0019	0.0016	0.0018	0.0023
Pelecaniformes	0.0013	0.0005	0.0027	0.0021	0.0013	0.0012	0.0011	0.0013	0.0018	0.0022	0.0016	0.0018	0.0015	0.0017	0.0025
Phaethontiformes	0.0014	0.0004	0.0028	0.0019	0.0012	0.001	0.0009	0.0012	0.0015	0.0019	0.0014	0.0016	0.0014	0.0016	0.0025
Phoenicopteriformes	0.0016	0.0004	0.0029	0.002	0.0012	0.0011	0.0011	0.0013	0.0017	0.002	0.0017	0.0019	0.0015	0.0017	0.0034
Piciformes	0.0016	0.0006	0.0027	0.002	0.0013	0.0011	0.0011	0.0014	0.0017	0.0023	0.0015	0.0018	0.0016	0.0018	0.0022
Podicipediformes	0.0008	0.0004	0.0022	0.002	0.0012	0.001	0.001	0.0014	0.0014	0.0019	0.0015	0.0016	0.0014	0.0016	0.002
Procellariiformes	0.001	0.0004	0.0026	0.0021	0.0012	0.0011	0.001	0.0013	0.0015	0.0021	0.0016	0.0017	0.0014	0.0017	0.0024
Psittaciformes	0.0015	0.0006	0.0027	0.0022	0.0013	0.0012	0.0011	0.0013	0.0018	0.0023	0.0016	0.0018	0.0015	0.0018	0.0024
Sphenisciformes	0.001	0.0005	0.0027	0.0021	0.0013	0.0011	0.001	0.0013	0.0017	0.0022	0.0016	0.0017	0.0015	0.0017	0.0024
Strigiformes	0.0015	0.0006	0.0029	0.0022	0.0012	0.0011	0.0011	0.0014	0.0017	0.0024	0.0016	0.0018	0.0015	0.0019	0.0025
Suliformes	0.0013	0.0004	0.0027	0.002	0.0013	0.0011	0.0011	0.0014	0.0018	0.0023	0.0016	0.0018	0.0016	0.0018	0.0025

Table S1: Estimation of the molecular clock substitution rates (in substitutions / site / lineage / My) for each mtDNA gene in the sampled avian orders

Appendix 6: Bayesian phylogenetic tree

Figure S1 (next pages): Time-calibrated avian phylogenetic tree based on complete mitochondrial genomes of from 621 bird species. Orders indicated in different colors.

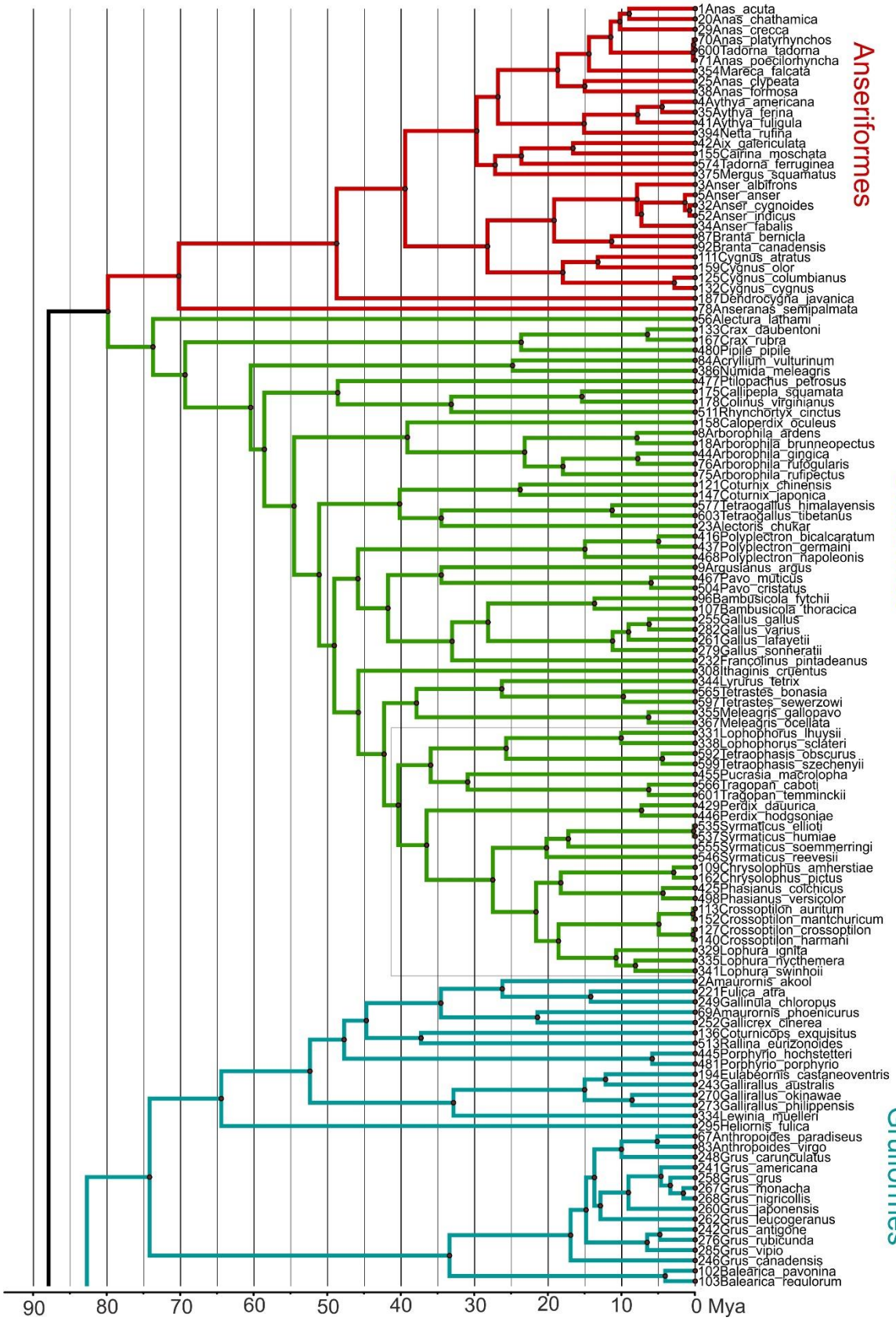
Anseriformes
Galliformes
Gruiformes
1Anas_acuta
20Anas_chathamica
29Anas_crecca
70Anas_platyrhynchos
600Tadorna_tadorna
71Anas_poecilorhyncha
354Mareca_falcata
25Anas_clypeata
38Anas_formosa
4Aythya_americana
35Aythya_ferina
41Aythya_fuligula
394Netta_rufina
42Aix_galericulata
155Cairina_moschata
574Tadorna_ferruginea
375Mergus_squamatus
3Anser_albifrons
5Anser_anser
32Anser_cygnoides
52Anser_indicus
34Anser_fabalis
87Branta_bernicla
92Branta_canadensis
111Cygnus_atratus
159Cygnus_olor
125Cygnus_columbianus
132Cygnus_cygnus
187Dendrocygna_javanica
78Anseranas_semipalmata
56Alectura_lathami
133Crax_daubentoni
167Crax_rubra
480Pipile_pipile
84Acryllium_vulturinum
386Numida_meleagris
477Ptilopachus_petrosus
175Callipepla_squamata
178Colinus_virginianus
511Rhynchortyx_cinctus
158Caloperdix_oculeus
8Arborophila_ardens
18Arborophila_brunneopectus
44Arborophila_gingica
76Arborophila_rufogularis
75Arborophila_rufipectus
121Coturnix_chinensis
147Coturnix_japonica
577Tetraogallus_himalayensis
603Tetraogallus_tibetanus
23Alectoris_chukar
416Polyplectron_bicalcaratum
437Polyplectron_germaini
468Polyplectron_napoleonis
9Argusianus_argus
467Pavo_muticus
504Pavo_cristatus
96Bambusicola_fytchii
107Bambusicola_thoracica
255Gallus_gallus
282Gallus_varius
261Gallus_lafayetii
279Gallus_sonneratii
232Francolinus_pintadeanus
308Ithaginis_cruentus
344Lyrurus_tetrix
565Tetrastes_bonasia
597Tetrastes_sewerzowi
355Meleagris_gallopavo
367Meleagris_ocellata
331Lophophorus_lhuysii
338Lophophorus_sclateri
592Tetraophasis_obscurus
599Tetraophasis_szechenyii
455Pucrasia_macrolopha
566Tragopan_caboti
601Tragopan_temminckii
429Perdix_dauurica
446Perdix_hodgsoniae
535Syrmaticus_ellioti
537Syrmaticus_humiae
555Syrmaticus_soemmerringi
546Syrmaticus_reevesii
109Chrysolophus_amherstiae
162Chrysolophus_pictus
425Phasianus_colchicus
498Phasianus_versicolor
113Crossoptilon_auritum
152Crossoptilon_mantchuricum
127Crossoptilon_crossoptilon
140Crossoptilon_harmani
329Lophura_ignita
335Lophura_nycthemera
341Lophura_swinhoii
2Amaurornis_akool
221Fulica_atra
249Gallinula_chloropus
69Amaurornis_phoenicurus
252Gallicrex_cinerea
136Coturnicops_exquisitus
513Rallina_eurizonoides
445Porphyrio_hochstetteri
481Porphyrio_porphyrio
194Eulabeornis_castaneoventris
243Gallirallus_australis
270Gallirallus_okinawae
273Gallirallus_philippensis
334Lewinia_muelleri
295Heliornis_fulica
67Anthropoides_paradiseus
83Anthropoides_virgo
248Grus_carunculatus
241Grus_americana
258Grus_grus
267Grus_monacha
268Grus_nigricollis
260Grus_japonensis
262Grus_leucogeranus
242Grus_antigone
276Grus_rubicunda
285Grus_vipio
246Grus_canadensis
102Balearica_pavonina
103Balearica_regulorum
90
80
70
60
50
40
30
20
10
0 Mya

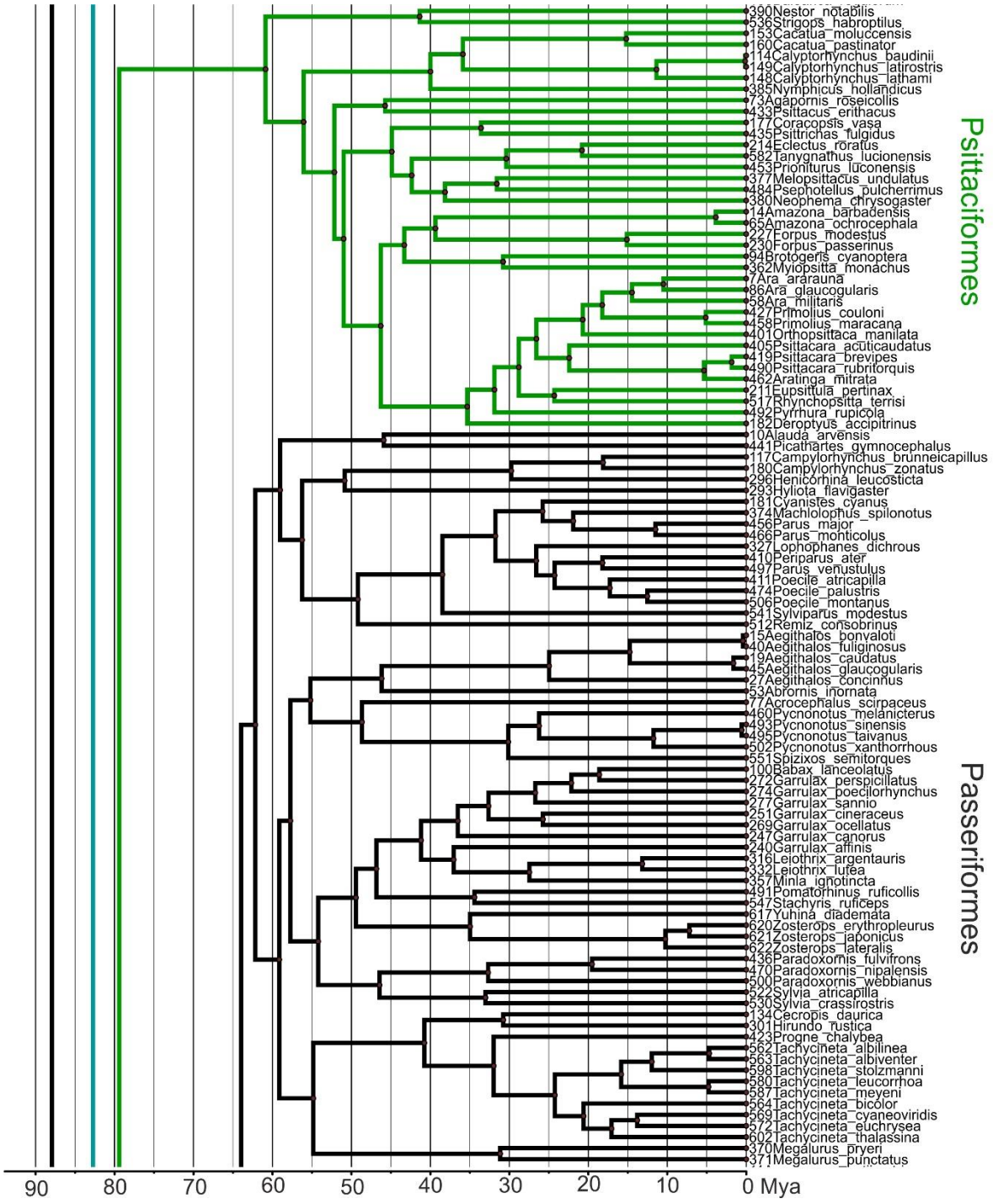
Psittaciformes
Passeriformes
390Nestor_notabilis
536Strigops_habroptilus
153Cacatua_moluccensis
160Cacatua_pastinator
114Calyptorhynchus_baudinii
149Calyptorhynchus_latirostris
148Calyptorhynchus_lathami
385Nymphicus_hollandicus
73Agapornis_roseicollis
433Psittacus_erithacus
177Coracopsis_vasa
435Psittrichas_fulgidus
214Eclectus_roratus
582Tanygnathus_lucionensis
453Prioniturus_luconensis
377Melopsittacus_undulatus
484Psephotellus_pulcherrimus
380Neophema_chrysogaster
14Amazona_barbadensis
65Amazona_ochrocephala
227Forpus_modestus
230Forpus_passerinus
94Brotogeris_cyanoptera
362Myiopsitta_monachus
7Ara_ararauna
86Ara_glaucogularis
58Ara_militaris
427Primolius_couloni
458Primolius_maracana
401Orthopsittaca_manilata
405Psittacara_acuticaudatus
419Psittacara_brevipes
490Psittacara_rubritorquis
462Aratinga_mitrata
211Eupsittula_pertinax
517Rhynchopsitta_terrisi
492Pyrrhura_rupicola
182Deroptyus_accipitrinus
10Alauda_arvensis
441Picathartes_gymnocephalus
117Campylorhynchus_brunneicapillus
180Campylorhynchus_zonatus
296Henicorhina_leucosticta
293Hyliota_flavigaster
181Cyanistes_cyanus
374Machlolophus_spilonotus
456Parus_major
466Parus_monticolus
327Lophophanes_dichrous
410Periparus_ater
497Parus_venustulus
411Poecile_atricapilla
474Poecile_palustris
506Poecile_montanus
541Sylviparus_modestus
512Remiz_consobrinus
15Aegithalos_bonvaloti
40Aegithalos_fuliginosus
19Aegithalos_caudatus
45Aegithalos_glaucogularis
27Aegithalos_concinnus
53Abrornis_inornata
77Acrocephalus_scirpaceus
460Pycnonotus_melanicterus
493Pycnonotus_sinensis
495Pycnonotus_taivanus
502Pycnonotus_xanthorrhous
551Spizixos_semitorques
100Babax_lanceolatus
272Garrulax_perspicillatus
274Garrulax_poecilorhynchus
277Garrulax_sannio
251Garrulax_cineraceus
269Garrulax_ocellatus
247Garrulax_canorus
240Garrulax_affinis
316Leiothrix_argentauris
332Leiothrix_lutea
357Minla_ignotincta
491Pomatorhinus_ruficollis
547Stachyris_ruficeps
617Yuhina_diademata
620Zosterops_erythropleurus
621Zosterops_japonicus
622Zosterops_lateralis
436Paradoxornis_fulvifrons
470Paradoxornis_nipalensis
500Paradoxornis_webbianus
522Sylvia_atricapilla
530Sylvia_crassirostris
134Cecropis_daurica
301Hirundo_rustica
423Progne_chalybea
562Tachycineta_albilinea
563Tachycineta_albiventer
598Tachycineta_stolzmanni
580Tachycineta_leucorrhoa
587Tachycineta_meyeni
564Tachycineta_bicolor
569Tachycineta_cyaneoviridis
572Tachycineta_euchrysea
602Tachycineta_thalassina
370Megalurus_pryeri
371Megalurus_punctatus
90
80
70
60
50
40
30
20
10
0 Mya

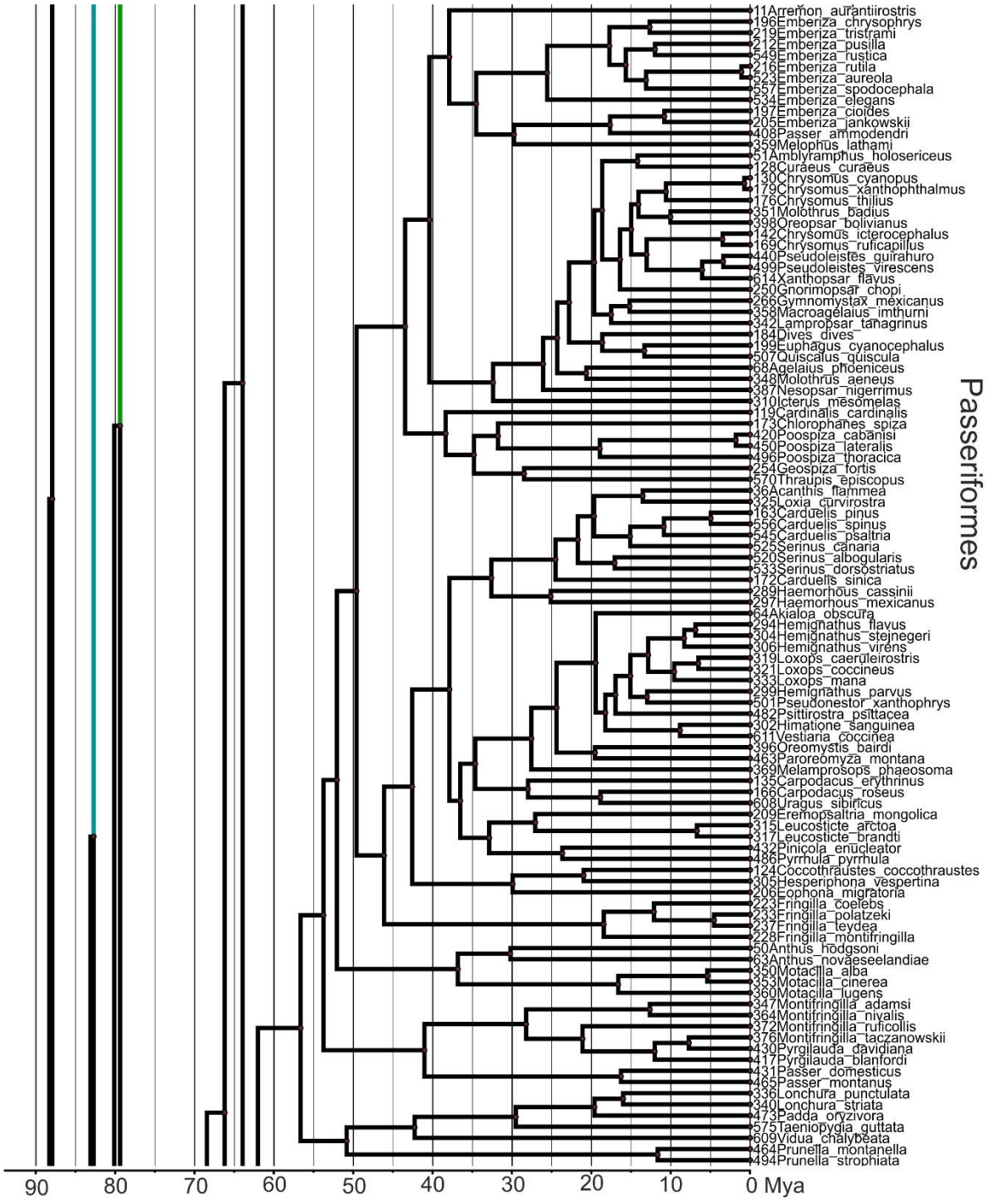
11Arremon_aurantiirostris
196Emberiza_chrysophrys
219Emberiza_tristrami
212Emberiza_pusilla
549Emberiza_rustica
216Emberiza_rutila
523Emberiza_aureola
557Emberiza_spodocephala
534Emberiza_elegans
197Emberiza_cioides
205Emberiza_jankowskii
408Passer_ammodendri
359Melophus_lathami
51Amblyramphus_holosericeus
128Curaeus_curaeus
130Chrysomus_cyanopus
179Chrysomus_xanthophthalmus
176Chrysomus_thilius
351Molothrus_badius
398Oreopsar_bolivianus
142Chrysomus_icterocephalus
169Chrysomus_ruficapillus
440Pseudoleistes_guirahuro
499Pseudoleistes_virescens
614Xanthopsar_flavus
250Gnorimopsar_chopi
266Gymnomystax_mexicanus
358Macroagelaius_imthurni
342Lampropsar_tanagrinus
184Dives_dives
199Euphagus_cyanocephalus
507Quiscalus_quiscula
68Agelaius_phoeniceus
348Molothrus_aeneus
387Nesopsar_nigerrimus
310Icterus_mesomelas
119Cardinalis_cardinalis
173Chlorophanes_spiza
420Poospiza_cabanisi
450Poospiza_lateralis
496Poospiza_thoracica
254Geospiza_fortis
570Thraupis_episcopus
36Acanthis_flammea
325Loxia_curvirostra
163Carduelis_pinus
556Carduelis_spinus
545Carduelis_psaltria
525Serinus_canaria
520Serinus_albogularis
533Serinus_dorsostriatus
172Carduelis_sinica
289Haemorhous_cassinii
297Haemorhous_mexicanus
64Akialoa_obscura
294Hemignathus_flavus
304Hemignathus_stejnegeri
306Hemignathus_virens
319Loxops_caeruleirostris
321Loxops_coccineus
333Loxops_mana
299Hemignathus_parvus
501Pseudonestor_xanthophrys
482Psittirostra_psittacea
302Himatione_sanguinea
611Vestiaria_coccinea
396Oreomystis_bairdi
463Pareoreomyza_montana
369Melamprosops_phaeosoma
135Carpodacus_erythrinus
166Carpodacus_roseus
608Uragus_sibiricus
209Eremopsaltria_mongolica
315Leucosticte_arctoa
317Leucosticte_brandti
432Pinicola_enucleator
486Pyrrhula_pyrrhula
124Coccothraustes_coccothraustes
305Hesperiphona_vespertina
206Eophona_migratoria
223Fringilla_coelebs
233Fringilla_polatzeki
237Fringilla_teydea
228Fringilla_montifringilla
50Anthus_hodgsoni
63Anthus_novaeseelandiae
350Motacilla_alba
353Motacilla_cinerea
360Motacilla_lugens
347Montifringilla_adamsi
364Montifringilla_nivalis
372Montifringilla_ruficollis
376Montifringilla_taczanowskii
430Pyrgilauda_davidiana
417Pyrgilauda_blanfordi
431Passer_domesticus
465Passer_montanus
336Lonchura_punctulata
340Lonchura_striata
473Padda_oryzivora
575Taeniopygia_guttata
609Vidua_chalybeata
464Prunella_montanella
494Prunella_strophiata
Passeriformes
90
80
70
60
50
40
30
20
10
0 Mya

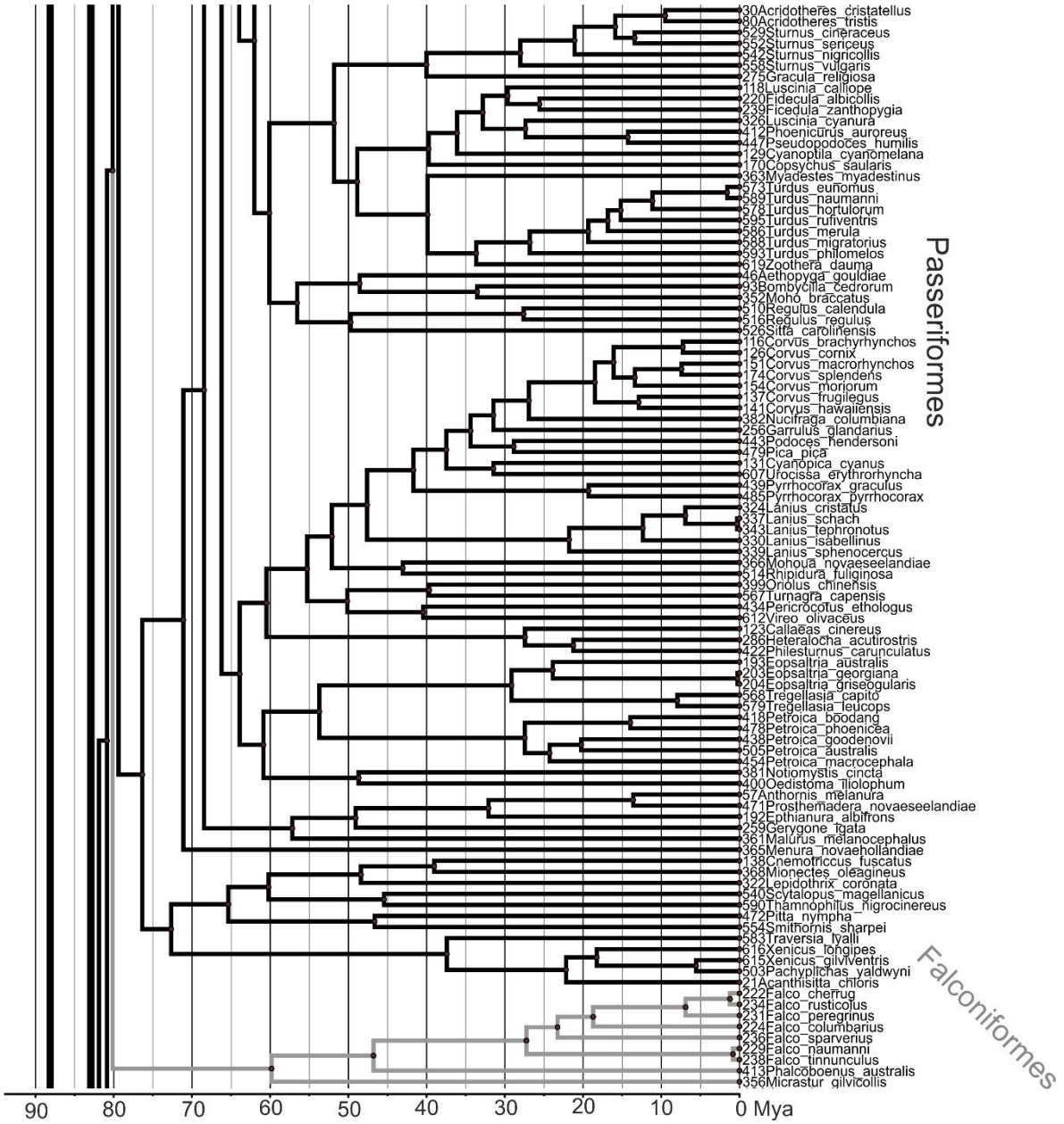
430Acridotheres_cristatellus
480Acridotheres_tristis
529Sturnus_cineraceus
552Sturnus_sericeus
542Sturnus_nigricollis
558Sturnus_vulgaris
275Gracula_religiosa
118Luscinia_calliope
220Fidecula_albicollis
239Ficedula_zanthopygia
326Luscinia_cyanura
412Phoenicurus_auroreus
447Pseudopodoces_humilis
129Cyanoptila_cyanomelana
170Copsychus_saularis
363Myadestes_myadestinus
573Turdus_eunomus
569Turdus_naumanni
578Turdus_hortulorum
595Turdus_ruficollis
586Turdus_merula
588Turdus_migratorius
593Turdus_philomelos
619Zoothera_dauma
46Aethopyga_gouldiae
93Bombycilla_cedrorum
352Mohoidae_braccatus
510Regulus_calendula
516Regulus_regulus
526Sitta_carolinensis
116Corvus_brachyrhynchos
126Corvus_cornix
151Corvus_macrorhynchos
174Corvus_splendens
154Corvus_moriorum
137Corvus_frugilegus
141Corvus_hawaiiensis
382Nucifraga_columbiana
256Garrulus_glandarius
443Podoces_hendersoni
479Pica_pica
131Cyanopica_cyanus
607Urocissa_erythrorhyncha
439Pyrrhocorax_graculus
435Pyrrhocorax_pyrrhocorax
324Lanius_cristatus
337Lanius_schach
343Lanius_tephronotus
330Lanius_isabellinus
339Lanius_sphenocercus
366Mohoua_novaeseelandiae
514Rhipidura_fuliginosa
399Oriolus_chinensis
567Turnagra_capensis
434Pericrocotus_ethologus
612Vireo_olivaceus
123Callaeas_cinereus
286Heteralocha_acutirostris
422Philesturnus_carunculatus
193Eopsaltria_australis
203Eopsaltria_georgiana
204Eopsaltria_griseogularis
568Tregellasia_capito
579Tregellasia_leucops
418Petroica_boodang
478Petroica_phoenicea
438Petroica_goodenovii
505Petroica_australis
454Petroica_macrocephala
381Notomystis_cincta
400Dicaeidae_Dicaeidae
57Anthornis_melanura
471Prosthemadera_novaeseelandiae
192Epthianura_albifrons
259Gerygone_igata
361Malurus_melanocephalus
365Menura_novaehollandiae
138Chamaeidae_Chamaeidae
368Mimidae_Mimidae
322Lepidothrix_coronata
540Scytalopus_magellanicus
590Thamnophilus_nigrocinereus
472Pittidae_Pittidae
554Smithornis_sharpei
583Traversia_lyalli
616Xenicus_longipes
615Xenicus_gilviventris
503Pachycephalidae_Pachycephalidae
21Acanthisitta_chloris
222Falco_cherrug
234Falco_rusticolus
231Falco_peregrinus
224Falco_columbarius
236Falco_sparverius
229Falco_naumanni
238Falco_tinnunculus
413Falconidae_Falconidae
356Micrastur_gilvicollis
Passeriformes
Falconiformes
90
80
70
60
50
40
30
20
10
0 Mya


16Athene_brama
244Glaucidium_brodiei
391Ninox_novaeseelandiae
518Sceloglaux_albifacies
395Ninox_scutulata
37Asio_flammeus
88Bubo_blakistoni
95Bubo_flavipes
90Bubo_bubo
538Strix_leptogrammica
403Otus_scops
397Otus_bakkamoena
415Phodilus_badius
561Tyto_alba
581Tyto_longimembris
28Aceros_corrugatus
65Aceros_waldeni
475Penelopides_panini
89Bycanistes_brevis
101Bucorvus_leadbeateri
606Upupa_epops
414Pteroglossus_azara
543Sasia_ochracea
191Dryocopus_pileatus
139Campephilus_guatemalensis
143Campephilus_imperialis
188Dendrocopos_leucotos
189Dendrocopos_major
483Picoides_pubescens
168Ceryle_rudis
290Halcyon_coromanda
300Halcyon_pileata
303Halcyon_smyrnensis
596Todiramphus_sanctus
210Eurystomus_orientalis
605Trogon_viridis
91Buteo_buteo
97Buteo_hemilasius
99Buteo_lagopus
43Accipiter_gentilis
61Accipiter_nisus
47Accipiter_gularis
82Accipiter_virgatus
79Accipiter_soloensis
22Aquila_chrysaetos
292Hieraaetus_fasciatus
378Nisaetus_alboniger
388Nisaetus_nipalensis
60Aegypius_monachus
527Spilornis_cheela
442Pandion_haliaetus
553Sagittarius_serpentarius
112Cathartes_aura
13Ardeola_bacchus
106Butorides_striata
24Ardea_cinerea
72Ardea_purpurea
54Ardea_intermedia
59Ardea_modesta
98Bubulcus_ibis
257Gorsachius_goisagi
265Gorsachius_melanolophus
392Nycticorax_nycticorax
62Ardea_novaehollandiae
201Egretta_eulophotes
217Egretta_sacra
202Egretta_garzetta
264Gorsachius_magnificus
185Dupetor_flavicollis
307Ixobrychus_cinnamomeus
309Ixobrychus_eurhythmus
312Ixobrychus_sinensis
105Botaurus_stellaris
215Eudocimus_ruber
389Nipponia_nippon
452Platalea_leucorodia
461Platalea_minor
560Threskiornis_aethiopicus
104Balaeniceps_rex
426Pelecanus_conspicillatus
235Fregata_sp.
373Morus_serrator
74Anhinga_rufa
320Leucocarbo_chalconotus
379Nannopterum_brasilianus
421Phalacrocorax_carbo
115Ciconia_boyciana
122Ciconia_ciconia
157Ciconia_nigra
17Aphrodroma_brevirostris
424Procellaria_cinerea
459Pelagodroma_marina
183Diomedea_chrysostoma
585Thalassarche_melanophrys
407Phoebastria_albatrus
448Phoebastria_immutabilis
469Phoebastria_nigripes
406Pygoscelis_adeliae
409Pygoscelis_antarcticus
39Aptenodytes_forsteri
195Eudyptes_chrysocome
208Eudyptula_minor
532Spheniscus_demersus
271Gavia_pacifica
280Gavia_stellata
451Phaethon_lepturus
489Phaethon_rubricauda
515Rhynochetos_jubatus
Strigiformes
Bucerotiformes
Piciformes
Pelecaniformes
Suliformes
Ciconiiformes
Procellariiformes
Sphenisciformes
Gaviiformes
Phaetontiformes
90
80
70
60
50
40
30
20
10
0 Mya

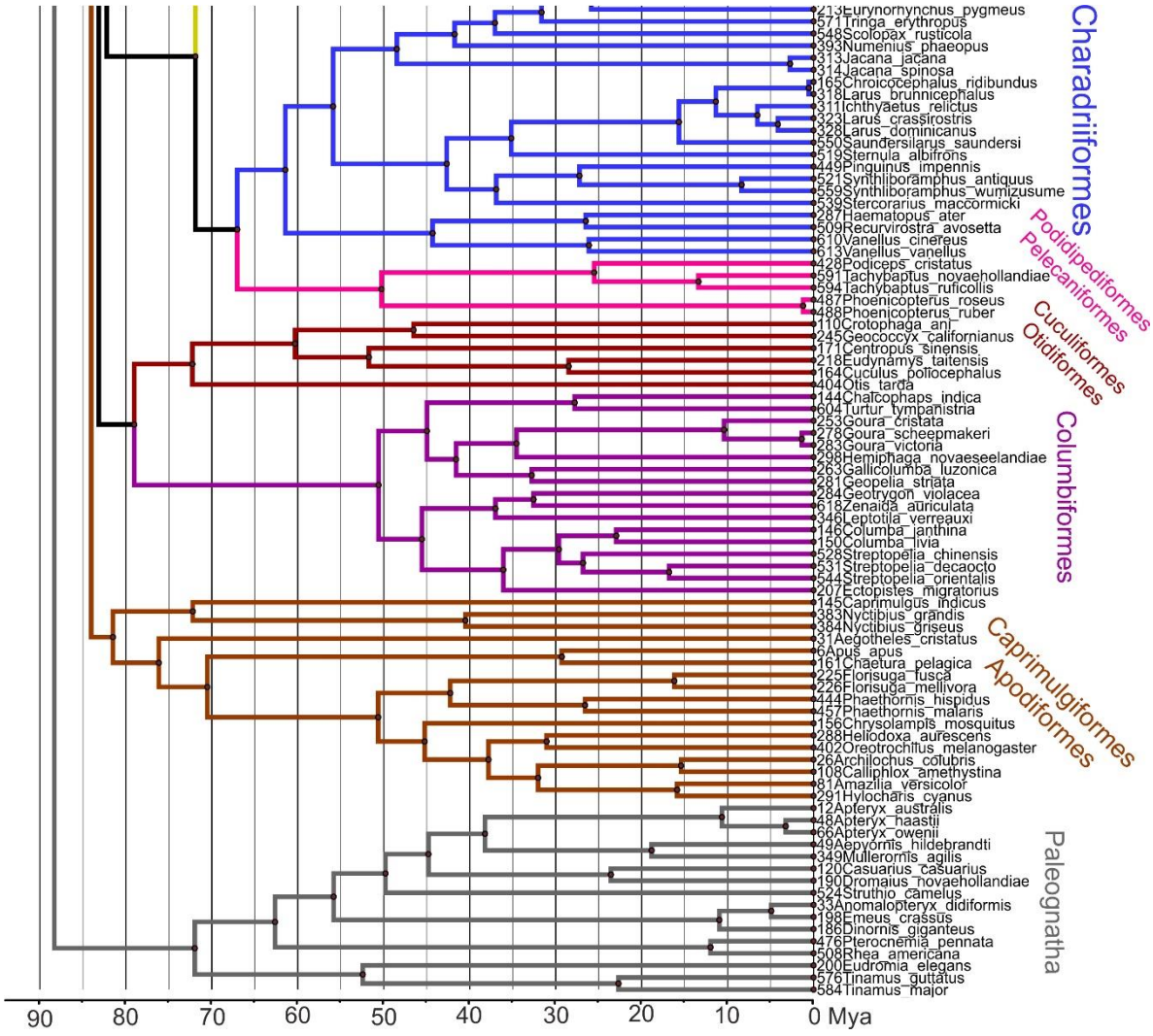
213Eurynorhynchus_pygmeus
571Tringa_erythropus
548Scolopax_rusticola
393Numenius_phaeopus
313Jacana_jacana
314Jacana_spinosa
165Chroicocephalus_ridibundus
318Larus_brunnicephalus
311Ichthyaetus_relictus
323Larus_crassirostris
328Larus_dominicanus
550Saundersilarus_saundersi
519Sternula_albifrons
449Pinguinus_impennis
521Synthliboramphus_antiquus
559Synthliboramphus_wumizusume
539Stercorarius_maccormicki
287Haematopus_ater
509Recurvirostra_avosetta
610Vanellus_cinereus
613Vanellus_vanellus
428Podiceps_cristatus
591Tachybaptus_novaehollandiae
594Tachybaptus_ruficollis
487Phoenicopterus_roseus
488Phoenicopterus_ruber
110Crotophaga_ani
245Geococcyx_californianus
171Centropus_sinensis
218Eudynamys_taitensis
164Cuculus_pollocephalus
404Otis_tarda
144Chalcophaps_indica
604Turtur_tympanistria
253Goura_cristata
278Goura_scheepmakeri
283Goura_victoria
298Hemiphaga_novaeseelandiae
263Gallicolumba_luzonica
281Geopelia_striata
284Geotrygon_violacea
618Zenaida_auriculata
346Leptotila_verreauxi
146Columba_janthina
150Columba_livia
528Streptopelia_chinensis
531Streptopelia_decaocto
544Streptopelia_orientalis
207Ectopistes_migratorius
145Caprimulgus_indicus
383Nyctibius_grandis
384Nyctibius_griseus
31Aegotheles_cristatus
6Apus_apus
161Chaetura_pelagica
225Florisuga_fusca
226Florisuga_mellivora
444Phaethornis_hispidus
457Phaethornis_malaris
156Chrysolampis_mosquitus
288Heliodoxa_aurescens
402Oreotrochilus_melanogaster
26Archilochus_colubris
108Calliphlox_amethystina
81Amazilia_versicolor
291Hylocharis_cyanus
12Apteryx_australis
48Apteryx_haastii
66Apteryx_owenii
49Aepyornis_hildebrandti
349Mullerornis_agilis
120Casuarius_casuarius
190Dromaius_novaehollandiae
524Struthio_camelus
33Anomalopteryx_didiformis
198Emeus_crassus
186Dinornis_giganteus
476Pterocnemia_pennata
508Rhea_americana
200Eudromia_elegans
576Tinamus_guttatus
584Tinamus_major
Charadriiformes
Podidipediformes
Pelecaniformes
Cuculiformes
Otidiformes
Columbiformes
Caprimulgiformes
Apodiformes
Paleognatha
90
80
70
60
50
40
30
20
10
0 Mya